



## RU GRANT FINAL REPORT FORM

Please email a softcopy of this report to rcmo@usm.my

<b>A</b>	<b>PROJECT DETAILS</b>
<b>i</b>	<b>Title of Research: Estimation of Probable Earthquake Ground Motion in Peninsular Malaysia</b>
<b>ii</b>	<b>Account Number: 1001/PAWAM/814179</b>
<b>iii</b>	<b>Name of Research Leader: Dr. Lau Tze Liang</b>
<b>iv</b>	<b>Name of Co-Researcher:</b>  1. Assoc. Prof. Dr. Choong Kok Keong 2. Prof. Dr. Taksiah A. Majid 3. Dr. Fadzli Mohamed Nazri 4. Dr. Neeraj Bhardwaj
<b>v</b>	<b>Duration of this research:</b>  a) Start Date : 15/12/2012 b) Completion Date : 14/12/2015 c) Duration : 36 months d) Revised Date (if any) : 14/6/2016
<b>B</b>	<b>ABSTRACT OF RESEARCH</b>
	<p><i>(An abstract of between 100 and 200 words must be prepared in Bahasa Malaysia and in English. This abstract will be included in the Report of the Research and Innovation Section at a later date as a means of presenting the project findings of the researcher/s to the University and the community at large)</i></p> <p>Malaysia is located in seismically stable Sunda plate and has not experienced any disastrous earthquake occurrences. However, due to the location close to two of the most seismically active plate boundaries, i.e. Indo-Australian and Eurasian plates, Malaysia has experienced numerous strong tremors caused by earthquakes in those two seismically active zones recently. Regions of moderate to low seismicity such as Peninsular Malaysia are currently facing an intricate condition involving the prediction of probable seismic hazard. Paucity of strong motion records in these areas hampers earthquake ground motion estimation as well as the conduct of a comprehensive regression analysis of available data. For this reason, the research was carried out to determine an appropriate ground motion attenuation model for Peninsular Malaysia out of</p>

28 pre-selected ground motion attenuation models. Evaluation of pre-selected models respective to actual weak ground motion records in Peninsular Malaysia resulted from Sumatra earthquakes was conducted. A total of 318 seismic records from 42 distant subduction and strike-slip Sumatra earthquakes with moment magnitude ranging from 5.2 to 9.1 spanning in a distance range of 284–1292 km from 19 seismic stations operated by Malaysian Meteorological Department were used in this study.

*Malaysia terletak di plat Sunda yang stable secara seismos dan tidak pernah mengalami kejadian gempa bumi yang teruk. Tetapi disebabkan lokasi yang berhampiran dengan dua sempadan plat yang sangat aktif secara seismos iaitu plat Indo-Australia dan plat Eurasian, Malaysia telah mengalami gegaran yang kuat akibat gempa bumi di kedua-dua zon aktif seismos ini baru-baru ini. Kawasan seismos rendah dan sederhana seperti Semenanjung Malaysia sedang menghadapi keadaan yang sukar untuk menganggarkan bahaya seismos yang berkemungkinan. Kekurangan catatan gegaran kuat di kawasan ini telah menghalang penganggaran gegaran gempa bumi dan pelaksanaan analisis regresi yang menyeluruh dengan menggunakan data yang sedia ada. Untuk tujuan ini, kajian ini telah dilakukan untuk menentukan satu model pengurangan gegaran tanah yang berseesuaian untuk Semenanjung Malaysia daripada 28 model pengurangan gegaran tanah terpilih. Penilaian untuk model terpilih dengan catatan gegaran lemah yang sebenar di Semenanjung Malaysia akibat gempa bumi di Sumatra telah dilakukan. Sebanyak 318 catatan gempa bumi dari 42 gempa bumi benam dan dan gelinciran jurus di Sumatra dengan magnitud antara 5.2 ke 9.1 dan berjarak dari 284-1292 km daripada 19 stesen gempa bumi yang dikendalikan oleh Jabatan Meteorologi Malaysia telah digunakan dalam kajian ini.*

## C BUDGET & EXPENDITURE

i

**Total Approved Budget** : RM 249,950.00

### Yearly Budget Distributed

Year 1 : RM 142,650.00

Year 2 : RM 75,150.00

Year 3 : RM 32,150.00

**Total Expenditure** : RM 249,947.39

**Balance** : RM 2.61

**Percentage of Amount Spent (%)** : 100

**# Please attach final account statement (eStatement) to indicate the project expenditure**

## ii Equipment Purchased Under Vot 35000

No.	Name of Equipment	Amount (RM)	Location	Status
1	Ambient vibration measuring instrument	81,841.00	School of Civil Engineering USM	Good

**# Please attach the Asset/Inventory Return Form (Borang Penyerahan Aset/Inventori) – Appendix 1**

<b>D RESEARCH ACHIEVEMENTS</b>		
<b>i</b>	<b>Project Objectives (as stated/approved in the project proposal)</b>	
	<b>No.</b>	<b>Project Objectives</b>
	<b>Achievement</b>	
	1	To determine the most suitable attenuation model for Peninsular Malaysia
	2	To provide a good estimate of the level of ground motion intensity in Penang and Kuala Lumpur

<b>ii</b>	<b>Research Output</b>		
	<b>a) Publications in ISI Web of Science/Scopus</b>		
	<b>No.</b>	<b>Publication (authors,title,journal,year,volume,pages,etc.)</b>	<b>Status of Publication (published/accepted/ under review)</b>
	1	Tze Che Van, Tze Liang Lau and Chai Fung Mok (2016) "Selection of ground motion attenuation models for Peninsular Malaysia due to far-field Sumatra earthquakes", Natural Hazards, 80(3), pp. 1865-1889, 10.1007/s11069-015-2036-8.	Published
	<b>b) Publications in Other Journals</b>		
	<b>No.</b>	<b>Publication (authors,title,journal,year,volume,pages,etc.)</b>	<b>Status of Publication (published/accepted/ under review)</b>
	1	Tze Che Van, Tze Liang Lau, Taksiah A. Majid, Kok Keong Choong and Fadzli Mohamed Nazri (2015) "Modification of Published Prediction Model of Ground Motion Due to Sumatra Subduction Earthquakes for the Application in Peninsulr Malaysia", Applied Mechanics and Materials, 802, pp. 34-39.	Published
	<b>c) Other Publications (book,chapters in book,monograph,magazine,etc.)</b>		
	<b>No.</b>	<b>Publication (authors,title,journal,year,volume,pages,etc.)</b>	<b>Status of Publication (published/accepted/ under review)</b>
	1	Tze Che Van and Tze Liang Lau (2014) "Estimation of Ground Motion in Kuala Lumpur Due to Sumatra Subduction Earthquake". InCIEC 2013 - Proceedings of the International Civil and Infrastructure Engineering Conference 2013, Hassan, R., Yusoff, M., Ismail, Z., Amin, N.M., Fadzil, M.A. (Eds.), Springer, 129-139.	Published
	<b>d) Conference Proceeding</b>		
	<b>No.</b>	<b>Conference (conference name,date,place)</b>	<b>Title of Abstract/Article</b>
			<b>Level (International/National)</b>
	1	International Civil and Infrastructure Engineering Conference, September 22-24, 2013, Kuching, Malaysia	Estimation of Ground Motion in Kuala Lumpur Due to Sumatra Subduction Earthquake
			International

# Please attach a full copy of the publication/proceeding listed above

**iii Other Research Output/Impact From This Project**  
(patent, products, awards, copyright, external grant, networking, etc.)

The completion of this project has provided a good foundation for the estimation of earthquake ground motion in Malaysia. This has contributed to the approval of an external grant from JICA AUN/SEED-Net and the grant is in collaboration with researchers from Japan and Thailand.

**E HUMAN-CAPITAL DEVELOPMENT**

**a) Graduated Human Capital**

Student	Nationality (No.)		Name
	National	International	
PhD			1. 2.
MSc	2		1. Chow Tze Liang 2. Van Tze Che
Undergraduate	1		1. Mok Chai Fung 2.

**b) On-going Human Capital**

Student	Nationality (No.)		Name
	National	International	
PhD			1. 2.
MSc			1. 2.
Undergraduate			1. 2.

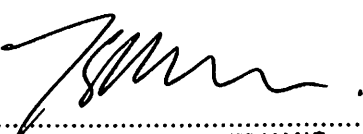
**c) Others Human Capital**

Student	Nationality (No.)		Name
	National	International	
Post Doctoral Fellow			1. 2.
Research Officer	1		1. Van Tze Che 2.
Research Assistant	4		1. Chong Kim Wee 2. Kenny Chia 3. Koon Foo Siong 4. Loh Mei Yee
Others (.....)			1. 2.



<b>F</b>	<b>COMPREHENSIVE TECHNICAL REPORT</b>
	<p>Applicants are required to prepare a comprehensive technical report explaining the project. The following format should be used (this report must be attached separately):</p> <ul style="list-style-type: none"> <li>• Introduction</li> <li>• Objectives</li> <li>• Methods</li> <li>• Results</li> <li>• Discussion</li> <li>• Conclusion and Suggestion</li> <li>• Acknowledgements</li> <li>• References</li> </ul>
<b>G</b>	<b>PROBLEMS/CONSTRAINTS/CHALLENGES IF ANY</b>
	<p><i>(Please provide issues arising from the project and how they were resolved)</i></p> <p>-</p>
<b>H</b>	<b>RECOMMENDATION</b>
	<p><i>(Please provide recommendations that can be used to improve the delivery of information, grant management, guidelines and policy, etc.)</i></p> <p>-</p>

**Project Leader's Signature:**

  
 .....  
 Name : **DR LAU TZE LIANG**  
           **SENIOR LECTURER**  
           **SCHOOL OF CIVIL ENGINEERING**  
           **UNIVERSITI SAINS MALAYSIA**  
 Date : **4/10/2016**

I COMMENTS, IF ANY/ENDORSEMENT BY PTJ'S RESEARCH COMMITTEE

This research has produced findings highly beneficial for engineering communities and also policy makers on issues related to consideration of earthquake in design and planning of structures especially critical in infrastructures. Publications produced will also serve as valuable sources for other researchers. Human resource training target is also achieved satisfactorily.



Signature and Stamp of Chairperson of PTJ's Evaluation Committee

Prof. Madya Dr. Choong Kok Keong  
Timbalan Dekan

Name :

Penyelidikan, Siswazah & Jaringan  
Pusat Pengajian Kejuruteraan Awam  
Kampus Kejuruteraan  
Universiti Sains Malaysia

Date :

7/10/2016



Signature and Stamp of Dean/ Director of PTJ

11/10/16

Name : Prof. Dr. Ahmad Farhan Mohd Sadullah  
Dekan

Date : Pusat Pengajian Kejuruteraan Awam  
Kampus Kejuruteraan  
Universiti Sains Malaysia



**JABATAN BENDAHARI**  
**PENYATA PERBELANJAAN SEHINGGA 1 OKTOBER 2016**

Tajuk projek ESTIMATION OF PROBABLE EARTHQUAKE GROUND MOTION IN PENINSULAR MALAYSIA  
Tempoh projek 15/12/2012 hingga 14/06/2016  
Taraf projek AKTIF  
Ahli LAU TZE LIANG (KETUA PROJEK)  
CHOONG KOK KEONG  
FADZLI BIN MOHAMED NAZRI  
NEERAJ BHARDWAJ  
TAKSIAH BINTI A. MAJID  
Nombor akaun 1001.PAWAM.814179

Vot	Nama Vot	Peruntukan Projek	Perbelanjaan Terkumpul Sehingga Thn Lalu	Baki Peruntukan Tahun Lalu	Peruntukan Thn Semasa	Jumlah Peruntukan Thn Semasa	Tanggungan Semasa	Bayaran Thn Semasa	Jum Belanja Thn Semasa	Baki Projek
111	GAJI	108,000.00	50,387.69	57,612.31	0.00	57,612.31	0.00	0.00	0.00	57,612.31
221	JALANAN & SARA HIDUP	42,500.00	20,961.62	21,538.38	0.00	21,538.38	0.00	2,902.00	2,902.00	18,636.38
222	P'ANGKUTAN BARANG	0.00	675.00	(675.00)	0.00	(675.00)	0.00	0.00	0.00	(675.00)
223	HUBUNGAN & UTILITI	450.00	203.90	246.10	0.00	246.10	0.00	0.00	0.00	246.10
224	SEWAAN	0.00	1,680.00	(1,680.00)	0.00	(1,680.00)	0.00	1,375.00	1,375.00	(3,055.00)
225	MAKANAN & MINUMAN	0.00	787.90	(787.90)	0.00	(787.90)	0.00	296.00	296.00	(1,083.90)
226	BAHAN MENTAH	0.00	220.50	(220.50)	0.00	(220.50)	0.00	88.00	88.00	(308.50)
227	BEKALAN BAHAN LAIN	15,000.00	18,386.32	(3,386.32)	0.00	(3,386.32)	27,500.00	17,294.22	44,794.22	(48,180.54)
229	KHIDMAT IKTISAS	9,000.00	14,178.95	(5,178.95)	0.00	(5,178.95)	0.00	11,286.89	11,286.89	(16,465.84)
335	HARTA MODAL	75,000.00	80,529.16	(5,529.16)	0.00	(5,529.16)	0.00	0.00	0.00	(5,529.16)
552	PERBELANJAAN LAIN	0.00	78.30	(78.30)	0.00	(78.30)	9.57	1,106.37	1,115.94	(1,194.24)
Jumlah		249,950.00	188,089.34	61,860.66	0.00	61,860.66	27,509.57	34,348.48	61,858.05	2.61

Penyata ini adalah cetakan komputer tiada tandatangan diperlukan

Penyata ini adalah dianggap tepat jika tiada maklumbalas dalam tempoh masa 14 hari dari tarikh penyata

# Selection of ground motion attenuation model for Peninsular Malaysia due to far-field Sumatra earthquakes

Tze Che Van<sup>1</sup>  · Tze Liang Lau<sup>1</sup> · Chai Fung Mok<sup>1</sup>

Received: 25 November 2014 / Accepted: 11 October 2015 / Published online: 19 October 2015  
© Springer Science+Business Media Dordrecht 2015

**Abstract** Establishment of quality seismic hazard assessment is governed by capability of an attenuation model to produce closest predictions to the actual ground motion. Therefore, a robust ground motion attenuation model must be selected to feed a logic tree. The scarcity of historical strong ground motion data hinders the development of attenuation model for the low-seismicity area such as Peninsular Malaysia. This paper aims to determine an appropriate ground motion attenuation model for Peninsular Malaysia out of 28 pre-selected ground motion attenuation models. Evaluation of pre-selected models respective to actual weak ground motion records in Peninsular Malaysia resulted from Sumatra earthquakes was conducted. A total of 327 seismic records from 44 distant subduction and strike-slip Sumatra earthquakes with moment magnitude ranging from 5.2 to 9.1 spanning in a distance range of 284–1292 km were obtained from 19 seismic stations operated by Malaysian Meteorological Department. The multi-channel analysis of surface waves was conducted on all seismic stations to characterise the sites. Based on graphs plotting and calculation of quantification measure, the best fitting model for distant subduction earthquakes is Nabilah and Balendra (2012) with RMSE value as low as 0.182 and 0.107 for interface and intraslab events, respectively. Si and Midorikawa (2000) and Somerville et al. (2009) models give closest prediction to distant strike-slip earthquakes.

**Keywords** Attenuation models · Sumatra earthquakes · Distant earthquake · Ground motion prediction · Peak ground acceleration · Ground motion prediction equation

---

✉ Tze Che Van  
cathvan\_911@hotmail.com

Tze Liang Lau  
celau@usm.my

Chai Fung Mok  
freedamok@gmail.com

<sup>1</sup> School of Civil Engineering, Universiti Sains Malaysia, Penang, Malaysia

## 1 Introduction

Inhabitants in Peninsular Malaysia often feel tremors from earthquakes generated by one of the world's most seismically active zone, the Sumatra subduction and fault zone, despite sitting on the stable Sunda plate and large distance in between, which is around 300–500 km. Due to the fact that most of the constructions in Peninsular Malaysia did not practise seismic resistant design and protection, the seismic impact and risk is high due to its dense population and economic importance. The earthquakes occurrence has increased since the Sumatra earthquake in 2004 as shown in Fig. 1. This has raised the awareness among public and questions on the structural stability of existing building structures in Malaysia, especially in Penang (Lau et al. 2005). Therefore, there is a need of a robust ground motion attenuation model that could predict ground motion with a sensible

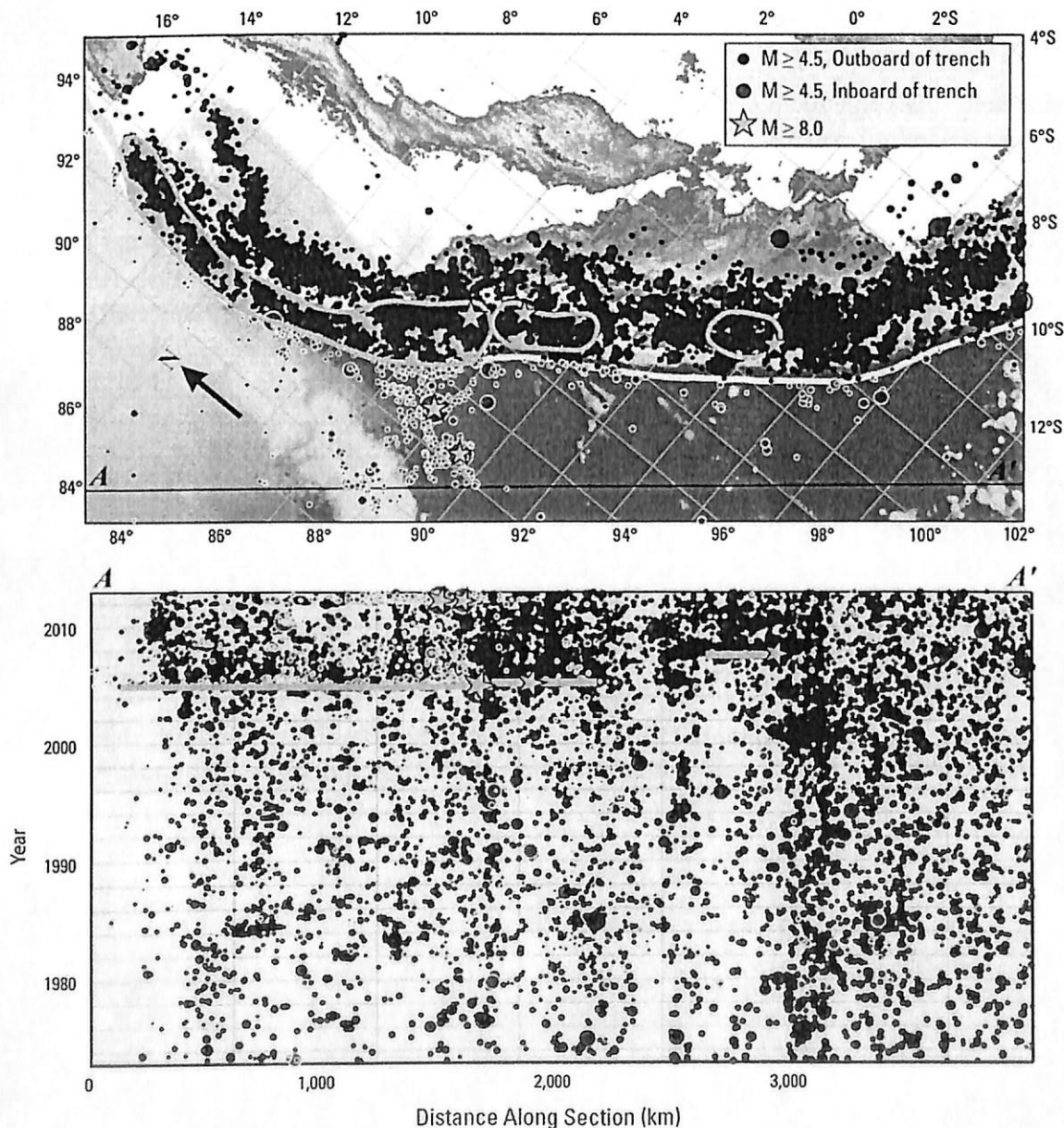


**Fig. 1** Time–space plot of seismicity in the Sumatra Arc from 1973–2011 (Hayes et al. 2013)

accuracy in order to develop a reliable national seismic building code for Peninsular Malaysia.

Ground motion attenuation model relates the estimation of the ground motion at particular area from a specified set of seismological parameters (Campbell 2003). It provides ground motion acceleration threshold for the assessment of seismic hazard, both deterministically and probabilistically, which in turn accounts for the establishment of reliable seismic building code for a particular country. Attenuation model with high uncertainties could lead to high probabilistic ground motion estimates at long return period (Zhao et al. 2006).

Most of the ground motion attenuation models, especially for seismically active regions, were derived based on strong ground motion by regression analysis. However, for regions where record of strong historical ground motion data is not profound, like Peninsular Malaysia, development of attenuation models is hindered. For countries having similar seismicity conditions to Malaysia, ground motion attenuation model was adopted among published equations (Allen 2010; Beauval et al. 2012a; Chintanapakdee et al. 2008). As adoption of existing ground motion attenuation model is a fast and economical method for subsequent seismic hazard assessment, a few researches have been conducted to determine the adoption of the best fitting attenuation model for Peninsular Malaysia (Adnan et al. 2004, 2010, 2012; Azizan 2012; Pappin et al. 2011; Petersen et al. 2004). However, these researches result in proposal of different attenuation models due to different criteria and

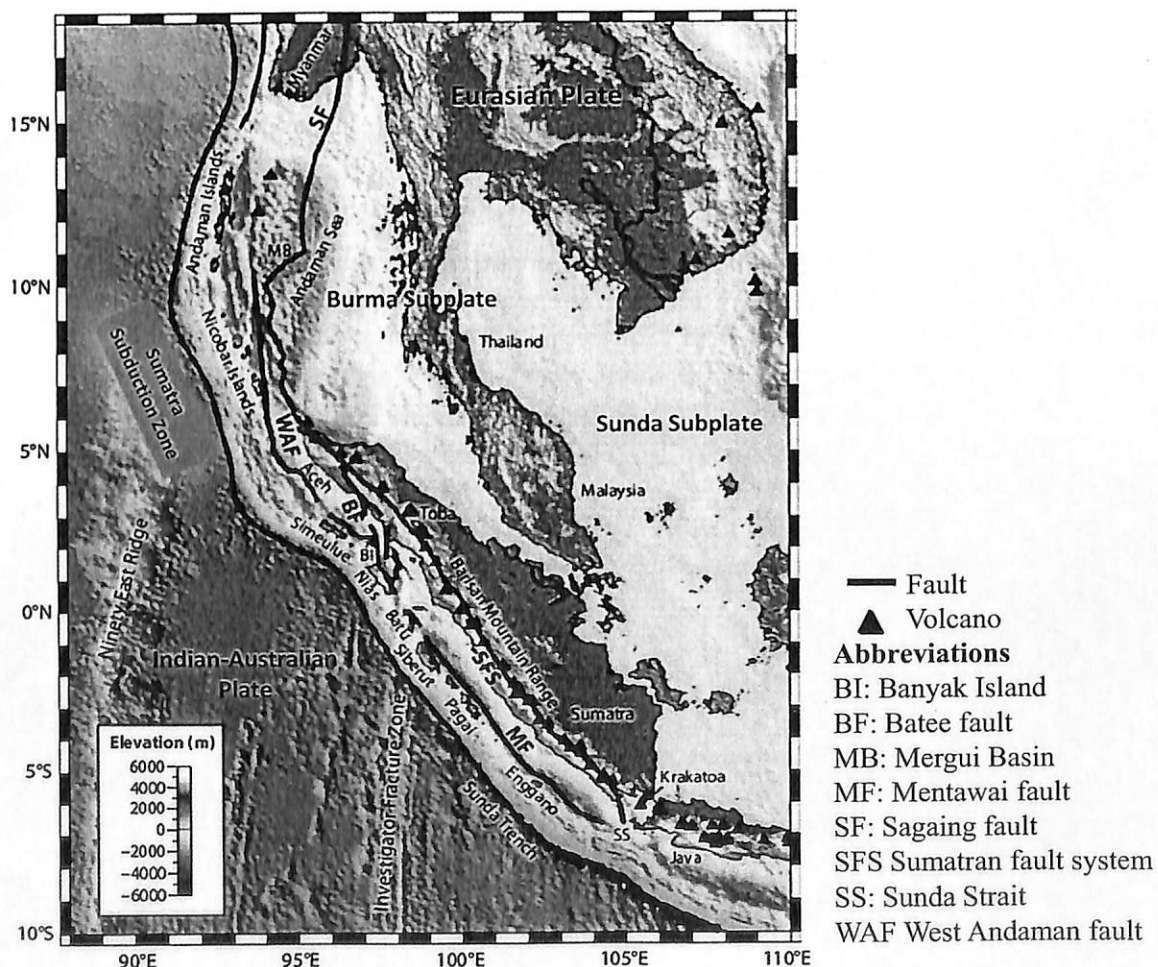


Fig. 2 Regional map showing tectonic setting and Sumatra zone (McCaffrey 2009)

considerations. Hence, a comprehensive study to incorporate all the suggested models with up-to-date ground motion records and seismological information has to be carried out for Peninsular Malaysia in order to establish an unambiguous outcome.

This study focuses on evaluating the suitability of various published prediction models and selecting ground motion attenuation model that gives closest prediction to recorded ground motion in Peninsular Malaysia, particularly for distant earthquakes. Thus, only distant earthquake events from Sumatra subduction and fault zone are considered in this study.

## 2 Tectonic settings and seismicity of Peninsular Malaysia

Peninsular Malaysia lies in the southern edge of the Eurasian plate which is close to the most seismically active zone, the Sumatra subduction zone (the interpolate boundary between the Indo-Australian and Eurasian plates) (Fig. 2). The west coast of Peninsular is about 500 km from this subduction zone. Sumatra subduction zone is a convergent belt extending at a length of more than 1600 km which running down from Himalayan to Java and the Sunda Islands. The Indian Ocean plate moves north-eastward and subducts under the Sumatra at about 40–50 mm/year (Lay et al. 2005; Sieh et al. 1999) and thus causes pressure to build up and eventually till the strength of the rock cannot resist the imposed stresses. Due to the sudden release of high pressure, the Sumatra subduction zone tends to produce large earthquake. The Sumatra subduction zone has generated a few massive historical earthquakes such as in 1797 event ( $M \sim 8.4$ ), 1833 event ( $M_w 8.75$ ), 1861 event ( $M_w 8.4$ ), 1881 event ( $M \sim 7.9$ ), 2004 event ( $M_w 9.1$ ), 2005 event ( $M_w 8.6$ ) and 2007 event ( $M_w 8.4$ ) (Newcomb and McCann 1987).

The highly oblique subducting motion of the Indian-Australian plate into the Eurasian plate results in slip-partitioning that causes the existence of 1900-km-long Sumatra fault on the in-land of Sumatra Island. As shown in Fig. 2, Peninsular Malaysia is closer to the Sumatra fault, with the closest distance from the earthquake source of about 260 km. The Sumatra fault has a slip rate ranges from 11 mm/year at southern fault to 27 mm/year at the northern part of the fault (Sieh and Natawidjaja 2000). The fault accommodates only strike-slip motion to share the large shear force of the Sumatra subduction zone. The energy released from this fault is at a relatively lower stress level compared with the Sumatran subduction zone due to the limited energy storage. Thus, the highest magnitude of this fault may not exceed  $M_w 7.8$ . However, the high seismicity of the fault is worth noticing. Between April 2008 and February 2009, Weller et al. (2012) recorded more than 1000 crustal events ranging from  $M_w 1.0$  to  $M_w 6.0$  produced along the fault.

## 3 Ground motion dataset

Seismic data utilised in this study are recorded from a total of 19 seismic stations located within Peninsular Malaysia. These seismic stations were monitored by Malaysian Meteorology Department (MMD). Catalogues from international open-access databases were used to supplement ground motion records with seismological information. Such catalogues are US Geological Survey (USGS) database, International Seismological Centre (ISC) database and National Earthquake Information Center (NEIC) database. A total of 73 earthquakes recorded from July 2004 to July 2013 were used in this study. As only distant



earthquakes originated from Sumatra subduction and fault zone with moment magnitude larger than 5 are of interest in this study, the size of events was reduced to 44, which comprised of 327 observed geometrical mean of two horizontal peak ground accelerations (PGA). The PGA value utilised in this study is the geometrical mean of two horizontal components (N and E components) of ground motion acceleration at a site. Vertical component PGA, that is Z component, diminishes faster than horizontal components, thus giving lesser effect on ground motion for far-field earthquake (Bozorgnia et al. 2000). Hence, vertical component is excluded in this study. Being the dataset of distant earthquakes, these data cover a wide range of epicentral distance, ranging from 284 to 1292 km. Figure 3 shows the epicentres of earthquakes considered in this study, while Fig. 4 portrays the location of seismic stations in Peninsular Malaysia.

Different source mechanism results in different ground motion as assured by Spudich et al. (1999) through theoretical study of Oglesby et al. (1998) and laboratory study by Brune and Anooshehpour (1999). Seismic waves from subduction earthquakes were proved to attenuate slower than those from crustal earthquakes (Atkinson and Boore 2003; Youngs et al. 1997). Thus, source mechanism categorisation was carried out on recorded ground motion data based on seismological information obtained from global centroid moment tensor (CMT) project moment tensor solution and NEIC moment tensor solution. As shown in Table 1, 33 events were identified as subduction events originated from Sumatra subduction zone having either normal or thrust faulting. Those subduction events were further classified into interface and intraslab earthquakes. The rest are strike-slip events produced by Sumatra fault zone except for two events on 11 April 2012 with  $M_w$  8.2 and  $M_w$  8.6, respectively. The foci of these two earthquakes were located at several hundred kilometres off west coast of northern Sumatra. The magnitude–distance distribution of the selected dataset is shown in Fig. 5.

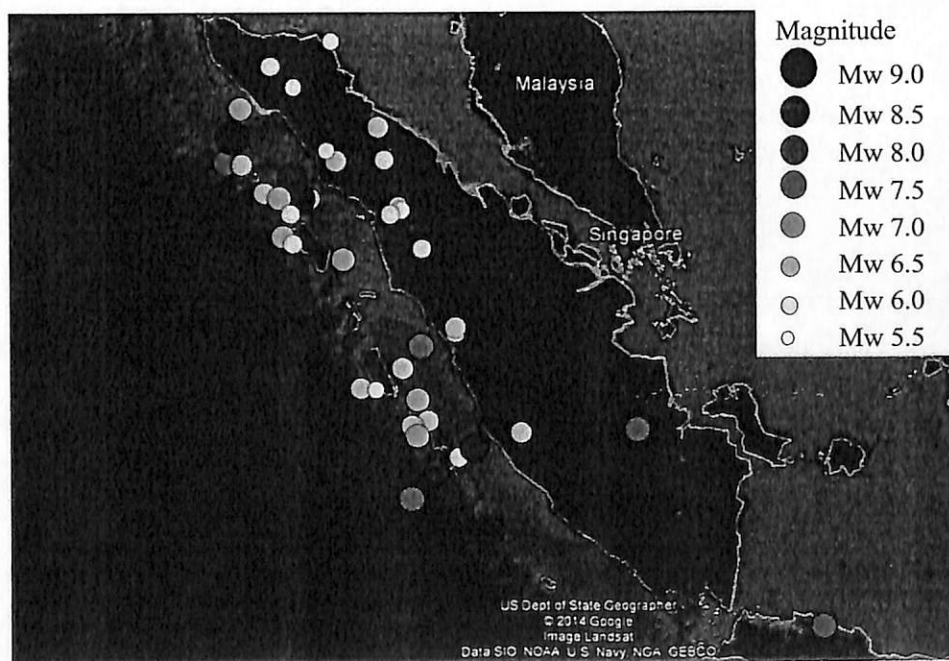


**Fig. 3** Map showing location and magnitude of distant earthquake events from July 2004 to July 2013





Fig. 4 Map showing location of seismic stations in Malaysia

#### 4 Site classification

Although seismic waves originated from the subduction and fault zone have to propagate through a long distance to reach Peninsular Malaysia, the long-period (low frequency) waves are less prone to energy dissipation. Arrival of these long-period waves on the ground surface could lead to large displacement properties, depending on the site condition. Soft soil sites tend to promote higher multiple reflection of shear compared to rock sites. Thus, building structures on soft soil sites tend to suffer severe vibration if resonances developed in the soil. The Mexico earthquake in 1985 is one of the observed examples for such implication. Due to the fact that site condition is a crucial parameter affecting ground motions, average shear-wave velocity in the upper 30 m ( $V_{S30}$ ) of seismic stations in Peninsular Malaysia was obtained by conducting multi-channel analyses of surface wave (MASW) using single GEODE for site classifying purpose. A total of 24 geophones with natural frequency of 4.5 Hz are deployed vertically into soil in a straight line with spacing interval of 1–1.5 m, depending on the area availability at site. These geophones were channelled together and connected to the GEODE. Offsets of 5, 10 and 15 m were measured at both ends on the spread length to meet different soil rigidity as suggested by Xu et al. (2006). Stacking limit of 5–12 blows using 8-kg sledgehammer was applied. The record length and sampling rate were adjusted to 1 s and 0.25 ms, respectively. The analysis of the collected seismographs, as shown in Fig. 6a, was carried out in two main steps. First, dispersion curves of Rayleigh waves (Fig. 6b) are developed from raw seismograph obtained from site testing. Secondly, dispersion curves are inverted to obtain  $V_S$  profiles. The fundamental mode of Rayleigh wave ranging from frequencies 4–75 Hz is taken in generating the dispersion curve by referring to signal-to-noise ratio (Fig. 6c). The final outcome is S-wave velocity profile against depth for each seismic station as shown in Fig. 6d.

Based on the field testing and analysis, the  $V_{S30}$  obtained for sites beneath seismic stations ranges from 182.7 to 792 m/s. The  $V_{S30}$  for each site has been determined and classified into respective site classes with reference to National Earthquake Hazard Reduction Program (NEHRP) 1997. As shown in Fig. 7, four of them were classified into class C, the class for soft rocks or very hard soils site, out of 19 stations. These stations are

**Table 1** List of earthquake events sorting based on source mechanisms

No.	Date	Time (UTC)	Epicentre coordinate (°)		Magnitude ( $M_w$ )	Focal depth (km)	Source mechanisms	No. of seismic stations with recordings
			Lat.	Long.				
1	2/7/2013	7:37:02	4.611	96.6041	6.1	10	Strike-slip	5
2	25/7/2012	0:27:45	2.657	96.126	6.4	22	Interface	4
3	23/6/2012	4:34:53	2.934	97.806	6.1	95	Intraslab	11
4	2012-04-11(a)	10:43:09	0.735	92.443	8.2	16.4	Strike-slip	14
5	2012-04-11(b)	8:38:38	2.36	93.01	8.6	22.9	Strike-slip	16
6	5/3/2012	6:55:28	4.187	97.093	5.5	10	Strike-slip	11
7	5/9/2011	17:55:13	2.73	98	6.6	91	Intraslab	13
8	18/6/2011	11:58:05	1.784	99.315	5.2	24.8	Strike-slip	16
9	2011-06-14(a)	3:01:29	1.856	99.254	5.6	10	Strike-slip	16
10	2011-06-14(b)	0:08:33	1.813	99.29	5.3	10	Strike-slip	15
11	6/4/2011	14:01:46	1.693	97.133	5.8	20	Interface	15
12	1/12/2010	0:50:23	2.758	98.95	5.9	163.4	Intraslab	15
13	25/10/2010	14:42:16	−3.838	99.604	7.7	20.6	Interface	14
14	9/5/2010	5:59:44	3.77	96.044	7.2	45	Interface	15
15	6/4/2010	22:15:06	2.412	97.145	7.8	31	Interface	11
16	23/12/2009	1:11:52	−1.721	98.894	5.7	22.6	Interface	14
17	1/10/2009	1:52:31	−2.49	101.685	6.6	15	Strike-slip	11
18	30/9/2009	10:16:09	−0.873	99.746	7.6	81	Intraslab	11
19	16/8/2009	7:38:18	−1.699	98.597	6.7	20	Interface	14
20	19/5/2008	14:26:00	1.7	99.1	6	14.8	Strike-slip	2
21	2008-02-25(a)	18:06:00	−2.3	99.9	6.3	33.1	Interface	2
22	2008-02-25(b)	8:36:00	−2.6	99.7	7.2	35	Interface	3
23	24/2/2008	14:46:00	−2.5	99.6	6.2	35	Interface	2
24	20/2/2008	8:08:00	2.7	95.8	7.4	35	Interface	2
25	22/1/2008	17:14:00	1.1	97.2	6.2	40.6	Interface	2
26	4/1/2008	7:29:00	−3	100.5	6	40.6	Interface	2
27	20/9/2007	8:31:00	−2.4	99.6	6.7	30	Interface	3
28	13/9/2007	3:35:00	−1.9	99.7	7	20	Interface	2
29	2007-09-12(a)	23:49:00	−2.8	100.8	7.9	30	Interface	3
30	2007-09-12(b)	11:10:00	−4.4	101.1	8.5	34	Interface	3
31	8/8/2007	17:04:00	−6.2	107.6	7.5	289.2	Intraslab	2
32	21/7/2007	12:53:00	5.1	97.8	5.2	25.6	Interface	3
33	2007-03-06(a)	5:49:00	−0.6	100.4	6.1	30.1	Strike-slip	3
34	2007-03-06(b)	3:49:00	−0.5	100.4	6.4	19	Strike-slip	4
35	1/12/2006	3:58:00	3.4	98.8	6.3	206.1	Intraslab	5
36	16/5/2006	15:28:00	0	97	6.8	16.2	Interface	4
37	19/5/2005	1:54:00	2	96.9	6.9	30	Interface	4
38	14/5/2005	5:05:00	0.8	98.2	6.8	34	Interface	5
39	28/4/2005	14:07:00	2.1	96.6	6.3	29	Interface	5
40	10/4/2005	10:29:00	−1.3	99.4	6.7	19	Interface	5

Table 1 continued

No.	Date	Time (UTC)	Epicentre coordinate (°)		Magnitude ( $M_w$ )	Focal depth (km)	Source mechanisms	No. of seismic stations with recordings
			Lat.	Long.				
41	3/4/2005	3:10:00	2	97.5	6.3	46.6	Interface	5
42	28/3/2005	16:09:00	2	97.3	8.6	30	Interface	5
43	26/12/2004	0:58:53	3.2	95.9	9.1	30	Interface	5
44	25/7/2004	14:35:19	−2.4	103.9	7.3	576	Intraslab	5

DTSM, JRM, KTM and PJSM. The rest of those stations were considered as class D, the class for hard soils sites.

## 5 Ground motion attenuation models

A reliable set of pre-selected ground motion attenuation models is the main concern to obtain a dependable outcome in this study. In the effort of pre-selecting ground motion attenuation models to be used in this study, exclusion criterion as suggested by Cotton et al. (2006) is performed on comprehensive list as reviewed by Douglas (2011).

Most of the published ground motion attenuation models were developed for seismically active regions. However, though Sumatra subduction zone is also listed as one of the most seismically active zones that are capable in producing world's top largest earthquakes, most of the published models that claimed to be derived globally did not consider or include earthquake events generated by Sumatra zone in their datasets. One of the obvious examples is the negligence of Sumatra earthquakes in the datasets of NGA models. Another difficulty faced when deciding in the adoption of published ground motion attenuation models is regarding the source-to-site distance. Most of the established ground motion attenuation models were developed for short distance, which is only up to 100 km, or at most 200 km, due to the interest in near-field effect and availability of strong motion datasets for empirical derivation. Thus, it should also be noted that pre-selected attenuation models in this study is not confined under magnitude and distance constraint to fit the collected data.

Based on the exclusion criteria for the pre-selection mentioned above and by obeying the pre-selection of 10 % out of available ground motion attenuation models as suggested by Douglas et al. (2012), a total of twenty-eight ground motion attenuation models were shortlisted. This study considers attenuation models for both subduction and shallow crustal earthquakes (Table 2). Thirteen models are for subduction earthquakes, while another fifteen models are for shallow crustal earthquakes.

## 6 Parameter calibration

It is crucial to calibrate and standardise certain parameters as models being considered in this paper utilised various parameter terms due to different considerations during the development of respective models.

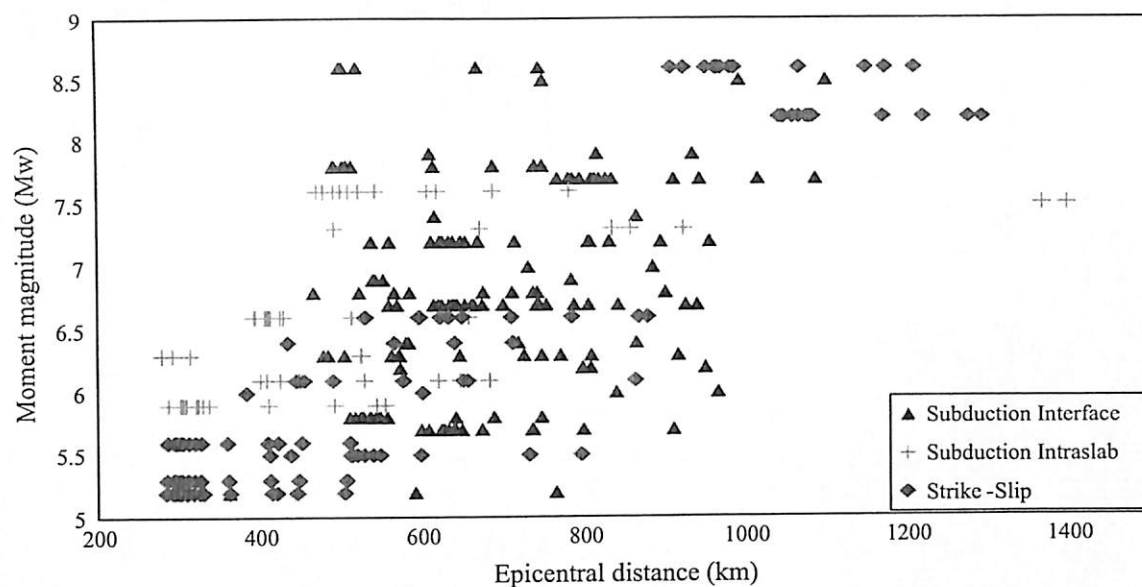


**Fig. 5** Magnitude–distance distribution for data from Peninsular Malaysia

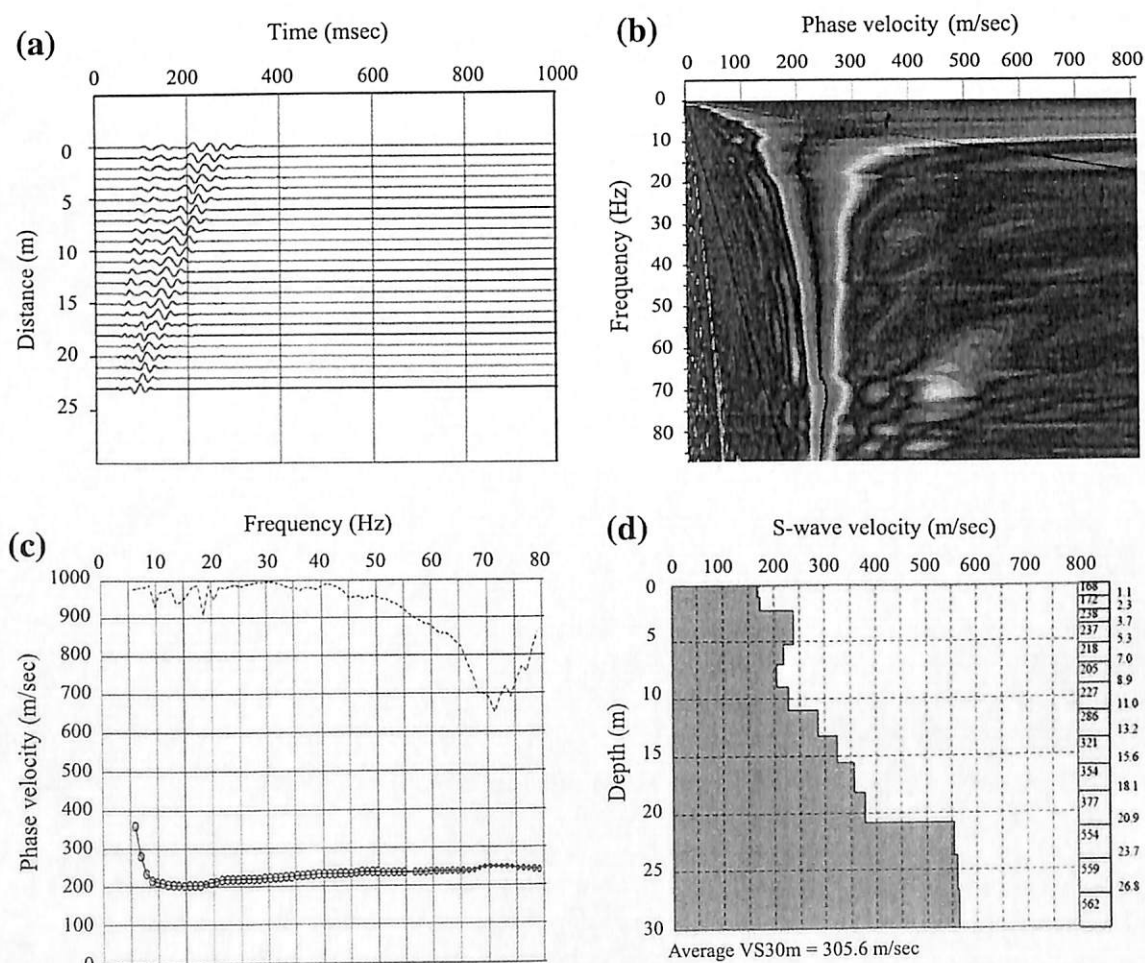


**Fig. 6** MASW data processing stages showing (a) collected accelerograph from the induced source (hammering), (b) plot of phase velocity against frequency, (c) dispersion curve and quality factor (dotted line) and (d) vertical shear-wave velocity profile

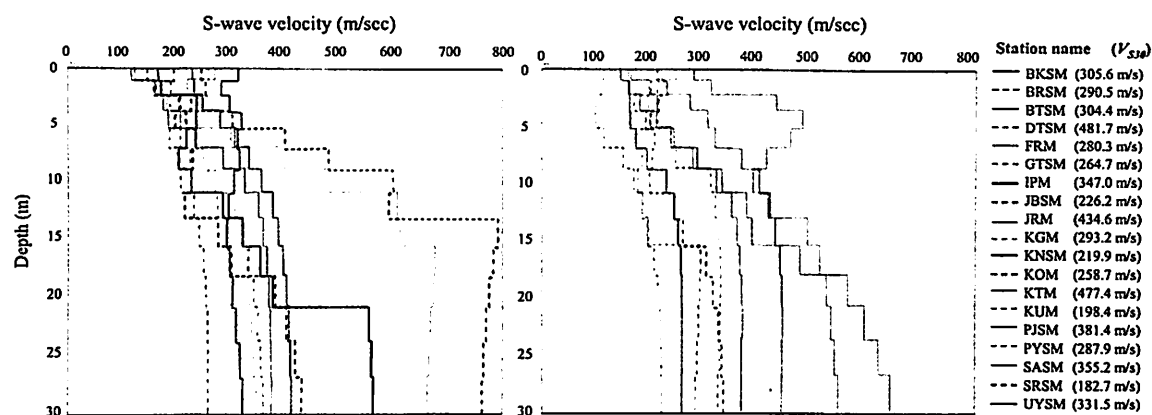


**Fig. 7** S-wave velocity profile against depth for seismic stations in Peninsular Malaysia

It should be emphasised that shallow crustal earthquakes included all types of faulting that occurred near to the ground surface and hence does not solely represent strike-slip earthquakes. A particular shallow crustal earthquakes model might be suitable to be used to predict strike-slip earthquakes or reverse faulting or normal faulting or combinations of any two of these faultings, or combination of all. While most of the models being considered in this paper provide coefficient values for strike-slip earthquakes as inputs, models such as Dahle et al. (1990), Frankel et al. (1996), Hwang and Huo (1997), Toro et al. (1997), Spudich et al. (1999) and Somerville et al. (2009) did not state their applicability to which types of faulting. Prior to comparison, adjustment was not made for models that did not mention the applicability to which faulting mechanism. On the other hand, Si and Midorikawa (2000) used geographical approach to describe earthquake source instead of using faulting mechanism. Equations for interplate earthquakes in this model were chosen to be applied on datasets from Peninsular Malaysia in this paper.

Different attenuation models adopt different distance terms. Each distance term has its own definition, strengths and weaknesses. Considering that the datasets in this paper were provided in epicentral distance and the nature of epicentral distance as point source measure which provides the simplest form of distance measure, it is adopted in this study during the plotting of recorded data. Distance terms other than epicentral distance used by some of these models were not converted into epicentral distance. This is because the difference among epicentral distance, hypocentral distance, closest distance to rupture surface and Joyner-Boore distance is apparently insignificant compared to the long distance being considered in the paper (Naguit 2007; Yeneir et al. 2008). Nonetheless, one should note that epicentral distance is not appropriate to be used for near-source prediction and large magnitude earthquake. Finite source distance measures such as Joyner-Boore distance and closest distance to rupture surface are more preferable when earthquake sources are well defined (Lee et al. 2002).

Most of the recently developed models used  $V_{S30}$  as variable for site classification which also suggest site classification schemes that provide equivalent classes according to ranges of  $V_{S30}$ . Such suggested classification schemes are Electric Power Research Institute (EPRI) 1993, National Earthquake Hazard Reduction Program (NEHRP) 2000, Boore et al. (1993) and Geomatrix site classification. However,  $V_{S30}$  was not used by older models, such as Dahle et al. (1990), Fukushima and Tanaka (1990), Crouse (1991) and Si and Midorikawa (2000), to define site classes. As these models distinguish site according to geology, stiffness and depth of soil, qualitative comparison was used to determine the

**Table 2** Pre-selected ground motion attenuation model with corresponding applicability range

Attenuation models	Focal depth (km)	Magnitude range	Source-to-site distance (km)	Target region
<i>Subduction earthquakes</i>				
Adnan et al. (2004)	5–56	$M_w$ 5.0–8.5	$r_{\text{epi}}$ 2–1122	Malaysia
Atkinson and Boore (2003)	0–100	$M_w$ 5.0–8.3	$r_{\text{rup}}$ 10–400	Cascadia
Crouse (1991)	0–238	$M_w$ 4.8–8.2	$r_{\text{epi}}$ 8–866	Cascadia
Fukushima and Tanaka (1990)	0–100	$M_w$ 4.5–8.2	$r_{\text{rup}}$ 10–300	Japan
Gregor et al. (2002)	–	$M_w$ 8.0–9.0	$r_{\text{rup}}$ 10–500	Cascadia
Kanno et al. (2006)	0–180	$M_w$ 5.0–8.2	$r_{\text{rup}}$ 1–450	Japan
Lin and Lee (2008)	5.5–161	$M_w$ 4.1–8.1	$r_{\text{hypo}}$ 15–630	Taiwan
Megawati et al. (2005)	15–33	$M_w$ 4.5–8.0	$r_{\text{epi}}$ 150–1500	Singapore
Megawati and Pan (2010)	12–44	$M_w$ 5.4–9.1	$r_{\text{epi}}$ 200–1500	Singapore
Nabilah and Balendra (2012)	0–35	$M_w$ 7.2–9.1	$r_{\text{epi}}$ 498–1021	Malaysia
Petersen et al. (2004)	0–229	$M_w$ 5.0–8.2	$r_{\text{rup}}$ > 200	Singapore and Peninsular Malaysia
Youngs et al. (1997)	0–229	$M_w$ 5.0–8.2	$r_{\text{rup}}$ 10–500	Global
Zhao et al. (2006)	0–162	$M_w$ 5.0–8.0	$r_{\text{rup}}$ 10–300	Japan
<i>Shallow crustal earthquakes at active tectonic region</i>				
Abrahamson and Silva (1997)	–	$M_w$ 4.4–7.4	$r_{\text{rup}}$ 0.1–200	Worldwide
Ambraseys et al. (2005)	1–30	$M_w$ > 5.0	$r_{\text{rup}}$ 1–100	Europe and Middle East
Atkinson and Boore (2006, 2011)	–	$M_w$ 3.5–8.0	Fault distance 1–1000	Eastern North America
Boore et al. (1997), Boore (2005)	0–20	$M_w$ 5.2–7.4	$r_{\text{jb}}$ 0–118	Western North America
Dahle et al. (1990)	–	$M_w$ 2.9–7.8	$r_{\text{hypo}}$ 1–1300	Worldwide
Megawati et al. (2003)	8–22	$M_w$ 4.0–8.0	$r_{\text{epi}}$ 174–1379	Singapore and Peninsular Malaysia
Sadigh et al. (1997)	–	$M_w$ 4.0–8.0	$r_{\text{rup}}$ 0–100	California
Si and Midorikawa (2000)	6–120	$M_w$ 5.8–8.2	$r_{\text{epi}}$ 0–118	Japan
Spudich et al. (1999)	–	$M_w$ 5.0–7.7	$r_{\text{jb}}$ 0–100	Worldwide
<i>Shallow crustal earthquakes at stable continental region</i>				
Campbell (2003, 2004)	–	$M_w$ 5.0–8.2	$r_{\text{rup}}$ 0–1000	Eastern North America
Frankel et al. (1996)	–	$M_w$ 4.4–8.0	$r_{\text{hypo}}$ 10–1000	Central and Eastern USA
Hwang and Huo (1997)	6–15	$M_w$ 5.0–7.5	$r_{\text{epi}}$ 5–200	Central and Eastern USA
Pezeshk et al. (2011)	–	$M_w$ 5.0–8.0	$r_{\text{rup}}$ 0–1000	Eastern North America
Somerville et al. (2009)	0–6	$M_w$ 5.0–7.5	$r_{\text{jb}}$ 0–500	Australia
Toro et al. (1997)	–	$M_w$ 5.0–8.0	$r_{\text{jb}}$ 1–500	Central and Eastern North America

classes of sites in Peninsular Malaysia according to definitions provided by these models. Generally, class C sites of NEHRP (2000) scheme were classified as rock sites by these older models, while class D sites were defined as soil sites.

## 7 Results and discussion

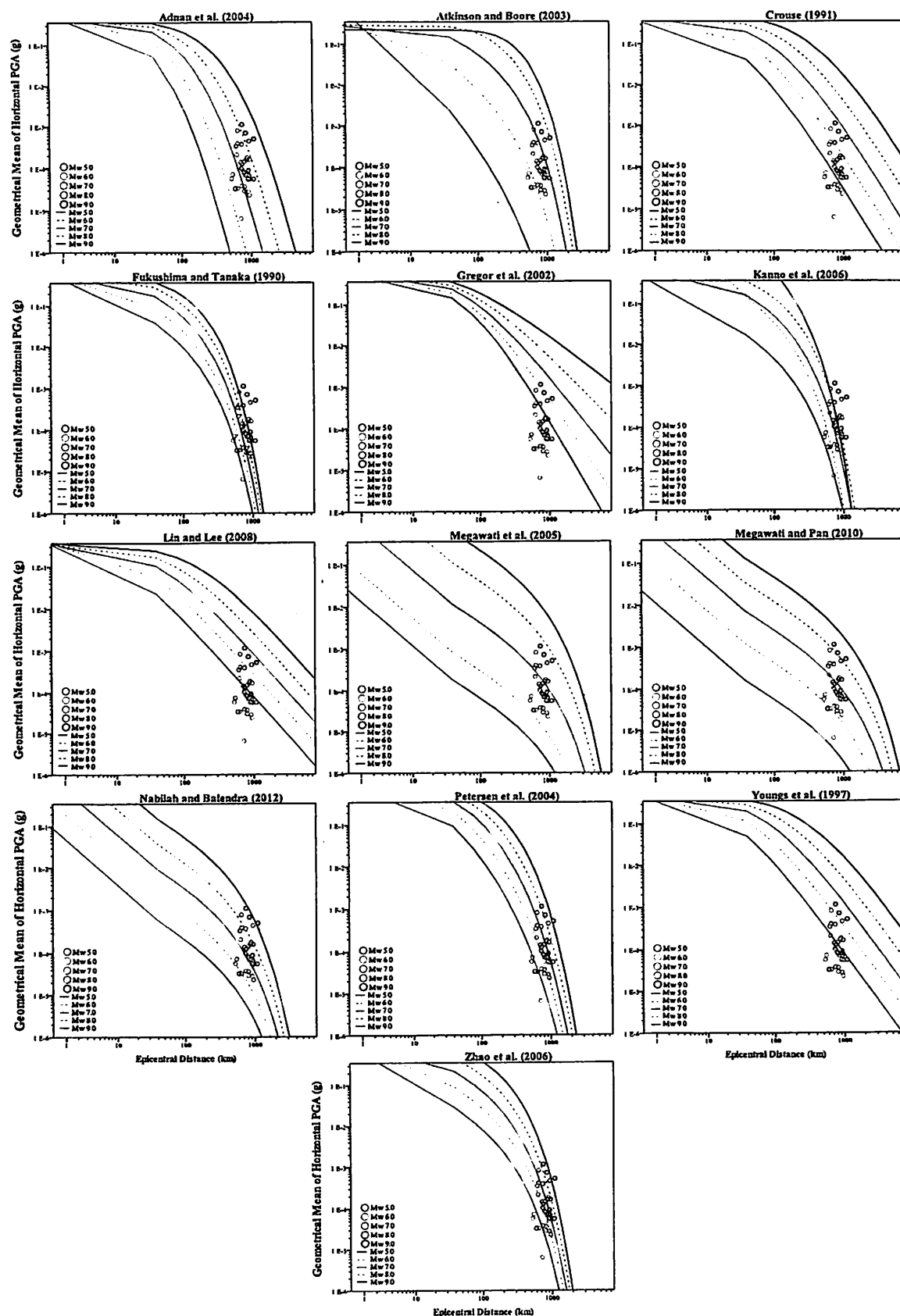
The comparisons of predicted attenuation curves of PGA and recorded PGA over epicentral distance were made. The actual ground motion records were grouped according to moment magnitude with 1.0 interval starting from  $M_w$  5.0 to  $M_w$  9.0 for plotting. Focal depth used for each group is the average of focal depth of events in respective magnitude groups. The comparisons have been made separately according to source mechanisms and site classes. This has resulted six groups of comparisons, namely: interface events on class C sites, interface events on class D sites, intraslab events on class C sites, intraslab events on class D sites, strike-slip events on class C sites and strike-slip events on class D sites.

Figure 8 illustrates plots of estimated PGA curves with actual records taken from seismic stations located on class C sites for interface subduction earthquakes. It can be seen that there are a few types of trend in the PGA prediction curves. First, Crouse (1991), Youngs et al. (1997), Gregor et al. (2002) and Lin and Lee (2008) deviated very much from the recorded ground motion data. Models like Atkinson and Boore (2003) and Megawati et al. (2005) tend to over-predict PGA at larger magnitude. There are also models that underestimated PGA at lower magnitude. Such models are Atkinson and Boore (2003), Adnan et al. (2004), Megawati et al. (2005), Megawati and Pan (2010) and Nabilah and Balendra (2012). It can be seen that Fukushima and Tanaka (1990), Petersen et al. (2004), Kanno et al. (2006) and Zhao et al. (2006) correspond to recorded data quite well and they have similar trends, that is having steeper drop at larger distance. However, Nabilah and Balendra (2012) has reasonably slower attenuation slope which makes it quite fit to the recorded ground motion, regardless of the underestimation of PGA at  $M_w$  5.0.

Figure 9 shows the attenuation curves established by 13 pre-selected subduction ground motion attenuation models and recorded PGA on class D sites for interface subduction earthquakes. Generally, the trend of the prediction curves for class D sites are similar to class C sites. However, Zhao et al. (2006) tends to give larger PGA estimation and deviated away from actual PGA collected on class D sites at large magnitude. Although Petersen et al. (2004) predicts better in class C site, it tends to overestimate PGA for class D site. In contrast, Nabilah and Balendra (2012) model seems to be more consistent in predicting PGA for class D sites. However, Fukushima and Tanaka (1990) and Kanno et al. (2006) produced curves fitter to the five magnitudes of data compared to the rest, despite the distance limitation.

Graphs plotted in Figs. 10 and 11 exhibit PGA curves estimated by models and scatter plot of actual ground motion records of intraslab events for class C sites and class D sites, respectively. Focal depth of intraslab events being considered in this study ranges from 81 to 576 km. However, average focal depth of events in each group of magnitude is used in the present study. Models that were developed mostly considering shallower foci depth exhibit only characteristics for interface events and might not be able to cater for intraslab events. From the graphs plotted for intraslab events and class C sites, such models are Gregor et al. (2002) and Megawati and Pan (2010). Both Gregor et al. (2002) and Megawati et al. (2005) models were derived to consider only interface earthquakes based on simulation of ground motion. This might be the reason for huge difference between





**Fig. 8** Comparison of attenuation curves and recorded PGA by seismic stations located on class C sites for interface subduction earthquakes



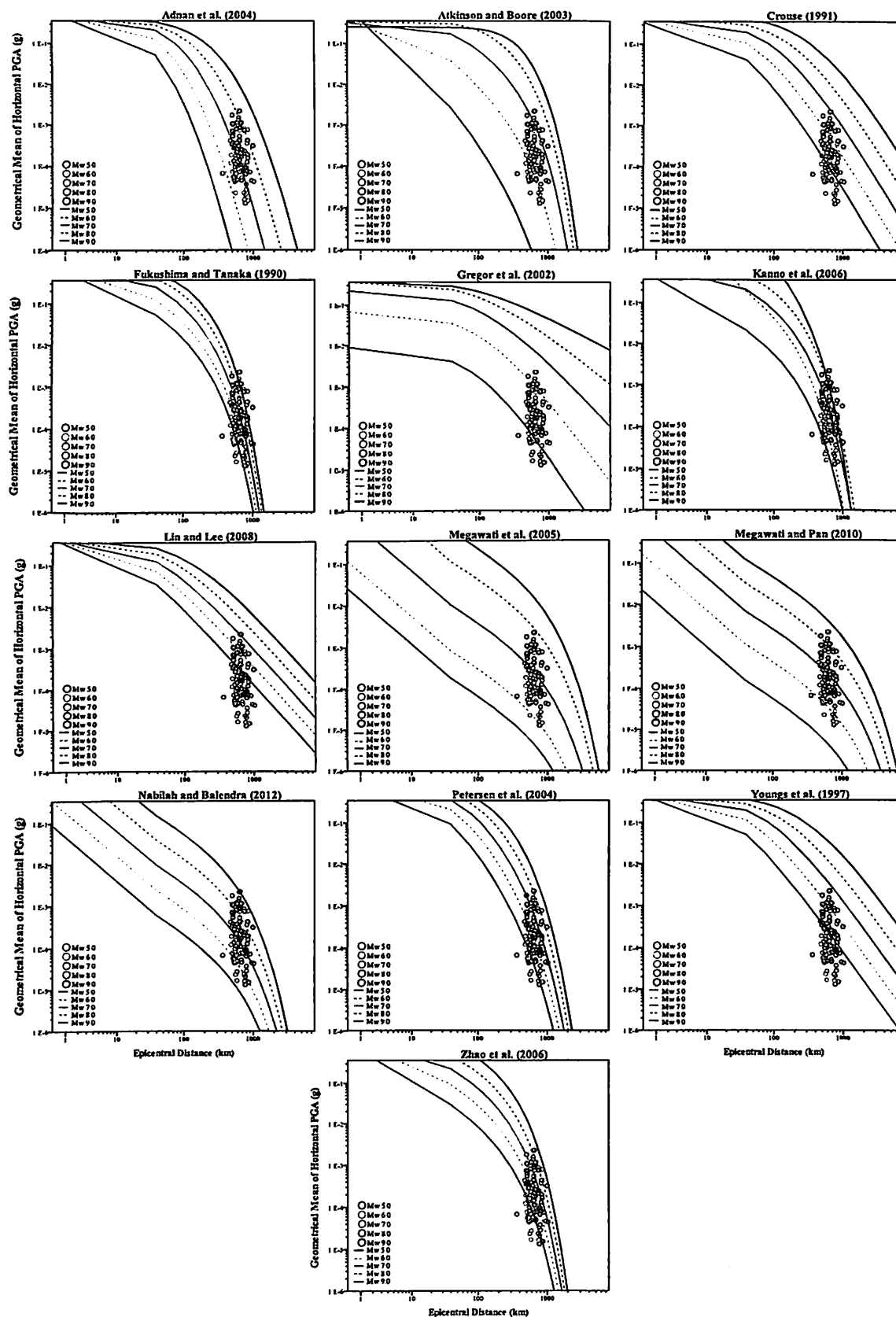


**Fig. 9** Comparison of attenuation curves and recorded PGA by seismic stations located on class D sites for interface subduction earthquakes

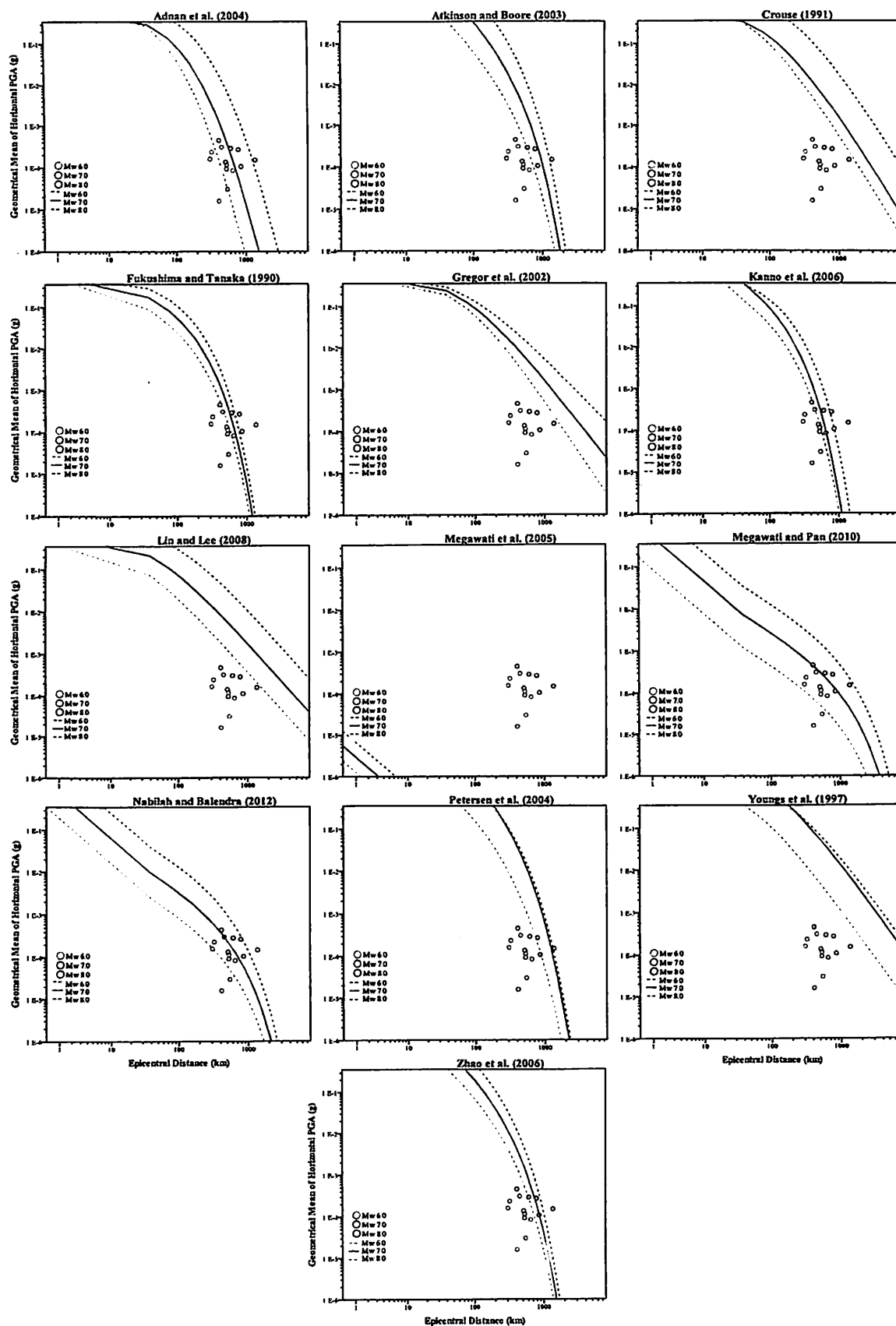


**Fig. 10** Comparison of attenuation curves and recorded PGA by seismic stations located on class C sites for intraslab subduction earthquakes

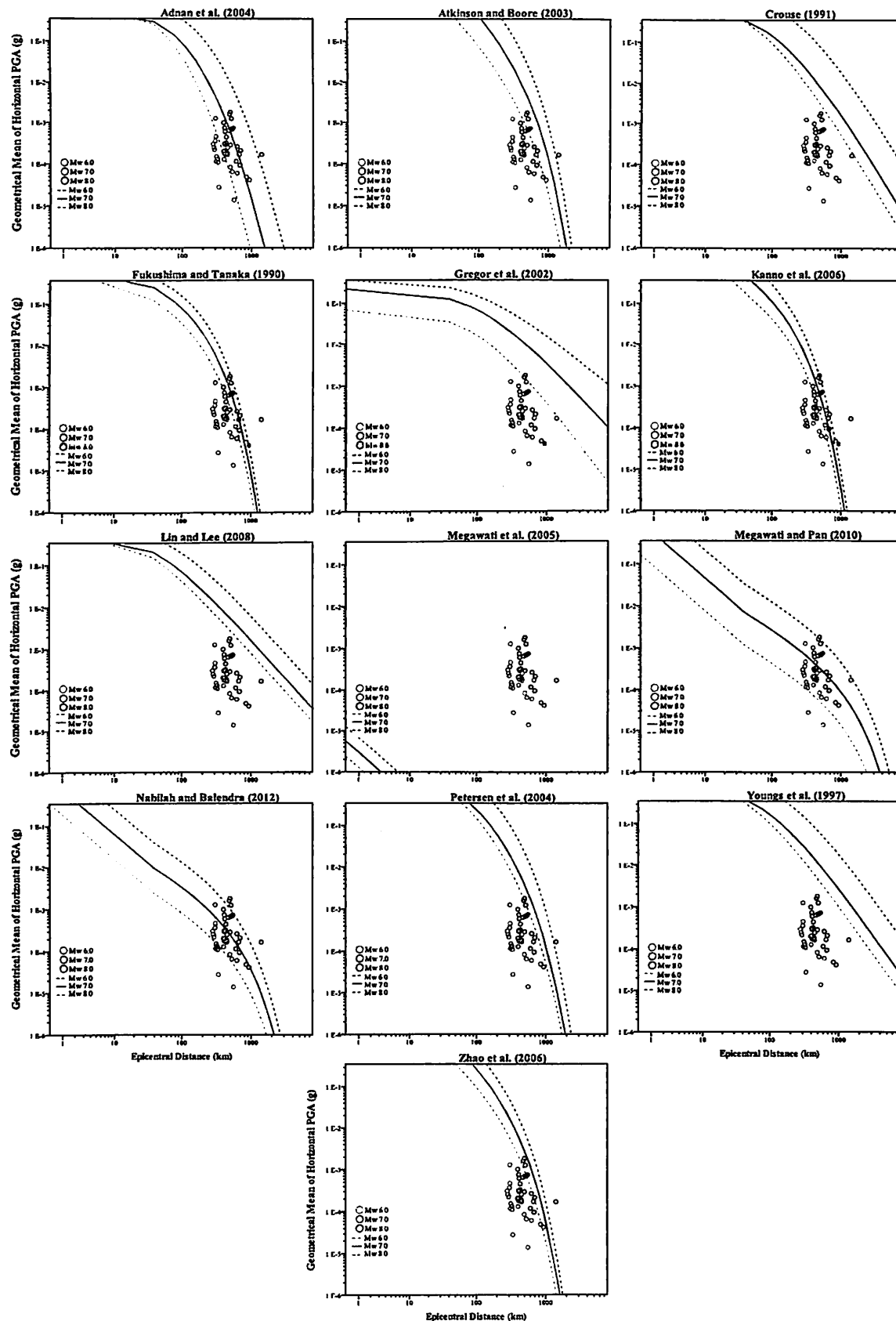


**Fig. 11** Comparison of attenuation curves and recorded PGA by seismic stations located on class D sites for intraslab subduction earthquakes

predictions from these two models and the actual records. Crouse (1991), Youngs et al. (1997) and Lin and Lee (2008) curves are seen having lower attenuation rate at large distance and constantly laying above recorded data compared to other attenuation models. This caused those models to over-predict PGA for intraslab events. In contrast, Fukushima and Tanaka (1990), Atkinson and Boore (2003), Adnan et al. (2004), Petersen et al. (2004), Kanno et al. (2006) and Zhao et al. (2006) curves have steeper attenuation at larger distance. However, Atkinson and Boore (2003) and Petersen et al. (2004) are slightly deviated from the recorded data compared to Fukushima and Tanaka (1990), Adnan et al. (2004), Kanno et al. (2006) and Zhao et al. (2006). Megawati and Pan (2010) and Nabilah and Balendra (2012) have similar trends of curve and fit better for all three magnitudes of data.

As an overall view in this set of graphs, prediction curves for class D sites are not much different from curves for class C sites. Nevertheless, Fukushima and Tanaka (1990) and Zhao et al. (2006) did not give prediction as fit as for class C site in predicting class D site. The two models tend to give higher prediction at  $M_W$  6.0 and  $M_W$  7.0. Megawati and Pan (2010) is also seen to be giving larger PGA for  $M_W$  8.0. However, Nabilah and Balendra (2012) model still estimates closely to actual PGA despite neglecting provision of equation for different soil classes.

On the whole, it can be seen that models developed for Cascadian subduction zone or global, such as Crouse (1991), Youngs et al. (1997), Gregor et al. (2002) and Atkinson and Boore (2003), tend to give higher prediction of PGA. This might be because the global data used in deriving those models could not describe the characteristic of subduction earthquakes originated from Sumatra. The locally derived Lin and Lee (2008), which predicts higher PGA compared to observed data from Peninsular Malaysia, is only suitable for Taiwan and Greece regions as stated by Beauval et al. (2012b). In contrast, all attenuation curves derived specifically for Japan seem to have similar trends to the actual data from Peninsular Malaysia. Such models are Fukushima and Tanaka (1990), Kanno et al. (2006) and Zhao et al. (2006). Magnitude–distance plot of distant Sumatra earthquakes seems to correspond to magnitude–distance plot of data used by Fukushima and Tanaka (1990), as shown in Fig. 12, for distance larger than 200 km in the magnitude range of 5–8. Magnitude–distance plot of Kanno et al. (2006) and Zhao et al. (2006) is incomparable to data in this study due to the short distance range of applicability of both models which is different from the longer distance range used in this study. Even so, the correspondence of Kanno et al. (2006) and Zhao et al. (2006) models to data from Peninsular Malaysia may be due to the abundance of Japanese data adopted in deriving those models which are more specific and similar in geological and geographical features to Peninsular Malaysia. Petersen et al. (2004), Megawati et al. (2005) and Megawati and Pan (2010) models were derived for Singapore and Peninsular Malaysia. Among these three models, Megawati et al. (2005) produces curves that deviate far from actual data for intraslab events. The model is derived based on simulation of shallow focal ground motion data and is not designed for intraslab events. Finally, the two models derived specifically for Peninsular Malaysia, namely Adnan et al. (2004) and Nabilah and Balendra (2012), seem to give reasonable correlation with the actual recorded data. However, the adoption of global data in deriving Adnan et al. (2004) leads to higher prediction at large magnitude and lower prediction at small magnitude compared to actual data. Nabilah and Balendra (2012) were derived using ground motion in Peninsular Malaysia; therefore, the model provides better fit for recorded PGA in Peninsular Malaysia.

Graphical presentations of shallow crustal attenuation curves together with scatter plot of actual records from strike-slip earthquakes are shown in Figs. 13 and 14 for class C and

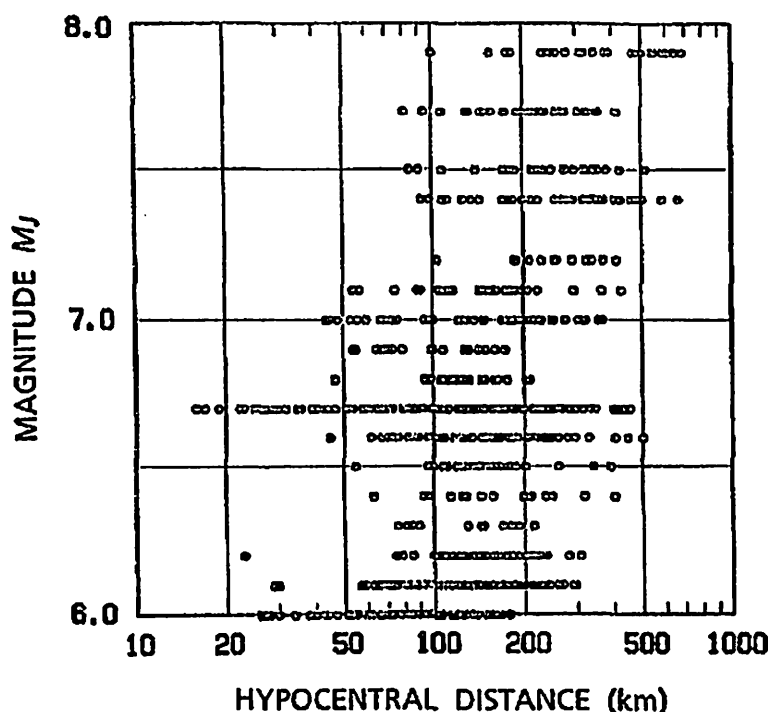


**Fig. 12** Magnitude–distance distribution of peak horizontal acceleration data observed in Japan that were utilised in the development of Fukushima and Tanaka (1990) ground motion attenuation model (Fukushima and Tanaka 1990)

class D sites, respectively. The scatter of actual PGA for both site classes portray almost vertical slope trend for all magnitudes. Thus, an attenuation model should have faster attenuation rate at larger distance in order to suit the trend of ground motion originating from strike-slip earthquakes for Peninsular Malaysia.

In models such as Abrahamson and Silva (1997), Campbell (2003), Boore et al. (1997), Boore (2005), Sadigh et al. (1997), Spudich et al. (1999) and Somerville et al. (2009), ground motion is assumed to be attenuated at slower rate once the waves travel beyond their defined near-source distance, regardless of the magnitude of the earthquake. On the other hand, models such as Frankel et al. (1996), Megawati et al. (2003), Atkinson and Boore (2006, 2011) and Pezeshk et al. (2011) illustrate a slight plateau after the cross point of short distance and long distance before a sudden steep drop of ground motion. On the other hand, the rest of the models, adopting other functional forms, showed dependencies of attenuation rate to magnitude of the earthquakes. Thus, the changes in slopes vary with distance at different magnitudes. The trend difference among these prediction curves is mainly due to the functional form of equation adopted in their derivations.

From the plotting of attenuation curves, Boore et al. (1997), Boore (2005) and Spudich et al. (1999) has slow attenuation rate and deviate greatly from actual PGA. Abrahamson and Silva (1997) and Ambraseys et al. (2005) generate curves that diverge for different magnitude as the distance increase. This is because these two models are magnitude-dependent models and were derived to give slower attenuation for higher magnitude. Campbell (2003) has constant attenuation rate for different magnitude, except for  $M_w$  9.0. Applicability of Campbell (2003) only lies within a magnitude constraint of  $M_w$  5.0 to  $M_w$  8.2. Nonetheless, the model trend could not fit the recorded data for magnitude that lies out of its applicability range. The rest of the models show steeper attenuation curve and

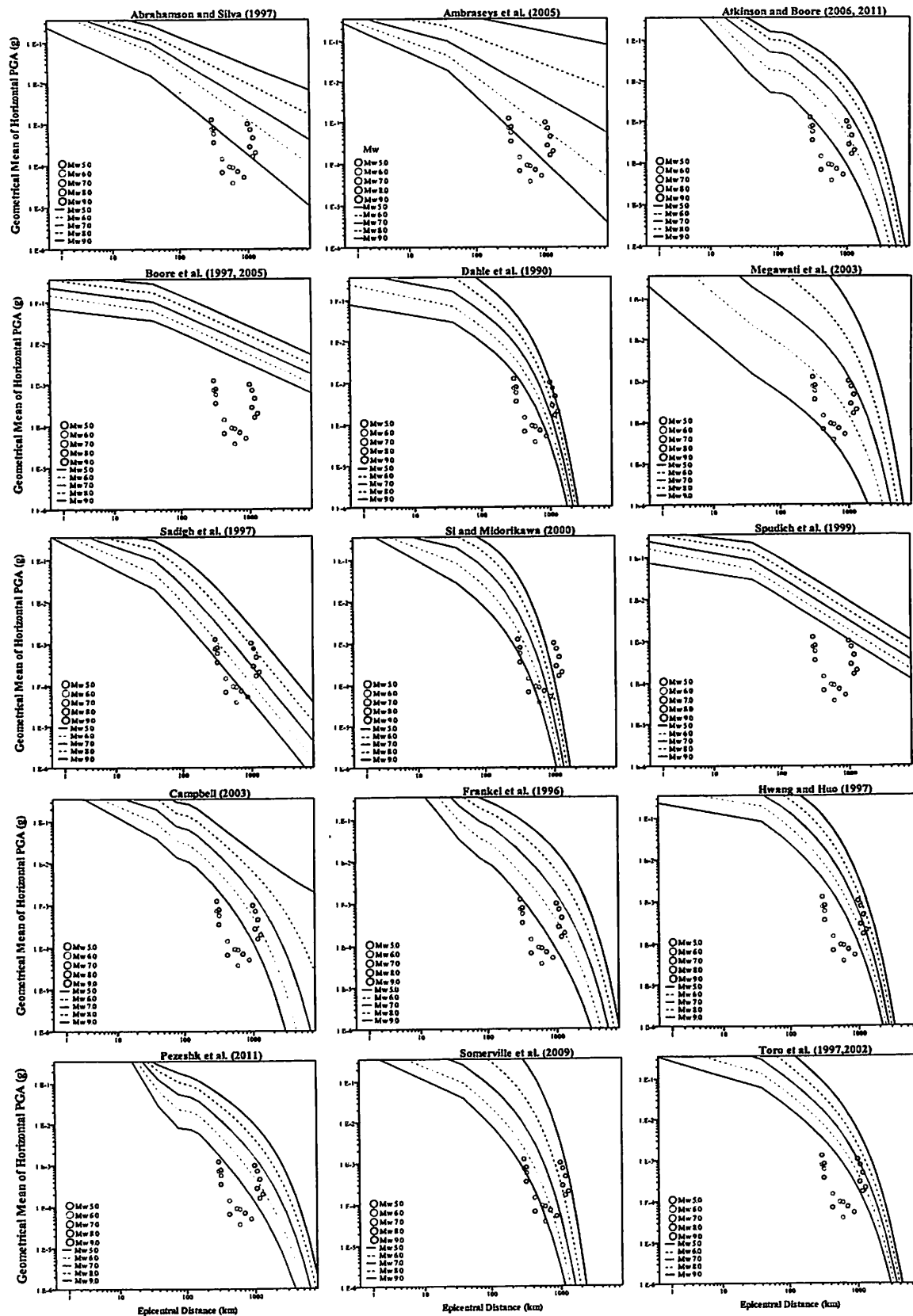


**Fig. 13** Comparison of attenuation curves and recorded PGA by seismic stations located on class C sites for strike-slip earthquakes

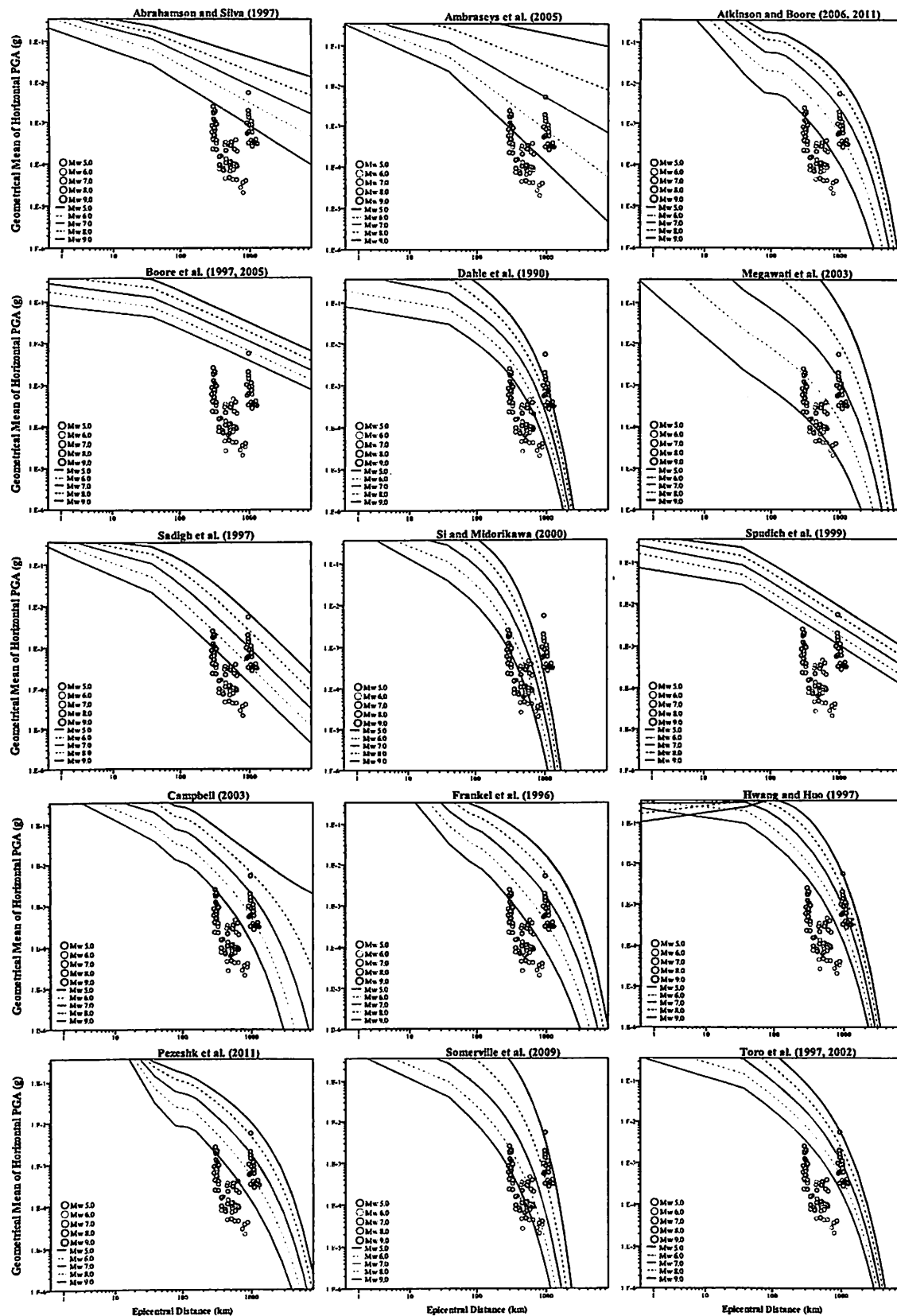


**Fig. 14** Comparison of attenuation curves and recorded PGA by seismic stations located on class D sites for strike-slip earthquakes

converging as the distance increases. Even so, only Somerville et al. (2009) and Si and Midorikawa (2000) correspond quite well to the actual records for both site classes. Comparison of magnitude–distance plots of both Somerville et al. (2009) and Si and Midorikawa (2000) to magnitude–distance plot in this study is not possible due to different ranges of distance considered and that Somerville et al. (2009) is derived stochastically.

In addition to the graphical presentation on PGA predictions by models, root-mean-squared error (RMSE) was also computed to quantify the goodness of fit for predicted and actual PGA as shown in Tables 3 and 4. Smaller RMSE value represents better estimation to actual records and vice versa. The RMSE has been normalised into the range of observed ground motion. These computed  $RMSE_{Nor}$  values were found agreeing well with plots of attenuation curves. Among subduction earthquake ground motion attenuation models, Nabilah and Balendra (2012) model provides the lowest overall  $RMSE_{Nor}$  for both interface and intraslab events. Fukushima and Tanaka (1990) also predicts rather well for interface earthquakes, while Megawati and Pan (2010) give second lower  $RMSE_{Nor}$  value for intraslab, after Nabilah and Balendra (2012). The lowest computed  $RMSE_{Nor}$  value for strike-slip earthquakes is provided by Somerville et al. (2009), following Si and Midorikawa (2000) yielding the second lowest  $RMSE_{Nor}$  value and Sadigh et al. (1997) the third lowest  $RMSE_{Nor}$  value.

In general, ground motion attenuation models that were developed for specific regions, especially Japan, are found to be producing trend that correspond well with the recorded field ground motion records. Global-based attenuation models, which were developed using worldwide events and ground motion data, tend to yield larger ground motion compared to recorded data in Peninsular Malaysia. Ground motion data in Peninsular

**Table 3** Summary of computed normalised root-mean-squared error ( $RMSE_{Nor}$ ) for subduction earthquake ground motion attenuation models

Models	$RMSE_{Nor}$					
	Interface Class C	Interface Class D	Intraslab Class C	Intraslab Class D	Overall interface	Overall intraslab
Fukushima and Tanaka (1990)	0.045	0.341	0.167	0.445	0.193	0.306
Crouse (1991)	2.292	4.125	27.212	50.355	3.208	38.783
Youngs et al. (1997)	2.327	3.987	13.917	23.279	3.157	18.598
Gregor et al. (2002)	2.469	7.855	2.087	4.513	5.162	3.300
Atkinson and Boore (2003)	0.936	3.090	0.746	1.866	2.013	1.306
Adnan et al. (2004)	0.339	1.008	0.111	0.388	0.674	0.250
Petersen et al. (2004)	0.279	1.028	1.841	7.291	0.653	4.566
Megawati et al. (2005)	0.849	1.641	0.104	0.292	1.245	0.198
Kanno et al. (2006)	0.075	0.528	0.145	0.375	0.302	0.260
Zhao et al. (2006)	0.223	0.889	0.553	1.040	0.556	0.796
Lin and Lee (2008)	1.225	1.840	9.874	4.641	1.532	7.257
Megawati and Pan (2010)	0.249	0.429	0.080	0.157	0.339	0.119
Nabilah and Balendra (2012)	0.110	0.253	0.049	0.164	0.182	0.107



**Table 4** Summary of computed normalised root-mean-squared error (RMSE<sub>Nor</sub>) for strike-slip earthquake ground motion attenuation models

Models	RMSE <sub>Nor</sub>		
	Class C	Class D	Overall
<i>Active tectonic region</i>			
Si and Midorikawa (2000)	0.057	0.132	0.094
Megawati et al. (2003)	1.439	1.785	1.612
Ambraseys et al. (2005)	4.270	5.452	4.861
Abrahamson and Silva (1997)	4.124	5.839	4.981
Sadigh et al. (1997)	0.087	0.309	0.198
Spudich et al. (1999)	0.556	0.783	0.670
Dahle et al. (1990)	0.288	0.379	0.334
Atkinson and Boore (2006)	0.591	0.834	0.713
Boore et al. (1997)	2.072	2.673	2.372
<i>Stable continental region</i>			
Campbell (2003)	0.832	0.938	0.885
Hwang and Huo (1997)	0.321	0.532	0.426
Toro et al. (1997)	0.387	0.519	0.453
Pezeshk et al. (2011)	0.516	0.598	0.557
Frankel et al. (1996)	0.673	0.795	0.734
Somerville et al. (2009)	0.045	0.110	0.077

Malaysia are predominantly attenuated due to the long propagation distance and thus have different characteristics compared to the worldwide strong ground motion data utilised for development of global-based model. For non-subduction regions, ground motion attenuation models for stable continental regions showed small deviation from the actual recorded data used in this study compared to models for active tectonic regions. Models for stable continental regions have broader range of applicability. Therefore, they are more suitable in predicting the long distance and weak ground motion.

## 8 Conclusion

The aim of this paper is to select a ground motion attenuation model that is able to predict ground motion in Peninsular Malaysia which resulted from distant earthquake from Sumatra zone. Among the pre-selected models, Nabilah and Balendra (2012) model appears to be the model that produce best fit to the interface and intraslab subduction events originated from Sumatra subduction zone. Meanwhile, the suitable attenuation models for estimating ground motion in Peninsular Malaysia due to distant strike-slip events include Si and Midorikawa (2000) and Somerville et al. (2009).

Most of the attenuation models being considered in this paper did not use data as narrow distant as Peninsular Malaysia data. Thus, the proposed best fit models in this paper are only applicable for long-distance earthquakes and might not be suitable for data with closer distance. The validation of proposed attenuation models to short-distance earthquakes is not included as it is out of the scope of study. However, the correspondence of magnitude–distance distribution of Japanese models to Peninsular Malaysia is noteworthy for the

evaluation of short-distance data surrounding Sumatra using Japanese models in future study.

The current study is only limited to comparison of peak acceleration. An extended study to evaluation of response spectral acceleration should be conducted in the future to enhance the consistency of the result. In addition, some of the models used in this paper may have been superseded by more recent publications such as 2014 NGA West 2 models. The results of this study should be revised with more updated models and more available ground motion data in future studies.

**Acknowledgments** The authors wish to express their deepest appreciation to Universiti Sains Malaysia for funding this research via a RU Grant (1001/PAWAM/814179). Credits are also extended to Malaysian Meteorological Department for providing seismological and ground motion data required for the analysis. Special thanks are also dedicated to Dr. Tan Chee Ghuan for his consultation and guidance in the conduction of multi-channel analysis of surface waves (MASW) in this study.

## References

- Abrahamson N, Silva W (1997) Empirical response spectral attenuation relations for shallow crustal earthquakes. *Seismol Res Lett* 68:94–127
- Adnan A, Hendriyawan, Marto A, Irsyam M (2004) Selection and development of appropriate attenuation relationship for Peninsular Malaysia. In: Paper presented at the Malaysian Science and Technology Congress 2004 (MSTC 2004), Cititel Hotel, Midvalley Kuala Lumpur, 18–20 April 2005
- Adnan A, Zaini Sooria S, Sawada S, Goto H (2010) An investigation of the attenuation characteristics of distant ground motions in Peninsular Malaysia by comparing values of recorded with estimated PGA and PGV. *Malays J Civil Eng* 2:38–52
- Adnan A, Tiong PLY, Chow YE (2012) Usability of the next generation attenuation equations for seismic hazard assessment in Malaysia. *Int J Eng Res Appl (IJERA)* 2:639–644
- Allen T (2010) The influence of attenuation in earthquake ground-motion and magnitude estimation: implications for Australian earthquake hazard. In: Proceedings of the 2010 Australian Earthquake Engineering Society Conference, Perth, Western Australia, 2010
- Ambraseys N, Douglas J, Sarma S, Smit P (2005) Equations for the estimation of strong ground motions from shallow crustal earthquakes using data from Europe and the Middle East: horizontal peak ground acceleration and spectral acceleration. *Bull Earthq Eng* 3:1–53
- Atkinson GM, Boore DM (2003) Empirical ground-motion relations for subduction-zone earthquakes and their application to Cascadia and other regions. *Bull Seismol Soc Am* 93:1703–1729
- Atkinson GM, Boore DM (2006) Earthquake ground-motion prediction equations for eastern North America. *Bull Seismol Soc Am* 96:2181–2205
- Atkinson GM, Boore DM (2011) Modifications to existing ground-motion prediction equations in light of new data. *Bull Seismol Soc Am* 101:1121–1135
- Azizan NZBN (2012) Building performance with different bedrock response spectrum. Universiti Teknologi Malaysia
- Beauval C, Tasan H, Laurendeau A, Delavaud E, Cotton F, Guéguen P, Kuehn N (2012a) On the testing of ground-motion prediction equations against small-magnitude data. *Bull Seismol Soc Am* 102:1994–2007
- Beauval C et al (2012b) Regional differences in subduction ground motions. In: World conference on earthquake engineering proceedings 2012, Portugal
- Boore DM (2005) Equations for estimating horizontal response spectra and peak acceleration from western North American earthquakes: a summary of recent work (Erratum). *Seismol Res Lett* 76:368–369
- Boore DM, Joyner WB, Fumal TE (1993) Estimation of response spectra and peak accelerations from western North American earthquakes: an interim report. US geological survey open-file report 93–509
- Boore DM, Joyner WB, Fumal TE (1997) Equations for estimating horizontal response spectra and peak acceleration from western North American earthquakes: a summary of recent work. *Seismol Res Lett* 68:128–153
- Bozorgnia Y, Campbell KW, Niazi M (2000) Observed spectral characteristics of vertical ground motion recorded during worldwide earthquakes from 1957 to 1995. In: Proceedings of the 12th world conference on earthquake engineering, 2000. vol 4. New Zealand

- Brune JN, Anooshehpour A (1999) Dynamic geometrical effects on strong ground motion in a normal fault model. *J Geophys Res Solid Earth* 104:809–815
- Campbell KW (2003) Prediction of strong ground motion using the hybrid empirical method and its use in the development of ground-motion (attenuation) relations in eastern North America. *Bull Seismol Soc Am* 93:1012–1033
- Campbell KW (2004) Prediction of strong ground motion using the hybrid empirical method and its use in the development of ground-motion (attenuation) relations in Eastern North America—Erratum. *Bull Seismol Soc Am* 93:1
- Chintanapakdee C, Naguit M, Charoenyuth M (2008) Suitable attenuation model for Thailand. In: Proceedings 14th world conference on earthquake engineering, Beijing, China, 12–17 October 2008
- Cotton F, Scherbaum F, Bommer JJ, Bungum H (2006) Criteria for selecting and adjusting ground-motion models for specific target regions: application to Central Europe and rock sites. *J Seismolog* 10:137–156
- Crouse C (1991) Ground-motion attenuation equations for earthquakes on the Cascadia subduction zone. *Earthq Spectra* 7:201–236
- Dahle A, Bungum H, Kvamme LB (1990) Attenuation models inferred from intraplate earthquake recordings. *Earthq Eng Struct Dynam* 19:1125–1141
- Douglas J (2011) Ground-motion prediction equations 1964–2010. Pacific Earthquake Engineering Research Center College of Engineering University of California, Berkeley: Bureau de Recherches Géologiques et Minières (BRGM)
- Douglas J, Cotton F, Di Alessandro C, Boore DM, Abrahamson N, Akkar S (2012) Compilation and critical review of GMPEs for the GEM-PEER Global GMPEs Project. In: Proceedings of the 15th world conference on earthquake engineering 2012, Lisbonne, Portugal
- Frankel AD et al (1996) National seismic-hazard maps: documentation June 1996. US Geological Survey
- Fukushima Y, Tanaka T (1990) A new attenuation relation for peak horizontal acceleration of strong earthquake ground motion in Japan. *Bull Seismol Soc Am* 80:757–783
- Gregor NJ, Silva WJ, Wong IG, Youngs RR (2002) Ground-motion attenuation relationships for Cascadia subduction zone megathrust earthquakes based on a stochastic finite-fault model. *Bull Seismol Soc Am* 92:1923–1932
- Hayes GP et al (2013) Seismicity of the Earth 1900–2012—Sumatra and Vicinity. U.S Geological Survey
- Hwang H, Huo J-R (1997) Attenuation relations of ground motion for rock and soil sites in eastern United States. *Soil Dyn Earthq Eng* 16:363–372
- Kanno T, Narita A, Morikawa N, Fujiwara H, Fukushima Y (2006) A new attenuation relation for strong ground motion in Japan based on recorded data. *Bull Seismol Soc Am* 96:879–897
- Lau TL, Majid TA, Choong KK, Zaini SS (2005) Public awareness on earthquake and tsunami survey in Penang. Vol. September 2005. Institute of Engineers Malaysia (IEM)
- Lay T et al (2005) The great Sumatra–Andaman earthquake of 26 December 2004. *Science* 308:1127–1133
- Lee WH, Jennings P, Kisslinger C, Kanamori H (2002) International handbook of earthquake & engineering seismology, vol. 81. Academic Press, London
- Lin P-S, Lee C-T (2008) Ground-motion attenuation relationships for subduction-zone earthquakes in northeastern Taiwan. *Bull Seismol Soc Am* 98:220–240
- McCaffrey R (2009) The tectonic framework of the Sumatran subduction zone. *Annu Rev Earth Planet Sci* 37:345–366
- Megawati K, Pan TC (2010) Ground-motion attenuation relationship for the Sumatran megathrust earthquakes. *Earthq Eng Struct Dynam* 39:827–845
- Megawati K, Pan TC, Koketsu K (2003) Response spectral attenuation relationships for Singapore and the Malay Peninsula due to distant Sumatran-fault earthquakes. *Earthq Eng Struct Dynam* 32:2241–2265
- Megawati K, Pan TC, Koketsu K (2005) Response spectral attenuation relationships for Sumatran-subduction earthquakes and the seismic hazard implications to Singapore and Kuala Lumpur. *Soil Dynam Earthq Eng* 25:11–25
- Nabilah A, Balendra T (2012) Seismic hazard analysis for Kuala Lumpur, Malaysia. *J Earthq Eng* 16(7):1076–1094
- Naguit ME (2007) Estimation of probable earthquake ground motions in Bangkok. Department of Civil Engineering, Faculty of Engineering, Chulalongkorn University, Bangkok
- Newcomb KR, McCann WR (1987) Seismic history and seismotectonics of the Sunda Arc. *J Geophys Res* 92(B1):421–439
- Oglesby DD, Archuleta RJ, Nielsen SB (1998) Earthquakes on dipping faults: the effects of broken symmetry. *Science* 280:1055–1059
- Pappin JW, Yim PHI, Koo CHR (2011) An approach for seismic design in Malaysia following the principles of Eurocode 8. Vol October 2011. Institute of Engineers Malaysia (IEM)

- Petersen MD, Dewey J, Hartzell S, Mueller C, Harmsen S, Frankel A, Rukstales K (2004) Probabilistic seismic hazard analysis for Sumatra, Indonesia and across the Southern Malaysian Peninsula. *Tectonophysics* 390:141–158
- Pezeshk S, Zandieh A, Tavakoli B (2011) Hybrid empirical ground-motion prediction equations for eastern North America using NGA models and updated seismological parameters. *Bull Seismol Soc Am* 101:1859–1870
- Sadigh K, Chang C-Y, Egan J, Makdisi F, Youngs R (1997) Attenuation relationships for shallow crustal earthquakes based on California strong motion data. *Seismol Res Lett* 68:180–189
- Si H, Midorikawa S (2000) New attenuation relations for peak ground acceleration and velocity considering effects of fault type and site condition. In: *Proceedings of twelfth world conference on earthquake engineering*
- Sieh K, Natawidjaja D (2000) Neotectonics of the Sumatran fault, Indonesia. *J Geophys Res Solid Earth* 105:28295–28326
- Sieh K, Ward SN, Natawidjaja D, Suwargadi BW (1999) Crustal deformation at the Sumatran subduction zone revealed by coral rings. *Geophys Res Lett* 26:3141–3144
- Somerville P, Graves R, Collins N, Song SG, Ni S, Cummins P (2009) Source and ground motion models for Australian earthquakes. In: *Proceedings of 2009 annual conference of Australian Earthquake Engineering Society*
- Spudich P, Joyner W, Lindh A, Boore D, Margaris B, Fletcher J (1999) SEA99: a revised ground motion prediction relation for use in extensional tectonic regimes. *Bull Seismol Soc Am* 89:1156–1170
- Toro GR, Abrahamson NA, Schneider JF (1997) Model of strong ground motions from earthquakes in central and eastern North America: best estimates and uncertainties. *Seismol Res Lett* 68:41–57
- Weller O, Lange D, Tilmann F, Natawidjaja D, Rietbrock A, Collings R, Gregory L (2012) The structure of the Sumatran Fault revealed by local seismicity. *Geophys Res Lett* 39:1–7
- Xu Y, Xia J, Miller RD (2006) Quantitative estimation of minimum offset for multichannel surface-wave survey with actively exciting source. *J Appl Geophys* 59:117–125
- Yeneir E, Erdogan O, Akkar S (2008) Empirical relationships for magnitude and source-to-site distance conversions using recently compiled Turkish strong-ground motion database. In: *Proceedings 14th world conference on earthquake engineering, Beijing, China, 12–17 October 2008*
- Youngs R, Chiou S-J, Silva W, Humphrey J (1997) Strong ground motion attenuation relationships for subduction zone earthquakes. *Seismol Res Lett* 68:58–73
- Zhao JX et al (2006) Attenuation relations of strong ground motion in Japan using site classification based on predominant period. *Bull Seismol Soc Am* 96:898–913

## **Modification of Published Prediction Model of Ground Motion Due to Sumatra Subduction Earthquakes for the Application in Peninsular Malaysia**

Tze Che, Van<sup>1,a\*</sup>, Tze Liang, Lau<sup>2,b</sup>, Taksiah A. Majid<sup>3,c</sup>,  
Kok Keong, Choong<sup>4,d</sup> and Fadzli Mohamed Nazri<sup>5,e</sup>

<sup>1,2,3,4,5</sup>School of Civil Engineering, Universiti Sains Malaysia, Penang, Malaysia

<sup>a</sup>cathvan\_911@hotmail.com, <sup>b</sup>celau@usm.my, <sup>c</sup>taksiah@usm.my, <sup>d</sup>cekkc@usm.my,  
<sup>e</sup>cefmn@usm.my

**Keywords:** Ground motion prediction model, Sumatra subduction zone, earthquakes, peak ground acceleration, intraslab, interface

### **Abstract**

Establishment of ground motion prediction model that is able to accurately predict ground motion for Peninsular Malaysia is always a challenge to local researchers due to the paucity of strong ground motion data. In this study, Fukushima and Tanaka (1990) model which was identified as the best prediction model in estimating ground motion in Peninsular Malaysia due to earthquakes originated from Sumatra subduction zone in previous study was modified in order to enhance its performance. Multiple regression analysis was conducted based on supplementation of 212 seismograms, which were produced by 32 subduction events ranging from Mw 5.2 to 9.1 from Sumatra. The modified Fukushima and Tanaka model is expected to perform well in estimating ground motion from NEHRP Class C and D in the distance range of 300 to 1200 km. The appropriateness of the modified model was verified with actual ground motion in Peninsular Malaysia and also through comparison with other published models that are popular in the region.

### **Introduction**

Sumatra subduction zone is one of the seismically active tectonic boundaries in the world. The Sumatra subduction zone has larger destructive potential compare to its neighbouring Sumatra strike-slip fault due to their ability to produce megathrust earthquakes. Among those deadliest historical events are Aceh earthquake (M<sub>w</sub> 9.1), Nias earthquake (M<sub>w</sub> 8.6), 1833 Bengkulu earthquake (M<sub>w</sub> 8.75), 1861 event (M<sub>w</sub> 8.4) and 2007 event (M<sub>w</sub> 8.4). Although Peninsular Malaysia sits on the stable Sunda plate with more than 300 km away from the Sumatra subduction zone, the tremors from the zone, although largely attenuated, often disturbed inhabitants in the peninsular, especially west coastal area. Added up with no practice of seismic resistant design for most of the buildings in Peninsular Malaysia, the seismic risk cannot be ignored. In this case, a development of a robust ground motion prediction model is essential as part of exhaustive seismic hazard assessment. An attenuation model expresses, in mathematical way, the relationship of earthquake source parameters and ground motion parameters [1].

This article aims to study the previous researches on adoption of ground motion prediction equations (GMPE) developed in Peninsular Malaysia and subsequently, modification of published GMPE to better fit far-field ground motions for Peninsular Malaysia subjected to earthquakes from Sumatra subduction zone.

### **Previous studies on GMPE in Peninsular Malaysia**

A few attenuation models have been developed to predict ground motions for Peninsular Malaysia. A model predicting ground motion from subduction earthquakes for Peninsular Malaysia had been developed [2]. In the same year, [3] model had been modified to cover distance beyond 200 km for the application in Singapore and southern Peninsular Malaysia [4]. In year 2005, a

stochastic attenuation model [5] was proposed for Singapore and Kuala Lumpur. In 2012, a simple empirical model to estimate ground motions for Kuala Lumpur had been derived [6].

Comparison and evaluation of ground motion attenuation models from other regions had been conducted for the applicability in Peninsular Malaysia [7,8,9]. Though so, these studies resulted in various proposals of GMPE to be used in the region. However, a comprehensive evaluation of GMPE for Peninsular Malaysia conducted by [10] found that [11] and [6] are best in representing actual PGA in Peninsular Malaysia. The [11] model attenuates slower at shorter distance and provide steeper attenuation curve at distance beyond 40km which correspond quite well with the PGA collected from Peninsular Malaysia. Thus, [11] model has been selected as the basic form to be modified in this study in order to improve its performance by reducing the deviation of its predictions. Table 1 shows models and respective notations that are to be used throughout the paper.

Table 1 Models and respective notations in this paper

Model	Notation
Fukushima and Tanaka (1990)[11]	FT90
Petersen et al. (2004)[4]	PT04
Nabilah and Balendra (2012)[6]	NB12

### Collection of datasets

In order to modify the FT90, far-field seismograms are required to extend the coverage of the model to larger distance and in this case, far-field seismograms from Peninsular Malaysia are used. Seismic data utilised in this study is recorded from 19 three-component and real time stations located within Peninsular Malaysia and is provided by Malaysian Meteorology Department. According to previous study [9], seismic stations within Peninsular Malaysia fall into NEHRP Class C and NEHRP Class D. Catalogues from international open-access databases were used for compilation to reduce informational error in selected earthquake events. Such catalogues are United States Geological Survey (USGS) database, International Seismological Centre (ISC) database and National Earthquake Information Center (NEIC) database. A total of 32 recorded distant earthquakes originated from Sumatra zone with 212 seismograms were selected from records between July 2004 and July 2012.

As subduction events are the main interest in this paper, source mechanism of recorded distant events has to be studied by the supplemented moment tensor solutions provided by Global Centroid Moment Tensor (GCMT) and National Earthquake Information Centre (NEIC). As a result, a total of 25 events were identified to be interface earthquakes while the rest are intraslab earthquakes. Fig.1 shows the magnitude-distance distribution plot of datasets in this study.

### Regression model

FT90 model is represented by the following equation:

$$\log_{10}(y) = C_1 M_S - \log_{10}[R + C_2 (10^{C_1 M_S})] - C_3 R + C_4 \quad (1)$$

where,  $y$  is the mean horizontal peak ground acceleration (PGA) in units of  $\text{cm/sec}^2$ ,  $M_S$  is the surface-wave magnitude and  $R$  is the shortest distance between site to fault rupture in km. The standard deviation of the model is 0.21. The coefficients ( $C_1$ ,  $C_2$ ,  $C_3$  and  $C_4$ ) are derived from regression analysis, and thus resulting the final equation as shown in Eq. 2.

$$\log_{10}(y) = 0.41 M_S - \log_{10}[R + 0.032(10^{0.41 M_S})] - 0.0034 R + 1.30 \quad (2)$$

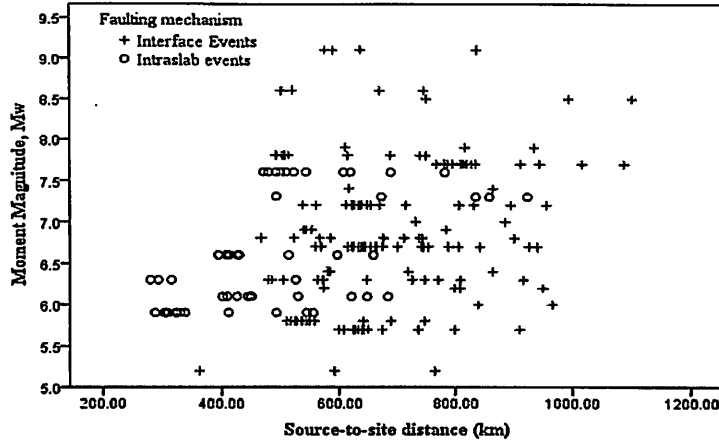


Fig. 1 Magnitude-distance distribution plot of utilised datasets for derivation of a new GMPE

This model is valid for shallow earthquakes with focal depth of up to 100 km and distance range between 10 and 300 km. The FT90 model was modified in the following way. Geometrical mean of two horizontal PGA were calculated from collected seismograms. The calculated geometrical mean of two horizontal PGA components ranges from 0.006867 gal to 2.1582 gal. Multiple regression analysis was constructed by constraining the distance coefficient,  $C_2$  and constant  $C_4$  to remain the near-field attenuation characteristics and prevent unrealistic low prediction at near distance. In this study, only the steepness of attenuation curves at longer distance were modified to fit the ground motion data in Peninsular Malaysia. Eq. 3 and Eq. 4 shows the resulting relationships for interface earthquakes and intraslab earthquakes, respectively.

$$\log_{10}(y) = 0.35M_w - \log_{10}[R + 0.032(10^{0.35M_w})] - 0.0028R + 1.30 \quad (3)$$

$$\log_{10}(y) = 0.35M_w - \log_{10}[R + 0.032(10^{0.35M_w})] - 0.003057R + 1.30 \quad (4)$$

where, PGA is in gal,  $M_w$  is the surface-wave magnitude and  $R$  is the source-to-site distance in km. The standard deviation of the Eq. 3 and Eq. 4 are 0.277 and 0.347, respectively.

### Validation of modified GMPE

Validation has been conducted for the modified GMPE by plotting it with the scatter of actual ground motion in Peninsular Malaysia, which originated from Sumatra subduction zone. Fig. 2 exhibits the curves of modified GMPE fits actual data quite well. However, the modified GMPE predict PGA larger than actual PGA for Mw 6.0 of intraslab events.

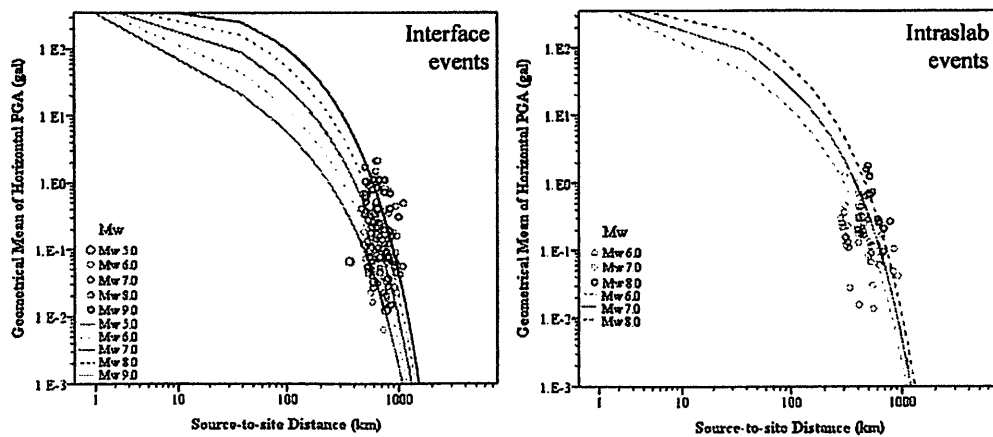


Fig. 2 Plot of modified GMPE curves and recorded PGA by seismic stations in Peninsular Malaysia

The modified GMPE was also compared with other GMPE's for this region, namely PT04 model and NB12 model. FT90 model was also included in the validation in order to evaluate the improvement of the modified GMPE. From Fig. 3, it can be seen that the curves of the modified GMPE correspond quite well to the trend of PGA from selected interface events. However, the modified GMPE seems to slightly under-predicts PGA for Mw 6.7 event. Though so, around 89 percentage of the data for selected events lies within the allowance of  $\pm 2$  standard deviation of the modified GMPE. The PT04 model seems to be only able to yield good prediction for Mw 6.7 event and more likely to over-predicts for other events. On the other hand, NB12 model predicts PGA in correspondence to recorded PGA for most of the events except Mw 9.1. Nevertheless, the gradient of the curves of NB12 model are gentler than the rest of the models which denoting unrealistic prediction as the distance decreases which could lead to extreme under-prediction. PGA prediction in short distance by NB12 model is lower compare to other existing GMPE for active subduction zone such as [3,10].

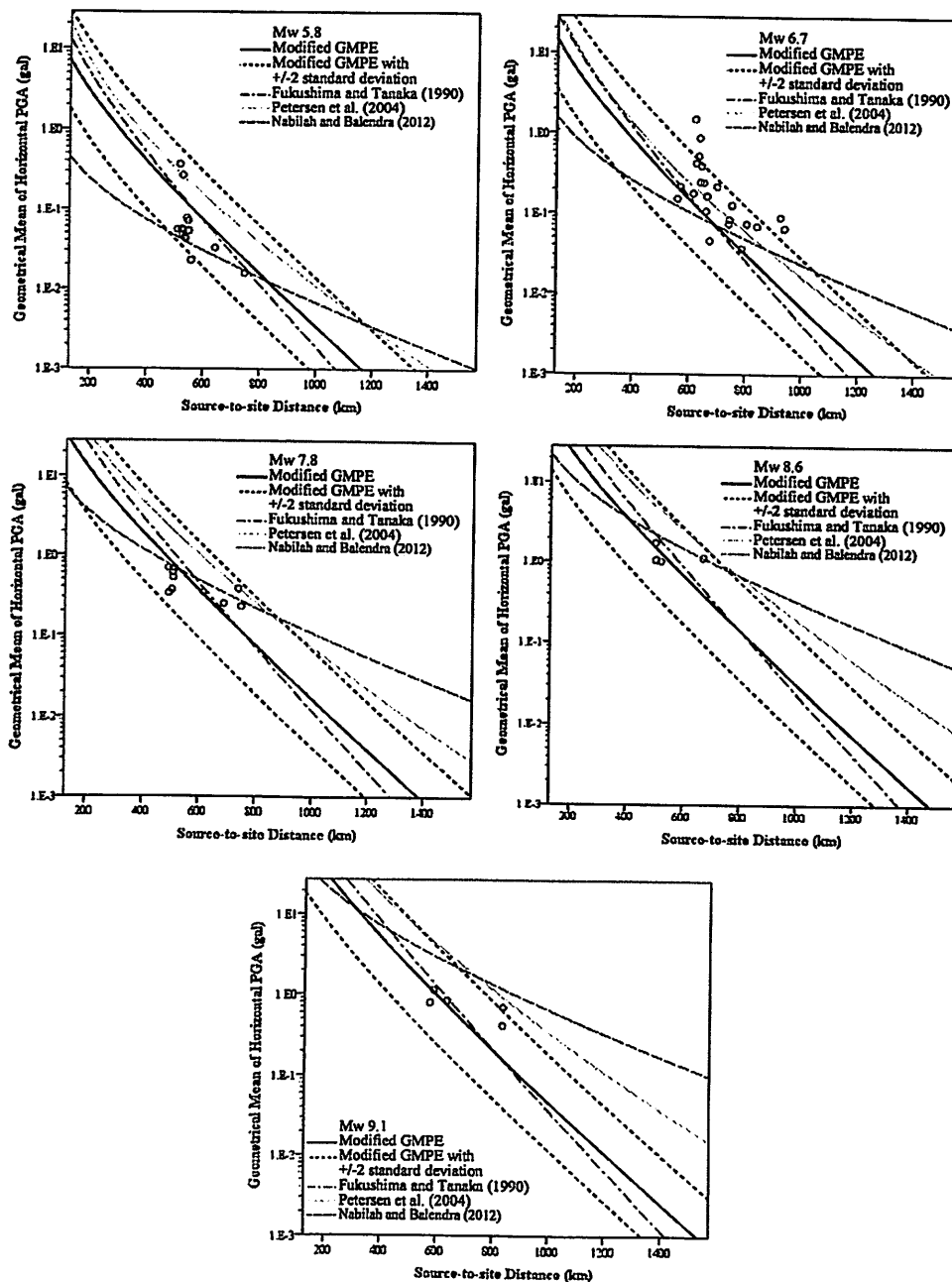


Fig. 3 Comparison of newly developed GMPE with FT9, PT04, NB12 and, recorded ground motion from interface earthquakes.



Fig. 4 shows the comparison of performance between modified GMPE and other GMPE's in the region for selected intraslab events. Being the only model which provides focal depth input in its prediction equation, PT04 over predicts PGA for both intraslab events with deep foci of up to 95 km for Mw 6.1 and 81 km for Mw 7.6 events. Despite not being derived to predict events with focal depth more than 30 km, NB12 model slightly predicts smaller PGA for Mw 6.1 event while predicts PGA close to the recorded PGA for Mw 7.6 intraslab. The modified GMPE produces curves that correspond to well with the trend of recorded PGA from selected intraslab events. For Mw 7.6 intraslab event, FT90 model predicts closer than modified GMPE to the recorded PGA. Even so, the deviated scatter of actual data still lies within the allowance of  $\pm 2$  standard deviation of prediction from modified GMPE. FT90 curves are slightly steeper than the modified GMPE.

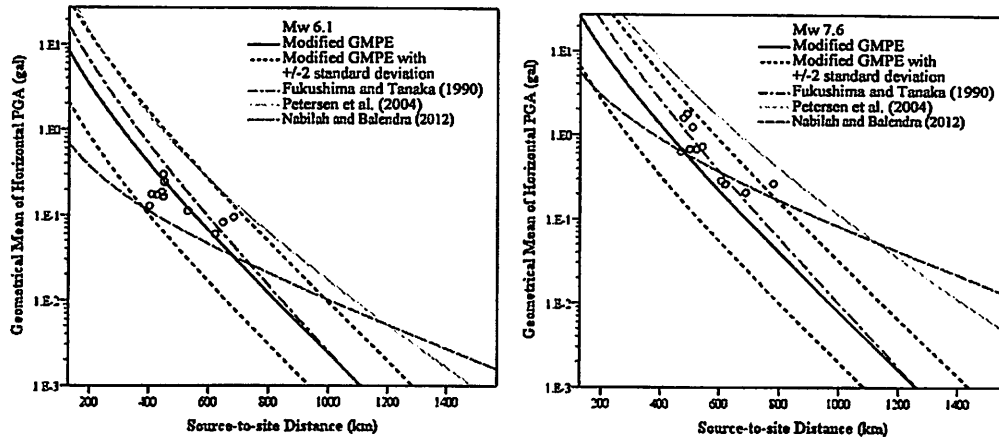


Fig. 4 Comparison of newly developed GMPE with FT9, PT04, NB12 and, recorded ground motion from intraslab earthquakes.

The small differences of steepness of prediction curves of FT90 model and modified GMPE can hardly be evaluated based on graphical presentation. Thus, the differences between collected PGA and predicted values from both FT90 model and modified GMPE were calculated. The sum of squared residuals between modified GMPE and full datasets used to for its derivation is compared with sum of squared residuals between FT90 model and the same datasets. Table 2 summarised the sum of squared residuals of respective models for each magnitude and faulting mechanisms. The median of each magnitude was adopted to classify the magnitude group. The sum of squared residuals of modified GMPE and FT90 model for interface events are 27.09 and 30.97, respectively while the sum of squared residuals of modified GMPE and FT90 model for intraslab events are 11.91 and 35.06, respectively. This shows that the modified GMPE quantitatively yield smaller differences and predicts closer to actual PGA than FT90 model, especially for intraslab events.

## Conclusion

A GMPE has been modified from the basic relationship form of Fukushima and Tanaka (1990) model to predict ground motions in Peninsular Malaysia due to interface and intraslab subduction earthquakes based on multiple regression analysis. The modified GMPE is applicable for both Class C and Class D sites in a distance range of 300 to 1200 km. The model has been validated with recorded data from Peninsular Malaysia and other GMPE that were popular in the region. The validation showed that the modified GMPE agrees well with the recorded data and gives closer prediction to recorded data than the Fukushima and Tanaka (1990) model. However, the model was improved under the insufficiency of near-field strong ground motions and far-field ground motions on rock. Thus, the modification of GMPE is the initial step to the derivation of a reliable GMPE specifically for Peninsular Malaysia. Further validation is required in the future, especially when more ground motion data from moderate to large earthquakes are available.

Table 2 Summary of sum of squared residuals under each magnitude category for modified GMPE and Fukushima and Tanaka (1990) model

Moment Magnitude	No. of data	Interface		No. of data	Intraslab	
		Modified GMPE	Fukushima and Tanaka (1990)		Modified GMPE	Fukushima and Tanaka (1990)
4.5 - 5.4	3	0.0810	0.1263	-	-	-
5.5 - 6.4	51	4.6424	4.7396	31	8.0416	30.3082
6.5 - 7.4	57	18.2581	18.0790	18	0.6879	3.3765
7.5 - 8.4	28	1.3522	3.0520	11	3.1781	1.3741
8.5 - 9.4	13	2.7558	4.9779	-	-	-
Total	152	27.0895	30.9748	60	11.9076	35.0588

### Acknowledgement

The authors wish to express their deepest appreciation to Universiti Sains Malaysia for funding this research via RU Grant (1001/PAWAM/814179). Credits are also extended to Malaysian Meteorological Department for providing seismological and ground motion data required for the analysis.

### References

- [1] W. K. Campbell. "Prediction of strong ground motion using the hybrid empirical method and its use in the development of ground-motion (attenuation) relations in eastern North America." *Bulletin of the Seismological Society of America*. 93(3) (2003) 1012-1033.
- [2] A. Adnan, Hendriyawan, and I. Masyhur. "Selection and Development of Appropriate Attenuation Relationship for Peninsular Malaysia." *Proceeding Malaysian Science and Technology Congress, Mid Valley, Kuala Lumpur* (2004).
- [3] R. Youngs, S. J. Chiou, W. Silva and J. Humphrey. "Strong ground motion attenuation relationships for subduction zone earthquakes." *Seismological Research Letters*. 68(1) (1997) 58-73.
- [4] M. D. Petersen, J. Dewey, S. Hartzell, C. Mueller, S. Harmsen, A. Frankel, and K. Rukstales. "Probabilistic seismic hazard analysis for Sumatra, Indonesia and across the Southern Malaysian Peninsula." *Tectonophysics*. 390(1) (2004) 141-158.
- [5] K. Megawati, T. C. Pan, and K. Koketsu. "Response spectral attenuation relationships for Sumatran-subduction earthquakes and the seismic hazard implications to Singapore and Kuala Lumpur." *Soil Dynamics and Earthquake Engineering*. 25(1) (2005) 11-25.
- [6] A. Nabilah and T. Balendra. "Seismic hazard analysis for Kuala Lumpur, Malaysia." *Journal of Earthquake Engineering*. 16(7) (2012) 1076-1094.
- [7] T.C. Van, and T. L. Lau. "Estimation of ground motion in Kuala Lumpur due to Sumatra subduction earthquake." *Proceedings of the International Civil and Infrastructure Engineering Conference 2013 (InCIEC 2013)* (2014) 129-139.
- [8] H. Husen, T. A. Majid, F. M. Nazri, M. R. Arshad, and A. Faisal. "Development of Design response Spectra Based on Various Attenuation Relationships at Specific Location." In *International Conference on Construction and Building Technology (ICCBT08)* (2008).
- [9] A. Adnan, Z. S. Shaerliza, S. Sumio, and G. Hiroyuki. "An investigation of the attenuation characteristics of distant ground motions in Peninsular Malaysia by comparing values of recorded with estimated PGA and PGV." *Malaysian Journal of Civil Engineering*. 2(1) (2010) 38-52.
- [10] T.C. Van. Evaluation of existing ground motion attenuation models for the application in Peninsular Malaysia. MSc. degree thesis (2014) School of Civil Engineering, Universiti Sains Malaysia.
- [11] Y. Fukushima and T. Tanaka. "A new attenuation relation for peak horizontal acceleration of strong earthquake ground motion in Japan." *Bulletin of the Seismological Society of America*. 80(4) (1990) 757-783.

Rohana Hassan · Marina Yusoff  
Zulhabri Ismail · Norliyati Mohd Amin  
Mohd Arshad Fadzil  
Editors

# InCIEC 2013

Proceedings of the International Civil  
and Infrastructure Engineering  
Conference 2013

 Springer

*Editors*

Rohana Hassan  
Marina Yusoff  
Norliyati Mohd Amin  
Mohd Arshad Fadzil  
Institute for Infrastructure Engineering  
and Sustainable Management (IIESM)  
Universiti Teknologi MARA  
Shah Alam, Selangor  
Malaysia

Zulhabri Ismail  
Architecture, Planning and Surveying  
Universiti Teknologi MARA  
Shah Alam, Selangor  
Malaysia

ISBN 978-981-4585-01-9      ISBN 978-981-4585-02-6 (eBook)  
DOI 10.1007/978-981-4585-02-6  
Springer Singapore Heidelberg New York Dordrecht London

Library of Congress Control Number: 2013956334

© Springer Science+Business Media Singapore 2014

This work is subject to copyright. All rights are reserved by the Publisher, whether the whole or part of the material is concerned, specifically the rights of translation, reprinting, reuse of illustrations, recitation, broadcasting, reproduction on microfilms or in any other physical way, and transmission or information storage and retrieval, electronic adaptation, computer software, or by similar or dissimilar methodology now known or hereafter developed. Exempted from this legal reservation are brief excerpts in connection with reviews or scholarly analysis or material supplied specifically for the purpose of being entered and executed on a computer system, for exclusive use by the purchaser of the work. Duplication of this publication or parts thereof is permitted only under the provisions of the Copyright Law of the Publisher's location, in its current version, and permission for use must always be obtained from Springer. Permissions for use may be obtained through RightsLink at the Copyright Clearance Center. Violations are liable to prosecution under the respective Copyright Law. The use of general descriptive names, registered names, trademarks, service marks, etc. in this publication does not imply, even in the absence of a specific statement, that such names are exempt from the relevant protective laws and regulations and therefore free for general use.

While the advice and information in this book are believed to be true and accurate at the date of publication, neither the authors nor the editors nor the publisher can accept any legal responsibility for any errors or omissions that may be made. The publisher makes no warranty, express or implied, with respect to the material contained herein.

Printed on acid-free paper

Springer is part of Springer Science+Business Media ([www.springer.com](http://www.springer.com))

# Estimation of Ground Motion in Kuala Lumpur Due to Sumatra Subduction Earthquake

Tze Che Van and Tze Liang Lau

**Abstract** Kuala Lumpur has undesirable subsurface features and yet is the most important and densely populated city in Peninsular Malaysia. Due to this, it should be covered and protected from seismic impact possibilities. An attenuation model that can best estimates ground motion is essential prior to conducting seismic hazard assessment. With the scarcity of historical data, an attenuation model is difficult to be developed for Peninsular Malaysia. The present research focuses on subjecting five existing attenuation models, particularly for subduction earthquakes, to comparison with the actual ground motion records in Kuala Lumpur. Seismic records of Sumatra subduction earthquakes with the moment magnitude from 5.7 to 9.1 spanning in a distance range of 395–834 km were obtained from Malaysian Meteorology Department and other catalogues. Results are presented in graphs and root mean squared error (RMSE) between estimated PGA and actual records was also computed for each attenuation model. The result shows that Adnan et al. (Selection and development of appropriate attenuation relationship for Peninsular Malaysia, Kuala Lumpur, 2004) provides the smallest RMSE of differences between predicted PGA and actual PGA on soil sites in Kuala Lumpur for interface mechanism and on both rock and soil sites for intraslab mechanism of subduction earthquakes while Zhao et al. (Attenuation relations of strong ground motion in Japan using site classification based on predominant period 96(3):898–913, 2006) gives best prediction to PGA on rock site for interface subduction earthquakes.

**Keywords** Attenuation models • Sumatra subduction zone • Distant earthquake • Seismic • Ground motion estimation • Peak ground acceleration

---

T. C. Van (✉) • T. L. Lau

School of Civil Engineering, Universiti Sains Malaysia (USM), Pulau Pinang, Malaysia  
e-mail: cathvan\_911@hotmail.com

T. L. Lau

e-mail: celau@eng.usm.my

## 1 Introduction

Kuala Lumpur is filled with modern structure and high rise building in almost every corner. Ensuring the safety of this capital of Malaysia is very important to protect residents and commercial activities importance. Peninsular Malaysia is located at the tectonically stable Sunda plate. Although there is no large earthquake originated within Malaysia, this country is often disturbed by tremors propagated from the most renowned seismically active Sumatra subduction zone and Sumatra fault despite its distance of more than 350 km from the zone. With increasing incidences of tremors felt from earthquakes originated from Sumatra, many start to worry if Peninsular Malaysia, including Kuala Lumpur, is still safe from seismic activities. The subsurface of Kuala Lumpur consists of limestone bedrock. The overlying soil deposits comprises of alluvium or/and mine tailings as Kuala Lumpur was once a popular area for tin mining industries [1]. The thick soil over the limestone bedrocks, which has a common depth of around 50 m, makes undesirable features for structural foundations. Kuala Lumpur, which has thick soil layer and long distance from epicenters of Sumatra earthquakes, has the similar geological and geographical features as in the case of Mexico City earthquake in 1985.

Although there is no major damage of structure and casualties experienced due to tremors felt in Kuala Lumpur, the occurrence of moderate level ground motions can be disastrous to structure with no seismic resistant design. According to prediction by Megawati et al. [2], subduction earthquake from Sumatra with a moment magnitude larger than 7.8 could yield catastrophic ground motion in Singapore and Kuala Lumpur, even at a distance of 700 km. Probabilistic seismic hazard assessment has to be carried out for Kuala Lumpur, knowing its importance as the main centre of the country. Prior to the seismic risk assessment, selection of a reliable ground motion attenuation model is yet another challenging task.

An attenuation model is a simple mathematical model that relates ground motion parameters (i.e. spectral acceleration, velocity and displacement) to earthquake source parameters (i.e. magnitude, source-to-site distance and mechanism) and local conditions [3]. Empirical method is the most reliable method to develop an attenuation model. However, due to limitation of well-documented historical ground motion information recorded in Malaysia, it is not possible to formulate a new model using that method as it requires regression analysis of abundant available data. Conventionally, subjecting a number of existing attenuation models which has the similarity in geology, seismo-tectonic features or source-to-site distance to comparison has been carried out in Malaysia.

A study on formulating distant attenuation model for subduction earthquake and shallow crustal earthquake has been carried out [4]. For comparative purposes, these models are plotted and compared with only a few existing attenuation models, which are considered not comprehensive enough to show any aspect of differences and errors of the formulated model for Peninsular Malaysia. Four distant attenuation models developed for Malaysia and Singapore were also

subjected into comparison and selection for design response study [5]. Reference [6] compared four models established for stable tectonic regions with actual ground motion data in Peninsular Malaysia. However, tectonic mechanism is not considered in the study.

None of the studies mentioned above clearly present a comprehensive and detailed method in processing ground motion data to suit those selected existing attenuation models. Since then, a greater amount of new data has been recorded with more stations distributed within Peninsular Malaysia. Although studies on attenuation models have already been carried out in Malaysia, different data sets utilized could lead to obtaining big differences in results [7]. Thus, despite the incomprehensive method used in the previous studies, a revision to the current adopted attenuation model is required.

This study is mainly to determine the most suitable attenuation models for subduction earthquakes for Kuala Lumpur by comparing peak ground acceleration (PGA).

## **2 Sumatra Subduction Zone and its Impact to Peninsular Malaysia**

Sumatra subduction zone is the extension of the convergent belt from Himalayan to south of Java and Sunda Islands, passing through front southward of Myanmar, Andaman, Nicobar Islands and Sumatra. It accommodates the northward motion of the Australian plate into Eurasia. With the subducting rate of 40–50 mm per year, this zone mostly produces shallow to intermediate thrust faulting earthquake [8]. Shallow earthquake can be more disastrous as waves propagate near the ground surface with less energy dissipation. This subduction zone had produced the two giant historical earthquakes: 1833 event and 2004 event with moment magnitude of 9 and 9.1 respectively.

Despite the distance of more than 400 km from Sumatra subduction earthquake sources, tremors can still be felt in Peninsular Malaysia. In 4 June 2000, the Bengkulu earthquake with Mw7.8 was reported to cause minor crack in building walls and fear among public especially in high rise building in Johor Bahru and also Klang Valley [9]. Tremors from two consecutive earthquakes from northern Sumatra of Indonesia in 14 June 2011 with Mw5.5 and Mw5.6 shocked public in Malacca, Selangor, Perak and Penang. And not to mention, the Mw9.1 megathrust earthquake generated from northern Sumatra on 26 December 2004 which triggers tsunami that took 68 lives, causing 6 missing and over 8,000 displaced in western coastal of Peninsular Malaysia [10]. Other than events mentioned above, there were a lot of subduction earthquake events that can be felt in Peninsular Malaysia.

### 3 Data Collection and Compilation

Seismic data used in this study were obtained from Malaysian Meteorology Department (MMD). These seismic data were recorded by a total of 13 stations located within Kuala Lumpur. Among those stations, 6 stations are set on soft soil Fig. 1. To fill in missing data and avoid inaccurate details, catalogues from other seismological centers such as United States Geological Survey (USGS) database, International Seismological Centre (ISC) database and National Earthquake Information Center (NEIC) database have also been referred. However, only data from December 2004 to June 2012 were included in this study due to the availability of time histories provided by MMD. Among 76 earthquake events, there are 29 distant earthquakes originated from Sumatra subduction and fault zone recorded by seismic station in Kuala Lumpur.

#### 3.1 Source Mechanisms

Global CMT project moment tensor solution and NEIC moment tensor solution were used to interpret and distinguish tectonic mechanism for each event. As a result, 15 events ranging from moment magnitude ( $M_w$ ) 5.7–9.1 with 69 ground motion data are subduction earthquakes originated from Sumatra subduction zone. Those events were further classified into two types of source mechanisms: interface earthquakes and intraslab earthquakes. Interface earthquake occurs at a depth less than 50 km on shallow dipping planes. It is associated with thrust faulting of subducting oceanic plate which is in contact with the overriding continental crust. Classified as shallow earthquakes, interface earthquakes are capable in producing megathrust earthquakes up to magnitude 9. Intraslab earthquake, on the other hand, have steep dipping planes. Producing earthquakes with magnitude not larger than 8, intraslab earthquake typically occurs along normal faults where the subducting plate experiences stress and physical changes as it is pulled deeper into the asthenosphere (Fig. 1).

However, thrust mechanism is also assumed to be intraslab event if the event occurs at depth greater than 50 km as it is below the crustal contact zone. By using rake angle, fault motion and focal depth from catalogues and moment tensors, 13 events were identified as interface earthquakes while only 2 events are intraslab earthquakes.

#### 3.2 Peak Ground Acceleration

The Peak Ground Acceleration (PGA) value utilized in this study is the geometrical mean of two horizontal components of ground motion acceleration at a site



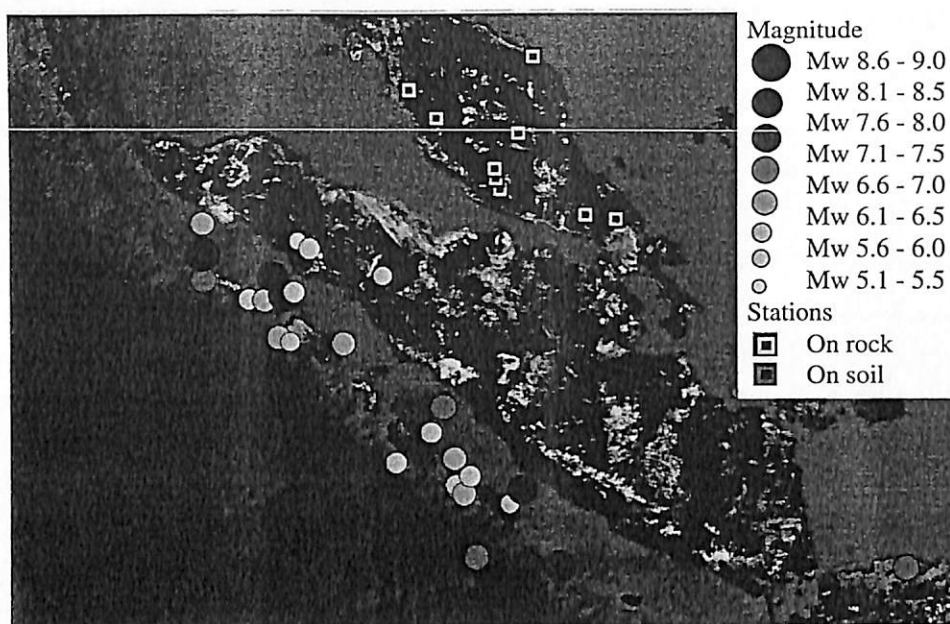


**Fig. 1** Location of Sumatra subduction earthquake events from December 2004 to June 2012 and location of seismic stations within Peninsular Malaysia

ranging from 0.000045 to 0.002220 g. Out of 69 PGA records, 42 records were from rock sites and the rest were measured from soil sites.

### 3.3 Source-to-site Distance

Source-to-site distance is yet another important parameter in this study. Different attenuation models utilized different types of distance terms. Whilst distance to rupture plane ( $r_{rup}$ ) and hypocentral distance ( $r_{hypo}$ ) are also used in some models, distance used in this study was standardized as epicentral distance ( $r_{epi}$ ) to ease comparison among attenuation models adopted. Moreover, the differences among  $r_{rup}$ ,  $r_{hypo}$  and  $r_{epi}$  are insignificant compare to the long distance from source to site. The definition of  $r_{epi}$  used in this study is the horizontal distance between epicenter of an earthquake and the site of recording instrument.

## 4 Selection of Attenuation Models

Only subduction earthquake attenuation models derived by using empirical method are selected and compared in this study. All selected models were derived by regression analysis using different sets of ground motion records. Selected attenuation models with magnitude and distance used in development of each model are tabulated in Table 1. It is noticeable that the distance ranges for some of

**Table 1** Summary of selected attenuation models

Attenuation model	Moment magnitude range	Distance range (km)	Site
Youngs et al. [11]	5.0–8.2	10–500	Mixed
Atkinson and Boore [12]	5.0–8.3	50–300	Rock and soil
Adnan et al. [4]	5.0–8.5	2–1122	Rock
Zhao et al. [13]	5.0–6.0	10–300	Rock and soil
Lin and Lee [14]	4.1–8.1	20–600	Rock and soil

the models were too small to cover the recorded long source-to-site distance from Sumatra subduction sources to seismic stations in Kuala Lumpur except Adnan et al. [4]. Nevertheless, these models may still provide the best match predictions to actual ground motions.

Different source mechanisms produce different level of motion. Thrust faulting at shallower surfaces generates the strongest motion compare to normal faulting from deeper ground. Thus, considering interface and intraslab mechanism separately is crucial in selection of attenuation model. In this study, all selected models weighed source mechanism as an essential aspect except Adnan et al. [4]. Being the only model developed for Peninsular Malaysia, Adnan et al. [4] model is included in the present study regardless to the exclusion of source mechanisms in the model. In addition, its consideration of farther source-to-site distance makes it a model worth to be compared with other models in this study.

Atkinson and Boore [12], Youngs et al. [11] and Adnan et al. [4] were developed for subduction zones at a global scale, which means seismic data were obtained from worldwide. On the other hand, Zhao et al. [13] and Lin and Lee [14] were derived by utilizing mainly local data from Japan and Taiwan respectively. An erratum for Atkinson and Boore [12] has been published in 2008 [15]. Therefore, the model adopted in this study has been corrected as suggested in the later paper.

## 5 Results and Discussions

The actual ground motion records were grouped according to moment magnitude with 1.0 interval starting from Mw6.0 to Mw9.0 for plotting. To provide better representation of actual conditions, focal depth varies for each group. Focal depth used for each group is the average of focal depth of events in respective groups. Each attenuation model has its own consideration for types of source mechanisms and site conditions. Thus, these data were also categorized into two site conditions namely, rock and soil sites.

Figure 2 shows the comparison of PGA estimated by attenuation models with actual records taken from rock site for interface subduction earthquake events. Most of the models predict larger PGA at higher moment magnitude. Lin and Lee [14] and Youngs et al. [11] predict PGA which differs significantly from the

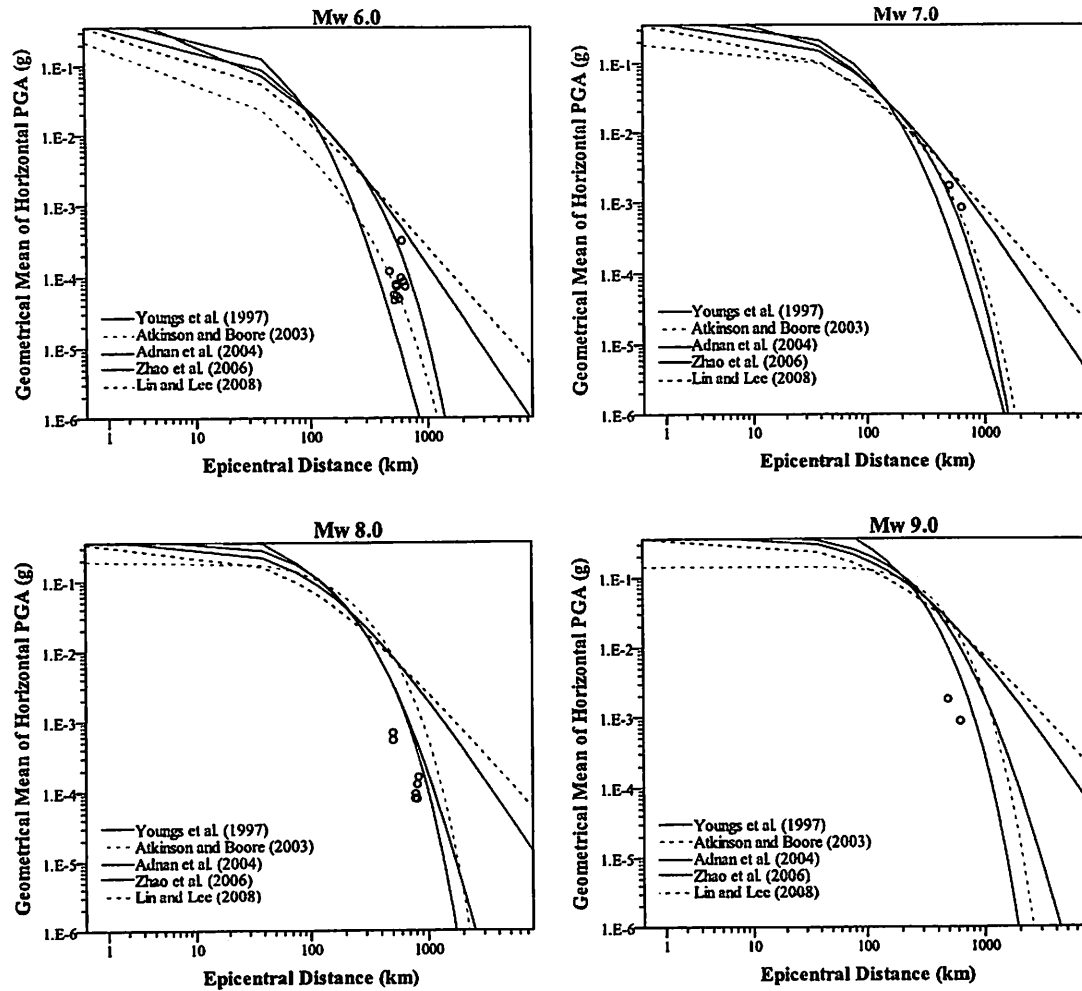
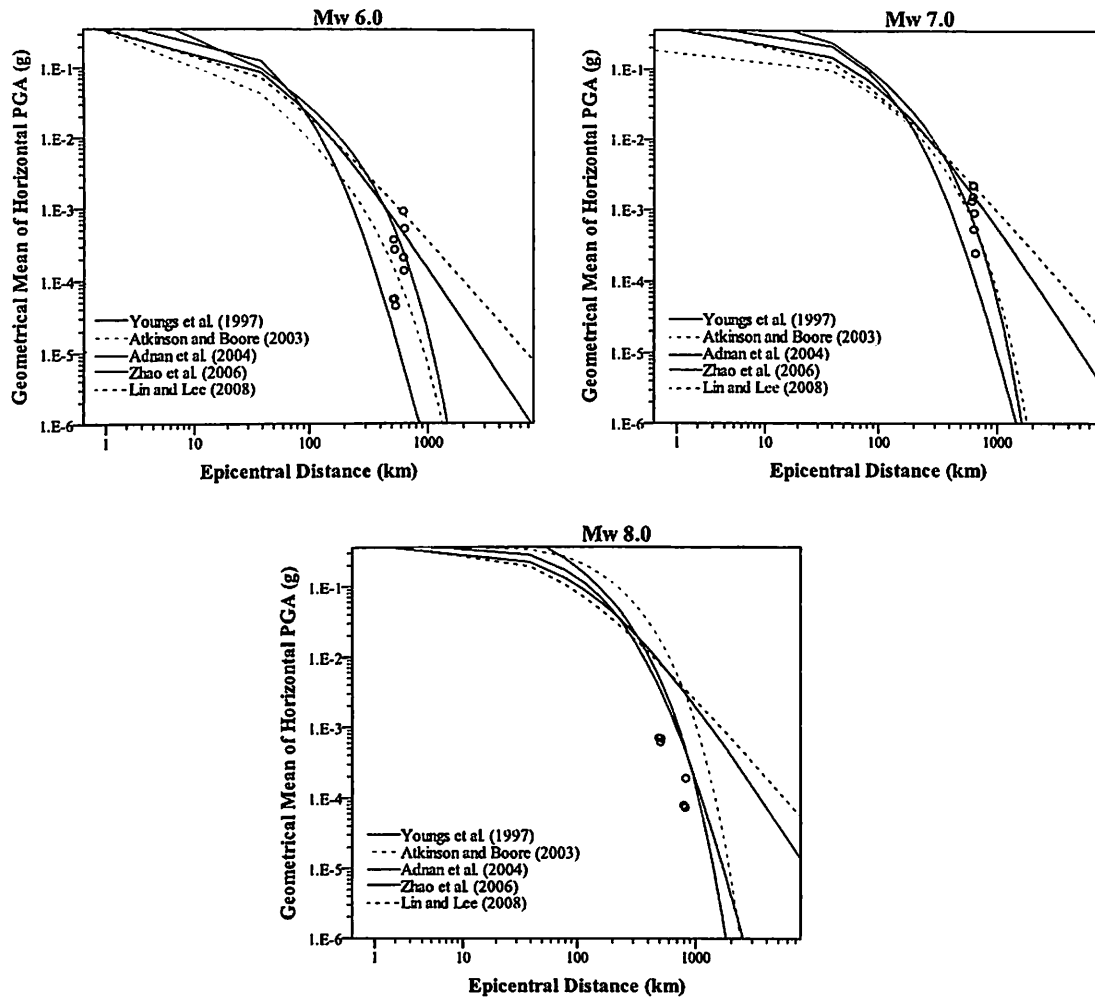


Fig. 2 Comparison of attenuation curves and recorded PGA on rock sites for interface subduction earthquakes with moment magnitude of 6.0, 7.0, 8.0 and 9.0 respectively

observed data. Atkinson and Boore [12] gives higher estimation as moment magnitude increases. Adnan et al. [4] also tends to saturate at higher magnitudes. It can be seen that Zhao et al. [13] produces curves fitter to the four magnitudes of data compare to the rest, despite the distance limitation.

On the other hand, graphs plotted in Fig. 3 exhibit comparison of PGA estimated by models with actual records taken from soil site for interface earthquake events. Zhao et al. [13] estimates PGA close to actual PGA from sites at lower magnitude. However, as magnitude increases, prediction from Zhao et al. [13] tends to deviate further from actual PGA. Adnan et al. [4] provides estimation with more consistency yet closest to actual PGA taken from soil site. Generally, Youngs et al. [11] and Lin and Lee [14] curves tend to attenuate slower and provide higher PGA value compare to recorded data.

The two intraslab earthquake events were binned into Mw7.0. With only 1 magnitude, only two graphs were produced for comparison purpose as shown in Fig. 4. From the graphs, Adnan et al. [4] curve attenuates faster than the rest and



**Fig. 3** Comparison of attenuation curves and recorded PGA on soil sites for interface subduction earthquakes with moment magnitude of 6.0, 7.0 and 8.0 respectively

gives the closest estimation of PGA. This is followed up by Zhao et al. [13], which provides the second best estimation of PGA for intraslab events. As there were only a few intraslab events, comparison between curves for each model for different moment magnitude could not be acquired.

In addition, root mean squared error (RMSE), which is also known as the standard error of the estimate, was also calculated to quantify the goodness of fit for predicted and actual value (Table 2). In other words, the smaller the RMSE value obtained, the better the estimation to the actual records. The RMSE is calculated after the data has been normalized into the range from 0 to 10. Among all, Adnan et al. [4] model provides the lowest RMSE for all types of source mechanisms and site conditions that were being considered in this study except for interface earthquakes on rock sites. The lowest RMSE on rock site for interface earthquakes is provided by Zhao et al. [13].

The locally-derived Lin and Lee [14], which predicts higher PGA compare to observed data from Kuala Lumpur, is only suitable for Taiwan and Greece regions

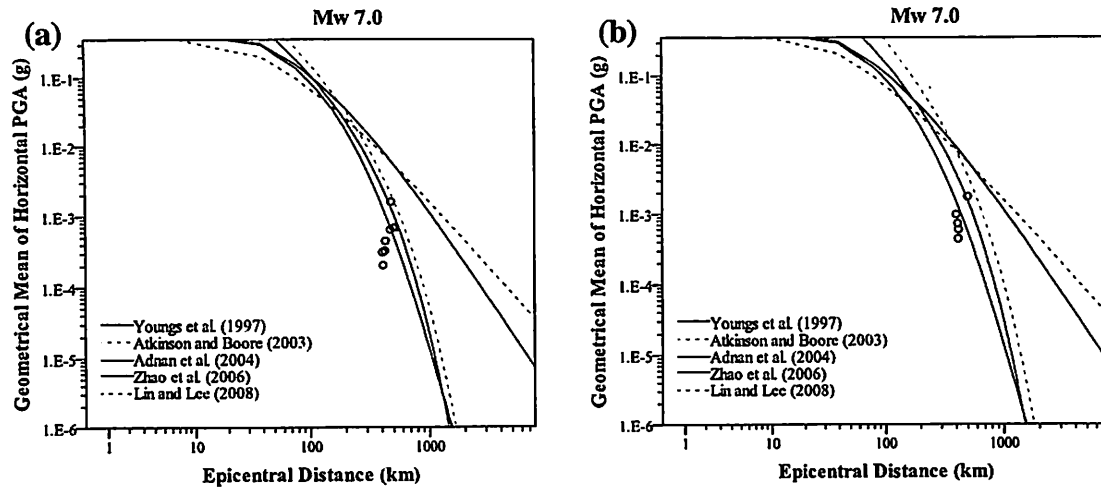


**Fig. 4** Comparison of attenuation curves and recorded PGA for intraslab subduction earthquakes with moment magnitude 7.0 on (a) rock and (b) soil sites respectively

**Table 2** Summary of root mean squared errors (RMSE)

Attenuation model	Moment magnitude (Mw)	Interface		Intraslab	
		Rock site	Soil site	Rock site	Soil site
Youngs et al. [11]	6	0.28	0.20	—	—
	7	0.71	0.23	4.58	3.33
	8	1.98	2.44	—	—
	9	8.64	—	—	—
	Mean RMSE	2.90	0.96	4.58	3.33
Atkinson and Boore [12]	6	0.06	0.21	—	—
	7	0.31	0.33	1.88	2.60
	8	1.73	4.67	—	—
	9	8.67	—	—	—
	Mean RMSE	2.69	1.74	1.88	2.60
Adnan et al. [4]	6	0.06	0.22	—	—
	7	0.34	0.72	0.59	0.18
	8	0.48	0.63	—	—
	9	5.29	—	—	—
	Mean RMSE	1.54	0.52	0.59	0.18
Zhao et al. [13]	6	0.13	0.19	—	—
	7	0.33	0.53	0.73	0.83
	8	0.61	1.20	—	—
	9	2.32	—	—	—
	Mean RMSE	0.85	0.64	0.73	0.83
Lin and Lee [14]	6	0.36	0.34	—	—
	7	0.85	0.40	4.33	3.05
	8	2.08	2.45	—	—
	9	8.26	—	—	—
	Mean RMSE	2.89	1.06	4.33	3.05

but not elsewhere [16]. Thus, the finding in this paper supports the results obtained in previous study [16]. Global-based Atkinson and Boore [12] and Youngs et al. [11] are unable to provide good estimations. This might be due to the worldwide data used in deriving those models that are too random and not specific for a certain region. Zhao et al. [13] gives closer prediction among all models in the present paper excluding Adnan et al. [4]. This might be due to the abundance of Japanese data (over 4,500 records) adopted in deriving the model which is more specific and similar in geological and geographical features to Sumatra subduction zone. Being the only attenuation model developed for Peninsular Malaysia, Adnan et al. [4] yields the lowest RMSE compare to other models considered in this paper except for interface events from rock sites.

## 6 Conclusions

Based on the results obtained, Adnan et al. [4] model provides the best fitting curve in estimating PGA on soil sites for interface mechanism and rock and soil sites for intraslab mechanism of subduction earthquakes compare to other selected models in the present study. On the other hand, Zhao et al. [13] yields the best estimation for PGA on rock sites for interface mechanism. In the future, this study will be extended to other attenuation models and further research on developing an attenuation model for Peninsular Malaysia should be carried out when recorded data are sufficient.

**Acknowledgments** The authors wish to express their sincere gratitude to Universiti Sains Malaysia for funding this research via a RU Grant (1001/PAWAM/814179). Special thanks also extended to Malaysian Meteorological Department for providing seismological data required for the analysis.

## References

1. B.B. Tan, K.A. Al-Suba, K.A. Barat, X. Li, Y. Yin, K. Zhang et al., Urban geology of Kuala Lumpur and Ipoh, Malaysia. *J. Struct. Geol.* **27**(2005), 1781 (1778)
2. K. Megawati, T.C. Pan, K. Koketsu, Response spectral attenuation relationships for Sumatran-subduction earthquakes and the seismic hazard implications to Singapore and Kuala Lumpur. *Soil Dyn. Earthq. Eng.* **25**(1), 11–25 (2005)
3. W.K. Campbell, Prediction of strong ground motion using the hybrid empirical method and its use in the development of ground-motion (attenuation) relations in eastern North America. *Bull. Seismol. Soc. Am.* **93**(3), 1012–1033 (2003)
4. A. Adnan, H. Hendriyawan, I. Masyhur, Selection and development of appropriate attenuation relationship for Peninsular Malaysia. *Proceeding Malaysian Science and Technology Congress*, Kuala Lumpur, (2004)
5. H. Husen, T.A. Majid, F.M. Nazri, M.R. Arshad, A. Faisal, Development of design response spectra based on various attenuation relationships at specific location. In *International Conference on Construction and Building Technology (ICCBT08)*, (2008)

6. A. Adnan, Z.S. Shaerliza, S. Sumio, G. Hiroyuki, An investigation of the attenuation characteristics of distant ground motions in Peninsular Malaysia by comparing values of recorded with estimated PGA and PGV. *Malays. J. Civ. Eng.* 2(1), 38–52 (2010)
7. N.A. Abrahamson, K.M. Shedlock, Overview. *Seism. Res. Lett.* 68, 9–23 (1997)
8. R. McCaffrey, The tectonic framework of the Sumatran subduction zone. *Annu. Rev. Earth Planet. Sci.* 37, 345–366 (2009)
9. M.R.C. Abas, Earthquake monitoring in Malaysia. *Seismic Risk Seminar 2001, Malaysia 2001*
10. OCHA-Geneva, OCHA situation report no. 18 earthquake and Tsunami Indonesia, Maldives, Sri Lanka. Ref: OCHA/GVA-2005/0010, January 2005, p. 9
11. R.R. Youngs, S.-J. Chiou, W.J. Silva, J.R. Humphrey, Strong ground motion attenuation relationships for subduction zone earthquakes. *Seismol. Res. Lett.* 68(1), 58–73 (1997)
12. G.M. Atkinson, D.M. Boore, Empirical ground-motion relations for subduction-zone earthquakes and their application to Cascadia and other regions. *Bull. Seismol. Soc. Am.* 93(4), 1703–1729 (2003)
13. J.X. Zhao, Z. Jian, A. Akihiro, O. Yuki, O. Taishi, T. Toshimasa et al., Attenuation relations of strong ground motion in Japan using site classification based on predominant period. *Bull. Seismol. Soc. Am.* 96(3), 898–913 (2006)
14. P.S. Lin, C.T. Lee, Ground-motion attenuation relationships for subduction-zone earthquakes in northeastern Taiwan. *Bull. Seismol. Soc. Am.* 98(1), 220–240 (2008)
15. G.M. Atkinson, M.B. David, Erratum to empirical ground-motion relations for subduction zone earthquakes and their application to Cascadia and other regions. *Bull. Seismol. Soc. Am.* 98(5), 2567–2569 (2008)
16. C. Beauval, F. Cotton, N. Abrahamson, N. Theodulidis, E. Delavaud, Rodriguez, et al., *Regional differences in subduction ground motions*. World Conference on Earthquake Engineering (Lisbonne, Portugal, 2012), p. 10

# Estimation of Ground Motion in Kuala Lumpur Due to Sumatra Subduction Earthquake

Tze Che Van<sup>1</sup>, Tze Liang Lau<sup>2</sup>

<sup>1</sup>School of Civil Engineering,  
Universiti Sains Malaysia(USM),  
Pulau Pinang, Malaysia.

<sup>2</sup>School of Civil Engineering,  
Universiti Sains Malaysia(USM),  
Pulau Pinang, Malaysia.

**Abstract**—Kuala Lumpur has undesirable subsurface features and yet is the most important and densely populated city in Peninsular Malaysia. Due to this, it should be covered and protected from seismic impact possibilities. An attenuation model that can best estimates ground motion is essential prior to conducting seismic hazard assessment. With the scarcity of historical data, an attenuation model is difficult to be developed for Peninsular Malaysia. The present research focuses on subjecting five existing attenuation models, particularly for subduction earthquakes, to comparison with the actual ground motion records in Kuala Lumpur. Seismic records of Sumatra subduction earthquakes with the moment magnitude from 5.7 to 9.1 spanning in a distance range of 395km to 834km were obtained from Malaysian Meteorology Department and other catalogues. Results are presented in graphs and root mean squared error (RMSE) between estimated PGA and actual records was also computed for each attenuation model. The result shows that Adnan et al.(2004) provides the smallest RMSE of differences between predicted PGA and actual PGA on soil sites in Kuala Lumpur for interface mechanism and on both rock and soil sites for intraslab mechanism of subduction earthquakes while Zhao et al. (2006) gives best prediction to PGA on rock site for interface subduction earthquakes.

**Keywords**— *attenuation models, Sumatra subduction zone, distant earthquake, seismic, ground motion estimation, peak ground acceleration*

## I. INTRODUCTION

Kuala Lumpur is filled with modern structure and high rise building in almost every corner. Ensuring the safety of this capital of Malaysia is very important to protect residents and commercial activities importance. Peninsular Malaysia is located at the tectonically stable Sunda plate. Although there is no large earthquake originated within Malaysia, this country is often disturbed by tremors propagated from the most renowned seismically active Sumatra subduction zone and Sumatra fault despite its distance of more than 350 km from the zone. With increasing incidences of tremors felt from earthquake originated from Sumatra, many start to worry if

Peninsular Malaysia, including Kuala Lumpur, is still safe from seismic activities. The subsurface of Kuala Lumpur consists of limestone bedrock. The overlying soil deposits comprises of alluvium or/and mine tailings as Kuala Lumpur was once a popular area for tin mining industries [1]. The thick soil over the limestone bedrocks, which has a common depth of around 50m, makes undesirable features for structural foundations. Kuala Lumpur, which has thick soil layer and long distance from epicenters of Sumatra earthquakes, has the similar geological and geographical features as in the case of Mexico City earthquake in 1985.

Although there is no major damage of structure and casualties experienced due to tremors felt in Kuala Lumpur, the occurrence of moderate level ground motions can be disastrous to structure with no seismic resistant design. According to prediction by Megawati (2005) [2], subduction earthquake from Sumatra with a moment magnitude larger than 7.8 could yield catastrophic ground motion in Singapore and Kuala Lumpur, even at a distance of 700km. Probabilistic seismic hazard assessment has to be carried out for Kuala Lumpur, knowing its importance as the main centre of the country. Prior to the seismic risk assessment, selection of a reliable ground motion attenuation model is yet another challenging task.

An attenuation model is a simple mathematical model that relates ground motion parameters (i.e. spectral acceleration, velocity and displacement) to earthquake source parameters (i.e. magnitude, source-to-site distance and mechanism) and local conditions [3]. Empirical method is the most reliable method to develop an attenuation model. However, due to limitation of well-documented historical ground motion information recorded in Malaysia, it is not possible to formulate a new model using that method as it requires regression analysis of abundant available data. Conventionally, subjecting a number of existing attenuation models which has the similarity in geology, seismo-tectonic features or source-to-site distance to comparison has been carried out in Malaysia.

A study on formulating distant attenuation model for subduction earthquake and shallow crustal earthquake has



been carried out [4]. For comparative purposes, these models are plotted and compared with only a few existing attenuation models, which are considered not comprehensive enough to show any aspect of differences and error of the formulated model for Peninsular Malaysia. Four distant attenuation models developed for Malaysia and Singapore were also subjected into comparison and selection for design response study [5]. Reference [6] compared four models established for stable tectonic regions with actual ground motion data in Peninsular Malaysia. However, tectonic mechanism is not considered in the study.

None of the studies mentioned above clearly present a comprehensive and detailed method in processing ground motion data to suit those selected existing attenuation models. Since then, a greater amount of new data has been recorded with more stations distributed within Peninsular Malaysia. Although studies on attenuation models have already been carried out in Malaysia, different data sets utilized could lead to obtaining big differences in results [7]. Thus, despite the incomprehensive method used in the previous studies, a revision to the current adopted attenuation model is required.

This study is mainly to determine the most suitable attenuation models for subduction earthquakes for Kuala Lumpur by comparing peak ground acceleration (PGA).

## II. SUMATRA SUBDUCTION ZONE AND ITS IMPACT TO PENINSULAR MALAYSIA

Sumatra subduction zone is the extension of the convergent belt from Himalayan to south of Java and Sunda Islands, passing through front southward of Myanmar, Andaman, Nicobar Islands and Sumatra. It accommodates the northward motion of the Australian plate into Eurasia. With the subducting rate of 40 to 50 mm per year, this zone mostly produces shallow to intermediate thrust faulting earthquake [8]. Shallow earthquake can be more disastrous as waves propagate near the ground surface with less energy dissipation. This subduction zone had produced the two giant historical earthquakes: 1833 event and 2004 event with moment magnitude of 9 and 9.1 respectively.

Despite the distance of more than 400km from Sumatra subduction earthquake sources, tremors can still be felt in Peninsular Malaysia. In 4 June 2000, the Bengkulu earthquake with Mw7.8 was reported to cause minor crack in building walls and fear among public especially in high rise building in Johor Bahru and also Klang Valley [9]. Tremors from two consecutive earthquakes from northern Sumatra of Indonesia in 14 June 2011 with Mw5.5 and Mw5.6 shocked public in Malacca, Selangor, Perak and Penang. And not to mention, the Mw9.1 megathrust earthquake generated from northern Sumatra on 26 December 2004 which triggers tsunami that took 68 lives, causing 6 missing and over 8000 displaced in western coastal of Peninsular Malaysia [10]. Other than events mentioned above, there were a lot of subduction earthquake events that can be felt in Peninsular Malaysia.

## III. DATA COLLECTION AND COMPILATION

Seismic data used in this study were obtained from Malaysian Meteorology Department (MMD). These seismic data were recorded by a total of 13 stations located within Kuala Lumpur. Among those stations, 6 stations are set on soft soil Fig. 1. To fill in missing data and avoid inaccurate details, catalogues from other seismological centers such as United States Geological Survey (USGS) database, International Seismological Centre (ISC) database and National Earthquake Information Center (NEIC) database have also been referred. However, only data from December 2004 to June 2012 were included in this study due to the availability of time histories provided by MMD. Among 76 earthquake events, there are 29 distant earthquakes originated from Sumatra subduction and fault zone recorded by seismic station in Kuala Lumpur.

### A. Source Mechanisms

Global CMT project moment tensor solution and NEIC moment tensor solution were used to interpret and distinguish tectonic mechanism for each event. As a result, 15 events ranging from moment magnitude (Mw) 5.7 to 9.1 with 69 ground motion data are subduction earthquakes originated from Sumatra subduction zone. Those events were further classified into two types of source mechanisms: interface earthquakes and intraslab earthquakes. Interface earthquake occurs at a depth less than 50km on shallow dipping planes. It is associated with thrust faulting of subducting oceanic plate which is in contact with the overriding continental crust. Classified as shallow earthquakes, interface earthquakes are capable in producing megathrust earthquakes up to magnitude 9. Intraslab earthquake, on the other hand, have steep dipping planes. Producing earthquakes with magnitude not larger than 8, intraslab earthquake typically occurs along normal faults where the subducting plate experiences stress and physical changes as it is pulled deeper into the asthenosphere.

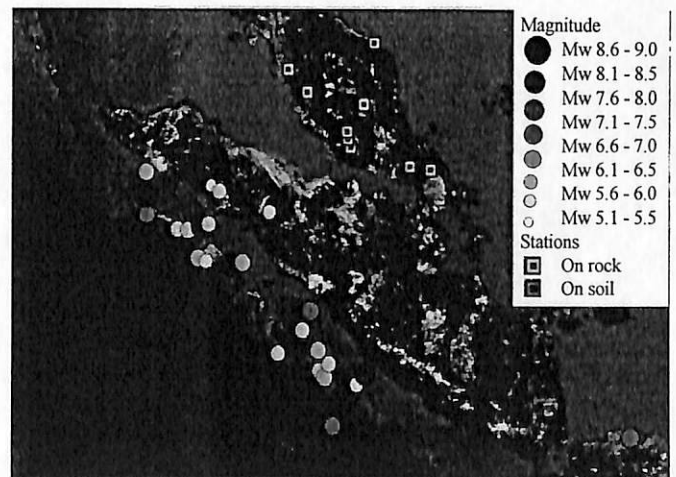


Fig. 1. Location of Sumatra subduction earthquake events from December 2004 to June 2012 and location of seismic stations within Peninsular Malaysia.

However, thrust mechanism is also assumed to be intraslab event if the event occurs at depth greater than 50km as it is below the crustal contact zone. By using rake angle, fault motion and focal depth from catalogues and moment tensors, 13 events were identified as interface earthquakes while only 2 events are intraslab earthquakes.

#### B. Peak Ground Acceleration (PGA)

The PGA value utilized in this study is the geometrical mean of two horizontal components of ground motion acceleration at a site ranging from 0.000045g to 0.002220g. Out of 69 PGA records, 42 records were from rock sites and the rest were measured from soil sites.

#### C. Source-to-site Distance

Source-to-site distance is yet another important parameter in this study. Different attenuation models utilized different types of distance terms. Whilst distance to rupture plane ( $r_{rup}$ ) and hypocentral distance ( $r_{hypo}$ ) are also used in some models, distance used in this study was standardized as epicentral distance ( $r_{epi}$ ) to ease comparison among attenuation models adopted. Moreover, the differences among  $r_{rup}$ ,  $r_{hypo}$  and  $r_{epi}$  are insignificant compare to the long distance from source to site. The definition of  $r_{epi}$  used in this study is the horizontal distance between epicenter of an earthquake and the site of recording instrument.

### IV. SELECTION OF ATTENUATION MODELS

Only subduction earthquake attenuation models derived by using empirical method are selected and compared in this study. All selected models were derived by regression analysis using different sets of ground motion records. Selected attenuation models with magnitude and distance used in development of each model are tabulated in Table 1. It is noticeable that the distance ranges for some of the models were too small to cover the recorded long source-to-site distance from Sumatra subduction sources to seismic stations in Kuala Lumpur except Adnan et al. (2004). Nevertheless, these models may still provide the best match predictions to actual ground motions.

Different source mechanisms produce different level of motion. Thrust faulting at shallower surfaces generates the strongest motion compare to normal faulting from deeper ground. Thus, considering interface and intraslab mechanism separately is crucial in selection of attenuation model. In this study, all selected models weighed source mechanism as an essential aspect except Adnan et al. (2004). Being the only model developed for Peninsular Malaysia, Adnan et al. (2004) model is included in the present study regardless to the exclusion of source mechanisms in the model. In addition, its consideration of farther source-to-site distance makes it a model worth to be compared with other models in this study.

TABLE 1. SUMMARY OF SELECTED ATTENUATION MODELS

Attenuation model	Moment Magnitude range	Distance range (km)	Site
Youngs et al. (1997)[11]	5.0 - 8.2	10 - 500	Mixed
Atkinson and Boore (2003)[12]	5.0 - 8.3	50 - 300	Rock and Soil
Adnan et al. (2004)	5.0 - 8.5	2 - 1122	Rock
Zhao et al. (2006)[13]	5.0 - 6.0	10 - 300	Rock and Soil
Lin and Lee (2008)[14]	4.1 - 8.1	20 - 600	Rock and Soil

Atkinson and Boore (2003), Youngs et al. (1997) and Adnan et al. (2004) were developed for subduction zones at a global scale, which means seismic data were obtained from worldwide. On the other hand, Zhao et al. (2006) and Lin and Lee (2008) were derived by utilizing mainly local data from Japan and Taiwan respectively. An erratum for Atkinson and Boore (2003) has been published in 2008[15]. Therefore, the model adopted in this study has been corrected as suggested in the later paper.

### V. RESULTS AND DISCUSSIONS

The actual ground motion records were grouped according to moment magnitude with 1.0 interval starting from Mw6.0 to Mw9.0 for plotting. To provide better representation of actual conditions, focal depth varies for each group. Focal depth used for each group is the average of focal depth of events in respective groups. Each attenuation model has its own consideration for types of source mechanisms and site conditions. Thus, these data were also categorized into two site conditions namely, rock and soil sites.

Fig. 2 shows the comparison of PGA estimated by attenuation models with actual records taken from rock site for interface subduction earthquake events. Most of the models predict larger PGA at higher moment magnitude. Lin and Lee (2008) and Youngs et al. (1997) predict PGA which differs significantly from the observed data. Atkinson and Boore (2003) gives higher estimation as moment magnitude increases. Adnan et al. (2004) also tends to saturate at higher magnitudes. It can be seen that Zhao et al. (2006) produces curves fitter to the four magnitudes of data compare to the rest, despite the distance limitation.

On the other hand, graphs plotted in Fig. 3 exhibit comparison of PGA estimated by models with actual records taken from soil site for interface earthquake events. Zhao et al. (2006) estimates PGA close to actual PGA from sites at lower magnitude. However, as magnitude increases, prediction from Zhao et al. (2006) tends to deviate further from actual PGA. Adnan et al. (2004) provides estimation with more consistency yet closest to actual PGA taken from soil site. Generally, Youngs et al. (1997) and Lin and Lee (2008) curves tend to attenuate slower and provide higher PGA value compare to recorded data.

The two intraslab earthquake events were binned into Mw 7.0. With only 1 magnitude, only two graphs were produced for comparison purpose as shown in Fig. 4. From the graphs, Adnan et al. (2004) curve attenuates faster than the rest and gives the closest estimation of PGA. This is followed up by Zhao et al. (2006), which provides the second best estimation of PGA for intraslab events. As there were only a few intraslab events, comparison between curves for each model for different moment magnitude could not be acquired.

In addition, root mean squared error (RMSE), which is also known as the standard error of the estimate, was also calculated to quantify the goodness of fit for predicted and actual value (Table 2). In other words, the smaller the RMSE value obtained, the better the estimation to the actual records. The RMSE is calculated after the data has been normalized into the range from 0 to 10. Among all, Adnan et al. (2004) model provides the lowest RMSE for all types of source mechanisms and site conditions that were being considered in this study except for interface earthquakes on rock sites. The

lowest RMSE on rock site for interface earthquakes is provided by Zhao et al. (2006).

The locally-derived Lin and Lee (2008), which predicts higher PGA compare to observed data from Kuala Lumpur, is only suitable for Taiwan and Greece regions but not elsewhere [16]. Thus, the finding in this paper supports the results obtained in previous study [16]. Global-based Atkinson and Boore (2003) and Youngs et al. (1997) are unable to provide good estimations. This might be due to the worldwide data used in deriving those models that are too random and not specific for a certain region. Zhao et al. (2006) gives closer prediction among all models in the present paper excluding Adnan et al. (2004). This might be due to the abundance of Japanese data (over 4500 records) adopted in deriving the model which is more specific and similar in geological and geographical features. Being the only attenuation model developed for Peninsular Malaysia, Adnan et al. (2004) yields the lowest RMSE compare to other models considered in this paper except for interface events from rock sites.

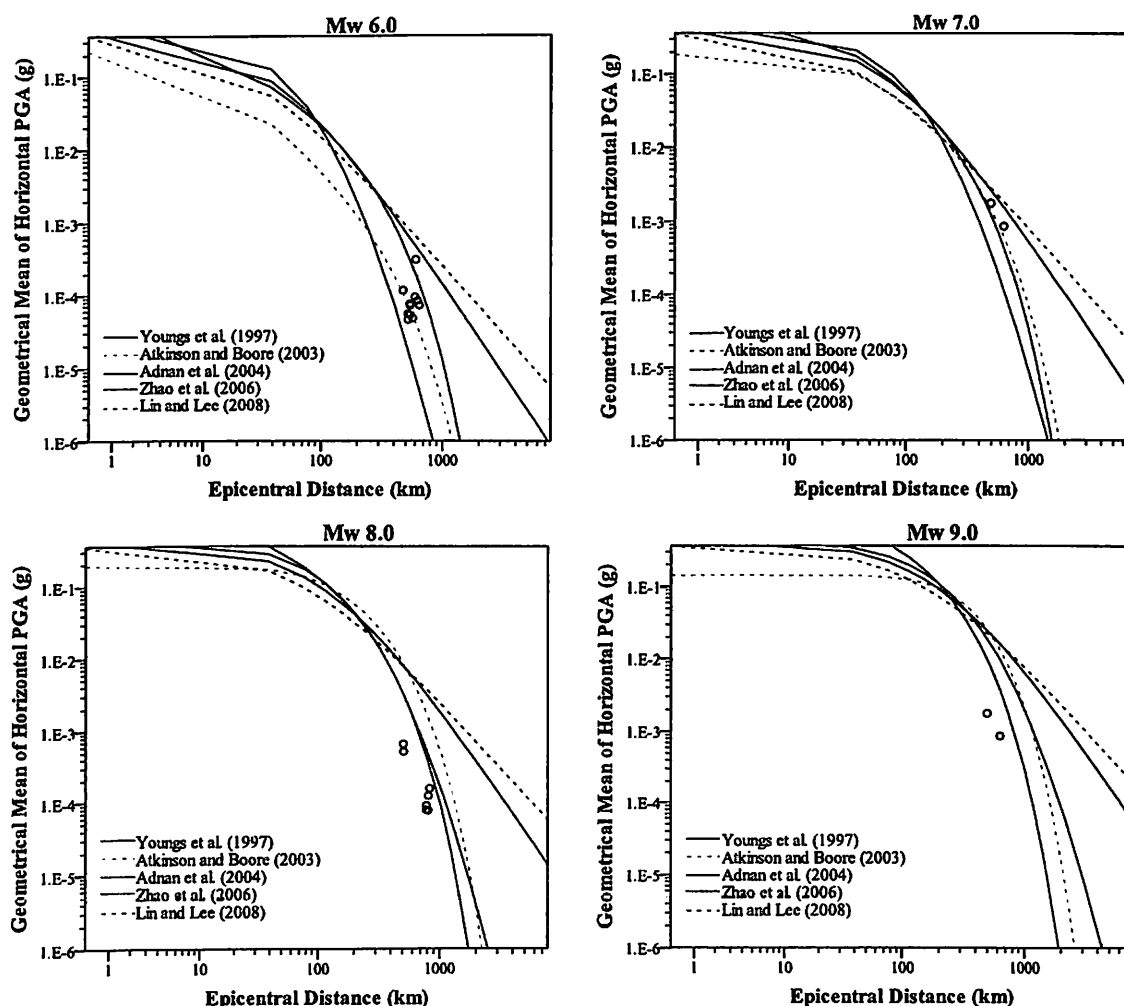


Fig. 2. Comparison of attenuation curves and recorded PGA on rock sites for interface subduction earthquakes with moment magnitude of 6.0, 7.0, 8.0 and 9.0 respectively.

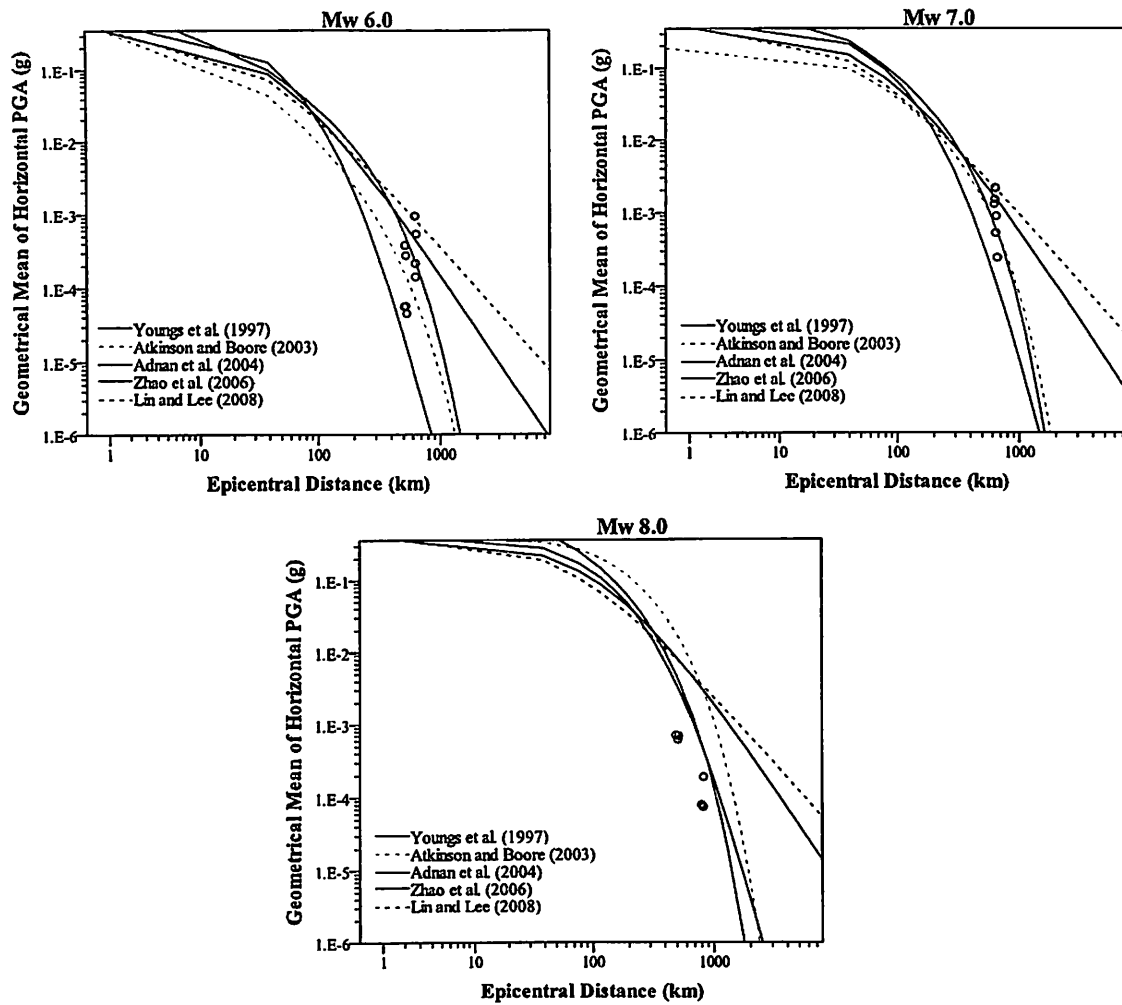


Fig. 3. Comparison of attenuation curves and recorded PGA on soil sites for interface subduction earthquakes with moment magnitude of 6.0, 7.0 and 8.0 respectively.

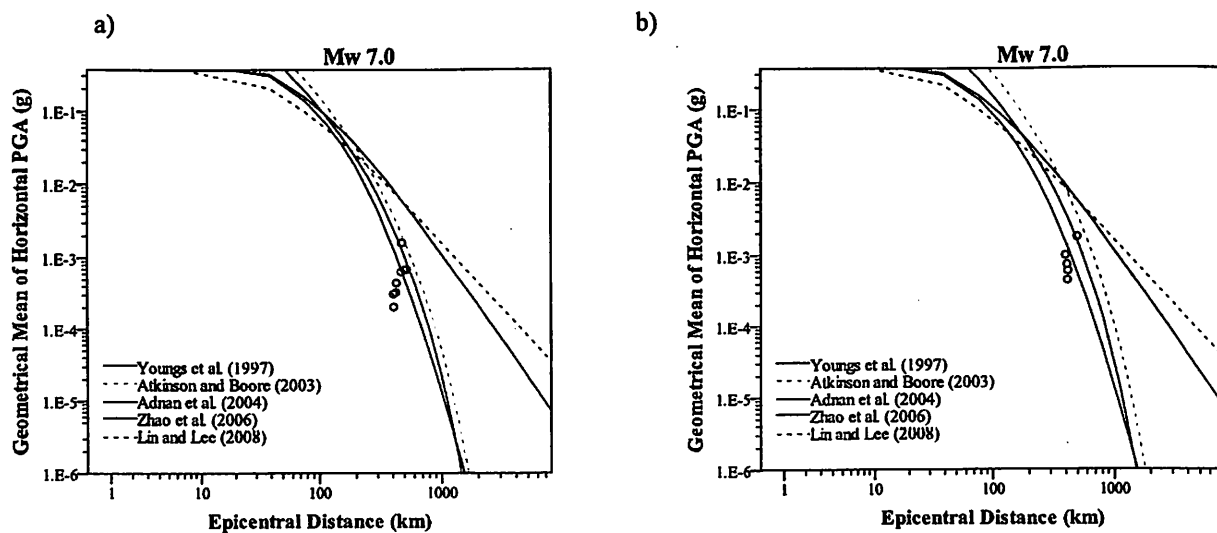


Fig. 4. Comparison of attenuation curves and recorded PGA for intraslab subduction earthquakes with moment magnitude 7.0 on a) rock and b) soil sites respectively.

TABLE 2 SUMMARY OF ROOT MEAN SQUARED ERRORS (RMSE)

Attenuation model	Moment magnitude (Mw)	Interface		Intraslab	
		Rock site	Soil site	Rock site	Soil site
Youngs et al. (1997)	6	0.28	0.20	-	-
	7	0.71	0.23	4.58	3.33
	8	1.98	2.44	-	-
	9	8.64	-	-	-
	Mean RMSE	2.90	0.96	4.58	3.33
Atkinson and Boore (2003)	6	0.06	0.21	-	-
	7	0.31	0.33	1.88	2.60
	8	1.73	4.67	-	-
	9	8.67	-	-	-
	Mean RMSE	2.69	1.74	1.88	2.60
Adnan et al. (2004)	6	0.06	0.22	-	-
	7	0.34	0.72	0.59	0.18
	8	0.48	0.63	-	-
	9	5.29	-	-	-
	Mean RMSE	1.54	0.52	0.59	0.18
Zhao et al. (2006)	6	0.13	0.19	-	-
	7	0.33	0.53	0.73	0.83
	8	0.61	1.20	-	-
	9	2.32	-	-	-
	Mean RMSE	0.85	0.64	0.73	0.83
Lin and Lee (2008)	6	0.36	0.34	-	-
	7	0.85	0.40	4.33	3.05
	8	2.08	2.45	-	-
	9	8.26	-	-	-
	Mean RMSE	2.89	1.06	4.33	3.05

## VI. CONCLUSIONS

Based on the results obtained, Adnan et al. (2004) model provides the best fitting curve in estimating PGA on soil sites for interface mechanism and rock and soil sites for intraslab mechanism of subduction earthquakes compare to other selected models in the present study. On the other hand, Zhao et al. (2006) yields the best estimation for PGA on rock sites for interface mechanism. In the future, this study will be extended to other attenuation models and further research on developing an attenuation model for Peninsular Malaysia should be carried out when recorded data are sufficient.

## ACKNOWLEDGEMENT

The authors wish to express their sincere gratitude to Universiti Sains Malaysia for funding this research via a RU Grant (1001/PAWAM/814179). Special thanks also extended to Malaysian Meteorological Department for providing seismological data required for the analysis.

## REFERENCES

- [1] B. B. Tan, K. A. Al-Suba, K. A. Barat, X. Li, Y. Yin, K. Zhang, et al. (1778). "Urban geology of Kuala Lumpur and Ipoh, Malaysia." *Journal of Structural Geology*, 27, 1781, 2005.
- [2] K. Megawati, T. C. Pan, and K. Koketsu. "Response spectral attenuation relationships for Sumatran-subduction earthquakes and the seismic hazard implications to Singapore and Kuala Lumpur." *Soil dynamics and earthquake engineering* 25, no. 1, 2005, pp.11-25.
- [3] W. K. Campbell. "Prediction of strong ground motion using the hybrid empirical method and its use in the development of ground-motion (attenuation) relations in eastern North America." *Bulletin of the Seismological Society of America* 93.3, 2003, pp. 1012-1033.
- [4] A. Adnan, Hendriyawan, and I. Masyhur. "Selection and Development of Appropriate Attenuation Relationship for Peninsular Malaysia." *Proceeding Malaysian Science and Technology Congress, Mid Valley, Kuala Lumpur*, 2004.
- [5] H. Husen, T. A. Majid, F. M. Nazri, M. R. Arshad, and A. Faisal. "Development of Design response Spectra Based on Various Attenuation Relationships at Specific Location." In *International Conference on Construction and Building Technology (ICCBT08)*, 2008.
- [6] A. Adnan, Z. S. Shaerliza, S. Sumio, and G. Hiroyuki. "An investigation of the attenuation characteristics of distant ground motions in Peninsular Malaysia by comparing values of recorded with estimated PGA and PGV." *Malaysian Journal of Civil Engineering* 2, no. 1, 2010, pp. 38-52.
- [7] N. A. Abrahamson, and K. M. Shedlock. *Overview*, *Seism. Res. Lett.* 68, 1997, pp. 9-23.
- [8] R. McCaffrey. "The tectonic framework of the Sumatran subduction zone." *Annual Review of Earth and Planetary Sciences* 37, 2009, pp. 345-366.
- [9] M. R. C. Abas. "Earthquake Monitoring in Malaysia." *Seismic Risk Seminar 2001, Malaysia*. 2001.
- [10] OCHA-Geneva. "OCHA Situation Report No. 18 Earthquake and Tsunami Indonesia, Maldives, Sri Lanka." Ref: OCHA/GVA-2005/0010, January 2005, 9 pp.
- [11] R. R. Youngs, S.-J. Chiou, W. J. Silva, and J. R. Humphrey. "Strong ground motion attenuation relationships for subduction zone earthquakes." *Seismological Research Letters* 68, no. 1, 1997, pp. 58-73.
- [12] G. M. Atkinson, and D. M. Boore. "Empirical ground-motion relations for subduction-zone earthquakes and their application to Cascadia and other regions." *Bulletin of the Seismological Society of America* 93, no. 4, 2003, pp. 1703-1729.
- [13] J. X. Zhao, Z. Jian, A. Akihiro, O. Yuki, O. Taishi, T. Toshimasa, et al. "Attenuation relations of strong ground motion in Japan using site classification based on predominant period." *Bulletin of the Seismological Society of America* 96, no. 3, 2006, pp. 898-913.
- [14] P. S. Lin, and C. T. Lee. "Ground-motion attenuation relationships for subduction-zone earthquakes in northeastern Taiwan." *Bulletin of the Seismological Society of America* 98, no. 1, 2008, pp. 220-240.
- [15] G. M. Atkinson, and M. B. David. "Erratum to empirical ground-motion relations for subduction zone earthquakes and their application to Cascadia and other regions." *Bulletin of the Seismological Society of America* 98, no. 5, 2008, pp. 2567-2569.
- [16] C. Beauval, F. Cotton, N. Abrahamson, N. Theodulidis, E. Delavaud, Rodriguez, et al. "Regional differences in subduction ground motions." *World Conference on Earthquake Engineering*, Lisbonne: Portugal, 2012, 10 pp.



**USM** UNIVERSITI  
SAINS  
MALAYSIA

Pusat Pengajian Kejuruteraan Awam  
School Of Civil Engineering

Kampus Kejuruteraan  
Engineering Campus  
Universiti Sains Malaysia  
Seri Ampangan, 14300 Nibong Tebal  
Seberang Perai Selatan  
Pulau Pinang  
Malaysia  
T : 04-599 6201  
F : 04-594 1009  
W : www.civil.eng.usm.my

Tarikh : 17 Oktober 2016

Pengarah  
Pejabat Pengurusan & Kreativiti Penyelidikan  
Bahagian Penyelidikan & Inovasi  
Universiti Sains Malaysia



Tuan,

**LAPORAN AKHIR GERAN PENYELIDIKAN UNIVERSITI (RU)  
LAPORAN AKHIR GERAN AGENSI LUAR**

Dengan hormatnya perkara di atas mohon dirujuk.

Bersama-sama ini dimajukan perkara berikut untuk perhatian dan tindakan pihak tuan selanjutnya.

**Laporan Akhir Geran Penyelidikan Universiti (RU)**

Bil.	Nama Penyelidik	Tajuk Penyelidikan
1.	Dr. Lau Tze Liang	'Estimation of Probable Earthquake Ground Motion in Peninsular Malaysia'

**Laporan Akhir Geran Agensi Luar**

Bil.	Nama Penyelidik	Tajuk Penyelidikan
1.	Dr. Fatehah Mohd Omar	'Importance of Flocculation Processes on the Fate and Transport of Nanoparticles in Natural and Water Treatment Processes'

Kerjasama tuan saya dahului dengan ucapan terima kasih.

Sekian.

**'BERKHIDMAT UNTUK NEGARA'**  
'Memastikan Kelestarian Hari Esok'

**PROF. MADYA DR. CHOONG KOK KEONG**  
Timbalan Dekan  
[Penyelidikan, Siswazah & Jaringan]

s.k. Dr. Lau Tze Liang  
Dr. Fatehah Mohd Omar

En. Iqam  
Untuk seliaan dan  
tindakan lanjut.  
Tt.

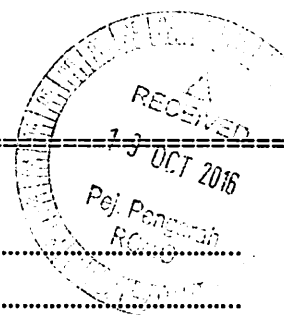
Dr. M  
24/10/16





**USM** UNIVERSITI  
SAINS  
MALAYSIA

**BORANG PENYERAHAN ASET / INVENTORI**



**A. BUTIR PENYELIDIK**


1. NAMA PENYELIDIK : Dr. Lau Tze Liang  
2. NO STAF : AE50261  
3. PTJ : Pusat Pengajian Kejuruteraan Awam  
4. KOD PROJEK :  
5. TARIKH TAMAT PENYELIDIKAN : 14/6/2016

**B. MAKLUMAT ASET / INVENTORI**

BIL	KETERANGAN ASET	NO HARTA	NO. SIRI	HARGA (RM)
1	Ambient vibration measuring instrument	AK00007180	12716270005	14,947.00
2	Ambient vibration measuring instrument	AK00007181	12716270004	14,947.00
3	Ambient vibration measuring instrument	AK00007182	12716270006	14,947.00
4	Ambient vibration measuring instrument	AK00007487	12716270037	18,500.00
5	Ambient vibration measuring instrument	AK00007488	12716270036	18,500.00

**C. PERAKUAN PENYERAHAN**

Saya dengan ini menyerahkan aset/ inventori seperti butiran B di atas kepada pihak Universiti:

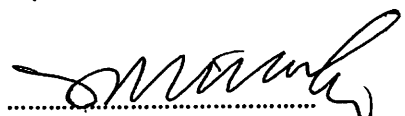
  
 ( DR LAU TZE LIANG  
 SENIOR LECTURER  
 SCHOOL OF CIVIL ENGINEERING  
 UNIVERSITI SAINS MALAYSIA )  
**D. PERAKUAN PENERIMAAN**

Tarikh: 4/10/2016

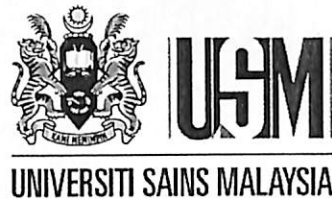
Saya telah memeriksa dan menyemak setiap alatan dan didapati :

- ☒ Lengkap  
☐ Rosak  
☐ Hilang : Nyatakan.....  
☐ Lain-lain : Nyatakan .....

Diperakukan Oleh :

  
 Tandatangan : Zulkapri Hassan  
 Pegawai Aset PTJ :  
 Nama :  
 Tarikh : 2/10/16

**\*Nota :** Sesalinan borang yang telah lengkap perlulah dikemukakan kepada Unit Pengurusan Harta, Jabatan Bendahari dan Pejabat RCMO untuk tujuan rekod.



## **RU Grant Technical Report**

**Title of Research:**  
**Estimation of Probable Earthquake Ground Motion in  
Peninsular Malaysia**

**Account Number:**  
**1001/PAWAM/814179**

**Duration:**  
**15/12/2012 – 14/6/2016**

**Name of Researcher: Dr. Lau Tze Liang**

**Name of Co-Researcher: Assoc. Prof. Dr. Choong Kok Keong  
Prof. Dr. Taksiah A. Majid  
Dr. Fadzli Mohamed Nazri  
Dr. Neeraj Bhardwaj**



## TABLE OF CONTENTS

	PAGE
TABLE OF CONTENTS	i
LIST OF TABLES	iv
LIST OF FIGURES	v
 <b>CHAPTER 1 - INTRODUCTION</b>	
1.1 General	1
1.2 Problem statement	2
1.3 Objective	3
1.4 Scope of Work	3
 <b>CHAPTER 2 – LITERATURE REVIEW</b>	
2.1 Tectonic setting of Peninsular Malaysia and its seismicity	4
2.1.1 Far field earthquake	4
2.1.1.1 Sumatra subduction zone	5
2.1.1.2 Sumatran fault zone	8
2.1.2 Local earthquake within Peninsular Malaysia	10
2.2 Seismicity network in Malaysia	11
2.3 Ground motion attenuation models	12
2.3.1 Theoretical background	14
2.3.2 Derivation of attenuation models	14
2.3.3 Factors affecting attenuation	17
2.3.3.1 Tectonic setting	18
2.3.3.2 Type of faulting and focal mechanism	18
2.3.3.3 Magnitude	18
2.3.3.4 Source-to-site distance	19
2.3.3.5 Site condition	20
2.3.3.6 Other factors	22
2.4 Ground motion attenuation model adoption from previous researches for Peninsular Malaysia	24
2.5 Pre-selection of attenuation models	26
2.5.1 Ground motion attenuation models for subduction earthquakes	28
2.5.1.1 Adnan et al. (2004)	28
2.5.1.2 Atkinson and Boore (2003, 2008)	28
2.5.1.3 Crouse (1991)	30

2.5.1.4	Fukushima and Tanaka (1990)	31
2.5.1.5	Gregor et al. (2002)	31
2.5.1.6	Kanno et al. (2006)	32
2.5.1.7	Lin and Lee (2008)	33
2.5.1.8	Megawati et al. (2005)	34
2.5.1.9	Megawati and Pan (2010)	35
2.5.1.10	Nabilah and Balendra (2012)	35
2.5.1.11	Petersen et al. (2004)	36
2.5.1.12	Youngs et al. (1997)	37
2.5.1.13	Zhao et al. (2006)	38
2.5.2	Ground motion attenuation models for shallow crustal earthquakes	40
2.5.2.1	Abrahamson and Silva (1997)	40
2.5.2.2	Ambraseys et al. (2005)	42
2.5.2.3	Atkinson and Boore (2006, 2011)	42
2.5.2.4	Boore et al. (1997, 2005)	44
2.5.2.5	Campbell (2003, 2004)	45
2.5.2.6	Dahle et al. (1990)	46
2.5.2.7	Frankel et al. (1996)	47
2.5.2.8	Hwang and Huo (1997)	47
2.5.2.9	Megawati et al. (2003)	49
2.5.2.10	Pezeshk et al. (2011)	50
2.5.2.11	Sadigh et al. (1997)	51
2.5.2.12	Si and Midorikawa (2000)	52
2.5.2.13	Somerville et al. (2009)	53
2.5.2.14	Spudich et al. (1999)	54
2.5.2.15	Toro et al. (1997)	55
2.6	Summary	56

## **CHAPTER 3 – RESEARCH METHODOLOGY**

3.1	Introduction	57
3.2	Data collection and selection	58
3.3	Data analysis and calibration	59
3.3.1	Source mechanism	59
3.3.2	Magnitude	61
3.3.3	Distance	61
3.3.4	Ground motion parameter	63
3.4	Site classification	65

3.5	Pre-selection of ground motion attenuation models	69
3.6	Result analysis	71
3.7	Summary	76

## **CHAPTER 4 – RESULTS AND DISCUSSION**

4.1	Introduction	77
4.2	Parameters calibration result	77
4.2.1	Source mechanism	77
4.2.2	Moment magnitude	78
4.2.3	Distance	80
4.3	Site classification	81
4.4	Examination of pre-selected ground motion attenuation model	90
4.4.1	Comparison of pre-selected models for subduction earthquakes	90
4.4.2	Comparison of pre-selected models for strike-slip earthquakes	111
4.4.3	Quantification of adequacy of pre-selected models	123
4.5	Summary	124

## **CHAPTER 5 – CONCLUSION AND RECOMMENDATIONS**

5.1	Conclusions	152
-----	-------------	-----

## **REFERENCES**

## **APPENDICES**

Appendix A	Compilation of moment magnitude from various catalogues
Appendix B	Computed epicentral distances between earthquake sources and seismic stations
Appendix C	Geometrical mean of two horizontal PGA for distant earthquakes

## LIST OF TABLES

	PAGE
Table 2.1 Top 17 largest earthquakes around the globe since year 1900 (USGS, 2011)	5
Table 2.2 Major Segments of Sumatra Fault (Sieh and Natawidjaja, 2000; Natawidjaja and Triyoso, 2007; Madlazim and Santosa, 2010)	9
Table 2.3 Details of earthquakes around Bukit Tinggi area (MMD, 2008)	10
Table 2.4 Codes, locations and geology of Malaysia Meteorological Department seismic stations (MMD, 2012)	13
Table 2.5 List of alternative functional form of median ground motion attenuation models (EPRI, 2004)	15
Table 2.6 Brief description of NEHRP 1997 site classification (BSSC, 1998)	23
Table 2.7 Number of records by source type, faulting mechanism and region	39
Table 2.8 Regression coefficients for various site categories	48
Table 3.1 Pre-selected ground motion attenuation model for subduction earthquakes with applicability range	72
Table 3.2 Pre-selected ground motion attenuation model for shallow crustal earthquakes at active tectonic region with applicability range	73
Table 3.3 Pre-selected ground motion attenuation model for shallow crustal earthquakes at stable continental region with applicability range	74
Table 4.1 List of events sorting based on source mechanisms	79
Table 4.2 Summary of moment magnitude range for each source mechanism	80
Table 4.3 Summary of computed epicentral distance	106
Table 4.4 Site classifications of 19 seismic stations in Peninsular Malaysia based on MASW result	88
Table 4.5 Summary of computed normalised root mean squared error ( $RMSE_{Nor}$ ) for subduction earthquake ground motion attenuation models	123
Table 4.6 Summary of computed normalised root mean squared error ( $RMSE_{Nor}$ ) for strike-slip earthquake ground motion attenuation models	124

## LIST OF FIGURES

	PAGE
Figure 1.1 Newspaper reports on the tremor felt in Penang and Kuala Lumpur	1
Figure 2.1 Seismic hazard map of Peninsular Malaysia (site class S <sub>B</sub> ) (Adnan et al., 2011)	4
Figure 2.2 Regional map showing the tectonic setting and faults in Sumatra (McCaffrey, 2009)	6
Figure 2.3 Block diagram showing slip-partitioning process and motion of silver plate under oblique movement of subducting plate beneath overriding plate (McCaffrey, 2009)	7
Figure 2.4 Map showing 19 segments of Sumatra fault	8
Figure 2.5 Map showing local earthquake locations and the lineaments at Bukit Tinggi area	11
Figure 2.6 Map showing location of seismic stations in Malaysia	12
Figure 2.7 Comparison of distance measures (Abrahamson and Shedlock, 1997)	20
Figure 3.1 Flow chart of research methodology	57
Figure 3.2 Map showing location and magnitude of distant earthquake events from July 2004 to July 2013	59
Figure 3.3 USGS Moment Tensor Solution for Sumatra megathrust earthquake on 26 December 2004 (USGS, 2013)	60
Figure 3.4 Chart of classification of source mechanism.	61
Figure 3.5 Graph of horizontal in E component time histories computed by MATLAB software by FRM station for Mw 6.8 event happened on 14 May 2005 originating from Northern Sumatera	64
Figure 3.6 Full set of MASW tools	66
Figure 3.7 Schematic diagram of MASW configuration at site	67
Figure 3.8 Collected accelerograph from the induced source (hammering)	68
Figure 3.9 Plot of phase velocity against frequency	68
Figure 3.10 Dispersion curve and quality factor (dotted line)	68
Figure 3.11 S-wave velocity against depth profile and $V_{S30}$	69

Figure 4.1 Classification of source mechanism from recorded distant earthquake events and ground motion data for Peninsular Malaysia.	78
Figure 4.2 S-wave velocity profile against depth for seismic stations in Peninsular Malaysia	81
Figure 4.3 Attenuation curves and recorded PGA by seismic stations located on Class C sites for interface subduction earthquakes	91
Figure 4.4 Attenuation curves and recorded PGA by seismic stations located on Class D sites for interface subduction earthquakes	96
Figure 4.5 Attenuation curves and recorded PGA by seismic stations located on Class C sites for intraslab subduction earthquakes	101
Figure 4.6 Attenuation curves and recorded PGA by seismic stations located on Class D sites for intraslab subduction earthquakes	106
Figure 4.7(a) Attenuation curves (active tectonic region) and recorded PGA by seismic stations located on Class C sites for strike-slip earthquakes	113
Figure 4.7(b) Attenuation curves (stable continental region) and recorded PGA by seismic stations located on Class C sites for strike-slip earthquakes	116
Figure 4.8(a) Attenuation curves (active tectonic region) and recorded PGA by seismic stations located on Class D sites for strike-slip earthquakes	118
Figure 4.8(b) Attenuation curves (stable continental region) and recorded PGA by seismic stations located on Class D sites for strike-slip earthquakes	121

# CHAPTER 1

## INTRODUCTION

### 1.1 General

Malaysia is located in seismically stable Sunda plate and has not experienced any disastrous earthquake occurrences. Because of this reason, there is no seismic code in Malaysia and most of our buildings and structures are designed without considering earthquake loading. However, due to the location close to two of the most seismically active plate boundaries, i.e. Indo-Australian and Eurasian plates, Malaysia has experienced numerous strong tremors caused by earthquakes in those two seismically active zones recently. This occurrence becomes more frequent in the last decade (Figure 1.1) with the increasing seismic activity since the major earthquake in Banda Aceh and the unprecedented Indian Ocean Tsunami in 2004. Even though Malaysia is located far from seismic sources, it has a substantial seismic risk from distant earthquakes to structures. Therefore, it is imperative to conduct a detailed site-specific seismic hazard assessment and investigate the potential risk from distant earthquake to Peninsular Malaysia.

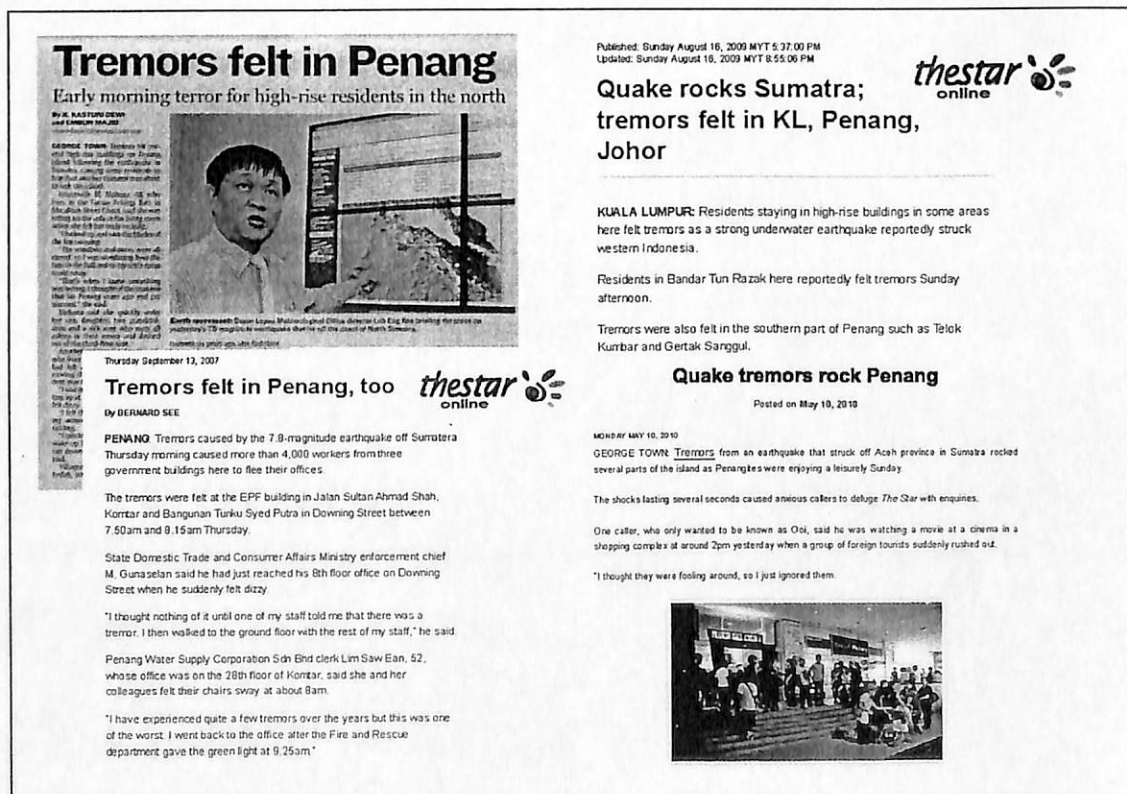


Figure 1.1 Newspaper reports on the tremor felt in Penang and Kuala Lumpur

Kuala Lumpur is the federal capital and most populous city in Malaysia. The city covers an area of 243 km<sup>2</sup> and has an estimated population of 1.6 million as of 2012. Greater Kuala Lumpur, also known as the Klang Valley, is an urban agglomeration of 7.2 million. It is among the fastest growing metropolitan regions in the country, in terms of population and economy. Penang is a state situated in northwest coast of Peninsular Malaysia. Georgetown is the capital of the state of Penang Island and is the second largest metropolitan in Malaysia by population. It is a highly urbanized and economically important state in Malaysia. The Northeast Penang Island District that covers 121 square kilometres has almost fully developed with high-rise buildings and important structures. Due to its close vicinity to Sumatra, numerous tremors have been experienced by the people especially the residents staying in high-rise buildings and some cracking on non-structural member of buildings are reported. Whenever moderate and strong earthquakes occur in Sumatra, tremors are felt and high-rise building dwellers flee their houses and scurry for safety. A growing population in these two cities calls for a need of a more reliable seismic design of structures. Distant earthquakes pose potential hazard to Peninsular Malaysia due in large part to the capability of the underlying soil to amplify earthquake ground motions. Thus, it is imperative to employ an appropriate seismic zone factor in the analysis and design of buildings and other infrastructures. This is to ensure a safe and sound environment.

This research is an independent assessment as well as confirmation of the probable earthquake ground motions in Peninsular Malaysia. Results of this study are critical factors in the formulation of seismic design criteria. As a fundamental step in seismic hazard analysis, a comprehensive evaluation of existing attenuation models is conducted for the main purpose of determining the most suitable model for the region. The possible earthquake ground motion that may induce a significant effect to the structures in the city is estimated by integrating as much information as possible to acquire a certain level of accuracy consistent with the available data.

## **1.2 Problem statement**

Regions of moderate to low seismicity such as Peninsular Malaysia are currently facing an intricate condition involving the prediction of probable seismic



hazard. Paucity of strong motion records in these areas hampers earthquake ground motion estimation as well as the conduct of a comprehensive regression analysis of available data. While it is fortunate to have low hazard, the associated seismic risk due to occasional but large earthquakes still exists. For this reason, the need to adopt appropriate attenuation relations arises that is able to approximately represent the geological and seismological conditions of the area under consideration. Even though few study on seismic hazard assessment have been conducted for the Peninsular Malaysia, the attenuation model developed for other countries are used in the analysis. The attenuation characteristic of seismic wave propagation is site specific and it can only be determined based on the recorded data at local sites.

### **1.3 Objective**

The objectives of this research are:

- i. To determine the most suitable attenuation model for Peninsular Malaysia
- ii. To provide a good estimate of the level of ground motion intensity in Penang and Kuala Lumpur

### **1.4 Scope of Work**

This research focuses on determining an appropriate existing attenuation model to be used in Peninsular Malaysia in predicting distant earthquakes. Hence, only distant earthquake events from Sumatra subduction and fault zone are considered in this study. The ground motion data utilised in this study was taken from July 2004 to June 2012 due to availability of time histories obtained from 19 seismic stations located in Peninsular Malaysia. Due to the fact that vertical acceleration diminished at faster rate and is insignificant at the distance more than 50 km, only the two horizontal component of PGA are utilised in this study. In addition, testing to obtain soil information of seismic stations in Peninsular Malaysia, where seismic data were obtained, will be carried out. Multichannel Analyses of Surface Wave (MASW) are conducted using Seismodule Controller software to obtain shear-velocity profile of ground where seismic stations sitting on. Computation of PGA using pre-selected existing attenuation models will be plotted for general graphical evaluation. On top of that, computed PGA will be compared with the collected actual seismic data in terms of root means square of errors (RMSE) in order to determine the prediction that has the least deviation from real ground motion data.

## CHAPTER 2

### LITERATURE REVIEW

#### 2.1 Tectonic setting of Peninsular Malaysia and its seismicity

Peninsular Malaysia is located on the stable Sunda plate. Sunda plate and Burma plate are the subplates of the Eurasian plate. Referring to the seismic hazard map for Peninsular Malaysia as shown in Figure 2.1, Peninsular Malaysia is considered having low seismicity. Based from the quantity and intensity of historical earthquake events, Peninsular Malaysia is more likely to be affected by far field earthquake generated at the neighbouring country, Indonesia, than local earthquake.

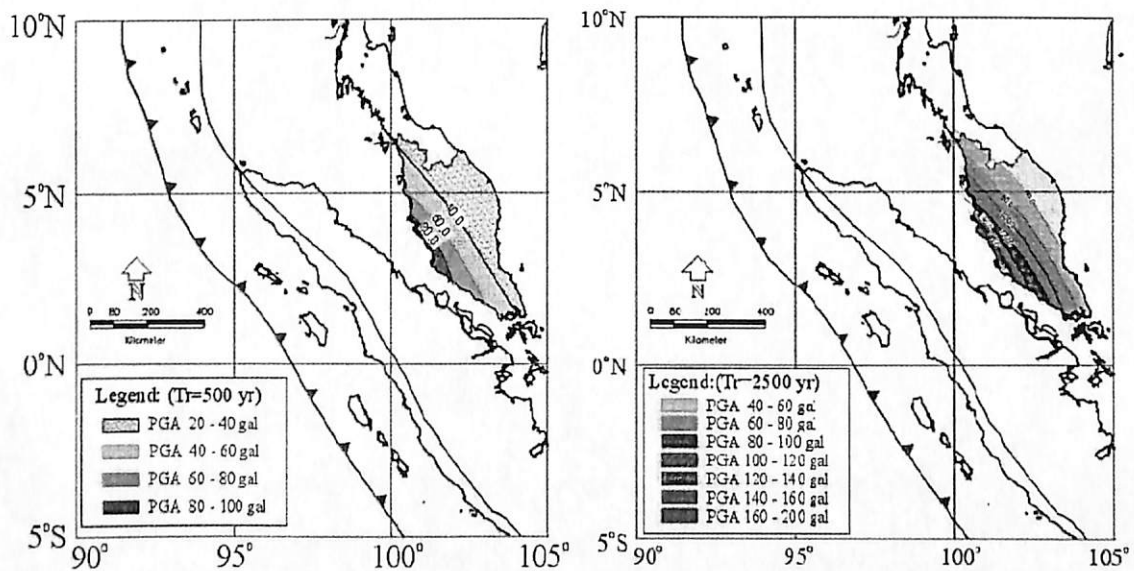


Figure 2.1 Seismic hazard map of Peninsular Malaysia (site class  $S_B$ )  
(Adnan et al., 2011)

##### 2.1.1 Far field earthquake

Indonesia, one of Malaysia's neighbouring countries, is well-known for its high seismic activity. Sumatera Island has been reported numerous times for producing large earthquakes that never fail to shock the world. According to database from United States Geological Survey (USGS), the top 17 deadliest earthquakes, exceeding magnitude of 8.5, that ever happened since 1900 are as listed in Table 2.1. Out of the 17 earthquakes listed, there are four earthquakes originated from Sumatera, Indonesia, regardless of the southern or northern regions. Thus, the Sumatera region is the mod in the top 17 earthquakes list.

Table 2.1 Top 17 largest earthquakes around the globe since year 1900  
(USGS, 2011)

No.	Location	Date (UTC)	$M_w$	Coordinate	
				°N	°E
1.	Chile	22/05/1960	9.5	-38.29	-73.05
2.	1964 Great Alaska Earthquake	28/03/1964	9.2	61.02	-147.65
3.	Off the West Coast of Northern Sumatera	26/12/2004	9.1	3.30	95.78
4.	Near the East Coast of Honshu, Japan	11/03/2011	9.0	38.322	142.369
5.	Kamchatka	04/11/1952	9.0	52.76	160.06
6.	Offshore Maule, Chile	27/02/2010	8.8	-35.846	-72.719
7.	Off the Coast of Ecuador	31/01/1906	8.8	1.0	-81.5
8.	Rat Islands, Alaska	04/02/1965	8.7	51.21	178.50
9.	Northern Sumatera, Indonesia	28/03/2005	8.6	2.08	97.01
10.	Assam, Tibet	15/08/1950	8.6	28.5	96.5
11.	Off the West Coast of Northern Sumatra	11/04/2012	8.6	2.311	93.063
12.	Andreanof Islands, Alaska	09/03/1957	8.6	51.56	-175.39
13.	Southern Sumatera, Indonesia	12/09/2007	8.5	-4.438	101.367
14.	Banda Sea, Indonesia	01/02/1938	8.5	-5.05	131.62
15.	Kamchatka	03/02/1923	8.5	54.0	161.0
16.	Chile-Argentina Border	11/11/1922	8.5	-28.55	-70.50
17.	Kuril	13/10/1963	8.5	44.9	149.6

Earthquake activity around Sumatra is not only contributed by a single source but many. These sources are thrust earthquakes on the subduction fault, strike-slip earthquakes on the Sumatra fault, in-slab earthquakes within the subduction lithosphere, and volcanic earthquakes. Compare to the rest, volcanic earthquake are rather less significant in exerting distant tremors. The most prominent sources of earthquakes are the Sumatra subduction zone and Sumatra fault zone. Figure 2.2 shows the location of Peninsular Malaysia in relative to Sumatra subduction zone and Sumatra faults.

#### 2.1.1.1 Sumatra subduction zone

Sumatra subduction zone, which is also locally known as Sunda subduction zone or Sunda trench, is a convergent belt extending more than 1600 km from Himalayan to Java and the Sunda Islands. It passes through south of Myanmar, and continues running down near west of Andaman and Nicobar Islands to Sumatra and

finally stretching coastwise the south of Java. Lithosphere of Indian Ocean seafloor is denser than continental Australian lithosphere. Thus, the subduction of the Indian-Australian plate into the Burma and Sunda subplates is in a highly oblique motion and becoming normal in front of Java. Generally, the Indian-Australian plate moves northward of about 40 to 50 mm/year (Sieh et al., 1999; Lay et al., 2005). The highly oblique motion is the root of the slip-partitioning process at the plate boundary, where two separate faults are needed to share the shear force instead of only one fault. While one fault predominated by dip-slip components and a little of strike-slip component, the other fault encounters purely strike-slip components. This denotes the Sumatra subduction zone as the former type of fault and Sumatra fault zone as the later type (Fitch, 1972). As shown in Figure 2.3, there is a wedge of forearc in between these two zones, known as silver plate. The motion rate of the silver plate and deformation within itself is highly unpredictable, especially in the Andaman section. Hence, the subduction vector is hard to be resolved (McCaffrey, 2009).

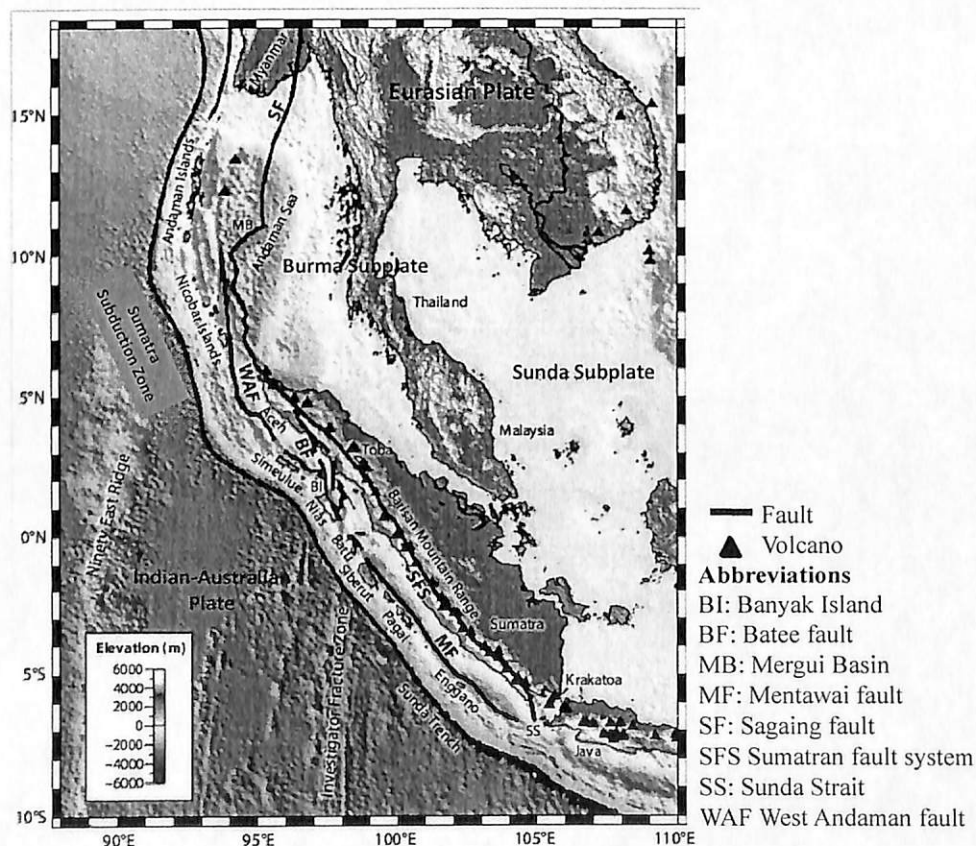


Figure 2.2 Regional map showing the tectonic setting and faults in Sumatra (McCaffrey, 2009)

The Australia plate thrust beneath Sunda subplate at a greater depths compare to the north of the trench. Therefore, the region near Java is seismically active to a depth up to 650 km, which is prone to produce intermediate-depth to deep-focus earthquakes (USGS, 2007). On the other hand, the northern Sumatra subduction zone generally produces shallower events. Sumatra subduction zone, both northern and southern, has generated a few massive historical earthquakes, such as in 1797 event ( $M \sim 8.4$ ), 1833 event ( $M_W$  8.75), 1861 event ( $M_W$  8.4), 1881 event ( $M \sim 7.9$ ), 2004 event ( $M_W$  9.1), 2005 event ( $M_W$  8.6) and 2007 event ( $M_W$  8.4).

There are a total of 19 subduction zones in the world. However, there was only little attention received by Sumatran subduction zone compared to other subduction zones around the world before the earthquake and tsunami incident on 26 December 2004 (Lay et al., 2005). This is due to lower seismic activities generated

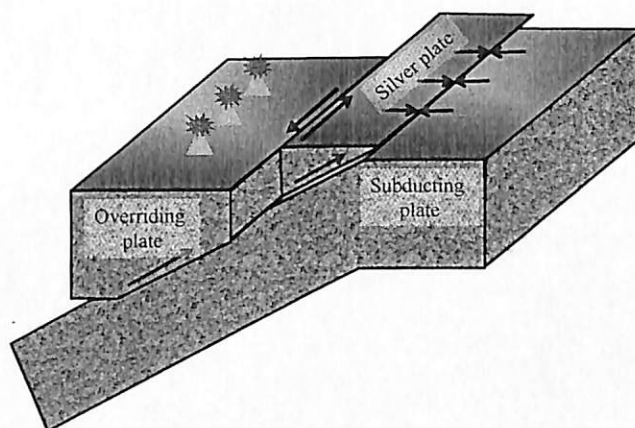


Figure 2.3 Block diagram showing slip-partitioning process and motion of silver plate under oblique movement of subducting plate beneath overriding plate (McCaffrey, 2009)

prior to that. It has been reported that the event has ruptured 1200 to 1300 km of a curved plate boundary and consequently altered the nature of the faulting. Since then, a series of moderate to large subduction earthquake events from the zone strikes more frequently. In addition, the fault alteration has also triggered more earthquakes to arise from surrounding fault, such as Sumatra fault. Potential slip width of the Sumatra subduction zone is the largest among 19 subduction zones in the world (Pacheco et al., 1993). Moreover, Pacheco et al. (1993) also found that the southern Java yielded the deepest underthrust earthquakes over the whole globe. These imply



that Sumatra subduction zone possesses a great potential in producing more and more massive earthquakes.

#### 2.1.1.2 Sumatran fault zone

As a result of oblique convergence of Indian-Australian plate into Eurasian plate, the Sumatra active fault accommodates a substantial amount of right lateral motion. Compare to the complicated neighbouring subduction zone, the Sumatra fault has a rather simple basic kinematic role, which is strike-slip motion. It has a slip rate ranges from 11 mm/year at southern fault to 27 mm/year at the northern part of the fault. The 1900-km-long fault that runs along the length of Sumatera Island, Indonesia were divided into 19 geometrically defined segments by Sieh and Natawidjaja (2000) as shown in Figure 2.4 and Table 2.2.

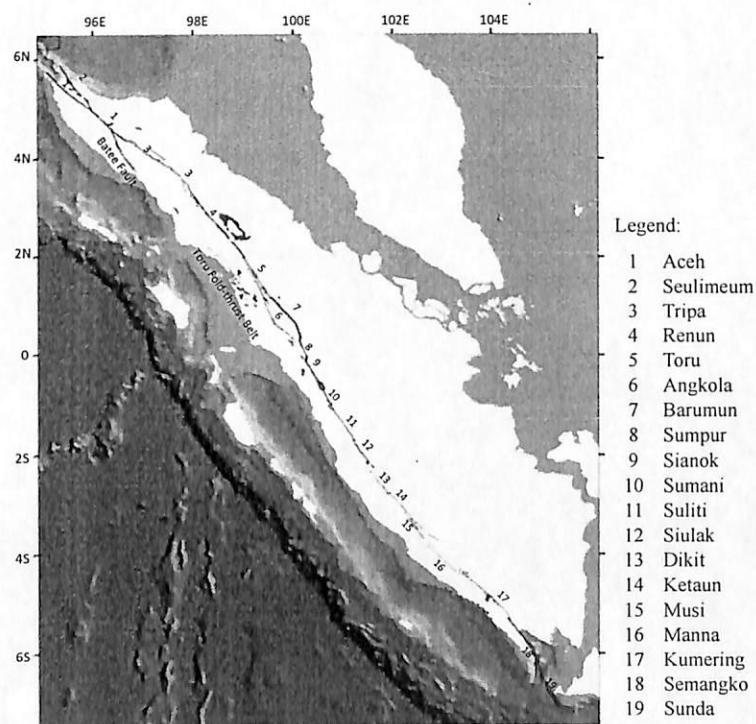


Figure 2.4 Map showing 19 segments of Sumatra fault

Due to these fault discontinuities, magnitude of earthquakes occurred in these segments is often limited under  $M_W$  7.8 (Balendra et al., 2002). The largest earthquake ever generated by this fault is in 1892 ( $M_W$  7.7) that produced dislocations of at least 2 m (Reid, 1913). However, the closest distance from

earthquake sources in this fault to the west coast of Peninsular Malaysia is about 260 km in 2011. Consequently, tremors could be felt in west Peninsular Malaysia when earthquake larger than  $M_W$  5.0 arise from this fault. Petersen et al. (2004) reported more than 42 earthquakes with  $M_W$  5.0 originated from this fault in the last 40 years. More than 1000 crustal events ranging  $M_W$  1.0 to  $M_W$  6.0 between April 2008 and February 2009 were also registered by Weller et al. (2012). In addition, this fault is an active surface strike-slip fault (Santosa, 2010). This amount and type of earthquakes as well as tremors not only brought outnumber loss of properties and casualties in Indonesia but also insecurity and discomfort to public in Malaysia.

Table 2.2 Major Segments of Sumatra Fault (Sieh and Natawidjaja, 2000; Natawidjaja and Triyoso, 2007; Madlazim and Santosa, 2010)

No.	Segment	Latitude	Length(km)	Large Historical Earthquakes
1	Aceh	4.4°N-5.4°N	200	No record
2	Seulimeum	5.0°N-5.9°N	120	1964 ( $M_S$ 6.5)
3	Tripa	3.4°N-4.4°N	180	1990 ( $M_S$ 6), 1997 ( $M_W$ 6)
4	Renun	2.0°N-3.5°N	220	1916, 1921 ( $m_b$ 6.8), 196 ( $M_S$ 7.2)
5	Toru	1.2°N-2.0°N	95	1984 ( $M_S$ 6.4), 1987 ( $M_S$ 6.6)
6	Angkola	0.3°N-1.8°N	160	189 ( $M_S$ 7.7)
7	Barumun	0.3°N-1.2°N	125	No record
8	Sumpur	0°-0.3°N	35	No record
9	Sianok	0.7°S-0.1°S	90	1822, 1926 ( $M_S$ 7)
10	Sumani	1.0°S-0.5°S	60	1943 ( $M_S$ 7.4), 1926 ( $M_S$ 7)
11	Suliti	1.75°S-1.0°S	95	1943 ( $M_S$ 7.4)
12	Siulak	2.25°S-1.7°S	70	1909 ( $M_S$ 7.6), 1995 ( $M_W$ 7.0)
13	Dikit	2.75°S-2.3°S	60	No record
14	Ketaun	3.35°S-2.75°S	85	1943 ( $M_S$ 7.3), 1952 ( $M_S$ 6.8)
15	Musi	3.65°S-3.25°S	70	1979 ( $M_S$ 6.6)
16	Manna	4.35°S-3.8°S	85	1893
17	Kumering	5.3°S-4.35°S	150	1933( $M_S$ 7.5), 1994 ( $M_W$ 7.0)
18	Semangko	5.9°S-5.25°S	65	1908
19	Sunda	6.75°S-5.9°S	~150	No record

### 2.1.2 Local earthquake within Peninsular Malaysia

In addition to tremors resulting from the neighbouring country, Peninsular Malaysia also experiences small magnitude local earthquakes. There were a series of small magnitude earthquakes generated from the Bukit Tinggi area in 2007 and 2008, as listed in Table 2.3. These earthquakes fell within a magnitude range of 1.7 to 3.7, which were considered mild. There was no property damage reported. Figure 2.5 shows that Bukit Tinggi area consists of 5 sets of distinct lineaments, that are, NW-SE fault, N-S fault, NE-SW fault, ENE-WSW fault and a less prominent E-W fault (Shuib, 2009).

Table 2.3 Details of earthquakes around Bukit Tinggi area (MMD, 2008)

No.	Date	Time (MST)	Latitude	Longitude	Magnitude ( $m_b$ )	Depth (km)
1.	30/11/2007	10.13 am	3.36°N	101.80°E	3.5	2.3
2.	30/11/2007	10.42 am	3.34°N	101.80°E	2.8	<10
3.	30/11/2007	08.42 pm	3.31°N	101.84°E	3.2	6.7
4.	04/12/2007	06.12 pm	3.40°N	101.80°E	3.0	<10
5.	05/12/2007	03.57 am	3.37°N	101.81°E	3.3	<10
6.	06/12/2007	11.23 pm	3.36°N	101.81°E	2.7	<10
7.	09/12/2007	08.55 pm	3.33°N	101.82°E	3.5	4.9
8.	12/12/2007	06.01 pm	3.48°N	101.76°E	3.2	<10
9.	31/12/2007	05.19 pm	3.32°N	101.81°E	2.5	<10
10.	10/01/2008	11.38 pm	3.39°N	101.73°E	3.0	<10
11.	13/01/2008	10.24 am	3.30°N	101.90°E	2.9	<10
12.	13/01/2008	06.18 pm	3.30°N	101.80°E	2.5	<10
13.	13/01/2008	11.59 pm	3.40°N	101.86°E	1.9	3.0
14.	14/01/2008	11.45 pm	3.42°N	101.79°E	3.4	<10
15.	15/01/2008	06.24 am	3.63°N	101.24°E	2.9	<10
16.	15/01/2008	12.41 pm	3.35°N	101.77°E	2.5	<10
17.	15/03/2008	08.50 am	3.30°N	101.70°E	3.3	<10
18.	15/03/2008	07.35 am	3.50°N	101.80°E	1.8	<10
19.	15/03/2008	07.16 am	3.30°N	101.70°E	2.8	<10
20.	27/03/2008	09.46 am	3.80°N	102.40°E	3.0	<10
21.	25/05/2008	09.36 am	3.31°N	101.65°E	3.0	<10



It is believed that the rising of the earthquake events from those hidden faults are due to the deformation of Sundaland core as a result from the Sumatran megathrust earthquake on 26 December 2004. Though so, lacking of solid evidences suspends the ascertainment of the relationship between earthquakes and geologically mapped faults in Bukit Tinggi area.

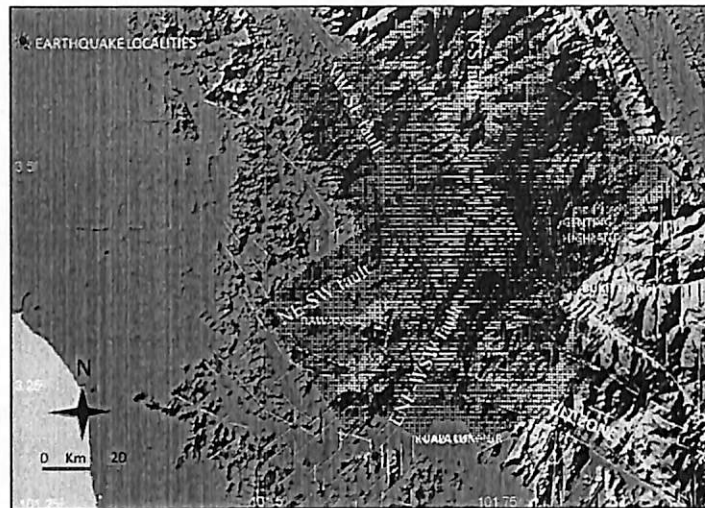


Figure 2.5 Map showing local earthquake locations and the lineaments at Bukit Tinggi area

## 2.2 Seismicity network in Malaysia

MMD serves as a seismology center providing seismological information in Malaysia. Through funding from United Nations Educational, Scientific and Cultural Organization (UNESCO) in 1979, the first four recording instruments installed in Malaysia were short period seismographs at Petaling Jaya, Kluang, Ipoh and Kota Kinabalu (Che Abas, 1998). Presently there are a total of 30 seismic stations distributed throughout the whole country. As shown in Figure 2.6, ten of them are in East Malaysia and the rest in Peninsular Malaysia.

Two of the seismic stations are located inside the Putrajaya building, where one placed at the basement and another at the 9<sup>th</sup> level of the building. All these stations provide real time and three-component digital seismic data via Very Small Aperture Terminal (VSAT) satellite to the central processing center at Malaysian Meteorological Department Headquarters in Petaling Jaya for processing and

analysis. Table 2.4 shows the geographical and geological information of seismic stations in Malaysia. Among all the seismic stations, 7 broadband stations are contributing real-time waveform data for regional and international exchange. Those stations are KUM, IPM, KOM, KSM, SBM, KKM, and LDM.

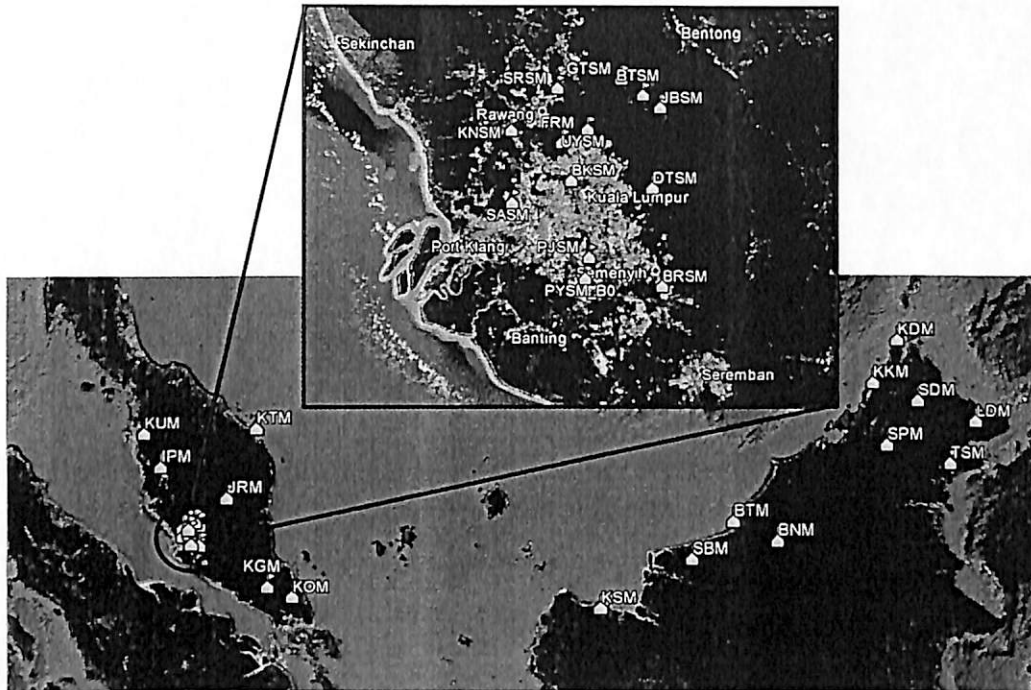


Figure 2.6 Map showing location of seismic stations in Malaysia

### 2.3 Ground motion attenuation models

Seismic waves that propagate inside the ground will eventually cause damaging effect on structure or human on the ground surface if the seismic waves manage to reach area with dense population or of high economic importance. To reduce the impact and damaging effects of earthquakes, incorporation of the likelihood of the called seismic hazard assessment. Evaluation of seismic hazard assessment, no characteristics of future earthquake ground motions in a given seismic area into seismic design is essential. This evaluation process of prediction is matter deterministic or probabilistic, requires the use of attenuation relationships.

Table 2.4 Codes, locations and geology of Malaysia Meteorological Department seismic stations (MMD, 2012)

No.	Station Code	Station Name	Latitude	Longitude	Foundation	Elevation
1	KUM	Kulim	5.29 N	100.65 E	Granite	74
2	IPM	Ipoh	4.58 N	101.03 E	Granite	247
3	FRM	Frim Kepong	3.24 N	101.63 E	Granite	97
4	KTM	Kuala Terengganu	5.33 N	103.14 E	Meta Sedimen	33
5	KGM	Kluang	2.01 N	103.32 E	Granite	103
6	KOM	Kota Tinggi	1.79 N	103.85 E	Granite	49
7	JRM	Jerantut	3.89 N	102.48 E	Sandstone	55
8	BNM	Bakun	2.78 N	114.03 E	Sandstone	166
9	SPM	Sapulut	4.71 N	116.46 E	Sandstone	275
10	KSM	Kuching	1.47 N	110.31 E	Volcanic Rock	66
11	SBM	Sibu	2.45 N	112.21 E	Sandstone	237
12	BTM	Bintulu	3.21 N	113.10 E	Sandstone	156
13	KKM	Kota Kinabalu	6.04 N	116.21 E	Sandstone	830
14	KDM	Kudat	6.94 N	116.80 E	Granite	3
15	SDM	Sandakan	5.64 N	117.19 E	Sandstone	463
16	TSM	Tawau	4.29 N	117.87 E	Granite	62
17	LDM	Lahad Datu	5.18 N	118.50 E	Sandstone	177
18	PYSM_B0	Putrajaya Basement	2.92 N	101.68 E	Granite	-10
19	PYSM_B9	Putrajaya Level 9	2.92 N	101.68 E	Concrete Floor	76
20	BKSM	Bukit Kiara	3.15 N	101.65 E	Soft Soil	66
21	SASM	Shah Alam	3.10 N	101.51 E	Soft Soil	28
22	GTSM	Goh Tong Jaya	3.39 N	101.77 E	Rocky	844
23	JBSM	Janda Baik	3.32 N	101.86 E	Rocky	577
24	KNSM	Kundang	3.27 N	101.51 E	Soft Soil	27
25	SRSM	Serendah	3.37 N	101.62 E	Soft Soil	61
26	BRSM	Beranang	2.90 N	101.86 E	Rocky	73
27	DTSM	Dusun Tua	3.13 N	101.84 E	Rocky	67
28	PJSM	Wetland, Putrajaya	2.97 N	101.69 E	Soft Soil	45
29	UYSM	Ulu Yam	3.27 N	101.69 E	Soft Soil	84
30	BTSM	Bukit Tinggi	3.35 N	101.82 E	Soft Soil	322

Nowadays, probabilistic seismic hazard analysis is more preferable as it take account of uncertainties of all variables. Thus, attenuation model with high uncertainties provide relatively undependable values. This, in turn, can lead to high probabilistic ground motion estimates at long return period (Zhao et al., 2006).

Being a crucial element of seismic hazard studies, many attenuation relations have been developed over the years. Basic understanding about attenuation relations is important for the selection of which models to be used for seismic hazard analysis.

### 2.3.1 Theoretical background

An attenuation model is a mathematical-based equation that expresses the relation of a specific ground motion to seismological parameters of the earthquake source (Campbell, 2003). The seismological parameters quantitatively characterising the source mechanism or faulting, wave propagation path between source to site and local site conditions. The typical fundamental form of an attenuation model is expressed (Lee et al., 2002) as:

$$\ln Y = c_1 + c_2 M - c_3 \ln R - c_4 r + c_5 F + c_6 S + \varepsilon \quad (2-1)$$

where,

$Y$	=	ground motion parameter of interest
$M$	=	magnitude
$r$	=	source-to-site distance
$R$	=	distance term given in other form
$F$	=	parameter characterising type of faulting
$S$	=	parameter expressing the geological or soil profiles of the site
$\varepsilon$	=	random error term at zero mean
$\sigma \ln Y$	=	standard deviations of estimates of $\ln Y$ , represented by the symbol
$c_1, c_2, \dots c_6$	=	Coefficients of regression analysis

Other than the form of attenuation model mentioned, there are also alternative forms of attenuation models. Suitability of these forms is determined by the epistemic uncertainty in the estimate of median ground motion. Table 2.5 lists alternative form of attenuation models.

### 2.3.2 Derivation of attenuation models

Generally, there are four methods used to obtain a ground motion relationship. The most common method is empirical method, which is based solely on historical earthquake data. This method requires abundant actual historical earthquake data in order to obtain statistically reliable results. Therefore, it can only be developed in regions where abundance of earthquake data was well-recorded such as Japan,

Table 2.5 List of alternative functional form of median ground motion attenuation models (EPRI, 2004)

No.	Functional form
1.	$\ln Y = c_1 + c_2 m - (c_3 + c_4 m) \times \ln(d_{JB} + e^{c_5}) + c_6 (m - m_1)^2$
2.	$\ln Y = c_1 + c_2 m - (c_3 + c_4 m) \times \ln(d_{JB} + e^{c_5}) + c_6 (m - m_1)^2 + (c_7 + c_8 m) d_{JB}$
3.	$\ln Y = c_1 + c_2 m - c_3 m^2 + (c_4 + c_5 m) \times \min \{ \ln(r), \ln(r_1) \} + (c_6 + c_7 m) \times \max \{ \ln(r / r_2), 0 \} + c_8 r$ $r = \sqrt{d_{JB}^2 + h^2}$ $h = e^{(c_9 + c_{10} m)}$
4.	$\ln Y = c_1 + c_2 m + c_3 (m_1 - m)^2 + c_4 \ln[f_1(m, d_{CD})] + f_2(d_{CD}) + (c_9 + c_{10} m) d_{CD}$ $f_1(m, d_{CD}) = \sqrt{d_{CD}^2 + (c_5 e^{c_6 m})^2}$ $f_2(d_{CD}) = 0 \quad ; \text{ for } d_{CD} \leq r_1$ $= c_7 \{ \ln(d_{CD}) - \ln(r_1) \} \quad ; \text{ for } r_1 < d_{CD} \leq r_2$ $= c_7 \{ \ln(d_{CD}) - \ln(r_1) \} + c_8 \{ \ln(d_{CD}) - \ln(r_2) \} \quad ; \text{ for } d_{CD} \geq r_2$
5.	$\ln Y = c_1 + c_2 (m - m_1) + c_3 \ln(d) + c_4 (m - m_1) \ln(d) + c_5 d_{JB} + c_7 (m_2 - m)^2 \quad ; \text{ for } d_{JB} < r_1$ $\ln Y = c_1 + c_2 (m - m_1) + c_3 \ln(d_1) + c_4 (m - m_1) \ln(d) + c_5 d_{JB} + c_6 (\ln(d) - \ln(d_1)) + c_7 (m_2 - m)^2 \quad ; \text{ for } d_{JB} \geq r_1$ $d = \sqrt{d_{JB}^2 + h^2}$ $d_1 = \sqrt{r_1^2 + h^2}$

Note:  $m$  is moment magnitude,  $d_{JB}$  is Joyner-Boore distance and  $d_{CD}$  is the closest distance to fault rupture.

California, New Zealand, Italy and Alaska. This is the method pioneering the development of attenuation models. Due to its simplicity and its ability to account aleatory of variability and epistemic variability, this is the most popular method to obtain the relationship. According to Toro et al. (1997), epistemic variability, which is also known as uncertainty, is due to the incomplete understanding about the mechanism of an earthquake. It can be reduced by providing more additional data.

Conversely, aleatory variability can be defined as uncertainty to unpredictable nature of future events. It corresponds to distinctive details of source, path and site response which is not able to be identified before an earthquake occurs. It is also sometimes referred as 'randomness'

Following the existence of empirical method, intensity method is introduced to account for regions with scarce earthquake data. This method assumes relationship between ground motions to be estimated and intensity, such as MMI or MSK intensity. However, one of the disadvantages of this method is that the developed relationship relied on the subjective measurement of observer regarding the intensity. Though this method was once frequently used, it has been found to have considerable uncertainties (Dahle et al., 1990). Thus, many other methods have been employed over this method for regions that lack of ground motion data to avoid uncertainties which affect the reliability of the results.

For places where historical ground motion recordings are sparse but good seismological network data are available, theoretical method can be used. This method is initiated by a careful selection of good-quality seismological parameters. Then, a simple seismological model is derived to describe the relationships of ground motions with earthquake source size and source-to-site distance. This method has been used in many regions in the world where strong ground motion data is limited. However, this method gives high possibility in underestimating the epistemic uncertainties as the method rely solely based on a common method (Campbell, 2003). Furthermore, attenuation model developed using this method might not fully represent characteristics of ground motion that are implicit in empirical attenuation relations.

The last method in developing a ground motion relation is the hybrid-empirical method. It was first introduced by Campbell (1981). Theoretical adjustment factors based on simple seismological models from ground motion estimates by using empirical ground motion relations for a host region, very often regions with abundant ground motion data (e.g. Eastern North America), to account for differences in target regions (e.g. Western North America). One of the advantages of this method is its ability to account for aleatory variability and epistemic uncertainty in estimating

ground motions. It relies on empirical model, indicating its accountability for the characteristics of ground motion inherent in empirical model rather than just solely depend on theoretical assumptions.

Peninsular Malaysia has low number of recorded ground motion data. Due to this matter, development of ground motion attenuation model specifically for Peninsular Malaysia could be a tough task. Epistemic variability of a ground motion attenuation model for a low seismicity region like Peninsular Malaysia could be easily overlooked. Among the four methods mentioned above, theoretical and hybrid empirical method are more suitable for Peninsular Malaysia if provided with good seismological parameters (Campbell, 2003; Megawati et al., 2005).

Despite all the shortcomings and difficulties for each method in developing ground motion attenuation model, Adnan et al. (2004) and Nabilah and Balendra (2012) had developed ground motion attenuation model using empirical method specifically for Peninsular Malaysia. A few ground motion attenuation models based on theoretical method have also been developed for Peninsular Malaysia and Singapore, a neighbouring country of Malaysia which has similar seismicity condition with Peninsular Malaysia (Megawati et al., 2003; Megawati et al., 2005; Megawati and Pan, 2010). These models have been tested and compared with actual recorded ground motion up to year 2008 in a study by Husen et al. (2008) and Petersen et al. (2004) was found to be able to give closest prediction to recorded ground motion instead of the models mentioned above. Nonetheless, applicability of these models has yet to be tested with up-to-date recorded ground motion data in Peninsular Malaysia. In another study, the proposed PGA values by Hendriyawan (2010) for western Peninsular Malaysia using probabilistic approach based on Adnan et al. (2004) model was said too high compared to actual recorded PGA provided by MMD (Jeffrey and Mun, 2011).

### **2.3.3 Factors affecting attenuation**

There are five primary factors affecting estimates of ground motion by an attenuation relation. They are tectonic setting, type of faulting and focal mechanism,

magnitude, source-to-site distance and site condition. Additional parameters can be estimated as amount of ground motion data increases.

#### **2.3.3.1 Tectonic setting**

There are three major types of tectonic settings. They are shallow crustal in active tectonic regions, shallow crustal in stable continental regions and subduction zones. According to Abrahamson and Shedlock (1997), seismic waves from subduction earthquakes were proved by various studies, for example Youngs et al. (1997) and Atkinson and Boore (2003), to attenuate slower than those from crustal earthquakes. Thus, it is more appropriate to develop attenuation model for these tectonic settings separately.

#### **2.3.3.2 Type of faulting and focal mechanism**

Type of faulting and focal mechanism depicts the orientation of the slip on the fault plane, which is characterised by the rake angle and dip angle. Generally, there are five types of faulting that defined by the slip angle, namely reverse, thrust, strike-slip, normal and vertical faulting. The values of slip angle for pure form of each of these mechanisms are  $0^\circ$  for left-lateral strike slip,  $180^\circ$  for right-lateral strike slip,  $90^\circ$  for reverse faulting, and  $270^\circ$  for normal faulting (Lay and Wallace, 1995). Spudich et al. (1999) assured the differences in source mechanism cause differences in ground motion through theoretical study of Oglesby et al. (1998) and the lab study by Brune and Anooshehpour (1999).

#### **2.3.3.3 Magnitude**

Magnitude is defined as the logarithm of certain peak ground motion parameter. The most widely used magnitude scales are  $M_L$ ,  $M_S$ ,  $m_b$ , and  $M_W$ . Due to the ability of  $M_W$  to withstand saturation at larger earthquakes, it is more favourable compare to the rest of magnitude scales. However, other magnitude scales were introduced earlier than  $M_W$  and were used in former development of ground motion attenuation models. Consequently, many attempts in converting other magnitude scales to  $M_W$  scale were carried out to promote standardisation. Some examples of developed magnitude conversion equations can be found in Sipkin (2003), Scordilis (2006),



Idriss and Archuleta (2005) and Das et al. (2011). It should be noted that each magnitude conversion is dependent on the number of earthquake events adopted, distribution of size of earthquakes, process of selecting earthquakes and analysis method adopted. Thus, it is sensible that the suitability of a magnitude conversion equation should be tested with earthquake event which the moment magnitude is known.

#### 2.3.3.4 Source-to-site distance

There are several distance measures introduced and commonly used in ground motion prediction models. Each distance measure has its own strength and weakness and their suitability is highly dependent on the characteristics of earthquake source. They can be classified into two main categories, namely point-source distance measures and finite-source distance measures.

Point-source distance measures are the simpler distance measures. Examples of point source distance measures are: epicentral distance ( $r_{epi}$ ); hypocentral distance ( $r_{hypo}$ ); distance to rupture centroid ( $r_c$ ); distance to energy center ( $r_E$ ). Epicentral distance is the distance from the site to the point on the Earth's surface directly above the hypocenter. Hypocentral distance is defined as distance from the site to the point within the Earth where the earthquake rupture initiated (the hypocentre). The value of  $r_{hypo}$  can be simply calculated using the following expression:

$$r_{hypo} = \sqrt{r_{epi}^2 + h_{hypo}^2} \quad (2-2)$$

where,

$h_{hypo}$  = depth from the Earth surface to the hypocentre (focal depth).

Distance to rupture centroid ( $r_c$ ) was first used in Zhao et al. (1997) while distance to energy centre ( $r_E$ ) was first appeared in Milne and Davenport (1969). Both  $r_c$  and  $r_E$  are not so popular and seldom being used in attenuation models.

Three of the most commonly used finite-source distance measures involves closest distance to the rupture plane are: closest horizontal distance to the vertical

projection of rupture plane ( $r_{jb}$ ) which also sometimes referred as Joyner-Boore distance (Joyner and Boore, 1981); closest distance to rupture surface ( $r_{rup}$ ) (slant distance) which was introduced by Schnabel and Seed (1973); distance to seismogenic rupture place ( $r_{seis}$ ). The  $r_{seis}$  was introduced by Campbell (1987; Campbell, 2000). It assumes near-surface rupture in sediments is non-seismogenic. Among the three finite-source distance measures,  $r_{jb}$  is the easiest to be used for future earthquake predictions.

Figure 2.7 illustrates definitions and compares of some of the distance measures. The closest distance measures are more preferable over point-source distances for large-magnitude earthquakes. The point source distances are normally used for small earthquakes when the fault-rupture plane cannot be identified for past or future earthquakes (Lee et al., 2002).

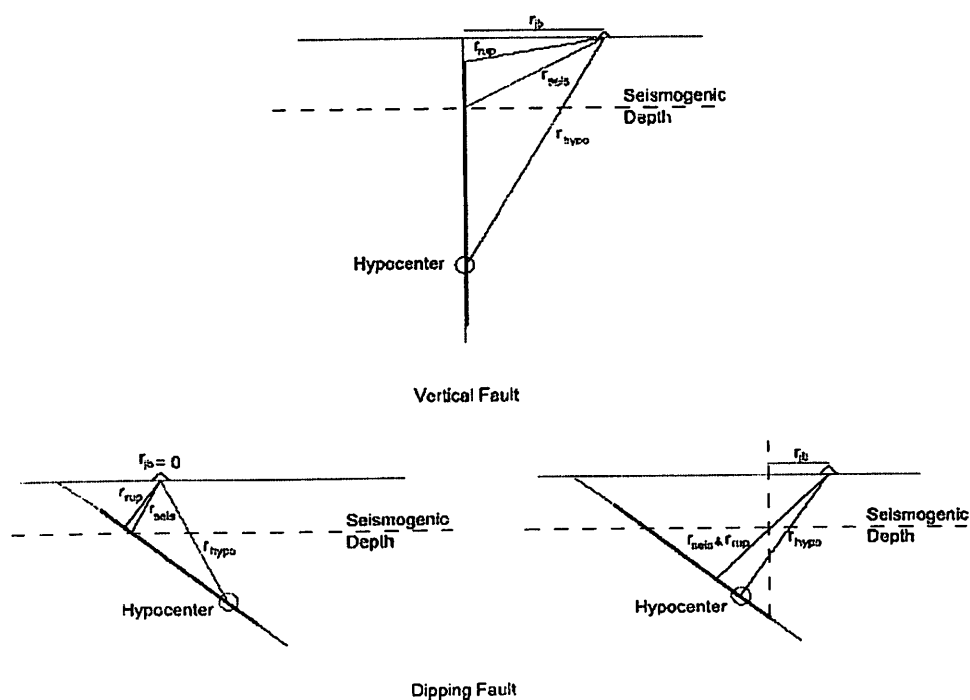


Figure 2.7 Comparison of distance measures (Abrahamson and Shedlock, 1997)

### 2.3.3.5 Site condition

The degree of earthquake force to the ground surface is very much depending on the state of aggregation of the terrain which the wave passes through. Site factors considers geological and properties of the surface topography underlying the

recording stations. There are many methods introduced in defining site classes since more than 30 years ago.

Back to the period between 1976 till 1994 when information regarding properties of ground is scarce, geology, stiffness and depth of soil at site are used to define site classes (Dobry et al., 2000). As an example, Joyner and Boore (1981) proposed a simple binary site classification method where they split local sites into two categories, namely rock and soil sites, based on visual inspection on geology. Sites described as granite, diorite, gneiss, chert, greywacke, limestone, sandstone or siltstone are considered as rock while soil sites are referring to alluvium, sand, gravel, clay, silt, mud, fill, or glacial outwash. For site with soil material less than 4 to 5 m thick overlying rock, it is classified as rock site.

Nowadays, most of the attenuation models developed after 1997 used average shear-wave velocity in the upper 30 m of site profile,  $V_{S30}$  as an approach in distinguishing sites into classes. The parameter  $V_{S30}$  is introduced to avoid ambiguous site measurement and classification. It is normally obtained from in-situ measurement or is deduced from borelog and geological map when in-situ measurement is inaccessible.  $V_{S30}$  is defined by Eq. 2-3:

$$V_{S30} = \frac{30}{\sum_{i=1}^n \frac{d_i}{v_{si}}} \quad (2-3)$$

where,

- $v_{si}$  = shear wave velocity of each layer having distinctly different soil layers (m/s)
- $d_i$  = Thickness of any layer between 0 to 30 m from the earth's surface
- $n$  = number of layers in the upper 30m
- $i$  = any one of the layers between 1 to n layers

The  $V_{S30}$  actually has been spotted being applied in Boore et al. (1993). However, Boore et al. (1933) only provide four site classes and was being modified to be incorporated into National Earthquake Hazards Reduction Program (NEHRP)

1997. International Building Code (IBC) 2000 has adopted site classification method as proposed by NEHRP (1997) as shown in Table 2.6 (ICC, 2000). If  $V_{S30}$  is not known, standard penetration resistance (N), undrained shear strength of soils ( $S_u$ ), plasticity index (PI) and water content ( $w$ ) can also be used to determine site classes. It should be noted that Class A and B shall not be used if there is more than 3 m of soil between rock surfaces.

There are also other guidelines adopting  $V_{S30}$  to determine site classes, such as EPRI (1993) and Eurocode 8 (2004). However, they provide different definition of site classes based on the ranges of  $V_{S30}$ . On the other hand, Geomatrix site classification, which was used by Abrahamson and Silva (1997), proposed a rather different definition and method by incorporating both qualitative and quantitative classification scheme. Comparison of some site classifications was listed and compared by Abrahamson (1996).

#### **2.3.3.6 Other factors**

There is no universal guideline or standard to be followed to derive an attenuation model. Thus, the selection of factors is not a confined process and is a personal choice. Other factors that may influence the attenuation rate of an attenuation model are stress drop, hanging-wall and footwall effects, geometrical spreading, crustal anelastic attenuation, crustal quality factor, mid crust amplification factor and upper crustal attenuation factor.

Stress drop, or to be exact dynamic stress drop, is the stress that is alleviated at the rupture surface during an earthquake. Theoretically, earthquake rupture with higher stress drop triggers higher ground motion. Stress drop is more likely to affect short-period ground motion, such as PGA, compare to long-period ground motion (Boore and Atkinson, 1987; Campbell and Bozorgnia, 2000). As magnitude increases, the aleatory uncertainty in stress drop is assumed to be smaller (Toro et al., 1997).

Table 2.6 Brief description of NEHRP 1997 site classification (BSSC, 1998)

Site classification	Description	Index
A	Very hard rocks	$V_{S30} > 1500\text{m/s}$
B	Rocks	$1500\text{m/s} > V_{S30} > 760\text{m/s}$
C	Hard or very hard soils, gravel, soft rocks	$760\text{m/s} > V_{S30e} > 360\text{m/s}$ or $N > 50$ , $S_u > 100\text{Kpa}$
D	Hard soils (sands, clays, and gravels)	$360\text{m/s} > V_{S30} > 180\text{m/s}$ or $50 > N > 15$ , $100 > S_u > 50\text{Kpa}$
E	Soft clay of thickness about H in site profiles	$V_{S30} < 180\text{m/s}$ or $N < 15$ , $S_u < 50\text{Kpa}$ or $H > 3\text{m}$ ( $PI > 20$ , $w > 40\%$ , $S_u < 25\text{Kpa}$
F	Easy subsidence or failure highly sensitive clays; poor cohesiveness soil; mudstone or organic matter clays; high plasticity clays	$H > 3\text{m}$ ; $H > 8\text{m}$ , and $PI > 75$ $H > 36\text{m}$

Hanging wall is the portion of crustal that lies above the rupture plane while foot wall is the crustal part that situated underneath the rupture plane. Several studies provide empirical evidence to show that higher ground motion is exhibited for sites located at the hanging wall of a normal or reverse fault (Somerville and Abrahamson, 1995; Abrahamson and Somerville, 1996; Abrahamson and Silva, 1997b; Somerville and Abrahamson, 2000).

Geometrical spreading and crustal anelastic attenuation are examples of the path parameters. Geometrical spreading describes the attenuation of amplitude of seismic waves due to the geometrical spreading of energy. Crustal anelastic attenuation ( $\beta$ ) is a parameter that defines the rate of attenuation of wave through which the wave propagates through and represents dissipation of energy. The number

of wave cycles along the path and the ability of the earth's crust to transmit wave controls the attenuation of wave amplitude per cycle. The number of wave cycles is proportional to the source-to-site distance and frequency of waves (Chandler and Lam, 2004). Geology of a given region governs the wave transmission quality. The crustal quality factor ( $Q$ ) is the factor designed for such adjustment. Higher  $Q$  value implies that the earth's crust enables better wave transmission. Normally, older rocks in stable continental regions have higher  $Q$  value than younger rocks in mountainous regions (Lam et al., 2000).

Combined crustal factor ( $\gamma$ ) represents mid-crust amplification and the upper crustal attenuation. Mid-crust amplification factor were adjusted by a mid-crust scaling factor ( $C$ ) based on density ( $\rho$ ) and shear wave velocity ( $V_s$ ) at source. The upper crustal attenuation factor ( $\kappa$ ) implies the attenuation of waves in the upper 4 km of the earth's crust.

#### **2.4 Ground motion attenuation model adoption from previous researches for Peninsular Malaysia**

As adoption of existing ground motion attenuation model is a fast and economical method for subsequent seismic hazard assessment, there were a few previous researches conducted to determine the adoption of the best fitting attenuation model for Peninsular Malaysia.

Adnan et al. (2004) had specifically developed an attenuation model for subduction earthquake for Peninsular Malaysia and also recommended attenuation model derived by Campbell (2003) to be used to predict ground motion resulting from shallow crustal earthquake for Peninsular Malaysia.

In an attempt to design response study on several selected locations in Kuala Lumpur, Petersen et al. (2004) model was proposed for subduction earthquakes while ground motions produced by shallow crustal earthquakes were said well-predicted by Megawati et al. (2003) (Husen et al., 2008).

On the other hand, Azizan (2012) proposed Campbell (2003) model and Petersen et al. (2004) model to be used in Peninsular Malaysia for shallow crustal earthquakes and subduction earthquakes, respectively, as both models provide larger distance ranges which are suitable for distant seismicity area.

In another study, four models established specifically for stable continental regions were compared in a study for Peninsular Malaysia by Adnan et al. (2010). However, tectonic mechanism is not considered in the study.

In an approach for seismic design in Malaysia using Eurocode 8, Pappin et al. (2011) claimed that Malaysia has a rigid crustal structure similar to ENA and adopted attenuation model developed by Atkinson and Boore (2006).

A study to determine the usability of Next Generation Attenuation (NGA) models for seismic hazard assessment for Malaysia has also been conducted by Adnan et al. (2012). It was stated in the paper that calibration and fine-tuning has to be carried out as the difference in predicted PGA and actual PGA value is not negligible. The large difference is due to the limitation in range of applicability of the NGA models. NGA models focused more on near-source ground motion prediction for distance not more than 200 km. Although NGA models are considered global models but, strong motion database utilised in developing those models does not include Sumatran earthquakes. Thus, none of the five NGA models could represent characteristics of seismic activities and tectonic region in Sumatra.

Due to different proposal of attenuation model from previous studies carried out by different researchers, a comprehensive study to incorporate all the suggested models have to be carried out for Peninsular Malaysia should be conducted. The study should also include more attenuation models for comparison. However, the pre-selection of ground motion attenuation models is another difficult task and requires careful considerations.

## 2.5 Pre-selection of attenuation models

The first attenuation model was formulated by Esteva and Rosenblueth in 1964. With more seismic stations installed around the world, more availability of ground motion records through online open-source, and more journals and conferences, over a dozen of ground motion attenuation models were established each year. In a review by Douglas (2011), a total of 289 empirical attenuation model for the prediction of PGA and 188 empirical attenuation model for the prediction of elastic response spectral ordinates are summarized. Besides that, there were also many dozens of simulation-based attenuation models listed in the review. The abundance of ground motion attenuation models creates difficulty as it is out of sense to use all those models for comparison in order to be applied at a specific region. Practically, it is realistic to carefully select 10% of the available ground motion attenuation models for any project but the large dispersion of prediction by models are worth to be noted since it can cause high epistemic uncertainty in the ground motion attenuation model (Douglas et al., 2012). Thus, it is necessary to apply a set of criteria to the comprehensive list of ground motion attenuation models to pre-select ground motion attenuation models that fulfil the aim of the project before the final examination.

Cotton et al. (2006) proposed a set of exclusion criteria in the pre-selection of ground motion attenuation models from a complete list, which requires to be followed in descending order:

1. The model is from a clearly irrelevant tectonic regime.
2. The model is not published in an international peer-reviewed journal.
3. The documentation of model and its underlying dataset is insufficient.
4. The model has been superseded by more recent publications.
5. The frequency range of the model is not appropriate for engineering application.
6. The model has an inappropriate functional form.
7. The regression method or regression coefficients are judged to be inappropriate.

The purpose of Criterion 1 is to exclude attenuation models for different tectonic mechanisms as the targeted one. Criterion 2 is applied to reject attenuation models that had not been published in peer-reviewed journal that is listed by ISI Web



of Knowledge. However, attenuation models that had been published in the grey literature or presented in international conference or forum pioneering the seismology and earthquake engineering are to be retained under Criterion 2. Criterion 3 refers to rejection of studies that did not present detailed information regarding the dataset used in the developed of the attenuation models presented. Criterion 4 is applied to exclude attenuation models that have been modified or improved using larger set of databases in more recent publications for the same particular area and tectonic regime. Criterion 5 is applied to omit all PGA-only attenuation models as well as those that do not provide coefficients for period less than 0.04s (25 Hz) and up to at least 2s (0.5 Hz). Criterion 6 leads to exclusion of attenuation models that do not use moment magnitude as well as those that do not provide ground motion prediction on rock sites. Criterion 7 is applied to exclude models based on simulation that do not account for modelling variability in the calculations of standard deviations. The last criterion also leads to exclusion of attenuation models that do not provide reliable ground motion prediction over a wide range of magnitude (roughly  $M_w$  5.0 to 7.5) and near-source distance to at least 100 km (Douglas et al., 2012).

The criteria has been modified and updated by Bommer et al. (2006) into a set of 10 criteria of exclusion. However, proposal by Bommer et al. (2006) is too strict to be followed (Douglas et al., 2012). In the project conducted by Pacific Earthquake Engineering Research Center (PEER) regarding the Global Component on GMPEs for the Global Earthquake Model (GEM), proposal by Cotton et al. (2006) was used for the pre-selection of attenuation model into a more manageable number for closer examination and testing in the effort of choosing representative global attenuation models.

A total of 28 most cited ground motion attenuation models were summarized in the following sub-sections. These models were pre-selected from the complete list of models as reviewed by Douglas (2011), except for Adnan et al. (2004), Petersen et al. (2004) and Nabilah and Balendra (2012). Criterion used in the pre-selection of these models will be discussed in Section 3.5. Grouping of these models were carried out based on tectonic setting.

### 2.5.1 Ground motion attenuation models for subduction earthquakes

Among these 28 models, 13 of them are ground motion attenuation models for subduction earthquakes. The tectonic setting identification was carried out based on the utilized databases and target regions of these models.

#### 2.5.1.1 Adnan et al. (2004)

A total of 29 worldwide subduction earthquake events with 776 ground motion records were utilized in the developing this attenuation relationship. By taking only dip slip mechanism as the source characteristic and rock condition as site characteristics, regression analysis was performed on the typical form of an attenuation relationship as suggested by Kramer (1996). The analysis led to the formation of attenuation relationship as follow:

$$\begin{aligned}\ln(y) &= 21.6187 + 3.3993M_w + 0.6040M_w^{1.1034} \\ &\quad - 7.7091\ln(R_{hypo} + 6.6233e^{0.5554M_w}) + 0.0061H \\ \sigma_{\ln y} &= 0.598\end{aligned}\tag{2-4}$$

where,

- $y$  = mean of peak ground acceleration (PGA) in units of gal
- $M_w$  = moment magnitude
- $R_{hypo}$  = hypocentral distance in km
- $H$  = focal depth in km
- $\sigma_{\ln(y)}$  = standard deviations of the model

#### 2.5.1.2 Atkinson and Boore (2003, 2008)

This global ground motion relation is derived empirically by using 1200 ground motion data for subduction earthquake events since 1989. The database is the compilation from the Youngs et al. (1997) and Crouse (1991) studies and with addition from events occurred in Japan, Mexico, Central America, and Cascadia. Maximum likelihood regression analysis is performed separately on different event classification namely, interface event and in-slab event. The resulting relations are as shown in Eq 2-5:

$$\log(y) = C_1 + C_2 M + C_3 H + C_4 R + g \log R + C_5 s/S_c + C_6 s/S_D + C_7 s/S_E \quad (2-5)$$

where,

$y$  = peak ground acceleration (PGA) or 5% damped pseudo-acceleration (PSA) in  $\text{cm/sec}^2$  random horizontal component

$M$  = moment magnitude (use M8.5 for interface events of  $M > 8.5$ , and M8.0 for in-slab events of  $M \geq 8$ )

$H$  = focal depth in km

$R$  =  $\sqrt{D_{\text{fault}}^2 + \Delta^2}$  with  $D_{\text{fault}}$  being the closest to fault surface, in km (use  $H=100\text{km}$  for events with depth  $> 100\text{km}$ )

$\Delta$  = near-source saturation term  
 $= 0.00724(10^{0.507M})$

$S_C$  = 1 for NEHRP C soils ( $360 < \beta \leq 760$  m/sec), = 0 otherwise

$S_D$  = 1 for NEHRP D soils ( $180 < \beta \leq 360$  m/sec), = 0 otherwise

$S_E$  = 1 for NEHRP E soils ( $\beta < 180$  m/sec), = 0 otherwise

$\beta$  = shear-wave velocity averaged over the top 30 m of the soil profile

$$sl = \begin{cases} 1 & \text{for } \text{PGA}_{\text{rx}} \leq 100 \text{ cm/sec}^2 \text{ or frequencies } \leq 1 \text{ Hz} \\ 1 - (f-1)(\text{PGA}_{\text{rx}} - 100)/400 & \text{for } 100 < \text{PGA}_{\text{rx}} < 500 \text{ cm/sec}^2 \text{ (1 Hz } < f < 2\text{Hz)} \\ 1 - (f-1) & \text{for } \text{PGA}_{\text{rx}} \geq 500 \text{ cm/sec}^2 \text{ (1 Hz } < f < 2\text{Hz)} \\ 1 - (\text{PGA}_{\text{rx}} - 100)/400 & \text{for } 100 < \text{PGA}_{\text{rx}} < 500 \text{ cm/sec}^2 \text{ (} f \geq 2\text{Hz and PGA)} \\ 0 & \text{for } \text{PGA}_{\text{rx}} \geq 500 \text{ cm/sec}^2 \text{ (} f \geq 2\text{Hz and PGA)} \end{cases}$$

$\text{PGA}_{\text{rx}}$  is predicted PGA on rock (NEHRP B) in  $\text{cm/sec}^2$

$\sigma$  = standard deviation of residuals

$= \sqrt{\sigma_1^2 + \sigma_2^2}$  where, 1, 2 denote estimated intra-event and inter-event variability, respectively

For interface events:

$C_1 = 2.991$ ,  $C_2 = 0.03525$ ,  $C_3 = 0.00759$ ,  $C_4 = -0.00206$ ,  $C_5 = 0.19$ ,  $C_6 = 0.24$ ,  
 $C_7 = 0.29$ ,  $g = 10^{(1.2-0.18M)}$ ,  $\sigma_1 = 0.20$ ,  $\sigma_2 = 0.11$  and  $\sigma = 0.23$ .

For in-slab events:

$$C_1 = -0.04713, C_2 = 0.6909, C_3 = 0.01130, C_4 = -0.00202, C_5 = 0.19, C_6 = 0.24, \\ C_7 = 0.29, g = 10^{(0.301-0.01M)}, \sigma_1 = 0.23, \sigma_2 = 0.14 \text{ and } \sigma = 0.27.$$

In 2008, there was an erratum paper published by the same authors to correct the error found in the previous article. According to Atkinson and Boore (2008), the correction is made for interface events and affecting only pseudo-acceleration at 2.5 Hz and 5Hz. As the correction is out of the interest in this research, further discussion regarding the erratum is not included here.

### 2.5.1.3 Crouse (1991)

This model is developed by using 697 peak ground acceleration (PGA) and 235 pseudo-velocity (PSV) horizontal component databases. Although database utilised in this relationship comprised of large amount of worldwide ground motion, the lack of data from true bedrock site made the model to be confined for use at shallow stiff soil sites. Being one of the earliest global scale attenuation relationships, this model has a relatively large standard deviation, which is 0.773. However, as the magnitude and distance increases, the residual appears to be decreasing. Thus, the model is more reliable at higher magnitude and larger distance. Eq. 2-6 shows the form of the model.

According to Crouse et al. (1988), center-of-energy-release distance was defined as the distance from the recording station to a point on the fault rupture where the energy was considered to be concentrated.

$$\ln(y) = 6.36 + 1.76M_w - 2.73 \ln(R + 1.58e^{0.608M_w}) + 0.00916h \quad (2-6)$$

where,

- $y$  = peak ground acceleration (PGA) in units of  $\text{cm/s}^2$
- $M_w$  = moment magnitude
- $R$  = center-of-energy-release distance in km
- $H$  = focal depth in km

#### 2.5.1.4 Fukushima and Tanaka (1990)

By performing two-step stratified regression analysis on strong motion data from 28 earthquakes originated in Japan and near source data from 15 earthquakes in United States and other countries, this empirically developed model has the form as in Eq. 2-7. Some of the ground condition for stations where the data were obtained, were classified into 4 types, according Numata (1960), namely: rock, hard soils, medium soils and soft soils. Examination to determine the effect of ground conditions on the model had been carried out by Fukushima and Tanaka (1990) and the result showed that observed peak horizontal accelerations are about 40% smaller than as predicted by the model for rock sites. As for soft-soil sites, the observed PGA were about 140% of the predictions by the model. Thus, this factor of amplification would be used for analysis in present study at the later part.

$$\begin{aligned}\log_{10}(y) &= 0.41M_s - \log_{10}[R + 0.032(10^{0.41M_s})] - 0.0034R + 1.30 \\ \sigma &= 0.21\end{aligned}\quad (2-7)$$

where,

- $y$  = mean horizontal peak ground acceleration (PGA) in units of  $\text{cm/sec}^2$
- $M_s$  = surface-wave magnitude
- $R$  = shortest distance between site to fault rupture in km
- $\sigma$  = standard deviations of the model

#### 2.5.1.5 Gregor et al. (2002)

The attenuation relationships by Gregor et al. (2002) are as below:

$$\ln(y) = C_1 + C_2M_w + (C_3 + C_4M_w) \ln[R + e^{C_5}] + C_6(M_w - 10)^3 \quad (2-8)$$

where,

- $y$  = peak ground acceleration (PGA) in units of  $g$
- $M_w$  = moment magnitude
- $R$  = closest distance to rupture plane in km
- $\sigma_{\ln(y)}$  = standard deviations of the model

Based on regression analysis, coefficients are for rock sites are:  $C_1 = 21.0686$ ,  $C_2 = -1.7712$ ,  $C_3 = -5.0631$ ,  $C_4 = 0.4153$ ,  $C_5 = 4.2$ ,  $C_6 = 0.0017$  and  $\sigma_{\ln(y)} = 0.7240$ . For soil sites, coefficient values are:  $C_1 = 23.8613$ ,  $C_2 = -2.2742$ ,  $C_3 = -4.8803$ ,  $C_4 = 0.4399$ ,  $C_5 = 4.7$ ,  $C_6 = 0.0366$  and  $\sigma_{\ln(y)} = 0.5436$ .

This stochastically developed attenuation relationships were used to account for megathrust earthquake from Mw 8.0 to Mw 9.0 from Cascadia subduction zone. Validation to the finite-fault numerical simulations were carried out using 15 earthquakes recorded from 500 sites and also two megathrust earthquakes namely, Mw 8.0 Michoacan, Mexico and Mw 8.0 Valpariso, Chile, earthquakes. As stated in the article, the model attenuates slower at greater distance, making it attributable to far-field softer soil profile. Hence, it is worth to be a candidate in the pre-selection.

#### 2.5.1.6 Kanno et al. (2006)

The relationship is expressed in two equations, one for the shallow events and another for deep events. This model was determined in a simple form in order to account for the uncertainty in necessity of some specific parameters. By computing maximum likelihood two-stage regression analysis method on 3769 ground motion data generated by 83 shallow earthquake events and 8150 peak acceleration values created by 111 deep events, the model acquired the following form:

For shallow events ( $D \leq 30\text{km}$ ),

$$\log \text{pre} = a_1 M_w + b_1 X - \log(X + d_1(10e_1 M_w)) + c_1 + \varepsilon_1 \quad (2-9)$$

For deep events ( $D > 30\text{km}$ ),

$$\log \text{pre} = a_2 M_w + b_2 X - \log(X) + c_2 + \varepsilon_2 \quad (2-10)$$

Site correction term,  $G$

$$G = -0.55 \log(V_{s30}) + 1.35 \quad (2-11)$$

$$\log A = \log \text{pre} + G \quad (2-12)$$

where,

- pre = predicted PGA (cm/sec<sup>2</sup>), PGV (cm/sec) or 5% damped response spectral accelerations (cm/sec<sup>2</sup>), without considering correction terms
- $A$  = PGA, PGV or 5% damped response spectral acceleration considering correction terms
- $M_W$  = moment magnitude
- $D$  = focal depth in km
- $X$  = distance in km
- $V_{S30}$  = average shear-wave velocity at depth of 30 m
- $\varepsilon_1, \varepsilon_2$  = standard deviation

Values of regression coefficients for horizontal PGA are:  $a_1 = 0.56$ ,  $a_2 = 0.41$ ,  $b_1 = -0.0031$ ,  $b_2 = -0.0039$ ,  $c_1 = 0.26$ ,  $c_2 = 1.56$  and  $d_1 = 0.0055$ .

#### 2.5.1.7 Lin and Lee (2008)

Although the predictive relations by Lin and Lee (2008) are developed specifically for north eastern Taiwan, ground motion data from foreign areas in addition to Taiwanese data were also utilised. Least-square method of non-linear regression model was used to process a total of 4383 sets after winnowed. Data utilised contains more intraslab earthquakes than interface earthquakes. The resultant PGA attenuation equations were classified into two groups, which are rock sites (B and C class in NEHRP) and soil sites (D and E class in NEHRP), by Lee et al. (2001). The relations are as following:

$$\ln(y) = C_1 + C_2 M + C_3 \ln(R + C_4 e^{C_5 M}) + C_6 H + C_7 Z_t \quad (2-13)$$

where,

- $y$  = geometric mean of two horizontal peak ground acceleration (PGA) in units of g
- $M$  = moment magnitude
- $R$  = hypocentral distance in km
- $H$  = focal depth in km
- $\sigma_{\ln(y)}$  = standard deviations of the model
- $Z_t$  = type of earthquake mechanism (0 for interface events, 1 for intraslab events)

Based on regression analysis, coefficients are for rock sites:  $C_1 = -2.500$ ,  $C_2 = 1.205$ ,  $C_3 = -1.905$ ,  $C_4 = 0.51552$ ,  $C_5 = 0.63255$ ,  $C_6 = 0.0075$ ,  $C_7 = 0.275$  and  $\sigma_{\ln(y)} = 0.5268$ . For soil sites:  $C_1 = -0.900$ ,  $C_2 = 1.000$ ,  $C_3 = -1.900$ ,  $C_4 = 0.99178$ ,  $C_5 = 0.52632$ ,  $C_6 = 0.004$ ,  $C_7 = 0.31$  and  $\sigma_{\ln(y)} = 0.6277$ .

### 2.5.1.8 Megawati et al. (2005)

Other than actual ground motion data, synthetic data can also be used to generate a ground motion prediction model. Megawati et al. (2005) is one of the models developed using simulation of ground motion data. A total of 11,520 sets of simulated data were generated at six stations from 60 random sources at four different focal depths and eight magnitude levels. The model is generated specifically for rock site. Another uniqueness of the model is that horizontal ground motions were aligned to the radial and tangential directions instead of to usual NS and EW directions. The final equation obtained is as follow:

$$\ln(y_H) = a_0 + a_1 M_W + a_2 M_W^2 + a_3 \ln(R) + a_4 R + a_5 H + \sigma_H \quad (2-14)$$

where,

$y_H$  = horizontal PGA, PGV or RSA (5% damping ratio) in units of  $\text{cm/s}^2$ ,  $\text{cm/s}$  and  $\text{cm/s}^2$ , respectively

$M_W$  = moment magnitude

$R$  = source-to-site distance in km

$H$  = focal depth in km

$\sigma_H$  = standard deviation

Values of regression coefficients for horizontal PGA are:  $a_0 = -7.198$ ,  $a_1 = 2.3691$ ,  $a_2 = -0.013856$ ,  $a_3 = -1.0000$ ,  $a_4 = -0.001548$ ,  $a_5 = -0.08909$  and standard deviation,  $\sigma_H = 0.4413$ .



### 2.5.1.9 Megawati and Pan (2010)

Unlike Megawati et al. (2005), this model is developed specifically for predicting ground motions for Sumatran megathrust earthquake. Generally, it is derived for very hard rock condition, which is class A according to NEHRP, and for distance range of 200 to 1500 km. Although derived for hard rock condition, the model can also be adopted for other site conditions by applying site response factor proposed by Boore and Joyner (1997). The model were derived based solely on synthetic seismograms and validation using ground motions recorded in Singapore from 12 massive earthquakes showed that the predictions are within an acceptable level of uncertainty. The functional form of the model is as described below:

$$\ln(y) = a_0 + a_1(M_w - 6) + a_2(M_w - 6)^2 + a_3 \ln(R) + (a_4 + a_5 M_w)R + \varepsilon_{\ln(y)} \quad (2-15)$$

where,

$y$  = geometrical mean of horizontal PGA, PGV or RSA (5% damping ratio) in units of  $\text{cm/s}^2$ ,  $\text{cm/s}$  and  $\text{cm/s}^2$ , respectively

$M_w$  = moment magnitude

$R$  = source-to-site distance in km

$H$  = focal depth in km

$\varepsilon_{\ln(y)}$  = standard deviation

Values of regression coefficients for horizontal PGA are:  $a_0 = 3.882$ ,  $a_1 = 1.8988$ ,  $a_2 = -0.11736$ ,  $a_3 = -1.0000$ ,  $a_4 = -0.001741$ ,  $a_5 = 0.0000776$  and standard deviation,  $\varepsilon_{\ln(y)} = 0.2379$ .

### 2.5.1.10 Nabilah and Balendra (2012)

Eq. 2-16 is derived solely based on ground motion records from Peninsular Malaysia and Singapore. A total of 35 records of 9 Sumatra subduction earthquakes occurred from 2004 to 2010 had been adopted. After a multiple regression analysis had been performed, a simple model based on magnitude and distance that is valid for shallow earthquakes with focal depth or around 30km is provided. Due to the site

condition of stations from where the records were obtained, the model were claimed to be only suitable for rock sites.

$$\ln(\text{PGA}) = a_1 M - \ln(R) - a_2 R + a_3 + \sigma_{\ln(\text{PGA})} \quad (2-16)$$

where,

PGA = maximum horizontal PGA in gal

$M$  = moment magnitude

$R$  = source-to-site distance in km

$\sigma_{\ln(\text{PGA})}$  = standard deviation, which has the value of 0.3917

Values of regression coefficients for horizontal PGA are:  $a_1 = 1.3858$ ,  $a_2 = 0.002478$ ,  $a_3 = 3.6589$ .

#### 2.5.1.11 Petersen et al. (2004)

This model is the extension version of Youngs et al. (1997) model. While Youngs et al. (1997) is used to predict ground motions of earthquake in global scale, Petersen et al. (2004) can give better estimation to ground motions at distance larger than 200 km. This is due to the inclusion of more distant ground motion data from Incorporated Research Institutions for Seismology (Data Management Center) IRIS (DMC) in the modification of the global scale model. Least-square fit was performed for peak ground acceleration after differences between observed data and those predicted by Youngs et al. (1997) model were determined and the result are as below:

$$\ln y_{\text{MODIFIED}}(M, x) = \ln y_{\text{YOUNGS}}(M, x) + [-0.0038(x - 200)] \quad (2-17)$$

where,

$y$  = PGA in g

$M$  = moment magnitude

$x$  = distance in km

### 2.5.1.12 Youngs et al. (1997)

This is a renowned global ground motion attenuation model developed using recorded ground motions from inter-plate earthquakes occurring in subduction regions such as Alaska, Chile, Cascadia, Japan, Mexico, Peru and Solomon islands. It considers two types of subduction earthquakes namely interface earthquakes and intraslab earthquakes. Although it took data from both rock and soil sites, most of the ground motion data for interface events are taken from soil sites. It has the form as the following:

For rock sites,

$$\begin{aligned}\ln(y) &= 0.2418 + 1.414M + C_1 + C_2(10 - M)^3 + C_3 \ln(r_{rup}) \\ &\quad + 1.7818e^{0.554M} + 0.00607H + 0.3846Z_T \\ \sigma &= C_4 + C_5M\end{aligned}\quad (2-18)$$

For soil sites,

$$\begin{aligned}\ln(y) &= -0.6687 + 1.438M + C_1 + C_2(10 - M)^3 + C_3 \ln(r_{rup}) \\ &\quad + 1.097e^{0.617M} + 0.00648H + 0.3643Z_T \\ \sigma &= C_4 + C_5M\end{aligned}\quad (2-19)$$

where,

- $y$  = geometrical mean of 2 horizontal components of PGA in g
- $M$  = moment magnitude
- $r_{rup}$  = distance to rupture plane in km
- $H$  = focal depth in km
- $Z_t$  = type of earthquake mechanism (0 for interface events, 1 for intraslab events)
- $\sigma$  = standard deviation

The coefficient values from regression analysis for rock sites are:  $C_1 = 0.0$ ,  $C_2 = 0.0$ ,  $C_3 = -2.552$ ,  $C_4 = 1.45$  and  $C_5 = -0.1$ . For soil sites the coefficient values are:  $C_1 = 0.0$ ,  $C_2 = 0.0$ ,  $C_3 = -2.329$ ,  $C_4 = 1.45$  and  $C_5 = -0.1$ .

### 2.5.1.13 Zhao et al. (2006)

This model had introduced site class terms which are more preferable in Japanese engineering design. Other than Japanese ground acceleration data, data from Iran and Western United States, as recorded in Table 2.7, were also collected and included in the empirical analysis.

The relationship adopted a simple form of attenuation function and the resultant coefficients after analysis are as shown in Eq. 2-20:

$$\ln(y_{i,j}) = aM_{wi} + bx_{i,j} + \ln(r_{i,j}) + e(h - h_c)\delta_h + F_R + S_I + S_S + S_{SL} \ln(x_{i,j}) + C_k \quad (2-20)$$

$$r_{i,j} = x_{i,j} + ce^{dM_{wi}}$$

where,

$y$  = geometrical mean of two horizontal components of peak ground acceleration (PGA) or 5% damped acceleration response spectrum in  $\text{cm/sec}^2$

$M_w$  = moment magnitude

$x$  = source to site distance in km

$h$  = focal depth in km (capped at 125 km)

$h_c$  = depth constant

= 15km for shallow events

$\delta_h$  = dummy variable =  $\begin{cases} 0 & \text{for } h < h_c \\ 1 & \text{for } h \geq h_c \end{cases}$

$F_R$  = reverse-fault parameter

= 1 for crustal events with reverse-faulting mechanism, 0 for otherwise

$S_I$  = 0.000 for interface events, 0 for otherwise

$S_S$  = 2.607 for subduction slab events, 0 for otherwise

$S_{SL}$  = magnitude-independent path modification term for slab events

= -0.528

$C_k$  = Site-class term for a given site class

$$= \begin{cases} 1.111 & \text{for SCI (NEHRP site class A+B)} \\ 1.344 & \text{for SCII (NEHRP site class C)} \\ 1.355 & \text{for SCIII (NEHRP site class D)} \\ 1.420 & \text{for SCIV (NEHRP site class E+F)} \end{cases}$$

$\sigma_T$  = Standard deviation

$$= \sqrt{\sigma^2 + \tau^2} \text{ where, } \sigma \text{ and } \tau \text{ denote estimated intra-event and inter-event variability, respectively.}$$

$$= 0.723$$

$i$  = Subscript denoting event number

$j$  = Subscript denoting record number from event  $i$

$$\left. \begin{aligned} a &= 1.101 \\ b &= -0.00564 \\ c &= 0.0055 \\ d &= 1.080 \\ e &= 0.01412 \end{aligned} \right\} \text{ for PGA}$$

Table 2.7 Number of records by source type, faulting mechanism and region

Focal Mechanism	Crustal	Interface	Slab	Total for Each Focal Mechanism
Japan				
Reverse	250	1492	408	2150
Strike-slip	1011	13	574	1598
Normal	24	3	735	762
Unknown			8	8
Total for each source type	1285	1508	1725	4518
Iran and Western United States				
Reverse	123	12		135
Strike-slip	73			73
Total for each source type	196	12		208
				Grand Total
Total for each source type from all regions	1481	1520	1725	4726

## 2.5.2 Ground motion attenuation models for shallow crustal earthquakes

Other than the 13 models, the remaining models, which are 15 of them, are to predict ground motion from shallow crustal earthquakes.

### 2.5.2.1 Abrahamson and Silva (1997)

The model has the following form:

$$\ln Sa_{(T=0.01s)} = f_1(M, r_{rup}) + Ff_3(M) + HWf_4(M, r_{rup}) + Sf_5(PGA_{rock}) \quad (2-21)$$

$$f_1(M, r_{rup}) = \begin{cases} 1.64 + 0.512(M - 6.4) \\ \quad + [-1.145 + 0.17(M - 6.4)] \ln R & ; \text{ for } M \leq 6.4 \\ 1.64 - 0.144(M - 6.4) \\ \quad + [-1.145 + 0.17(M - 6.4)] \ln R & ; \text{ for } M > 6.4 \end{cases}$$

$$R = \sqrt{r_{rup}^2 + 5.6^2}$$

$$F = \begin{cases} 1 & ; \text{ for reverse faulting earthquakes} \\ 0.5 & ; \text{ for reverse/oblique faulting earthquakes} \\ 0 & ; \text{ otherwise} \end{cases}$$

$$f_3(M) = \begin{cases} 0.610 & ; \text{ for } M \leq 5.8 \\ 0.610 - \frac{0.26 - 0.61}{6.4 - 5.8} & ; \text{ for } 5.8 < M < 6.4 \\ 0.260 & ; \text{ for } M > 6.4 \end{cases}$$

$$HW = \begin{cases} 1 & ; \text{ for hanging wall} \\ 0 & ; \text{ otherwise} \end{cases}$$

$$f_4(M, r_{rup}) = f_{HW}(M) f_{HW}(r_{rup})$$

$$f_{HW}(M) = \begin{cases} 0 & ; \text{ for } M \leq 5.5 \\ M - 5.5 & ; \text{ for } 5.5 < M < 6.5 \\ 1 & ; \text{ for } M \geq 6.5 \end{cases}$$

$$f_{HW}(r_{rup}) = \begin{cases} 0 & ; \text{for } r_{rup} < 4 \\ 0.370 \left( \frac{r_{rup} - 4}{4} \right) & ; \text{for } 4 < r_{rup} < 8 \\ 0.370 & ; \text{for } 8 < r_{rup} < 18 \\ 0.370 \left( \frac{r_{rup} - 18}{7} \right) & ; \text{for } 18 < r_{rup} < 25 \\ 0 & ; \text{for } r_{rup} > 25 \end{cases}$$

$$S = \begin{cases} 0 & ; \text{for rock site} \\ 1 & ; \text{for soil site} \end{cases}$$

$$f_5(PGA_{rock}) = -0.417 - 0.230 \ln(PGA_{rock} + 0.03)$$

$$\sigma_{total}(M) = \begin{cases} 0.70 & ; \text{for } M \leq 5.0 \\ 0.565(M - 5) & ; \text{for } 5.0 < M < 7.0 \\ 0.430 & ; \text{for } M \geq 7.0 \end{cases}$$

where,

- $Sa_{(T=0.01s)}$  = geometrical mean of two perpendicular horizontal components of spectral acceleration at period, T of 0.01s, in g
- $M$  = moment magnitude
- $r_{rup}$  = closest distance to the rupture plane in km
- $F$  = type of faulting mechanism
- $HW$  = hanging wall effect
- $\sigma$  = standard deviation
- $S$  = site category
- $PGA_{rock}$  = expected peak acceleration on rock in g (as predicted by the median attenuation relation with  $S = 0$ )
- $\sigma_{total}(M)$  = total standard error

Random effects model for regression analysis were conducted upon 655 recordings from 58 shallow crustal events produced in worldwide active tectonic regions. Geomatrix site classification is applied in the model with simplification. Rock sites were referred to class A and class B in Geomatrix while soil sites were referred to class C and class D.

### 2.5.2.2 Ambraseys et al. (2005)

This empirical model is developed based on the combination of moderate to strong motion data from Europe and Middle East. A set of 595 strong-motion records were analysed by using weighted regression analysis to derive the ground motion equations. The model classified local site conditions proposed by Boore et al. (1993). The functional form adopted was:

$$\begin{aligned} \log y &= \frac{a_1 + a_2 M_W + (a_3 + a_4 M_W) \log \sqrt{d^2 + a_5^2} + a_6 S_s}{+ a_7 S_A + a_8 F_N + a_9 F_T + a_{10} F_O} \quad (2-22) \\ S_s &= 1 \text{ for soft soil } (180 < V_{s30} \leq 360 \text{ m/s}), \text{ otherwise } 0 \\ S_A &= 1 \text{ for stiff soil } (360 < V_{s30} \leq 750 \text{ m/s}), \text{ otherwise } 0 \\ F_N &= 1 \text{ for normal faulting earthquake, otherwise } 0 \\ F_T &= 1 \text{ for thrust faulting earthquakes, otherwise } 0 \\ F_O &= 1 \text{ for odd faulting earthquakes, otherwise } 0 \end{aligned}$$

where,

$$\begin{aligned} y &= \text{peak ground acceleration and spectral acceleration for 5\% critical} \\ &\quad \text{damping ratio in m/s} \\ M_W &= \text{moment magnitude} \\ d &= \text{distance to the surface projection of the rupture} \end{aligned}$$

Values for coefficients  $a_1$  to  $a_{10}$  for PGA are as follows:  $a_1 = 2.522$ ,  $a_2 = -0.142$ ,  $a_3 = -3.184$ ,  $a_4 = 0.314$ ,  $a_5 = 7.6$ ,  $a_6 = 0.137$ ,  $a_7 = 0.050$ ,  $a_8 = -0.084$ ,  $a_9 = 0.062$  and  $a_{10} = -0.044$ .

### 2.5.2.3 Atkinson and Boore (2006, 2011)

This is a stochastic finite-fault model prediction which incorporated ground motion data from hard-rock sites from northeastern United States and southeastern Canada and also generation of synthetic seismograms. A total of 38,400 horizontal component ground motion were generated with 20 random trials performed on 10



magnitude (from Mw 3.5 to Mw 8.0 with 0.5 increment each), 24 fault distance (between 1 to 1000 km), and 8 azimuth. This model provides an updated version of Atkinson and Boore (1995) in terms of amount of data available and method in defining the fault model. An even more updated modification was published in 2011 (Atkinson and Boore, 2011). However, the modification is focused on stress-adjustment factor. The stress drop proposed in Atkinson and Boore (2006) is 140 bars, which is not much different from the stress drop assumed for Sumatra fault in Megawati et al. (2003), that is, 100 bars. Thus, the modification would not give large effect on present study and therefore Atkinson and Boore (2006) is used. The prediction curve is expressed in the following equations:

$$\begin{aligned} \log PGA = & c_1 + c_2 M + c_3 M^2 + (c_4 + c_5 M) \times \min \left\{ \log(R_{cd}), \ln(70) \right\} \\ & + (c_6 + c_7 M) \times \max \left\{ \log \left( \frac{R_{cd}}{140} \right), 0 \right\} \\ & + (c_8 + c_9 M) \times \max \left\{ \log \left( \frac{10}{R_{cd}} \right), 0 \right\} \\ & + c_{10} R_{cd} + S \end{aligned} \quad (2-23)$$

where,

- $PGA$  = peak ground acceleration in  $\text{cm/s}^2$
- $R_{cd}$  = distance to fault in km
- $M$  = moment magnitude
- $S$  = soil amplification term

Values of coefficients after conduction of regression analysis for hard rock site are:  $c_1 = 0.907$ ,  $c_2 = 0.983$ ,  $c_3 = -0.060$ ,  $c_4 = -2.70$ ,  $c_5 = 0.159$ ,  $c_6 = -2.80$ ,  $c_7 = 0.212$ ,  $c_8 = -0.301$ ,  $c_9 = -0.0653$  and  $c_{10} = -0.000448$ . As for BC boundary site ( $V_{S30} = 760$  m/s) which is used for soil amplification, values for coefficients are:  $c_1 = 0.523$ ,  $c_2 = 0.969$ ,  $c_3 = -0.062$ ,  $c_4 = -2.44$ ,  $c_5 = 0.147$ ,  $c_6 = -2.34$ ,  $c_7 = 0.191$ ,  $c_8 = -0.087$ ,  $c_9 = -0.0829$  and  $c_{10} = -0.000630$ .

Equations for soil amplification are divided into linear and nonlinear ranges as shown in next page:

$$S = \begin{cases} \log \left\{ e^{-0.361 \left[ \ln \left( \frac{V_{S30}}{760} \right) \right] + bnl \left[ \ln \left( \frac{60}{100} \right) \right]} \right\} & ; \text{ for } pgaBC \leq 60 \text{ cm/s}^2 \\ \log \left\{ e^{-0.361 \left[ \ln \left( \frac{V_{S30}}{760} \right) \right] + bnl \left[ \ln \left( \frac{pgaBC}{100} \right) \right]} \right\} & ; \text{ for } pgaBC > 60 \text{ cm/s}^2 \end{cases}$$

$$bnl = \begin{cases} -0.641 & ; \text{ for } V_{S30} \leq 180 \text{ m/s} \\ (-0.641 + 0.144) \left[ \frac{\ln \left( \frac{V_{S30}}{300} \right)}{\ln \left( \frac{180}{300} \right)} \right] - 0.144 & ; \text{ for } 180 < V_{S30} \leq 300 \text{ m/s} \\ -0.144 \left[ \frac{\ln \left( \frac{V_{S30}}{760} \right)}{\ln \left( \frac{300}{760} \right)} \right] & ; \text{ for } 300 < V_{S30} \leq 760 \text{ m/s} \\ 0.0 & ; \text{ for } V_{S30} > 760 \text{ m/s} \end{cases}$$

#### 2.5.2.4 Boore et al. (1997, 2005)

The effect of types of faulting, distance term, magnitude and site conditions were implemented in the development of the model. The model is empirically for shallow earthquakes with fault rupture lies above the depth of 20 km for western north America (WNA) (Boore et al., 1997). A total of 271 ground motion data from 19 earthquake events happened in the period of year 1940 to 1992 were selected. The model proposed a simple functional form:

$$\ln Y = b_1 + b_2(M - 6) + b_3(M - 6)^2 + b_5 \ln r + b_v \ln \frac{V_s}{V_A} \quad (2-24)$$

$$r = \sqrt{r_{jb}^2 + h^2}$$

$$b_1 = \begin{cases} b_{ISS} & ; \text{ for strike-slip earthquakes} \\ b_{IRS} & ; \text{ for reverse-slip earthquakes} \\ b_{ALL} & ; \text{ for unspecified mechanism} \end{cases}$$

where,

$Y$  = peak horizontal acceleration or pseudoacceleration response in g

- $r_{jb}$  = closest horizontal distance to the surface projection of the rupture plane  
in km
- $M$  = moment magnitude
- $V_S$  = shear-wave velocity to 30 m in m/s

Results of two stage regression for peak horizontal acceleration are:  $b_{ISS} = -0.313$ ,  $b_{IRV} = -0.117$ ,  $b_{IALL} = -0.242$ ,  $b_2 = 0.527$ ,  $b_3 = 0.000$ ,  $b_5 = -0.778$ ,  $b_V = -0.371$ ,  $V_A = 1396$  and  $h = 5.57$ . After an erratum published in year 2005, the standard deviation for the ground motion equation ( $\sigma_{lnY}$ ) was corrected to 0.495 (Boore, 2005).

#### 2.5.2.5 Campbell (2003, 2004)

Campbell (2003) developed a model based on hybrid stochastic-empirical method for ENA based on WNA. The site condition for both ENA and WNA were assumed by using Boore and Joyner (1997). The local soil profile for WNA is generic rock ( $V_{S30}$  620 m/s) and ENA is hard rock ( $V_{S30}$  2800 m/s). Although there is a more updated version of model developed by Campbell (2007) for CEUS, the model is not being selected in this study due to its smaller distance range, which is less than 100 km, and also adoption of complicated seismological parameters that makes it difficult to be applied. Campbell (2003) provide larger distance range, that is, less than 1000 km, which is more proper to the field of interest in this study. Eq. 2.21 shows the corrected version of Campbell (2003) based on erratum published in Campbell (2004).

$$\begin{aligned}
 \ln Y &= c_1 + c_2 M_W + c_3 (8.5 - M_W)^2 + c_4 \ln R \\
 &\quad + (c_5 + c_6 M_W) r_{rup} + f_3(r_{rup}) \quad (2-25) \\
 R &= \sqrt{r_{rup}^2 + (c_7 e^{c_8 M_W})^2} \\
 f_3(r_{rup}) &= \begin{cases} 0 & ; \text{for } r_{rup} \leq r_1 \\ c_9 (\ln r_{rup} - \ln r_1) & ; \text{for } r_1 < r_{rup} \leq r_2 \\ c_9 (\ln r_{rup} - \ln r_1) + c_{10} (\ln r_{rup} - \ln r_2) & ; \text{for } r_{rup} > r_2 \end{cases} \\
 \sigma_{lnY} &= \begin{cases} c_{11} + c_{12} M_W & ; \text{for } M_W < M_1 \\ c_{13} & ; \text{for } M_W \geq M_1 \end{cases}
 \end{aligned}$$

where,

- $Y$  = geometrical mean of the two horizontal components of PGA or 5%  
 damped PSA in gravitational acceleration (g)  
 $r_{rup}$  = closest distance to fault rupture (km)  
 $M_W$  = moment magnitude  
 $\sigma_{\ln Y}$  = standard deviation

Values for coefficients  $c_1$  to  $c_{13}$  for PGA are as follows:  $c_1 = 0.0305$ ,  $c_2 = 0.633$ ,  $c_3 = -0.0427$ ,  $c_4 = -1.591$ ,  $c_5 = -0.00428$ ,  $c_6 = 0.000483$ ,  $c_7 = 0.683$ ,  $c_8 = 0.416$ ,  $c_9 = 1.140$ ,  $c_{10} = -0.873$ ,  $c_{11} = 1.030$ ,  $c_{12} = -0.0860$ , and  $c_{13} = 0.414$ . Values for  $M_1$ ,  $r_1$  and  $r_2$  are 7.16, 70 km, and = 130 km, respectively.

#### 2.5.2.6 Dahle et al. (1990)

This model is empirically-derived to address prediction of ground motions resulted from intraplate earthquakes. According to Dahle et al. (1990), intraplate regions are area with more stable tectonic and uniform geography compare to plate boundaries. The model is dedicated to predict ground motion on rock site (presumably with hard rock or firm ground soil). Two-step regression analysis was performed on 87 recordings resulting from 56 intraplate earthquakes, which also comprised earthquakes from intraplate regions such as Eastern North America (ENA), Europe, China and Australia.

Proposed ground motion model is:

$$\ln A = C_1 + C_2 M + C_4 R + \ln G(R, R_0) \quad (2-26)$$

$$R = \sqrt{d^2 + h^2}$$

$$G(R, R_0) = \begin{cases} R^{-1} & ; R \leq R_0 \\ R_0^{-1} \left( \frac{R_0}{R} \right)^{5/6} & ; R > R_0 \end{cases}$$

where,

- $A$  = peak ground acceleration in  $\text{cm/s}^2$   
 $R$  = hypocentral distance in km

- $M$  = surface-wave magnitude
- $d$  = epicentral distance in km
- $h$  = focal depth in km (if focal depth is unknown, assume 15 km)
- $R_0$  = distance at which spreading for S waves overtaken by cylindrical spreading for Lg waves (recommended value is 100 km)

Values for coefficients  $C_1$ ,  $C_2$ ,  $C_4$  are -1.471, 0.84 and -0.00418 respectively.

#### 2.5.2.7 Frankel et al. (1996)

The CEUS model is found tabulated in Frankel et al. (1996) and parameterized by (EPRI, 2004) Electric-Power-Research-Institute-(EPRI) (2004). The stochastic model is derived by simulation of firm rock ground motion data representing boundary site of Class B-C ( $V_{S30}$  760 m/s) in NEHRP. The model was parameterized into the following form:

$$\begin{aligned} \ln(SA) = & C_1 + C_2M + C_3M^2 + (C_4 + C_5M) \times \min \{ \ln(r), \ln(70) \} \\ & + (C_6 + C_7M) \times \max \left\{ \min \left\{ \ln \frac{r}{70}, \ln \frac{130}{70} \right\}, 0 \right\} \\ & + (C_8 + C_9M) \times \max \left\{ \ln \frac{r}{130}, 0 \right\} \\ & + C_{10}r \end{aligned} \quad (2-27)$$

where,

- $SA$  = Spectral acceleration in g
- $r$  = hypocentral distance in km
- $M$  = moment magnitude

Values of coefficients for  $SA$  at period 0.01 sec (approximation of PGA) are:  $C_1 = -4.052$ ,  $C_2 = 1.665$ ,  $C_3 = -0.08898$ ,  $C_4 = -1.949$ ,  $C_5 = 0.09514$ ,  $C_6 = -1.410$ ,  $C_7 = 0.09549$ ,  $C_8 = -2.855$ ,  $C_9 = 0.2287$  and  $C_{10} = -0.001189$ .

#### 2.5.2.8 Hwang and Huo (1997)

Ground motion recordings in central and eastern United States (CEUS) are scarce compare to western United States (WUS). Thus, many attempted to develop attenuation relationships for CEUS using stochastic method rather than empirical

method. Hwang and Huo (1997) is one of them. 56 pairs of moment magnitude and epicentral distance were used to generate 550 synthetic ground motions. The model applied the site classifications as proposed in 1994 NEHRP provisions. The model expresses ground motion prediction in the form as shown in Eq. 2-28:

$$\ln(Y_{BR}) = C_1 + C_2 M + C_3 \ln[\sqrt{R^2 + H^2} + R_0(M)] + C_4 \sqrt{R^2 + H^2} \quad (2-28)$$

$$\ln[F_S(T)] = a(T)Y_{BR} + b(T)$$

$$Y_s(T) = Y_{BR}(T)F_S(T)$$

where,

$Y_{BR}$  = ground motion parameter at the bedrock sites in g

$R$  = epicentral distance in km

$M$  = moment magnitude

$H$  = focal depth in km, which 10km was usually taken

$R_0(M) = 0.06e^{(0.7M)}$

$\sigma_{\ln(Y_{BR})}$  = standard deviation for  $\ln Y_{BR}$

$F_S(T)$  = site coefficients for each sites

$\beta_{FS}$  = variability of site coefficients

Coefficient values for Eq. 2-10 for peak ground acceleration are:  $C_1 = -2.904$ ,  $C_2 = 0.926$ ,  $C_3 = -1.271$ ,  $C_4 = -0.00302$  and  $\sigma_{\ln(Y_{BR})} = 0.309$ . Regression coefficients  $a(T)$ ,  $b(T)$  and  $\beta_{FS}$  for each site category for PGA are as shown in Table 2.8.

Table 2.8 Regression coefficients for various site categories

Site category	Coefficient $a(T)$	Coefficient $b(T)$	$\beta_{FS}$
A	0.00	0.34	0.05
B	0.00	0.46	0.08
C	-0.96	0.77	0.22
D	-2.71	1.00	0.32
E	-3.01	1.19	0.27

### 2.5.2.9 Megawati et al. (2003)

Source parameters of synthetic seismograms for Sumatra fault as proposed by Megawati et al. (2003) consist of information as shown as following:

Strike direction	=	N 35° W
Focal depth	=	8 to 22 km
Dip angle	=	75° to 105°
Rake angle	=	150° to 210°
Source to site azimuth	=	63.4° from strike of fault clockwise

A total 20 random cases of simulation were performed on each of 6 stations, 7 segments of faults, and Mw 4.0 to 8.0 with an interval of 0.2, resulting in 6×7×21×20 = 17 640 sets of ground motions. Similar to Megawati et al. (2005), the model also took radial and tangential directions as the alignment for horizontal ground motions rather than NS and EW directions. Lastly, attenuation relationships were derived based on the simulated ground motions. The functional form of the horizontal ground motion model and its value for related coefficients are as in Eq. 2-29.

$$\ln(y_H) = a_0 + a_1 M_W + a_2 M_W^2 + a_3 \ln(R) + a_4 R + \ln \{ \max[\cos(2\phi), a_5 |\sin(2\phi)|] \} + \sigma_H \quad (2-29)$$

where,

$y_H$	=	horizontal PGA in units of $\text{cm/s}^2$
$R$	=	source-to-site distance (epicentral distance) in km
$M_W$	=	moment magnitude
$\phi$	=	source-to-station azimuth measured from the strike of the fault plane clockwise

Values of regression coefficients for horizontal PGA are:  $a_0 = -8.167$ ,  $a_1 = 2.7779$ ,  $a_2 = -0.045945$ ,  $a_3 = -1.0000$ ,  $a_4 = -0.001906$ ,  $a_5 = 0.1356$  and standard deviation,  $\sigma_H = 0.3511$ .

### 2.5.2.10 Pezeshk et al. (2011)

A hybrid empirical ground motion prediction model for ENA by using 5 new NGA models is developed. Ground motion prediction of the target region (ENA in this case) was derived from empirical models for host region which is WNA using theoretical modification factors between the two regions. The model is applicable for a magnitude range of 5 to 8 and closest distance to the fault rupture up to 1000 km. The resulting ground motion relationship derived for hard rock site (NEHRP site class A) is as shown in Eq. 2-30. The model can also be used to generate estimations for other site conditions by using appropriate site amplification factors.

$$\begin{aligned} \log(Y) = & c_1 + c_2 M_W + c_3 M_W^2 + (c_4 + c_5 M_W) \times \min \{ \log(R), \log(70) \} \\ & + (c_6 + c_7 M_W) \times \max \left\{ \min \left\{ \log \frac{R}{70}, \log \frac{140}{70} \right\}, 0 \right\} \\ & + (c_8 + c_9 M_W) \times \max \left\{ \log \frac{R}{140}, 0 \right\} \\ & + c_{10} R \end{aligned} \quad (2-30)$$

$$R = \sqrt{R_{rup}^2 + c_{11}^2}$$

$$\sigma_{\log Y}^T = \sqrt{\sigma_{\log Y}^2 + \sigma_{Reg}^2}$$

$$\sigma_{\log Y} = \begin{cases} c_{12} M_W + c_{13} & ; \text{ for } M \leq 7 \\ -6.95 \times 10^{-3} M_W + c_{14} & ; \text{ for } M > 7 \end{cases}$$

where,

$Y$  = median value for PGA or PSA in g

$R_{rup}$  = closest distance to fault rupture in km

$M_W$  = moment magnitude

$\sigma_{\log Y}$  = mean aleatory standard deviation of  $\log(Y)$

$\sigma_{Reg}$  = standard deviation of regression analysis

$\sigma_{\log Y}^T$  = total aleatory standard deviation

Regression coefficients  $c_1$  to  $c_4$  for PGA are calculated using nonlinear least-square method and are follows:  $c_1 = 1.5828$ ,  $c_2 = 0.2298$ ,  $c_3 = -0.03847$ ,  $c_4 = -3.8325$ ,



$c_5 = 0.3535, c_6 = 0.3321, c_7 = -0.09165, c_8 = -2.5517, c_9 = 0.1831, c_{10} = -0.0004224,$   
 $c_{11} = 6.6521, c_{12} = -0.0210, c_{13} = 0.3778, c_{14} = 0.2791$  and  $\sigma_{Reg} = 0.021$ .

#### 2.5.2.11 Sadigh et al. (1997)

Sadigh et al. (1997) is a specially-designed model for shallow crustal earthquakes originated from California. A total of 121 ground motion data utilized in the development of the model were selected from 79 earthquakes which lie within magnitude range of 4 to 8 and distances less than 100 km. In the model, sites, where data were collected, were categorized into two main classes, namely rock and deep soil. Rock site denotes site with bedrock less than 1 m from the ground surface while the term deep soil site implies to site with soil thickness greater than 20 m over bedrock. The attenuation equations are given as follows:

For rock sites,

$$\ln(y)_{roc.} = \frac{c_1 + c_2 M + c_3 (8.5M)^{2.5} + c_4 \ln[r_{rup} + e^{(c_5 + c_6 M)}]}{+ c_7 \ln(r_{rup} + 2)} \quad (2-31)$$

For  $M \leq 6.5$ ;

$$c_1 = -0.624, c_2 = 1.0, c_3 = 0.0, c_4 = -2.100, c_5 = 1.29649, c_6 = 0.250 \text{ and } c_7 = 0.0.$$

For  $M > 6.5$ ;

$$c_1 = -1.274, c_2 = 1.1, c_3 = 0.0, c_4 = -2.100, c_5 = -0.48451, c_6 = 0.524 \text{ and } c_7 = 0.0.$$

For soil sites,

$$\ln(y)_{soil} = \frac{c_1 + c_2 M + c_3 \ln[r_{rup} + c_4 e^{(c_5 M)}]}{+ c_6 + c_7 (8.5 - M)^{2.5}} \quad (2-32)$$

For  $M \leq 6.5$ ;

$$c_1 = -2.17, c_2 = 1.0, c_3 = 1.70, c_4 = 2.1863, c_5 = 0.32, c_6 = 0.0 \text{ and } c_7 = 0.0.$$

For  $M > 6.5$ ;

$$c_1 = -2.17, c_2 = 1.0, c_3 = 1.70, c_4 = 0.3825, c_5 = 0.5882, c_6 = 0.0 \text{ and } c_7 = 0.0.$$

where,

$y$  = geometrical mean of 2 horizontal components of PGA in g

$$\begin{aligned}
M &= \text{moment magnitude} \\
r_{rup} &= \text{distance to rupture surface in km} \\
\sigma \ln(y)_{rock} &= \begin{cases} 1.39 - 0.14M_w & ; M_w < 7.21 \\ 0.38 & ; M_w \geq 7.21 \end{cases} \\
\sigma \ln(y)_{soil} &= 1.52 - 0.16M_w
\end{aligned}$$

#### 2.5.2.12 Si and Midorikawa (2000)

Considering distance term as an essential parameter in deriving near-source model, Si and Midorikawa (2000) has included two types of distance term namely, closest distance to rupture plane and equivalent hypocentral distance, in their work. The model is derived by using 856 peak ground acceleration data from 21 Japan earthquakes. It classified fault types into three categories, that are, crustal, inter-plate and intra-plate earthquakes. Besides referring to the definition of rock and soil conditions as proposed by Joyner and Boore (1981), Si and Midorikawa (2000) also suggested conversion of PGA at rock site into PGA for soil site by multiplying the value with a factor of 1.4.

The model takes the following forms:

Attenuation model for rupture distance:

$$\begin{aligned}
\log A &= aM_w + hD + \sum d_i S_i + e - \log(X + c_1 10^{c_2 M_w}) - kX \\
S_i &= 0S_1 + 0.09S_2 + 0.28S_3
\end{aligned} \tag{2-33}$$

where,

$$\begin{aligned}
A &= \text{peak ground acceleration (PGA) in units of cm/sec}^2 \\
X &= \text{rupture distance in km} \\
M_w &= \text{moment magnitude} \\
D &= \text{focal depth in km}
\end{aligned}$$

Values of regression coefficients for PGA are:  $a = 0.50$ ,  $h = 0.0036$ ,  $d_1 = 0$ ,  $d_2 = 0.09$ ,  $d_3 = 0.28$ ,  $e = 0.60$ ,  $c_1 = 0.0055$ ,  $c_2 = 0.50$ ,  $k = 0.003$ , and standard deviation,  $\sigma = 0.27$ .

Attenuation model for equivalent hypocentral distance:

$$\begin{aligned}\log A &= aM_W + hD + \sum d_i S_i + e - \log(X_{eq}) - kX_{eq} \\ S_i &= 0S_1 + 0.01S_2 + 0.22S_3\end{aligned}\quad (2-34)$$

where,

$$\begin{aligned}A &= \text{peak ground acceleration (PGA) in units of cm/sec}^2 \\ X_{eq} &= \text{equivalent hypocentral distance in km} \\ M_W &= \text{moment magnitude} \\ D &= \text{focal depth in km}\end{aligned}$$

Values of regression coefficients for PGA are:  $a = 0.50$ ,  $h = 0.0043$ ,  $d_1 = 0$ ,  $d_2 = 0.01$ ,  $d_3 = 0.22$ ,  $e = 0.61$ ,  $k = 0.003$ , and standard deviation,  $\sigma = 0.28$ .

Dummy variable,  $S_i$  is referring to the fault type where;

$$S_i = \begin{cases} S_1=1, S_2=0, S_3=0 & \text{; for crustal} \\ S_1=0, S_2=1, S_3=0 & \text{; for interplate} \\ S_1=0, S_2=0, S_3=1 & \text{; for intraplate} \end{cases}$$

### 2.5.2.13 Somerville et al. (2009)

This is a stochastic model for several regions in Australia. Ground motions were simulated based on regional crustal velocity models and earthquake source scaling relations. Equations for cratonic region and noncratonic region are developed separately. This renders the non-homogeneous regions within Australia itself. Cratonic region can also be defined as stable continental platform. Thus, only the cratonic model is discussed in the present study. The form of ground motion model for rock sites having  $V_{S30}$  865 m/s appeared as follows:

For  $M < 6.4$ ,  $r < 50$  km

$$\begin{aligned}\ln PGA &= c_1 + c_2(M - 6.4) + c_3 \ln R + c_4(M - 6.4) \ln R \\ &\quad + c_5 r + c_8(8.5 - M)^2\end{aligned}\quad (2-35)$$

For  $M < 6.4$ ,  $r \geq 50$  km

$$\ln PGA = c_1 + c_2(M - 6.4) + c_3 \ln \sqrt{50^2 + 6^2} + c_4(M - 6.4) \ln R + c_5 r + c_6 (\ln R - \ln \sqrt{50^2 + 6^2}) + c_8 (8.5 - M)^2 \quad (2-36)$$

For  $M \geq 6.4$ ,  $r < 50$  km

$$\ln PGA = c_1 + c_7(M - 6.4) + c_3 \ln R + c_4(M - 6.4) \ln R + c_5 r + c_8 (8.5 - M)^2 \quad (2-37)$$

For  $M < 6.4$ ,  $r \geq 50$  km

$$\ln PGA = c_1 + c_7(M - 6.4) + c_3 \ln \sqrt{50^2 + 6^2} + c_4(M - 6.4) \ln R + c_5 r + c_6 (\ln R - \ln \sqrt{50^2 + 6^2}) + c_8 (8.5 - M)^2 \quad (2-38)$$

where,

PGA = peak ground acceleration in g

$$R = \sqrt{r^2 + 6^2}$$

r = Joyner Boore distance in km

M = moment magnitude

Values for coefficients are as follows:  $c_1 = 1.54560$ ,  $c_2 = 1.45650$ ,  $c_3 = -1.11510$ ,  $c_4 = 0.16640$ ,  $c_5 = -0.00567$ ,  $c_6 = -1.04900$ ,  $c_7 = 1.05530$ ,  $c_8 = 0.20000$  and standard deviation of the model,  $\sigma = 0.5513$ .

#### 2.5.2.14 Spudich et al. (1999)

The model is developed to predict ground motion of crustal earthquakes rose from extensional regions. Extensional regions are regions which the lithosphere is expanding areally. Strong motion recordings were collected globally which include Europe, New Zealand, Central America, Turkey, and Western United States. By using one-step regression method, a total of 142 records were analysed to obtain coefficients for equation form as shown in Eq. 2-39.

$$\log(Z) = b_1 + b_2(M - 6) + b_3(M - 6)^2 + b_5 \log D + b_6 \Gamma \quad (2-39)$$

$$D = \sqrt{r_{jb}^2 + h^2}$$

$$\sigma_{\log(Z)} = \sqrt{\sigma_1^2 + \sigma_2^2}$$

where,

- $Z$  = peak horizontal acceleration in g or pseudovelocity response in cm/sec at 5% damping for the geometrical mean horizontal component of motion  
 $r_{jb}$  = Joyner-Boore distance  
 $M$  = moment magnitude  
 $\Gamma$  = 0 for rock site and 1 for soil site  
 $h$  = focal depth in km  
 $\sigma_{\log(Z)}$  = standard deviation of  $\log(Z)$

Values for coefficients for peak horizontal acceleration are:  $b_1 = 0.299$ ,  $b_2 = 0.229$ ,  $b_3 = 0$ ,  $b_5 = -1.052$ ,  $b_6 = 0.112$ ,  $\sigma_1 = 0.172$  and  $\sigma_2 = 0.108$ .

#### 2.5.2.15 Toro et al. (1997)

Four sets of attenuation equations are stochastically-developed for CENA with 2 crustal regions  $\times$  2 magnitude scales to provide flexibility to user. The two magnitude terms used were moment magnitude and body-wave magnitude ( $Lg$ ). Compare to Gulf region, midcontinent is more suitable to describe conditions in Peninsular Malaysia. Thus, only equation incorporating moment magnitude and midcontinent for rock site, as shown in Eq. 2-40, is considered in present study. Toro (2002) had make changes to the model. However, the modification was only subjected for large magnitude and short distance. Thus, the modification is irrelevant and Toro et al. (1997) is more preferable in this study.

$$\begin{aligned}
 \ln Y &= C_1 + C_2(M - 6) + C_3(M - 6)^2 - C_4 \ln R_M \\
 &\quad - (C_5 - C_4) \max \left[ \ln \left( \frac{R_M}{100} \right), 0 \right] - C_6 R_M \\
 R_M &= \sqrt{R_{jb}^2 + C_7^2}
 \end{aligned} \tag{2-40}$$

where,

- $Y$  = spectral acceleration or peak ground acceleration in g  
 $R_{jb}$  = closest horizontal distance to earthquake rupture in km  
 $M$  = moment magnitude

Values for coefficients for PGA are:  $C_1 = 2.20$ ,  $C_2 = 0.81$ ,  $C_3 = 0.00$ ,  $C_4 = 1.27$ ,  $C_5 = 1.16$ ,  $C_6 = 0.0021$  and  $C_7 = 9.3$ .

When using this model, amplification factor of rock sites for application on soil sites can be conducted by referring to (EPRI, 1993).

## 2.6 Summary

This chapter provides an overall literature review on earthquakes and insight of ground motion attenuation models. It is indisputable that understanding towards the nature of earthquake sources and characteristics of earthquakes that they generate is essential in order to decrease our vulnerability to earthquakes.

Sumatra subduction zone and Sumatra fault zone has always been a major seismicity source to Peninsular Malaysia despite the long distance in between. Sumatra zone has been recognized as the most active earthquake source in the world. Previous studies and researches in discovering the characteristics in terms of seismicity, topography and geology of the Sumatra subduction zone and Sumatra fault zone has provide discernment for present study.

In order to determine the most suitable ground motion attenuation models, understanding in characteristics and mechanisms of earthquake source alone is not sufficient without knowledge about ground motion attenuation models. Since more than half century ago, hundreds of ground motion attenuation models have been developed for numerous regions as well as different types of earthquake source and distance. These models utilised different datasets and several distinct methods in their derivation. Hence, a set of exclusion criteria has to be adopted in the pre-selection phase in the present study. This enables a manageable number of attenuation models for closer examination. A number of renowned ground motion attenuation models have been reviewed in this chapter. And finally, some attenuation models that are suitable to be used in Peninsular Malaysia can be discovered.

## CHAPTER 3

### RESEARCH METHODOLOGY

#### 3.1 Introduction

This chapter describes method employed in determining the most appropriate ground motion attenuation model to describe ground motion in Peninsular Malaysia. The research methodology activities carried out in this study is presented in the form of flow chart as illustrated in Figure 3.1.

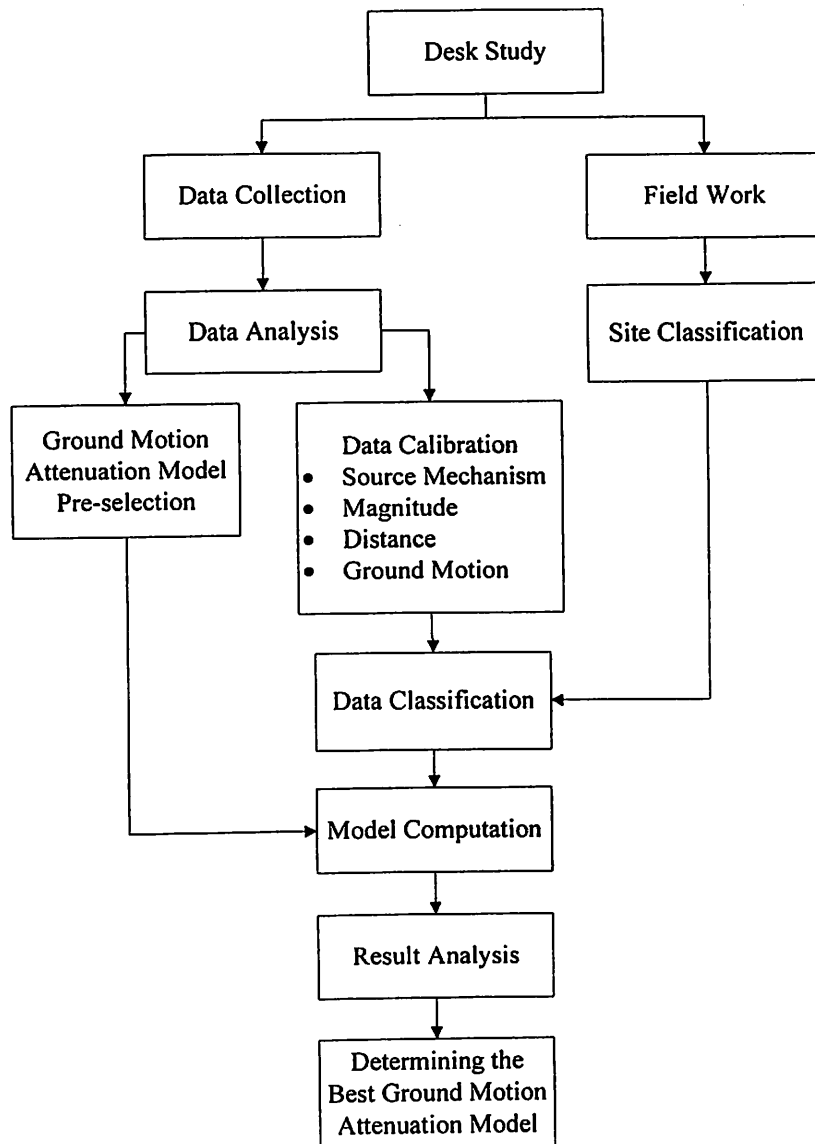


Figure 3.1 Flow chart of research methodology

The chapter begins with discussion about analysis of ground motion data collected from some authorities and international databases. Data analysis is an essential stage, which involves processing of collected data to obtain parameters in the correct scale that are required in the computational and analysis in this study. Prior to scale standardization, selection of ground motion data to be used in this study is considered based on the interest of the study as well as completeness of seismological information supplied by local authorities and international seismological databases.

Thus, this chapter also includes method used to classify earthquake source mechanism, conversion of parameters into universal scale as well as introducing new site classification scheme for ground condition beneath seismic stations in Peninsular Malaysia. Exemption criterion for pre-selection of ground motion attenuation models in order to regulate models into manageable amount in this study is reviewed.

Finally, method in computing ground motion by using ground motion attenuation models of concern as well as software involved is discussed. Statistical measures to give quantitative comparison measures among models with recorded ground motion data is also considered in this chapter.

### **3.2 Data collection and selection**

Time histories of acceleration recorded in Peninsular Malaysia were obtained from MMD. The recorded accelerations are in three components, which are two horizontal components (N and E component) and one vertical component (Z component). The accelerations time histories were originally recorded by 20 seismic stations located all over Peninsular Malaysia. From the listed record of earthquakes that affected Peninsular Malaysia, data from July 2004 to July 2013 were taken due to the availability of ground motion data provided. As shown in Figure 3.2, a total of 73 events were recorded in the time frame mentioned above. Based from the events locations, 44 are distant earthquakes originated from Sumatra subduction and fault zone. The rest are small local earthquakes originated within Peninsular Malaysia and were excluded as they are not of interest in this study.



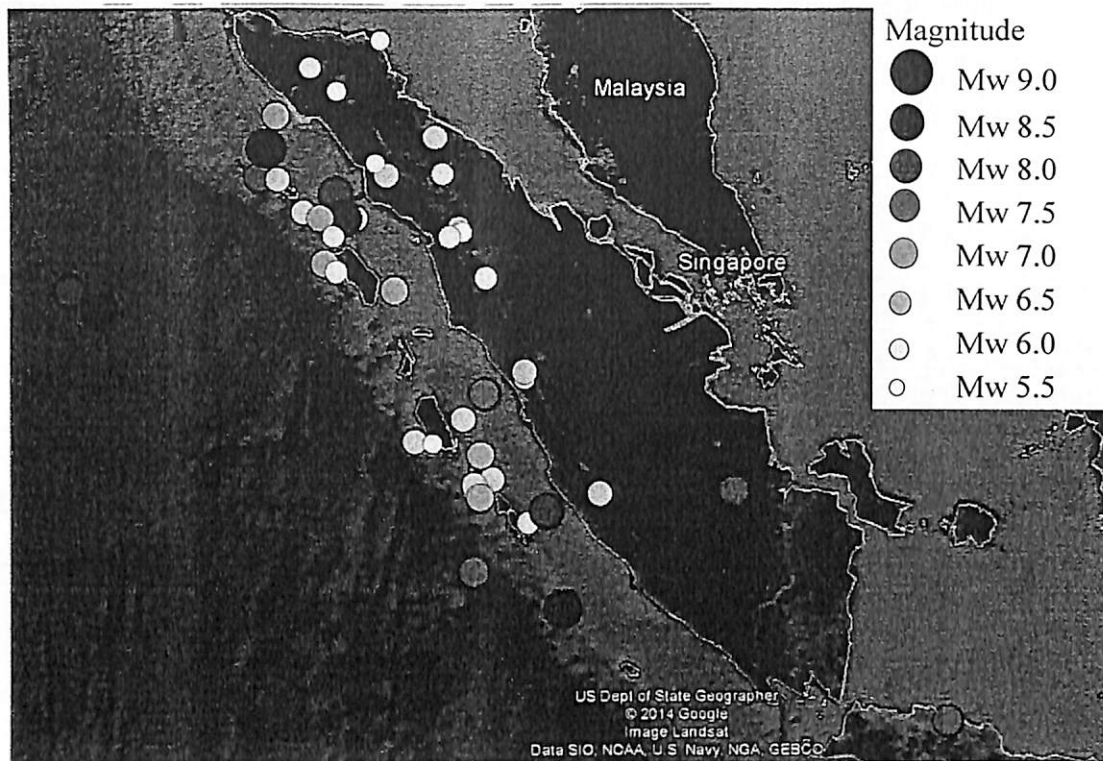


Figure 3.2 Map showing location and magnitude of distant earthquake events from July 2004 to July 2013

### 3.3 Data analysis and calibration

Data analysis is a process to study data collected and convert data into format that is ready to be analyzed in the next step. This study referred to some databases from other seismological centers to fill in missing data and avoid inaccurate details. The three international free-access databases, namely United States Geological Survey (USGS) database, International Seismological Centre (ISC) database and National Earthquake Information Center (NEIC) database, are cited in this study. Missing data or details involves some important parameters such as distance, magnitude, ground motion, source mechanism and site classification. These data has to be calibrated and standardized into readily-used scale for analysis.

#### 3.3.1 Source mechanism

Global Centroid Moment Tensor (CMT) project moment tensor solution and NEIC moment tensor solution were used to interpret and distinguish tectonic mechanism for each event. The two moment tensor solutions were international

open-access databases. USGS databasc provide the illustration of stereonet projection that better represent the focal mechanism of an event. Figure 3.3 exhibits the format and seismological information obtained from USGS database. On the other hand, ISC database only provide information of moment tensor solution in values. Thus, some of the events used in this study require stereonet to be self-drawn.

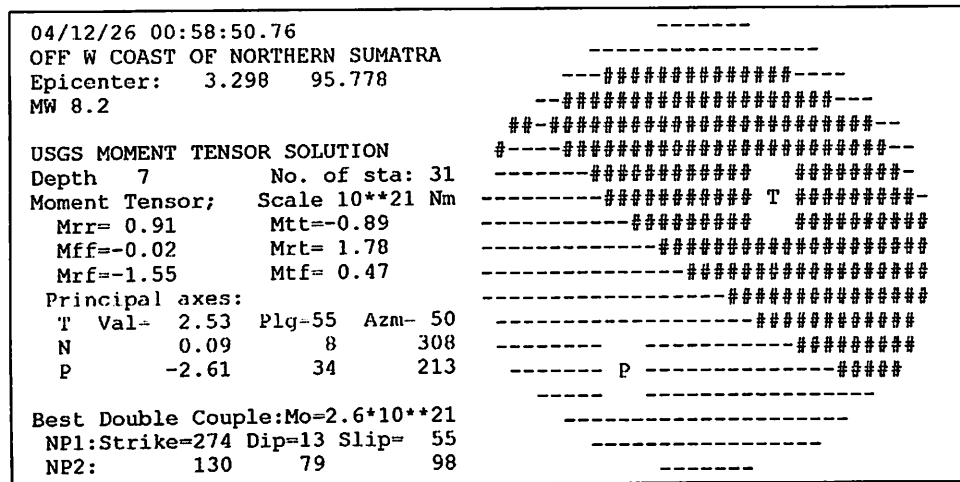


Figure 3.3 USGS Moment Tensor Solution for Sumatra megathrust earthquake on 26 December 2004 (USGS, 2013)

Based from geological and seismological information regarding Sumatra zone, Sumatra subduction produces earthquakes that falls into two types of source mechanisms, namely interface earthquakes and intraslab earthquakes while Sumatra fault zone only involves in producing strike-slip earthquakes. Interface earthquakes occur at a depth less than 50 km on shallow dipping planes. They are associated with thrust faulting of subducting oceanic plate which is in contact with the overriding continental crust. Classified as shallow earthquakes, interface earthquakes are capable in producing megathrust earthquakes up to magnitude 9. Intraslab earthquakes, on the other hand, have steep dipping planes. Intraslab earthquakes have magnitude not larger than 8 and are typically occur along normal faults where the subducting plate suffers stress and physical changes as it is pulled deeper into the aesthenosphere. However, thrust mechanism is also assumed to be intraslab event if the event occurs at depth greater than 50 km as it is below the crustal contact zone.

Slip angle, fault motion and focal depth from catalogues and moment tensors are used to distinguish earthquakes into interface, intraslab and shallow strike-slip

mechanisms. The determination of source mechanisms is important in pre-selection of ground motion attenuation model and also analysis in the later stage. The resulting classification based on source mechanism shall be as shown in Figure 3.4.

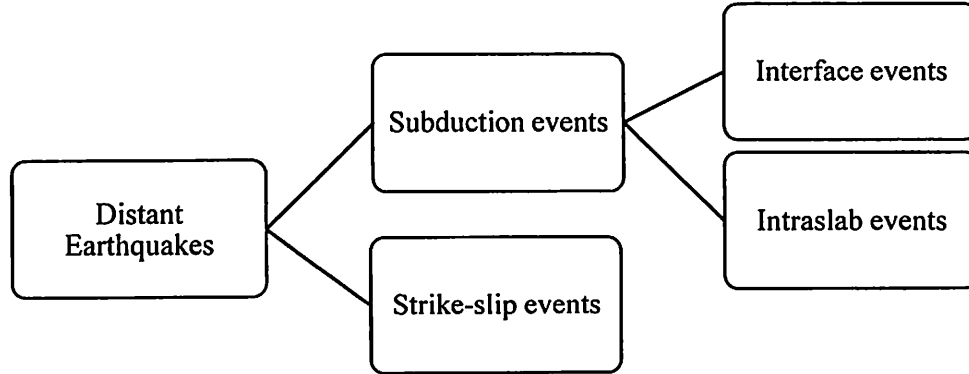


Figure 3.4 Chart of classification of source mechanism.

### 3.3.2 Magnitude

Moment magnitude ( $M_W$ ) is preferred over other types of magnitude scale due to its ability of withstanding saturation at larger earthquakes. However, instead of providing  $M_W$ , MMD recorded events in the  $M_L$ ,  $M_S$  or  $m_b$ . Thus, compilation of  $M_W$  from other international databases such as USGS, ISC and NEIC has been carried out.

Though majority of pre-selected ground motion attenuation models utilised  $M_W$ , there is also model using  $M_S$  as magnitude scales. Such model in this study is Fukushima and Tanaka (1990). Therefore, magnitude conversion equations developed by Scordilis (2006) is benefited in the present study. The magnitude conversion equation takes the form as shown below:

$$M_W = \begin{cases} 0.67M_S + 2.07 & ; 3.0 \leq M_S \leq 6.1 \\ 0.99M_S + 0.08 & ; 6.2 \leq M_S \leq 8.2 \end{cases} \quad (3-1)$$

### 3.3.3 Distance

Source-to-site distance is one of the important parameter in this study. Different attenuation models utilized different types of distance terms. Among so many models, epicentral distance ( $r_{epi}$ ), hypocentral distance ( $r_{hypo}$ ), distance to rupture plane ( $r_{rup}$ ) and Joyner-Boore distance ( $r_{jb}$ ) are the most commonly used distance terms in existing ground motion attenuation models. Though so, only one distance term is proposed in this study to ease comparison among attenuation models adopted. Among all,  $r_{epi}$  has been chose for the standardisation purposed. Moreover,

the differences among  $r_{epi}$ ,  $r_{hypo}$ ,  $r_{rup}$  and  $r_{jb}$  is only below 10 to 20 km, depending on focal depth or seismogenic depth. Thus, these differences are considered insignificant compare to the long distance from source to site (Naguit, 2007). The definition of  $r_{epi}$  used in this study is the horizontal distance between epicenter of an earthquake and the site of recording instrument.

MMD provides coordination for epicentres of each earthquake source as well as coordination for seismic stations within Peninsular Malaysia. Thus, calculation to obtain distance between each earthquake source and respective stations where ground motion can be detected has to be performed. The Carlson and Clay (1999) model is benefited for the distance computation purpose as the model use WGS84 spheroid earth model considering the major and minor axis of the earth. On top of that, the model is accurate in providing distance in kilometre up to 2 decimals. Below is the formula of distance conversion developed by Carlson and Clay (1999).

Latitude of point 1	= lat_p1
Longitude of point 1	= long_pt1
Latitude of point 2	= lat_p2
Longitude of point 2	= long_pt2
Elev	= elevation
maj_axis	= Earth's major axis (6378137 m)
min_axis	= Earth's minor axis (6356752.3142 m)

$$\text{True angle, TA1} = \left[ \tan^{-1} \left( \frac{(\text{min\_axis})}{(\text{maj\_axis})} \tan(\text{lat\_p1})(\pi/180) \right) \right] (180/\pi) \quad (3-2)$$

$$\text{True angle, TA2} = \left[ \tan^{-1} \left( \frac{(\text{min\_axis})}{(\text{maj\_axis})} \tan(\text{lat\_p2})(\pi/180) \right) \right] (180/\pi) \quad (3-3)$$

$$\text{Radius pt 1, RA1} = \left[ \sqrt{\frac{1}{\frac{\cos(TA1(\pi/180))^2}{\text{maj\_axis}^2} + \frac{\sin(TA1(\pi/180))^2}{\text{min\_axis}^2}}} \right] + \text{elev} \quad (3-4)$$

$$\text{Radius pt 2, RA2} = \left[ \sqrt{\frac{1}{\frac{\cos^2(\text{TA2}(\pi/180))}{\text{maj\_axis}^2} + \frac{\sin^2(\text{TA2}(\pi/180))}{\text{min\_axis}^2}}} \right] + \text{elev} \quad (3-5)$$

X-Y earth coordinates;

$$\text{xy1} = \text{RA1}[\cos(\text{TA1}(\pi/180))] \quad (3-6)$$

$$\text{xy2} = \text{RA1}[\sin(\text{TA1}(\pi/180))] \quad (3-7)$$

$$\text{xy3} = \text{RA2}[\cos(\text{TA2}(\pi/180))] \quad (3-8)$$

$$\text{xy4} = \text{RA2}[\sin(\text{TA2}(\pi/180))] \quad (3-9)$$

$$\text{X coordinate, x} = \sqrt{(\text{xy1} - \text{xy3})^2 + (\text{xy2} - \text{xy4})^2} \quad (3-10)$$

$$\text{Y coordinate, y} = (2\pi) \left[ \frac{((\text{xy1} + \text{xy3})/2)}{360} \right] (\text{long\_pt1} - \text{long\_pt2}) \quad (3-11)$$

$$\text{Distance in meter} = \sqrt{x^2 + y^2} \quad (3-12)$$

### 3.3.4 Ground motion parameter

The PGA is the maximum amplitude of the ground acceleration time-history. It is also known as zero period acceleration. In this study, PGA is chosen over spectral ordinates because of its simplicity in indicating the most critical condition (Bradley, 2011). Adoption of only PGA in examination of ground motion attenuation model has also been performed by (Chintanapakdee et al., 2008). Time histories obtained from MMD were plotted into graphs by using MATLAB software. From those graphs, peak accelerations, peak velocities and peak displacements were identified. Figure 3.5 shows an example of time histories computed by MATLAB software. The peak accelerations were then converted from  $\text{cm/sec}^2$  into g unit.

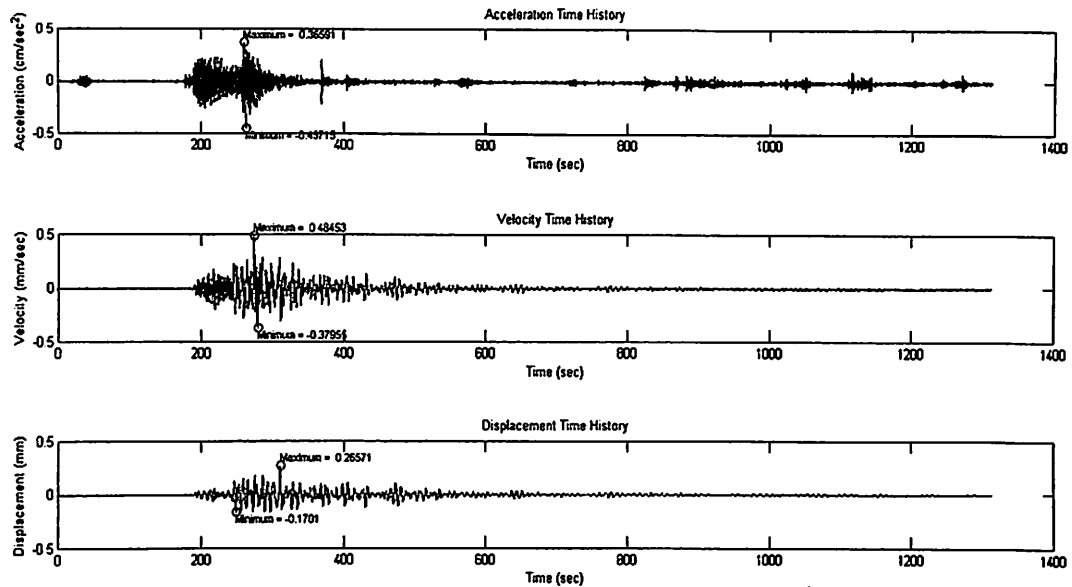


Figure 3.5 Graph of horizontal in E component time histories computed by MATLAB software by FRM station for Mw 6.8 event happened on 14 May 2005 originating from Northern Sumatera

The PGA value utilized in this study is the geometrical mean of two horizontal components of ground motion acceleration at a site. Vertical component PGA, that is Z component, diminishes faster than horizontal components, thus giving lesser effect on ground motion for far-field earthquake (Bozorgnia et al., 2000). Hence, vertical component is excluded in this study. The PGA of E and N component are added together and then divided by two to obtain the geometrical mean of PGA. As a result, geometrical mean of PGA for Peninsular Malaysia from July 2004 to July 2013 range from 0.000015g to 0.002220g.

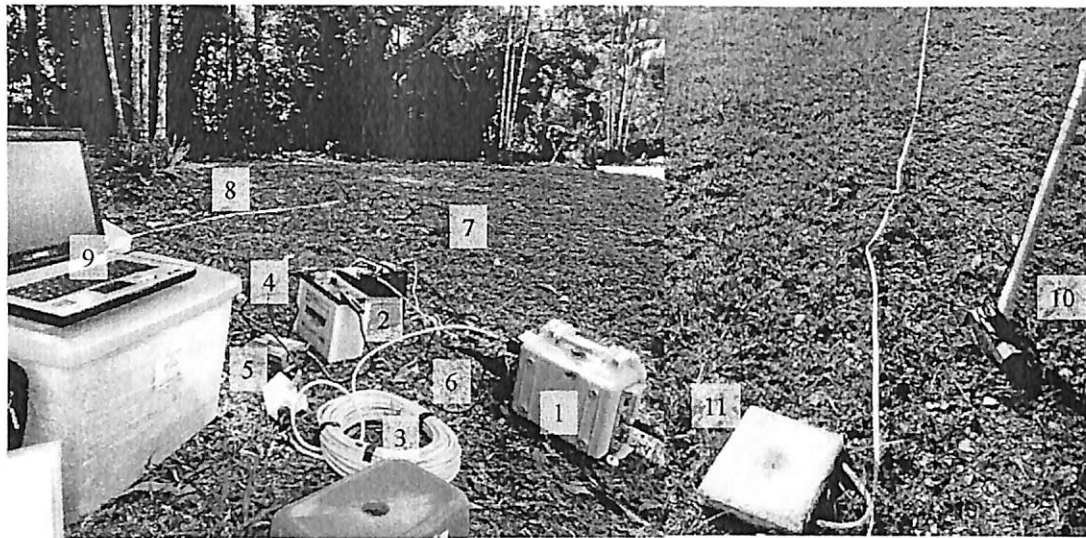
The geometrical mean of horizontal PGA of actual site recordings were compared with PGA computed from equations provided by pre-selected models. For models that do not provide coefficient values in determining PGA, approximation of PGA was carried out. According to Douglas et al. (2012), coefficients for periods less than 0.04 s, that is 25 Hz can be used to estimate PGA.

### 3.4 Site classification

There are a total of 20 seismic stations located by MMD within Peninsular Malaysia. However, PYSM\_B9 is placed on the ninth floor of the Putrajaya building and not on the ground level. Thus, it has been excluded in this study, leaving 19 seismic stations that are useful in this study. These seismic stations are described to be sitting on granite, sandstone, soft soil, meta-sediment or rocky foundations, as shown in Table 2.4. However, the descriptions on the ground conditions for respective seismic stations were found to be too general. Information such as type, depth and strength of soil layers sitting on top of these rocks are lacking. Hence, a better description and classification of ground underneath seismic stations within Peninsular Malaysia has to be proposed and this requires conduction of some field works. Most of the attenuation models and seismic design guidelines and provisions established after 1997 make use of shear-wave velocity in the upper 30 m,  $V_{S30}$  of the site profile to classify sites. Hence, site classification based on  $V_{S30}$  is also adopted in this study.

$V_{S30}$  can be obtained from in-situ measurement or deduced from borelog and geological map. Instead of using expensive, time consuming and contaminating borehole measurements, multichannel surface wave (MASW) analysis as one of the non-invasive method in measuring shear-wave velocity is used in this study. The reliability of MASW has been tested comparing with other invasive method. Xia et al. (2002) found that results from MASW analysis and borelog deductions are less than 15 % for both rock sites and soil sites. This finding was supported by results from other studies at different sites such as at Fraser River Delta, Canada (Xia et al., 2000), Turkey (Yilmaz et al., 2008), Norway and Ireland (Donohue and Long, 2008). These findings had implicitly proved that MASW produces reliable results on all types of sites.

MASW test was used to obtain the relationship of S-wave velocity with depth by inverting the dispersive surface of Rayleigh wave phase velocity. A full set of 1D MASW tools is shown in Figure 3.6. Lastly, the Seismodule Controller software is required to run the test.



Legends:

- |                   |                      |                    |
|-------------------|----------------------|--------------------|
| 1. GEODE          | 5. Inverter          | 9. Laptop          |
| 2. Battery        | 6. Trigger Extension | 10. Sledgehammer   |
| 3. Ethernet Cable | 7. Spread Cable      | 11. Striking Plate |
| 4. Battery Cable  | 8. Geophones         |                    |

Figure 3.6 Full set of MASW tools

Figure 3.7 illustrates the field configuration of MASW tools. A total of twenty-four 4.5 Hz geophones are deployed vertically on the soil in a straight line with spacing interval of 1 to 1.5 m, depending on the area availability at site. Spread cables were then connected to each geophones and finally to the GEODE. Offsets of 5 m, 10 m, and 15 m were measured from the first and the last geophones. These offsets are the coordination where the 8 kg hammer-striking took place as recommended by Xu et al. (2006) with the very soft soil to hard soil in ascending offsets distance. Two set of tests were carried out for each offset and blows of hammer were fixed according to the condition at site. Sites with higher traffic volume or near to undergoing construction sites are more likely to be affected by noises. Thus, higher stacking limit (number of hammer blows) are required. As a result, a range of 5 to 12 blows were applied to seismic stations depending on condition. The record length and sampling rate were adjusted to 1 s and 0.25 ms respectively.



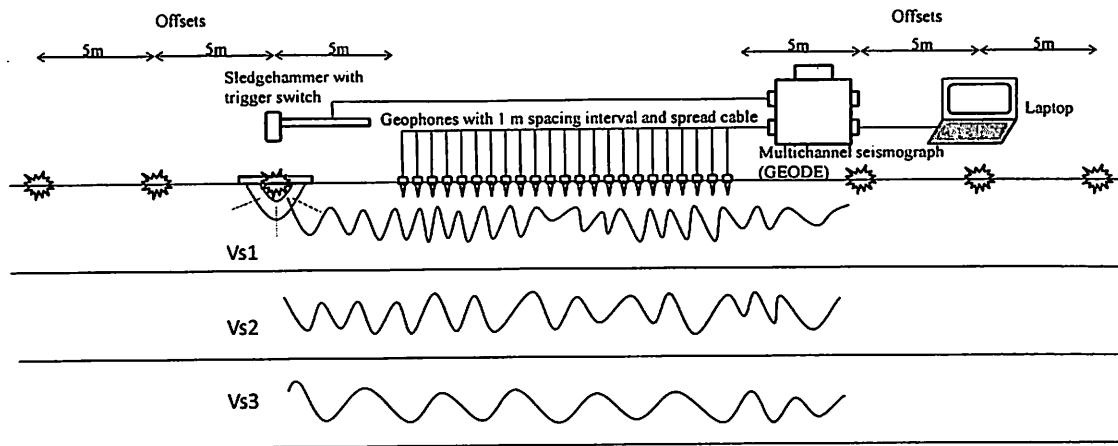


Figure 3.7 Schematic diagram of MASW configuration at site

Analysis of the collected data was conducted using SeisImager/SW<sup>TM</sup> software. Collected accelerographs take the form as shown in Figure 3.8. Unnecessary noise from these accelerographs was filtered out and only wave within a range of 3 Hz to 85 Hz are taken as S-wave frequency falls within that range. Due to the different speed in high frequency wavelength and low frequency wavelength, dispersion occurs.

Then, accelerographs were transformed into a phase velocity over frequency plot. Phase velocity is the velocity of each frequency. The blue regions and yellow regions in Figure 3.9 denote the value amplitudes with blue regions showing the highest amplitudes to yellow regions showing smaller amplitude. Phase velocity picking of the maximum amplitudes, denoted by red dots, from the graphs were carried out to obtain the dispersion curve. Figure 3.10 shows the plot of phase velocity-frequency in an inverted form with phase velocity plotted on vertical axis and frequency plotted on horizontal axis. The bottom line denotes the dispersion curve. The circles along the dispersion curves show the quality factor of the picked dispersion curve. Larger circles symbolize higher quality factor. The above dotted line stands for ratio of signal to noise.

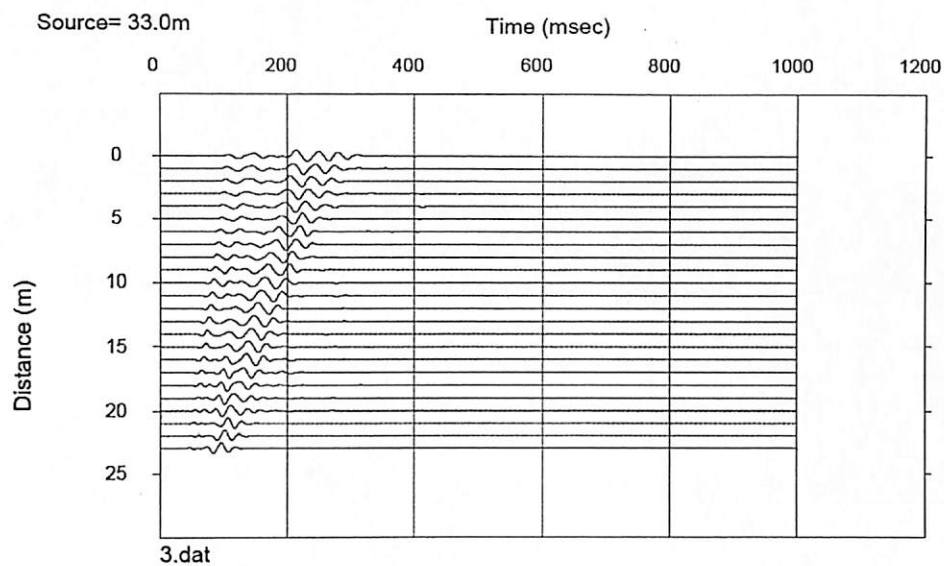


Figure 3.8 Collected accelerograph from the induced source (hammering)

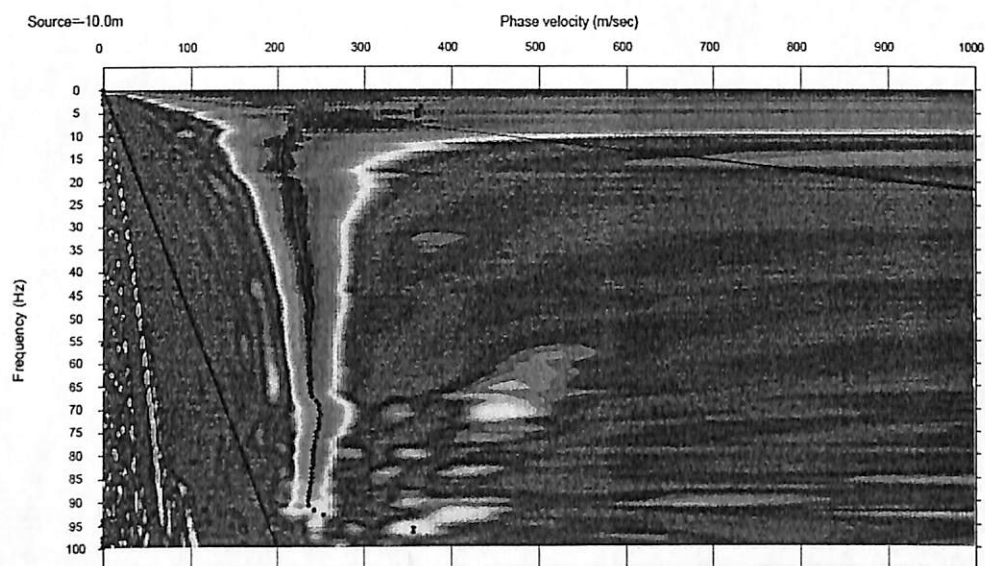


Figure 3.9 Plot of phase velocity against frequency

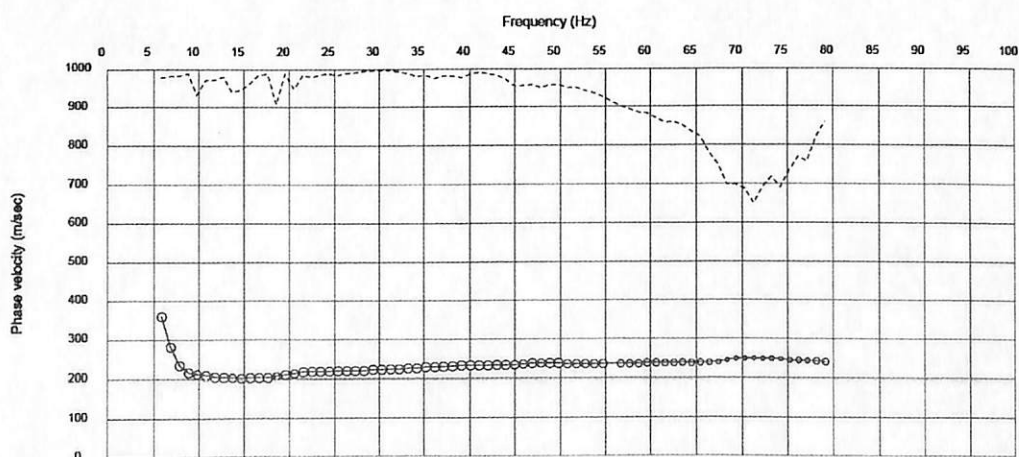


Figure 3.10 Dispersion curve and quality factor (dotted line)

There are two steps in transforming the picked dispersion curve into shear wave profile. First, an initial S-wave velocity of the site profiles was plotted. This was done by inserting required depth and number of layers. For this study, the depth of interest and number of layers is 30 m and 15 layers, respectively. Inversion was conducted next, to converge on the best fit of the initial model to the observed data. The resulting S-wave velocity against depth profile as shown in Figure 3.11 and the value of  $V_{S30}$  is obtained. The resulting  $V_{S30}$  were used to classify seismic stations into categories by referring to NEHRP 1997 site classification as shown in Table 2.6.

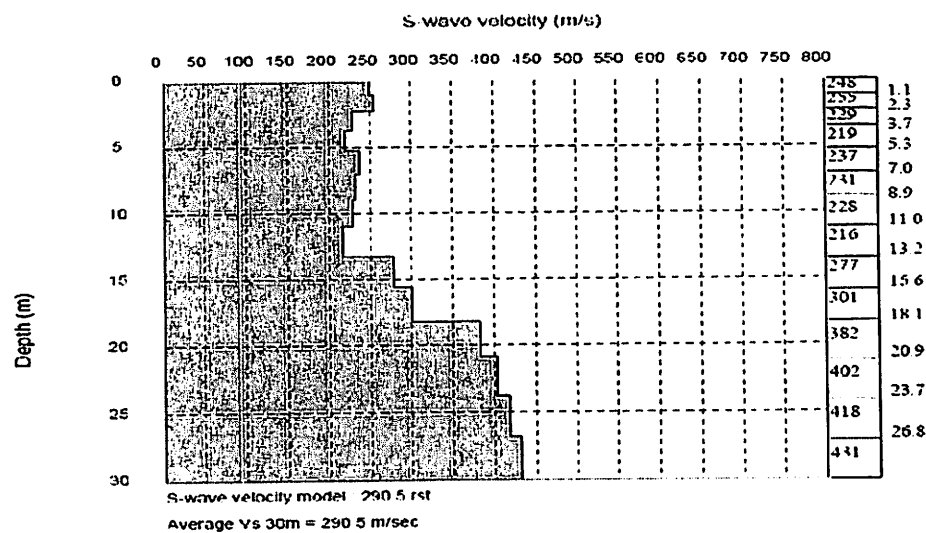


Figure 3.11 S-wave velocity against depth profile and  $V_{S30}$

### 3.5 Pre-selection of ground motion attenuation models

A reliable set of ground motion attenuation models is the main concern to obtain a dependable outcome in this study. Pre-selection of ground motion attenuation models from a comprehensive list as done by Douglas (2011) into a handy number of models is a crucial stage prior to the final examination. A proper set of criteria of exclusion could facilitate reliable examination and finally, consistent result. Generally, exclusion criterion as proposed by Cotton et al. (2006) which is also used by Douglas et al. (2012) in the effort to obtain global earthquake model is referred in this study. The exclusion criterion can be referred in Section 2.5.

However, some exceptions have been carried out to suit the circumstances in the present study. For instance, criterion 6 is excluded in the present study as the criterion requires only consideration on models developed using moment magnitude

and predictions on rock site. There has been numbers of handy magnitude conversion formula developed to standardise the magnitude parameter for analysis. Due to the ease provided for conversions of magnitude, models utilising other magnitude scale should not be excluded. Prediction on rock sites is vital, however, all amplification factors for other sites has also been developed. Thus, the criterion is not valid and is excluded from present study.

It should also be noted that pre-selected models in this study is not confined under magnitude and distance constraint to fit the data collected. This is because there are only a few numbers of ground motion attenuation models developed for far-field earthquake, so distance confinement might overlook models with small distance range but having the attenuation curve that could match actual ground motion at long distance when extrapolated. Sumatra subduction zone is capable in producing large earthquakes which are absent in other regions. Therefore, excluding models with small upper limit magnitude might neglect their potential.

Based from the exclusion criteria for the pre-selection mentioned above and by obeying the pre-selection of 10% out of available ground motion attenuation models as suggested by Douglas et al. (2012), a total of 28 ground motion attenuation models were shortlisted. Naguit (2007) had pre-selected 18 attenuation models for examination, which also comply with the 10% rule of the available models back then. All 28 shortlisted models, except Adnan et al. (2004), Petersen et al. (2004) and Nabilah and Balendra (2012) are taken from the list of ground motion attenuation models reviewed by Douglas (2011). The 3 exceptional models are included in this study despite not being listed in the review due to the target regions of their derivations, which is Peninsular Malaysia.

Out of these models, 13 of them are models to predict subduction earthquakes while the rest are for prediction of shallow crustal earthquake. Table 3.1 lists attenuation models for subduction earthquakes together with brief description regarding distance, focal depth and magnitude ranges as well as method of derivation and host and target regions. Table 3.2 summarises attenuation models for shallow crustal earthquakes according to tectonic regimes, namely active tectonic regions and stable continental regions.

### 3.6 Result analysis

After all parameters were standardized and identified, result analysis was carried out. In this study, result analysis involves input of seismological parameters, which were processed earlier, into the list of pre-selected ground motion attenuation models in order to compute predictions of ground motions. Each ground motion attenuation models were established using different data from different regions in the world, different considerations in source, path and site conditions and thus, results in different curves when the same set of seismological parameters were applied. Hence, examination of these ground motion attenuation models was carried out both qualitatively and quantitatively.

For qualitative examination, SPSS software was used to plot ground motion attenuation curves together with scatter of recorded ground motion for Peninsular Malaysia. This enables the visual comparison between predicted and recorded ground motion.

There are several statistical term in measuring variations of a sample data to a prediction model. They are such as coefficient of determination ( $R^2$ ), Pearsen product-moment correlation coefficient, and root mean squared error (RMSE). As for quantitative comparison, computations of RMSE among ground motion attenuation models in relation to recorded data were conducted. RMSE is chosen over Pearsen product-moment correlation coefficient because of the applicability of the term to

Table 3.1 Pre-selected ground motion attenuation model for subduction earthquakes with applicability range

No.	Attenuation models	Types of model	Focal depth (km)	Magnitude range	Source-to-site distance (km)	Origin of ground motion database utilised in model development	Target region
1.	Adnan et al. (2004)	Empirical	5-56	Mw 5.0-8.5	$r_{epi}$ 2-1122	Worldwide	Malaysia
2.	Atkinson and Boore (2003)	Empirical	0-100	Mw 5.0-8.3	$r_{rup}$ 10-400	Japan, Mexico, Central America and Cascadia	Cascadia
3.	Crouse (1991)	Empirical	0-238	Mw 4.8-8.2	$r_{epi}$ 8-866	Chile, Peru, Mexico, Alaska, and Japan	Cascadia
4.	Fukushima and Tanaka (1990)	Empirical	0-100	Mw 4.5-8.2	$r_{rup}$ 10-300	Japan and worldwide	Japan
5.	Gregor et al. (2002)	Stochastic	Unknown	Mw 8.0-9.0	$r_{rup}$ 10-500	Mexico, Chile and synthetic data	Cascadia
6.	Kanno et al. (2006)	Empirical	0-180	Mw 5.0-8.2	$r_{rup}$ 1-450	Japan	Japan
7.	Lin and Lee (2008)	Empirical	5.5-161	Mw 4.1-8.1	$r_{hypo}$ 15-630	Taiwan and worldwide	Taiwan
8.	Megawati et al. (2005)	Stochastic	15-33	Mw 4.5-8.0	$r_{epi}$ 150-1500	Singapore and synthetic seismograms	Singapore
9.	Megawati and Pan (2010)	Stochastic	12-44	Mw 5.4-9.1	$r_{epi}$ 200-1500	Singapore and synthetic seismograms	Singapore
10.	Nabilah and Balendra (2012)	Empirical	0-35	Mw 7.2-9.1	$r_{epi}$ 498-1021	Singapore and Peninsular Malaysia	Malaysia
11.	Petersen et al. (2004)	Numerical	0-229	Mw 5.0-8.2	$r_{rup}$ >200	Database from Youngs et al. (1997) and Sumatra	Singapore and Peninsular Malaysia
12.	Youngs et al. (1997)	Empirical	0-229	Mw 5.0-8.2	$r_{rup}$ 10-500	Alaska, Chile, Cascadia, Japan, Mexico, Peru and Solomon island	Global
13.	Zhao et al. (2006)	Empirical	0-162	Mw 5.0-8.0	$r_{rup}$ 10-300	Japan, United States and Iran	Japan

Table 3.2 Pre-selected ground motion attenuation model for shallow crustal earthquakes at active tectonic region with applicability range

No.	Attenuation models	Types of model	Focal depth (km)	Magnitude range	Source-to-site distance (km)	Origin of ground motion database utilised in model development	Target region
1.	Abrahamson and Silva (1997)	Empirical	-	Mw 4.4-7.4	$r_{rup}$ 0.1-200	Worldwide	Worldwide
2.	Ambraseys et al. (2005)	Empirical	1-30	Mw >5.0	$r_{rup}$ 1-100	Europe and Middle East (mainly Italy, Turkey, Greece, Iceland)	Europe and Middle East
3.	Atkinson and Boore (2006, 2011)	Stochastic	-	Mw 3.5-8.0	Fault distance 1-1000	Synthetic data	Eastern North America
4.	Boore et al. (1997, 2005)	Empirical	0-20	Mw 5.2-7.4	$r_{jb}$ 0-118	North Eastern US, South Eastern Canada	Western North America
5.	Dahle et al. (1990)	Empirical	-	Mw 2.9-7.8	$r_{hypo}$ 1-1300	Worldwide intraplate	Worldwide
6.	Megawati et al. (2003)	Stochastic	8-22	Mw 4.0-8.0	$r_{epi}$ 174-1379	Singapore and synthetic seismograms	Singapore and Peninsular Malaysia
7.	Sadigh et al. (1997)	Empirical	-	Mw 4.0-8.0	$r_{rup}$ 0-100	California	California
8.	Si and Midorikawa (1999)	Empirical	6-120	Mw 5.8-8.2	$r_{epi}$ 0-118	Japan	Japan
9.	Spudich et al. (1999)	Empirical	-	Mw 5.0-7.7	$r_{jb}$ 0-100	Worldwide	Worldwide

Table 3.3 Pre-selected ground motion attenuation model for shallow crustal earthquakes at stable continental region with applicability range

No.	Attenuation models	Types of model	Focal depth (km)	Magnitude range	Source-to-site distance (km)	Origin of ground motion database utilised in model development	Target region
1.	Campbell (2003, 2004)	Hybrid empirical	-	Mw 5.0-8.2	$r_{rup}$ 0-1000	Used empirical model to establish theoretical factor	Eastern North America
2.	Frankel et al. (1996)	Stochastic		Mw 4.4-8.0	$r_{hypo}$ 10-1000	Synthetic seismograms	Central and Eastern USA
3.	Hwang and Huo (1997)	Stochastic	6-15	Mw 5.0-7.5	$r_{epi}$ 5-200	Synthetic data	Central and Eastern United States
4.	Pezeshk et al. (2011)	Hybrid empirical		Mw 5.0-8.0	$r_{rup}$ 0-1000	-	Eastern North America
5.	Somerville et al. (2009)	Stochastic	0-6	Mw 5.0-7.5	$R_{jb}$ 0-500	Synthetic seismograms	Australia
6.	Toro et al. (1997)	Stochastic	-	Mw 5.0-8.0	$r_{jb}$ 1-500	Synthetic data	Central and Eastern North America



only linear predictive model. Coefficient of determination is not appropriate to be used on testing data sample that is not included in dataset for derivation of the predictive models. RMSE is known as the standard error of the estimate of the differences between out-of-sample predictive model and actually observed value. It is a good measure of accuracy to compare forecasting errors of different models (Hyndman and Koehler, 2006). This measure has also seen being used to compare a group of ground motion attenuation models for the application in Thailand (Naguit, 2007). The formula of RMSE is as shown below:

$$RMSE = \sqrt{\frac{\sum_{i=1}^n (X_{obs,i} - X_{model,i})^2}{n}} \quad (3-13)$$

where,

$$\begin{aligned} X_{obs} &= \text{observed value at time } i \\ X_{model} &= \text{predicted value by model at time } i \\ n &= \text{total number of value} \end{aligned}$$

Unlike coefficient of determination, RMSE does not have range of acceptability. However, it can be normalised over the range of observed values. The normalised RMSE are often expressed in percentage value, similar to average percentage of difference, with smaller value representing smaller residual variance (Terrell, 1999). The formula of normalised RMSE,  $RMSE_{Nor}$  is as following:

$$RMSE_{Nor} = \frac{RMSE}{X_{obs,max} - X_{obs,min}} \quad (3-14)$$

where,

$$\begin{aligned} X_{obs,max} &= \text{maximum observed value} \\ X_{obs,min} &= \text{minimum observed value} \end{aligned}$$

### 3.7 Summary

Several international free-access databases such as USGS, ISC and NEIC has been referred to limit errors and fill in missing data (e.g. moment magnitude in this study) in order to optimize the usage of data obtained from MMD. Formula of conversion of distance and magnitude from other studies and researches has also been utilized in this study.

Discovering the most appropriate ground motion attenuation models to be used in describing seismic conditions for Peninsular Malaysia involved a lot of critical steps from selection of reliable data, careful standardization of magnitude and distance scales, selection of ground motion parameter of interest, distinguishing of source mechanisms and classification of sites. Pre-selection of which ground motion attenuation models to be examined in this study has also been conducted based on strict exemption criterion in order to provide consistent analysis and results.

Lastly, the final examination of pre-selected models was followed by plotting of graphs for visual presentations while quantitative results are provided by calculation of RMSE.

## **CHAPTER 4**

### **RESULTS AND DISCUSSION**

#### **4.1 Introduction**

This chapter starts off with presentations of outcomes of the calibration of each important parameter in this study. This chapter also discusses about the shear-wave velocity results from field work done on the 19 seismic stations in Peninsular Malaysia using MASW. The calibrations and site classifications were used for analysis.

Thus, this chapter also includes graphical presentations of attenuation curves of 28 ground motion attenuation models and collected actual ground motion data. Together with computed RMSE value, discussion about curve trend and differences among each attenuation model is performed. Models with low RMSE value and curve trend similar to actual data are identified and proposed.

Validation of proposed ground motion attenuation model with two new earthquake events is conducted and presented in this chapter. Finally, a summary of findings is presented in the end of this chapter.

#### **4.2 Parameters calibration result**

Important parameters such as source mechanism, magnitude and distance were calibrated prior to analysis of result. Result of calibrations is discussed in following sub-sections.

##### **4.2.1 Source mechanism**

Tensor moment solutions for a total of 44 distant earthquakes were studied to identify mechanism of the earthquake sources. This information was obtained from open-access ISC database and USGS database. Due to the format of the ISC database, stereonet that often be used in determining focal mechanism was not provided. Thus, stereonets for events obtained from ISC database was projected manually.

From a total of 44 distant events, 33 were identified as subduction events having either normal or thrust faulting. Based on the type of faulting, depth of foci and also location of the source, these events were further categorised into interface and intraslab events. Out of 33 events, 26 exhibit characteristics of interface events while 7 events are classified as intraslab events. The faults of remaining 11 events have nearly 90° of dip angle, making them more appropriate to be defined as strike-slip faulting events. The resulting event classification based on source mechanism is as shown in Figure 4.1 and Table 4.1.

Based on strike, dip and rake angle obtained from international catalogues, two events with  $M_W$  8.2 and  $M_W$  8.6 occurred on 11 April 2012 are classified into strike-slip faulting. However, it should be noted that they were not originated from Sumatran fault zone. The foci of these two earthquakes were located at several hundred kilometres off west coast of northern Sumatera.

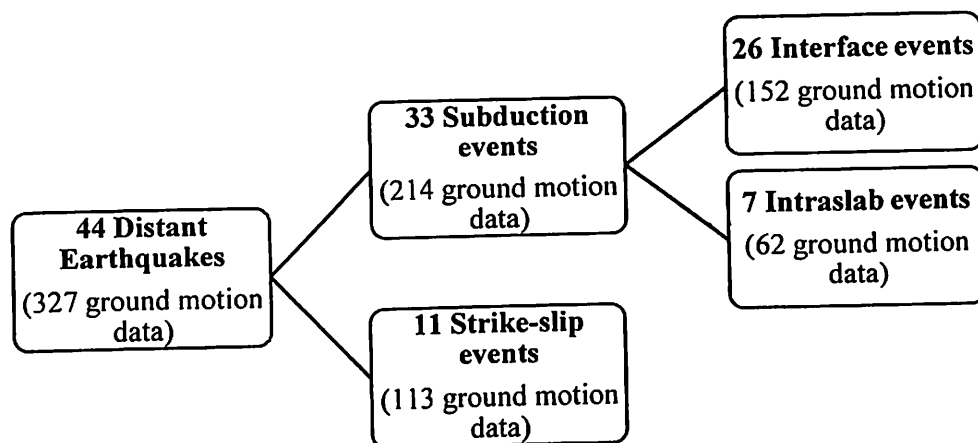


Figure 4.1 Classification of source mechanism from recorded distant earthquake events and ground motion data for Peninsular Malaysia

#### 4.2.2 Moment magnitude

From information provided by MMD, there are some events without moment magnitude being stated. Thus, checking and comparing of moment magnitude provided by MMD together with moment magnitude as recorded in USGS catalogue, NEIC catalogue, Geophysical Survey of Russian Academy of Sciences (MOS) catalogue and Badan Meteorologi dan Geofizika (Indonesia) (DJA) catalogue has been carried out. Finally, a compilation of moment magnitude is as shown in

Table 4.1 List of events sorting based on source mechanisms

No.	Date	Time (UTC)	Coordinate		Subduction		Faulting	Mw
			Lat.	Long.	Interface	Intraslab	Strike-slip	
1	2013-07-02	07:37:02	4.611	96.6041			*	6.1
2	2012-07-25	00:27:45	2.657	96.126	*			6.4
3	2012-06-23	04:34:53	2.934	97.806		*		6.1
4	2012-04-11 (a)	10:43:09	0.735	92.443			*	8.2
5	2012-04-11 (b)	08:38:38	2.360	93.010			*	8.6
6	2012-03-05	06:55:28	4.187	97.093			*	5.5
7	2011-09-05	17:55:13	2.730	98.000		*		6.6
8	2011-06-18	11:58:05	1.784	99.315			*	5.2
9	2011-06-14 (a)	03:01:29	1.856	99.254			*	5.6
10	2011-06-14 (b)	00:08:33	1.813	99.290			*	5.3
11	2011-04-06	14:01:46	1.693	97.133	*			5.8
12	2010-12-01	00:50:23	2.758	98.950		*		5.9
13	2010-10-25	14:42:16	-3.838	99.604	*			7.7
14	2010-05-09	05:59:44	3.770	96.044	*			7.2
15	2010-04-06	22:15:06	2.412	97.145	*			7.8
16	2009-12-23	01:11:52	-1.721	98.894	*			5.7
17	2009-10-01	01:52:31	-2.490	101.685			*	6.6
18	2009-09-30	10:16:09	-0.873	99.746		*		7.6
19	2009-08-16	07:38:18	-1.699	98.597	*			6.7
20	2008-05-19	14:26:00	1.700	99.100			*	6.0
21	2008-02-25 (a)	18:06:00	-2.300	99.900	*			6.3
22	2008-02-25 (b)	08:36:00	-2.600	99.700	*			7.2
23	2008-02-24	14:46:00	-2.500	99.600	*			6.2
24	2008-02-20	08:08:00	2.700	95.800	*			7.4
25	2008-01-22	17:14:00	1.100	97.200	*			6.2
26	2008-01-04	07:29:00	-3.000	100.500	*			6.0
27	2007-09-20	08:31:00	-2.400	99.600	*			6.7
28	2007-09-13	03:35:00	-1.900	99.700	*			7.0
29	2007-09-12 (a)	23:49:00	-2.800	100.800	*			7.9
30	2007-09-12 (b)	11:10:00	-4.400	101.100	*			8.5
31	2007-08-08	17:04:00	-6.200	107.600		*		7.5
32	2007-07-21	12:53:00	5.100	97.800	*			5.2
33	2007-03-06 (a)	05:49:00	-0.600	100.400			*	6.1
34	2007-03-06 (b)	03:49:00	-0.500	100.400			*	6.4
35	2006-12-01	03:58:00	3.400	98.800		*		6.3
36	2006-05-16	15:28:00	0.000	97.000	*			6.8
37	2005-05-19	01:54:00	2.000	96.900	*			6.9
38	2005-05-14	05:05:00	0.800	98.200	*			6.8
39	2005-04-28	14:07:00	2.100	96.600	*			6.3
40	2005-04-10	10:29:00	-1.300	99.400	*			6.7
41	2005-04-03	03:10:00	2.000	97.500	*			6.3
42	2005-03-28	16:09:00	2.000	97.300	*			8.6
43	2004-12-26	00:58:53	3.200	95.900	*			9.1
44	2004-07-25	14:35:19	-2.400	103.900		*		7.3

Appendix A and moment magnitude range for each mechanism is highlighted in Table 4.2. The moment magnitude range for the 44 distant earthquakes considered in this study is 5.2 to 9.1. This moment magnitude range falls in moderate to large-sized earthquake.

Table 4.2 Summary of moment magnitude range for each source mechanism

Event	Magnitude Limit	Date	Time (UTC)	Coordinate		$M_w$
				Lat.	Long.	
Interface Event	Lower Limit	2007-07-21	12:53:00	5.1	97.8	5.2
	Upper limit	2004-12-26	00:58:53	3.2	95.9	9.1
Intraslab Event	Lower Limit	2010-12-01	00:50:23	2.758	98.95	5.9
	Upper limit	2009-09-30	10:16:09	-0.873	99.746	7.6
Strike-slip Event	Lower Limit	2011-06-18	11:58:05	1.784	99.315	5.2
	Upper limit	2012-04-11 (b)	08:38:38	2.36	93.0104	8.6

Moment magnitude for interface events falls in the range of 5.2 to 9.1. Meanwhile,  $M_w$  5.9 is the lower limit and  $M_w$  7.6 is the upper limit for intraslab events. Strike-slip events show  $M_w$  5.2 as the smallest event and  $M_w$  8.6 being the largest event. It can be seen that interface events from Sumatra subduction zone possesses the potential in generating huge destruction due to the large moment magnitude and shallow focal depths.

#### 4.2.3 Distance

By using Carlson (1999) model, the epicentral distances between earthquake sources and seismic stations were calculated. The resulting epicentral distance is listed in Appendix B. Table 4.3 shows the summary of computed epicentral distance for distant earthquakes considered in this study.

Table 4.3 Summary of computed epicentral distance

Distance limit	Distance (km)	Date	Time (UTC)	Coordinate		Station
				Lat.	Long.	
Lower limit	284.1	2011-06-18	11:58:05	1.784	99.315	SASM
Upper limit	1291.6	2012-04-11 (a)	10:43:09	0.735	92.443	KTM

The smallest epicentral distance is only 284.1 km, which is from event originated from northern Sumatera on 18 June 2011 to a seismic station located at Shah Alam that is denoted by the code SASM. The farthest epicentral distance recorded is between event generated from off west coast of northern Sumatera and KTM stations that is located at Kuala Terengganu. The epicentral distance recorded a value of 1291.6 km.

### 4.3 Site classification

MASW has been carried out for all 19 seismic stations located throughout the whole Peninsular Malaysia as shown in Figure 2.6. Based from field testing and also computational analysis,  $V_{S30}$  has been obtained and classification has been carried out with reference from the NEHRP 1997. Figure 4.2 exhibits the S-wave velocity profile against depth for each seismic station while Table 4.4 shows the summary of  $V_{S30}$  and site classifications for seismic stations being considered in this study. Among all, only four seismic stations are classified into Class C, namely DTSM, JRM, KTM and PJSM. The rest are in Class D. According to NEHRP 1997, Class C is defined as soft rocks or very hard soils and gravels with range of 360 m/s to 760 m/s while Class D were defined as hard soils with  $V_{S30}$  range of 180 m/s to 360 m/s. Site at DTSM station has the largest  $V_{S30}$  recording a value of 481.7 m/s while SRSM site has the softest foundation, that is with  $V_{S30}$  of 182.7 m/s.

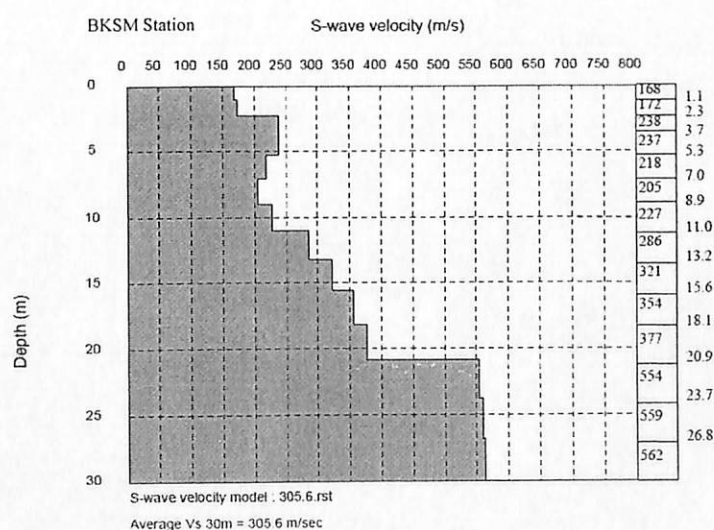


Figure 4.2 S-wave velocity profile against depth for seismic stations in Peninsular Malaysia

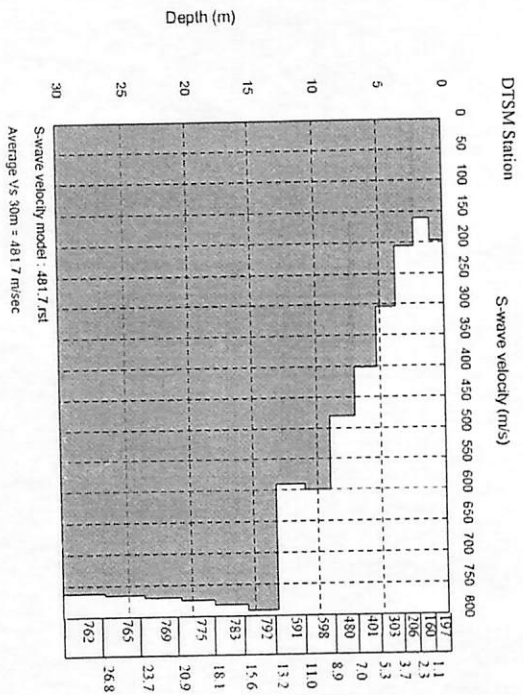
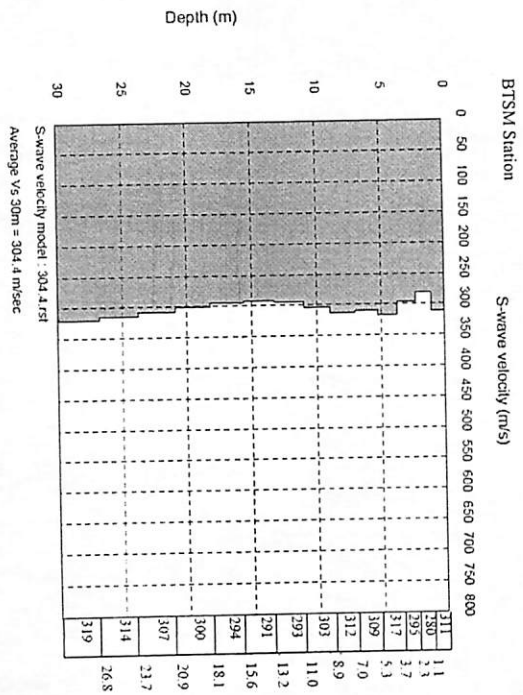
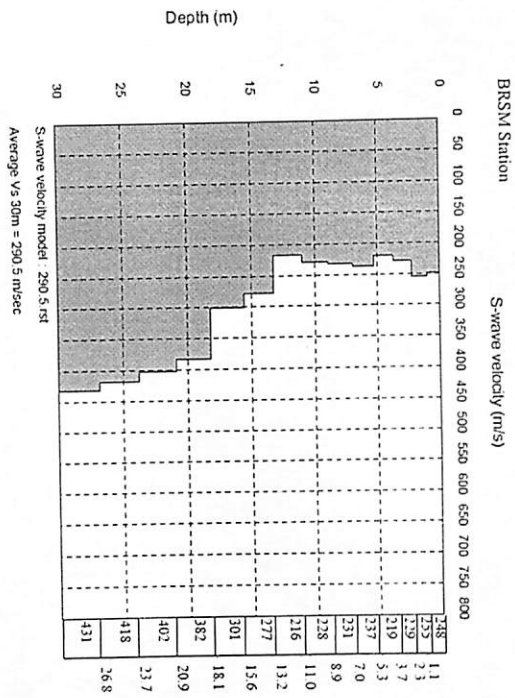


Figure 4.2 Continued



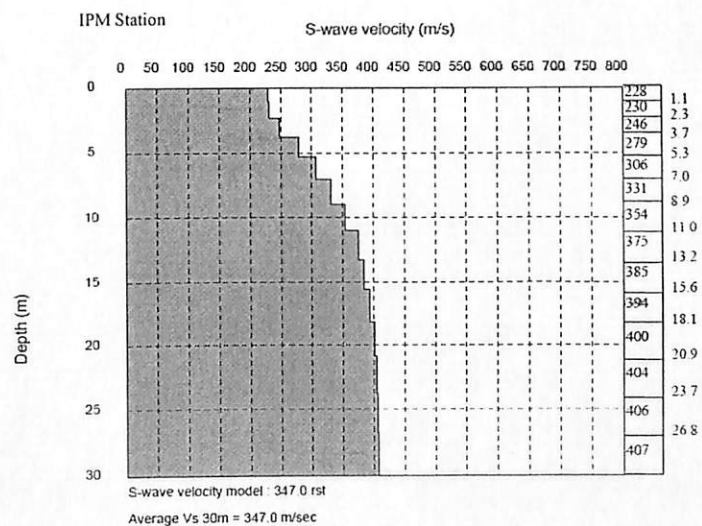
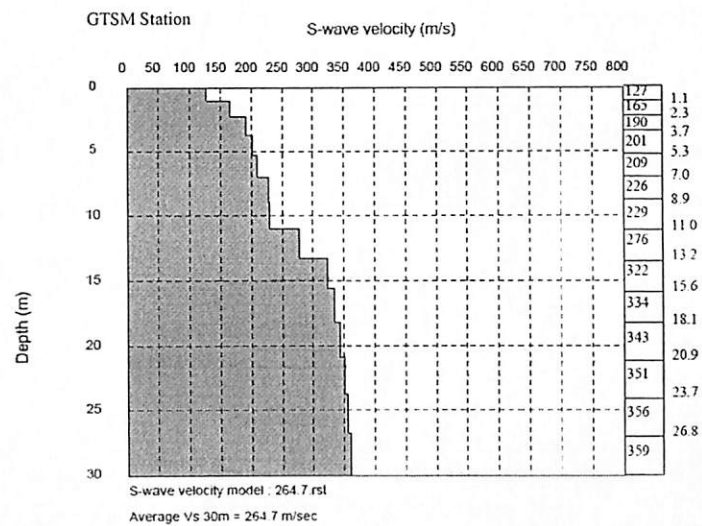
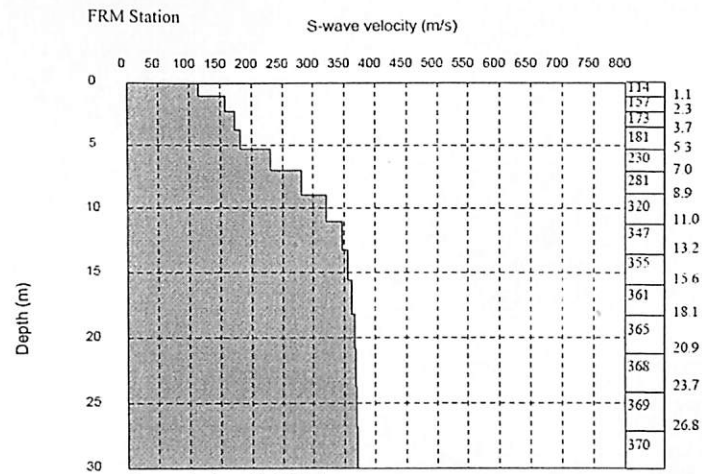


Figure 4.2 Continued

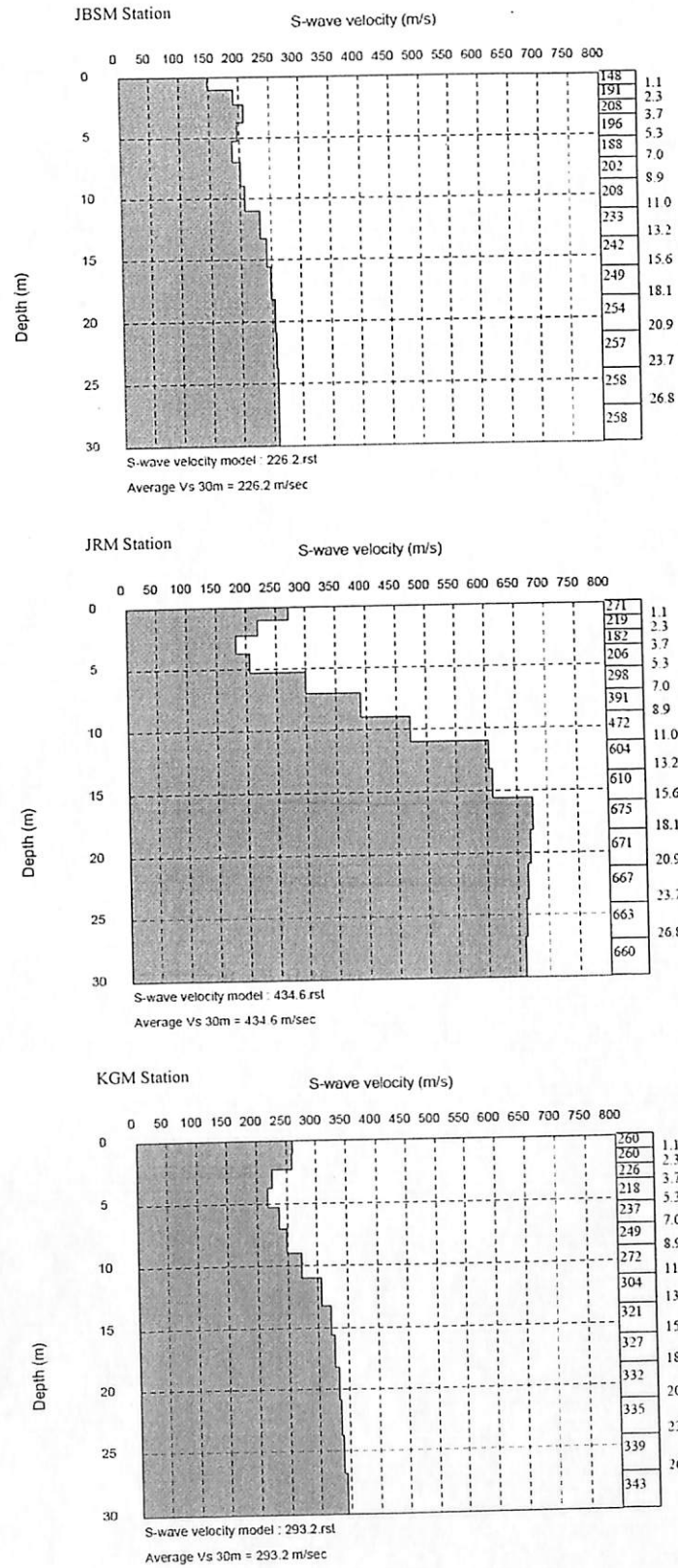


Figure 4.2 Continued

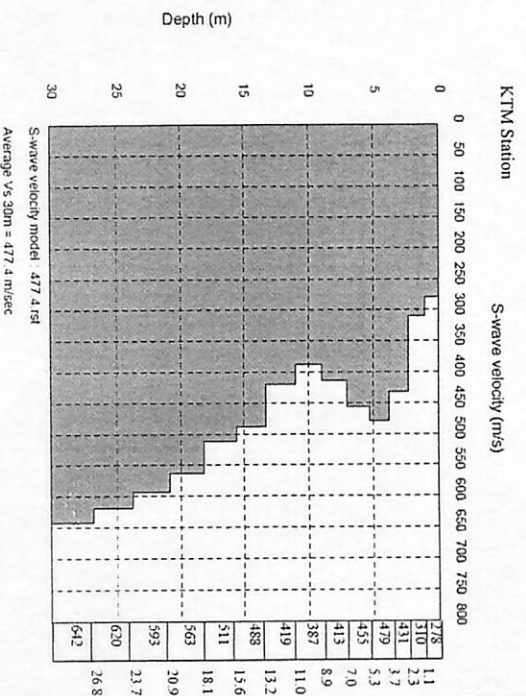
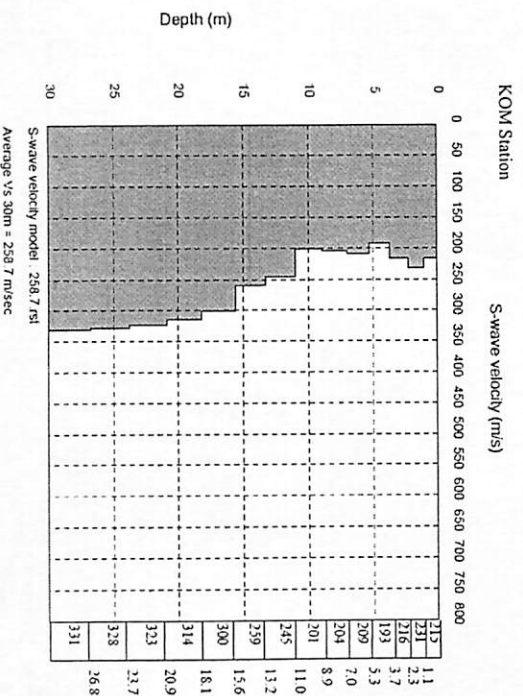
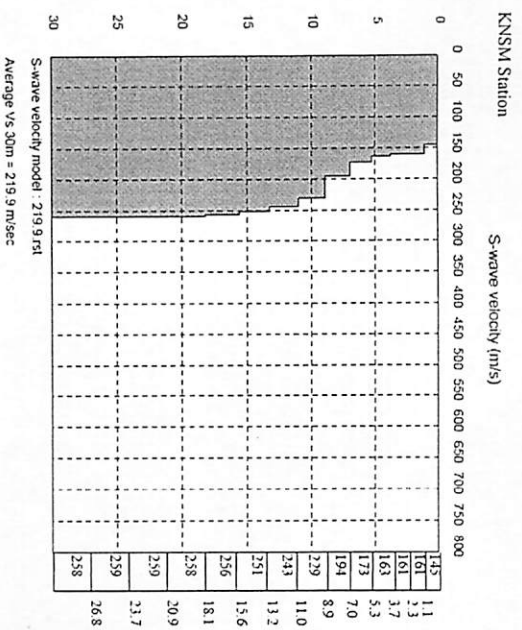


Figure 4.2 Continued

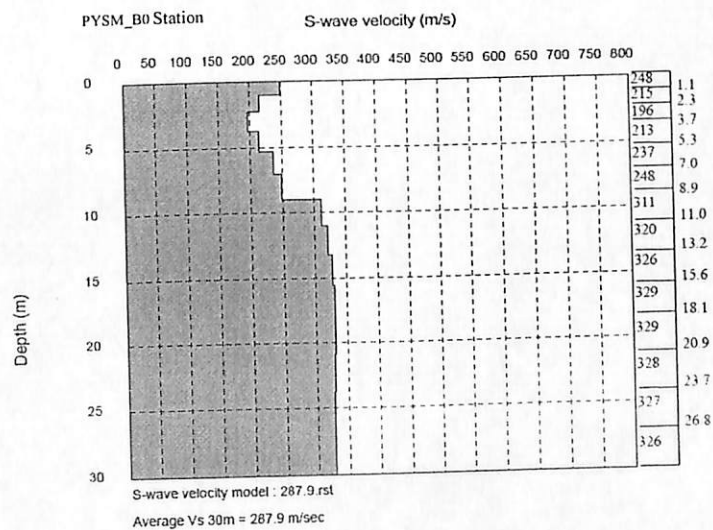
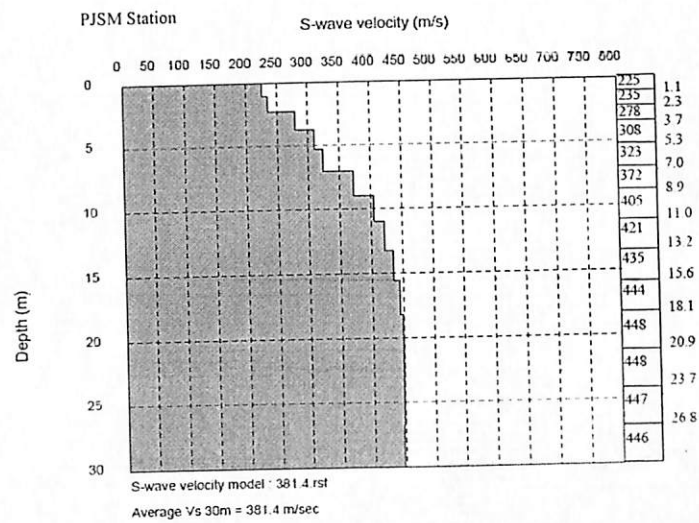
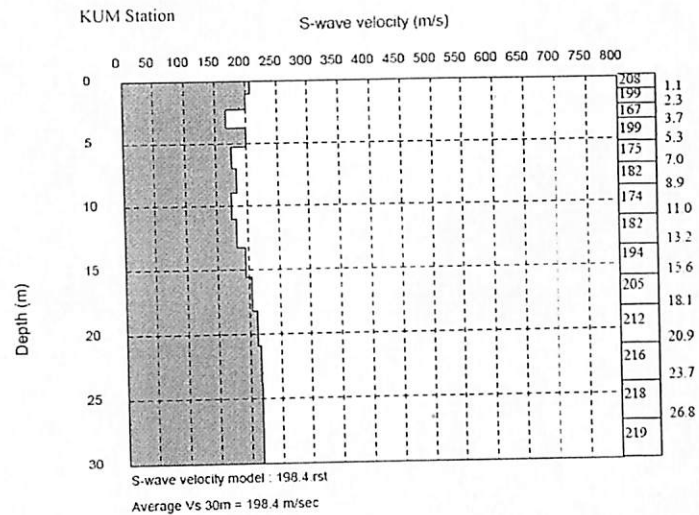


Figure 4.2 Continued

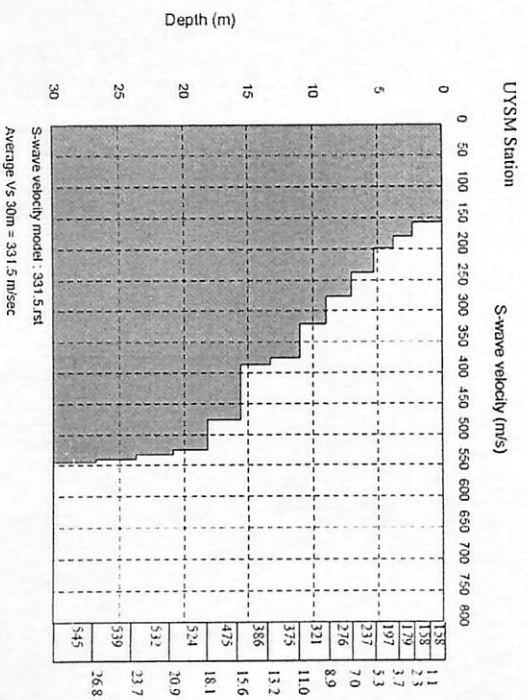
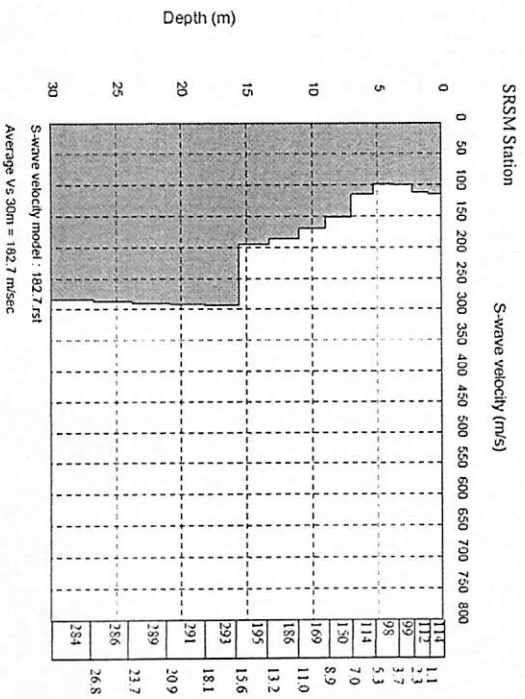
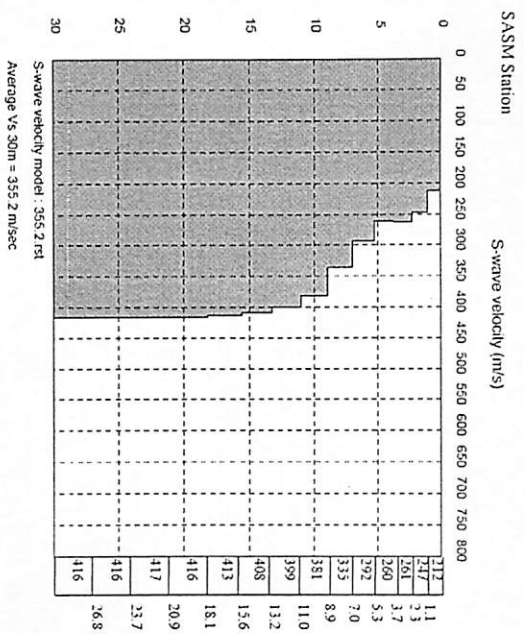


Figure 4.2 Continued



Table 4.4 Site classifications of 19 seismic stations in Peninsular Malaysia based on MASW result

No.	Station	Stations code	Coordinate		Elevation (m)	$V_{S30}$ (m/s)	Highest $V_S$ (m/s)	Class (according to NEHRP)
			Latitude(°N)	Longitude (°E)				
1	Pusat Sains, Bukit Kiara	BKSM	3.147	101.644	66	305.6	562.0	D
2	Kolej Mara, Beranang	BRSM	2.902	101.683	73	290.5	431.0	D
3	Bukit Tinggi	BTSM	3.350	101.820	322	304.4	319.0	D
4	Dusun Tua, Hulu Langat	DTSM	3.131	101.839	67	481.7	792.0	C
5	FRIM, Kepong	FRM	3.237	101.625	97	280.3	370.0	D
6	Aminuddin Baki, Goh Tong Jaya	GTSM	3.390	101.775	844	264.7	359.0	D
7	Ipoh, Perak	IPM	4.581	101.025	247	347.0	407.0	D
8	Janda Baik	JBSM	3.320	101.683	577	226.2	258.0	D
9	Jerantut, Pahang	JRM	3.887	102.477	55	434.6	675	C
10	Kluang, Johor	KGM	2.015	103.316	103	293.2	343	D
11	Mardi, Kundang	KNSM	3.271	101.515	27	219.9	258.0	D
12	Kota Tinggi, Johor	KOM	1.792	103.847	49	258.7	331	D
13	Kuala Terengganu, Terengganu	KTM	5.328	103.134	33	477.4	642	C
14	Kulim Kedah	KUM	5.290	100.649	74	198.4	219	D
15	Perbadanan Putrajaya (Basement)	PYSM_B0	2.918	101.684	N.A	287.9	326.0	D
16	Wetland, Putrajaya	PJSM	2.970	101.690	45	381.4	446.0	C
17	Bukit Cerakah, Shah Alam	SASM	3.096	101.511	28	355.2	417.0	D
18	Pusat Serenti, Serendah	SRSM	3.365	101.629	61	182.7	293.0	D
19	Empangan Batu, Hulu Yam	UYSM	3.272	101.685	84	331.5	545.0	D

MMD presumes the foundations of each seismic station solely based on general geological map and visual inspection, which are lack of quantitative measurements. From Table 2.4, all the seismic stations that claimed to be located on granite are found sitting on Class D sites. In contrast to the presumption for foundation as soft soil, such as for PJSM station, the site is discovered to fall in Class C site based on the MASW result in the present study. The term 'rocky' foundations for some of the seismic stations were too general and confusing. Based on the result obtained, only one out of four 'rocky' sites where seismic stations are sitting is in Class C that is, DTSM station.

The site classes for seismic stations located within or surrounding Kuala Lumpur (e.g. BKSM, BRSM, DTSM, FRM, KNSM, PYSM\_B0, PJSM, SASM and UYSM) found in present study is similar to findings of site at Kuala Lumpur City Center by Adnan et al. (2011). While some stations were claimed to be located on rock foundation, the result in present study shows that none of the stations belongs to NEHRP Class A or Class B. Thus, misinterpreting terms 'granite' foundation as 'rock' or 'hardrock' site could lead to underestimation of the dynamic properties of the ground. It was undeniable that the underlying bedrocks of these seismic stations might be granite or sandstone, however, the depth of the overlying soils and the weathering degree on the rock surface is the key point of the incompatibility of the results with the description provided by MMD.

A few studies have to be conducted before selecting a site for the installation of seismic stations. One of the most important criteria is to do off studies on geological map and field testing to obtain an ideal site for the installation of the seismic stations. According to (Trnkoczy et al., 2012), the most favourable geological site for seismic stations is on rock sites, preferably un-weathered magmatic rock with shear wave velocity,  $V_s$  of 2500 to 4000 m/s. Generally, higher acoustic impedance of a bedrock leads to smaller seismic noise and higher possible gain of a stations. Contradicting to this reference, all seismic stations in Peninsular Malaysia are located on either hard soils or soft rocks, which means they have high possibility in subjecting to seismic noise interruption and short-period signals might be unrepresentative. Although there is amplification factors developed to obtain ground motion on soil sites from rock sites and vice versa, factorising observed ground motion could introduce uncertainties to the datasets. Thus, it is advisable for local authorities to place new seismic station on bedrock in the future to enhance the reliability of recorded ground motion in Peninsular Malaysia.

The MASW test as well as the computational analysis of shear wave velocity in the present study managed to provide a more detailed site classes for seismic stations in Peninsular Malaysia which in turns, reducing the uncertainties due to assumptions on site classes. This implies that the result is dependable and reasonable for seismic stations located in Peninsular Malaysia compare to the site presumptions that were conventionally used in previous studies of seismic hazard analysis for Peninsular Malaysia. For more accurate site classification, further geotechnical investigation should be conducted. With the provision of borelog to obtain soil profile underneath the ground, validation to the site classification provided in this study can be carried out.

#### **4.4 Examination of pre-selected ground motion attenuation model**

The comparison of attenuation curves of PGA over epicentral distance were performed in magnitude range of  $M_W$  5.0 to  $M_W$  9.0. The actual ground motion records were grouped according to moment magnitude with 1.0 interval starting from  $M_W$  6.0 to  $M_W$  9.0 for plotting. To provide better representation of actual conditions, focal depth varies for each group. Focal depth used for each group is the average of focal depth of events in respective groups. Each attenuation model has its own consideration for types of source mechanisms and site conditions. Thus, the comparisons were divided into two main categories, namely for subduction earthquakes and shallow crustal strike-slip earthquakes.

##### **4.4.1 Comparison of pre-selected models for subduction earthquakes**

The comparison of attenuation curves has been conducted separately on interface events and intraslab events. Due to the fact that site conditions plays an effect on ground motions, the comparison of attenuation curves were also divided according to site classes. This resulted in four groups of comparison, namely: interface events with Class C site, interface events with Class D site, intraslab events with Class C site and intraslab events with Class D site. Geometrical mean of two horizontal PGA is used in this study and are tabulated in Appendix C.

The curve of PGA estimated by 13 subduction attenuation models with actual ground motion records taken from seismic stations located on Class C sites for interface subduction earthquake events is shown in Figure 4.3.



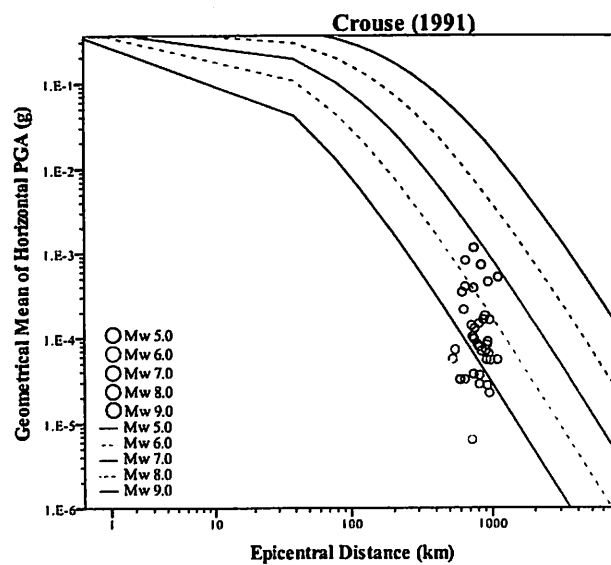
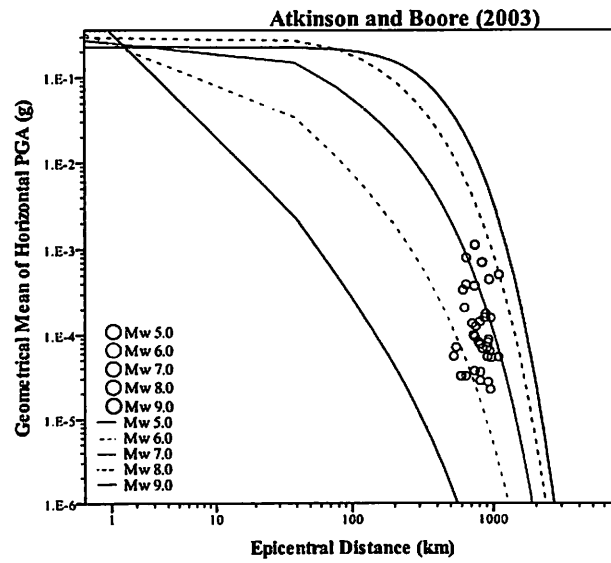
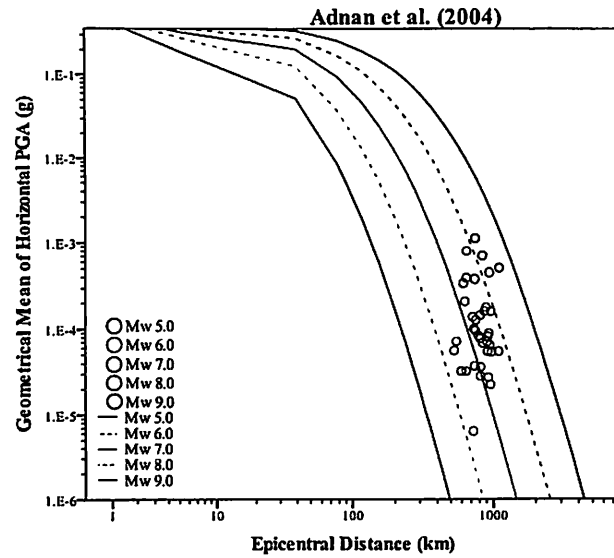


Figure 4.3 Attenuation curves and recorded PGA by seismic stations located on Class C sites for interface subduction earthquakes

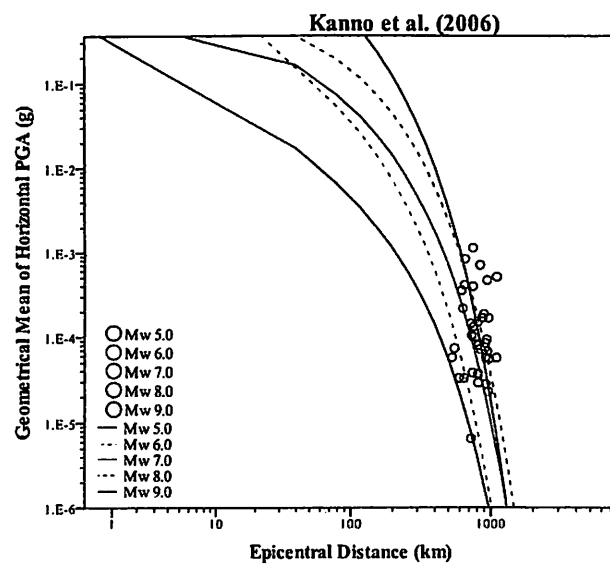
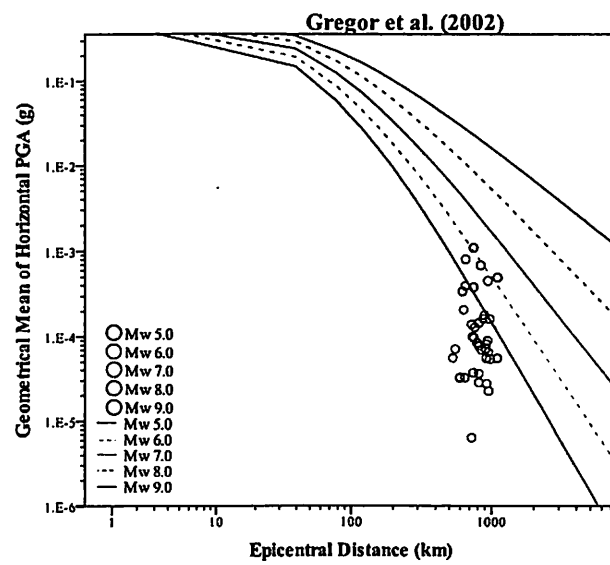
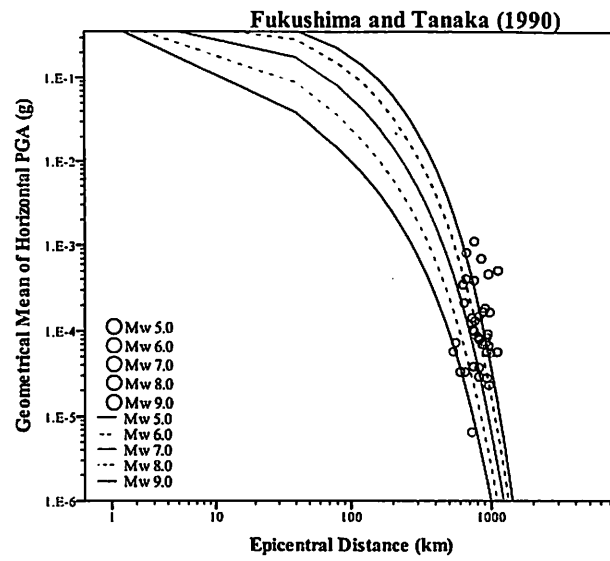


Figure 4.3 Continued

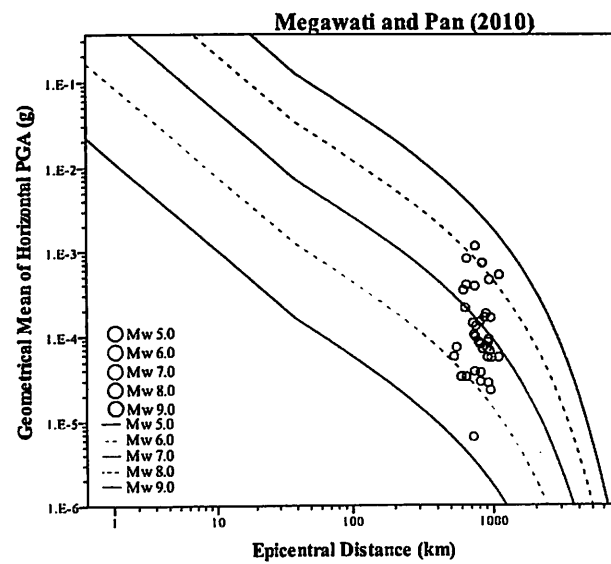
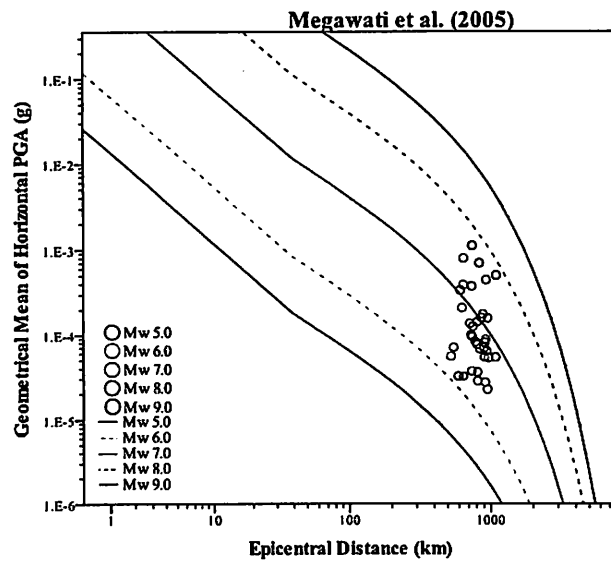
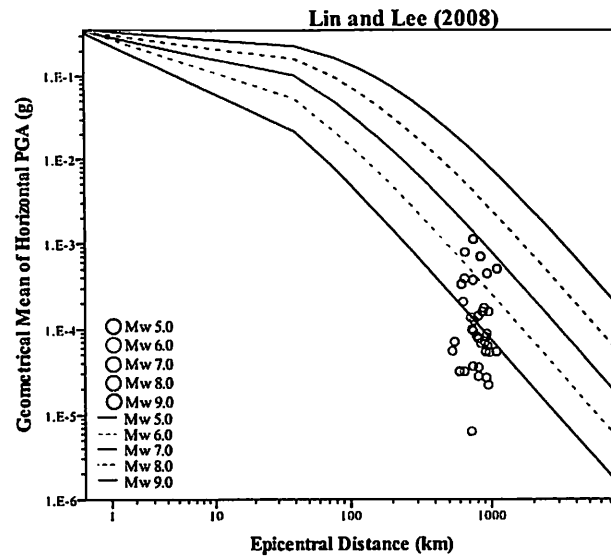


Figure 4.3 Continued

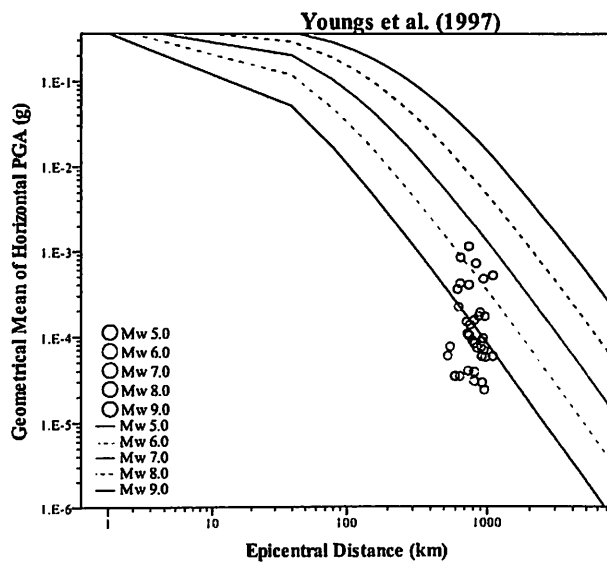
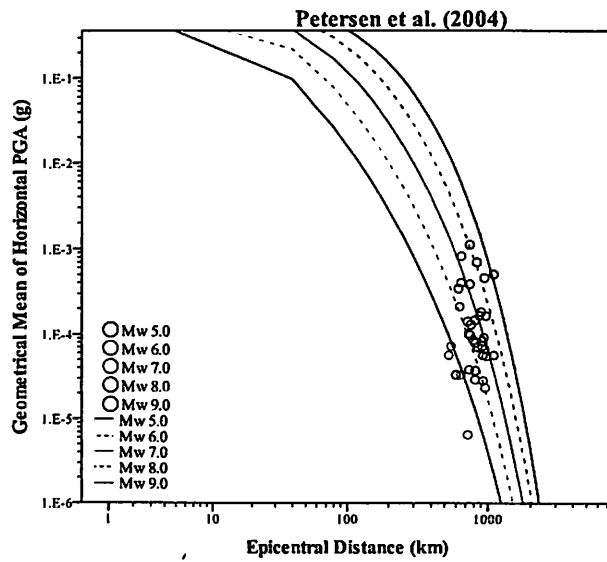
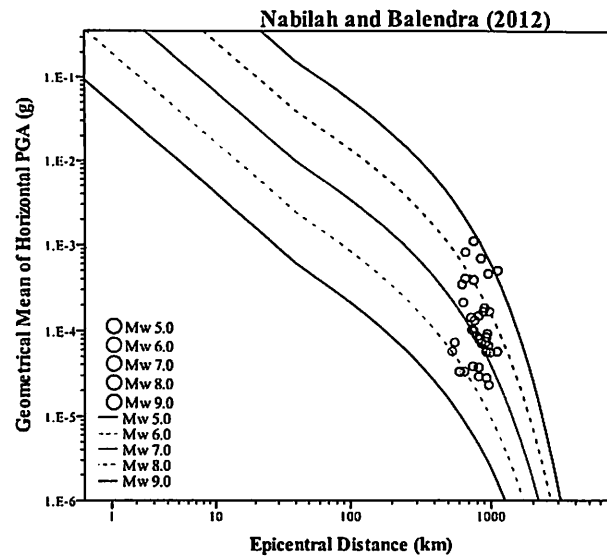


Figure 4.3 Continued

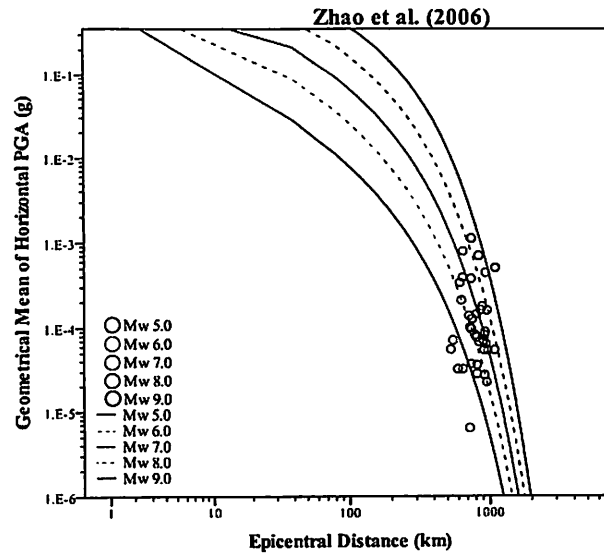


Figure 4.3 Continued

From Figure 4.3, it can be seen that there are a few types of trend in the PGA prediction curves. First, Crouse (1991), Youngs et al. (1997), Gregor et al. (2002) and Lin and Lee (2008) deviated very much from the recorded ground motion data. Models like Atkinson and Boore (2003) and Megawati et al. (2005) tends to over-predict PGA at larger magnitude. There are also models underestimated PGA at lower magnitude. Such models are Atkinson and Boore (2003), Adnan et al. (2004), Megawati et al. (2005), Megawati and Pan (2010) and Nabilah and Balendra (2012). It can be seen that Fukushima and Tanaka (1990), Petersen et al. (2004), Kanno et al. (2006), and Zhao et al. (2006) correspond to recorded data quite well and they have similar trends, that is having steeper drop at larger distance. However, Nabilah and Balendra (2012) has reasonably slower attenuation slope which makes it quite fit to the recorded ground motion, regardless of the underestimation of PGA at  $M_w$  5.0.

Regardless of the performance of attenuation models in predicting PGA on Class C site for interface earthquake events, they might be corresponding well for other earthquake source mechanisms and site classes due to the different trend in the recorded PGA scatter plot. Figure 4.4 shows the attenuation curves established by 13 pre-selected subduction ground motion attenuation models and recorded PGA on Class D sites for interface subduction earthquakes. Again, Crouse (1991), Youngs et al. (1997), Gregor et al. (2002) and Lin and Lee (2008) predict PGA which differs significantly from the

observed data. On the other hand, Atkinson and Boore (2003), Adnan et al. (2004), Megawati et al. (2005) and Megawati and Pan (2010) gives lower predictions at small magnitude and larger estimations at larger magnitude. This caused them only can predict well at  $M_w$  7.0, except for Atkinson and Boore (2003) which cannot fit for any moment magnitude. Zhao et al. (2006) tends to gives larger PGA estimation at large magnitude. Although Petersen et al. (2004) predicts better in Class C site but it tends to overestimate PGA for Class D site. In contrast, Nabilah and Balendra (2012) model seems to be more consistent in predicting PGA for Class D sites. However, Fukushima and Tanaka (1990) and Kanno et al. (2006) produced curves fitter to the five magnitudes of data compare to the rest, despite the distance limitation.

Graphs plotted in Figure 4.5 exhibit PGA curves estimated by models and scatter plot of actual ground motion records of intraslab events for Class C sites. Due to smaller number of intraslab events compare to interface events, the ground motion data are fewer and only cover the moment magnitude range of 6.0 to 8.0. Intraslab events have deeper foci. Focal depth of intraslab events being considered in this study ranges from 81 km to 576 km. However, average focal depth of events in each group of magnitude is used in the present study.

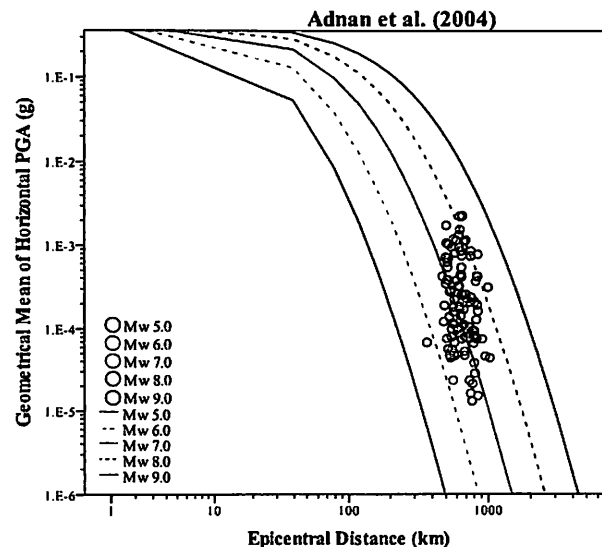


Figure 4.4 Attenuation curves and recorded PGA by seismic stations located on Class D sites for interface subduction earthquakes

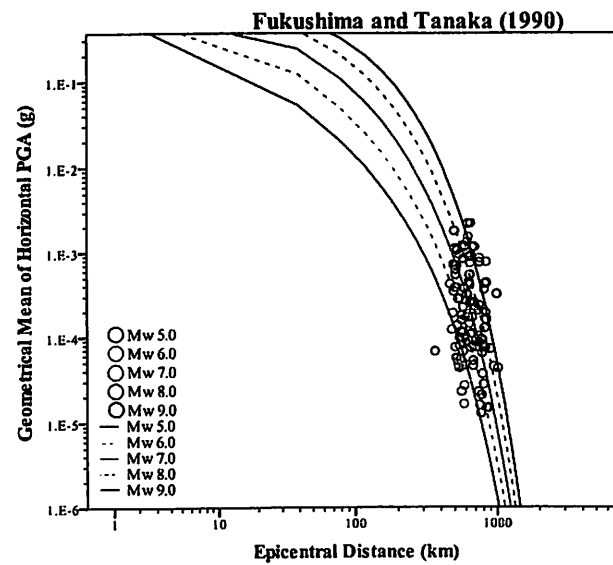
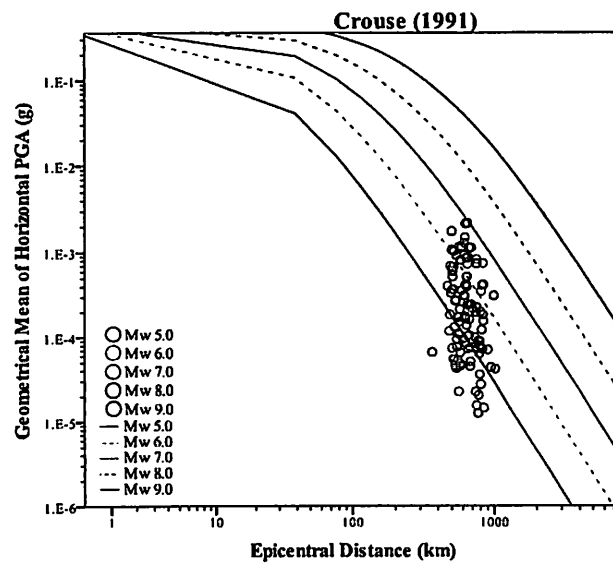
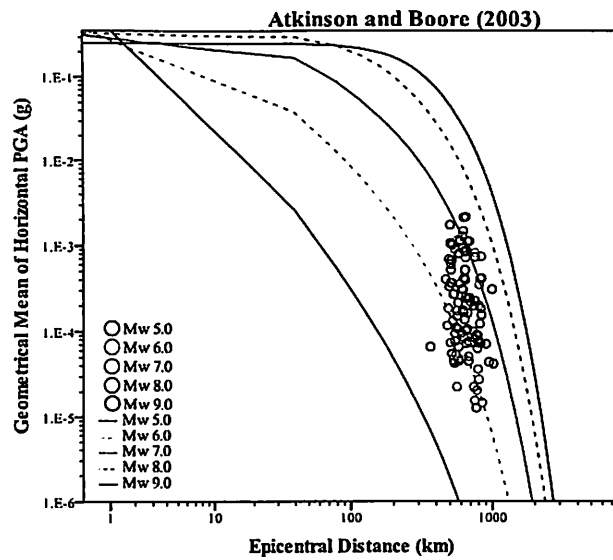


Figure 4.4 Continued

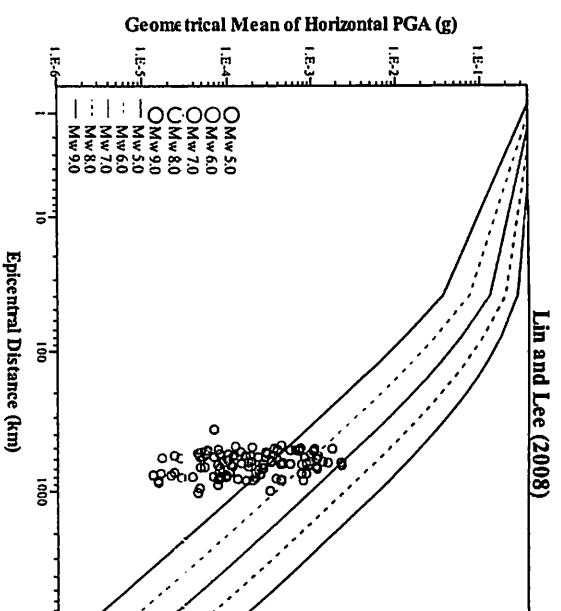
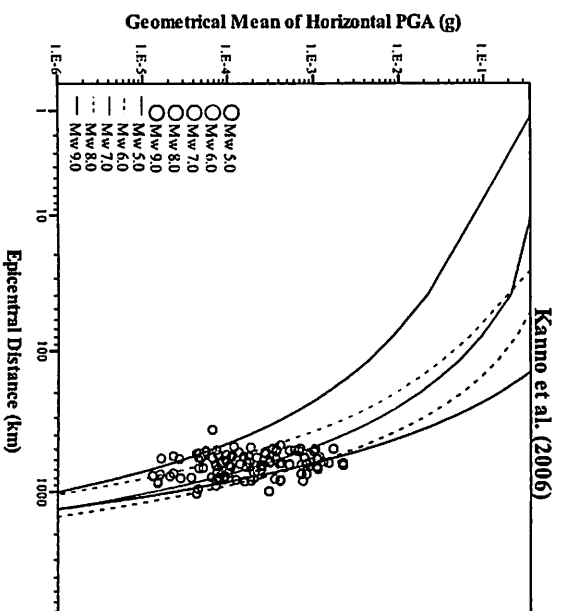
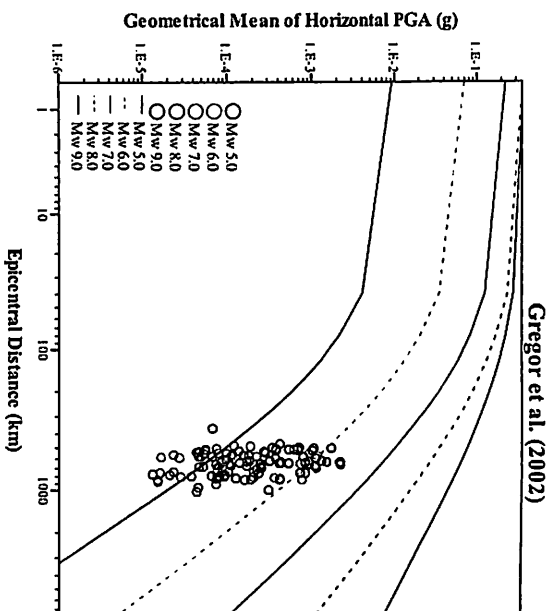


Figure 4.4 Continued



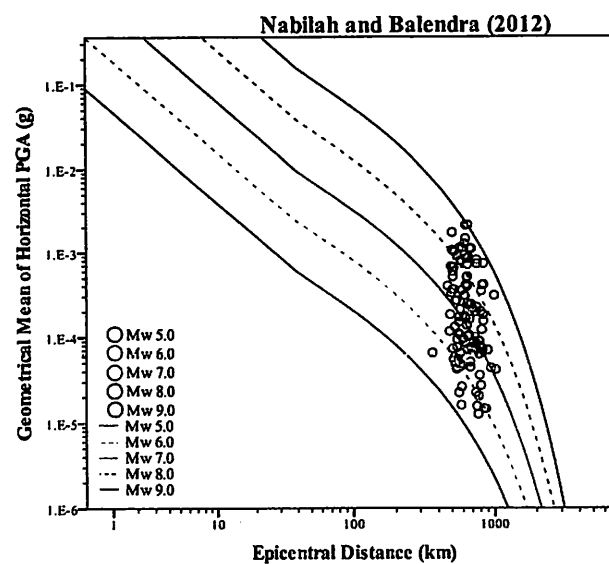
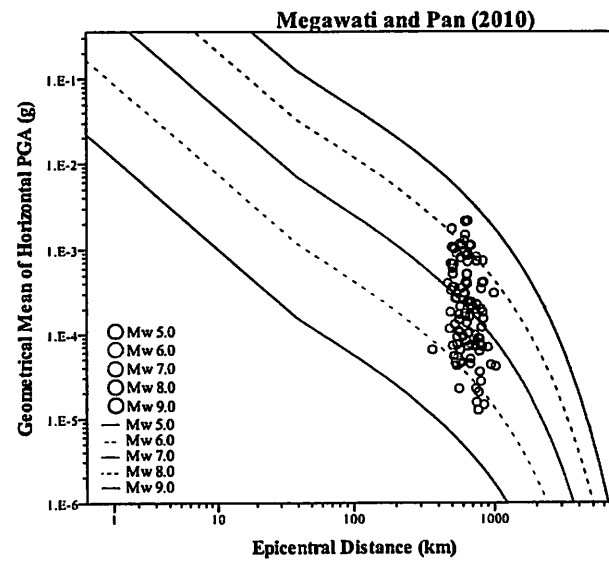
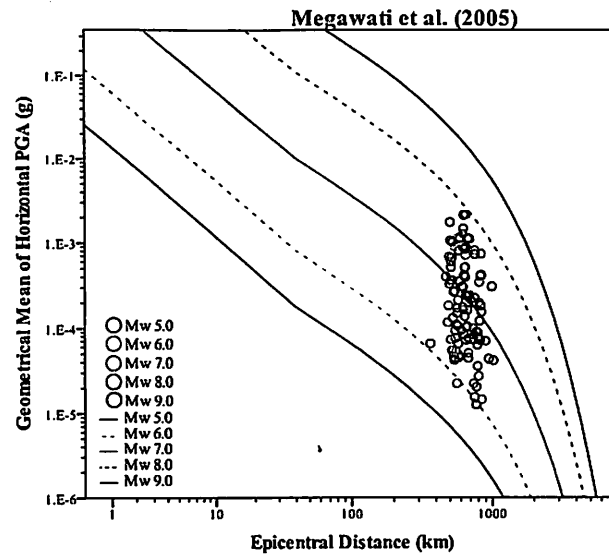


Figure 4.4 Continued

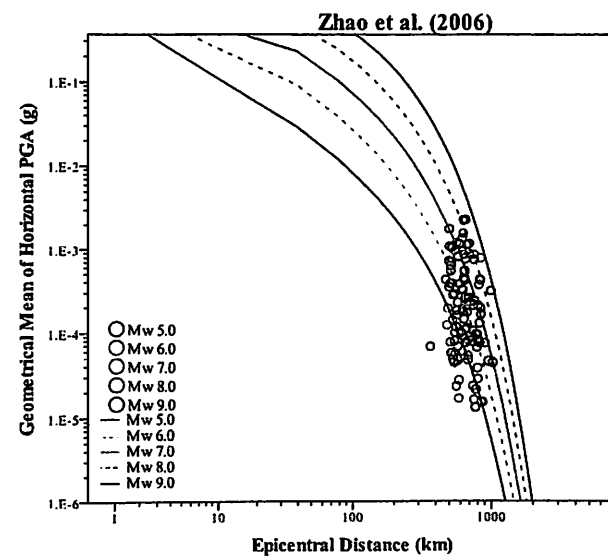
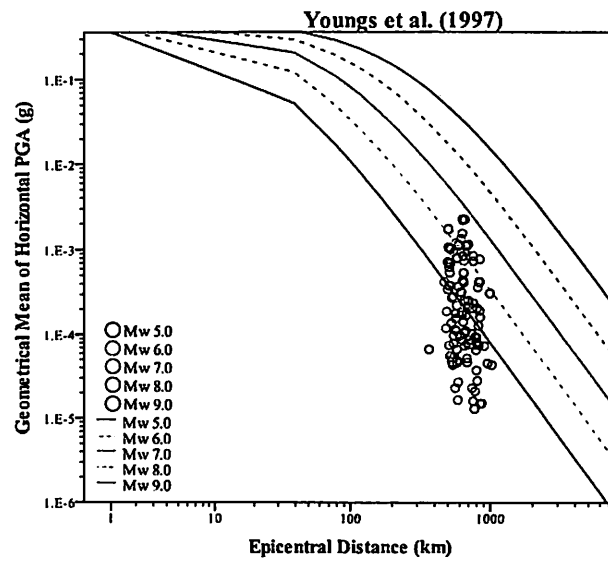
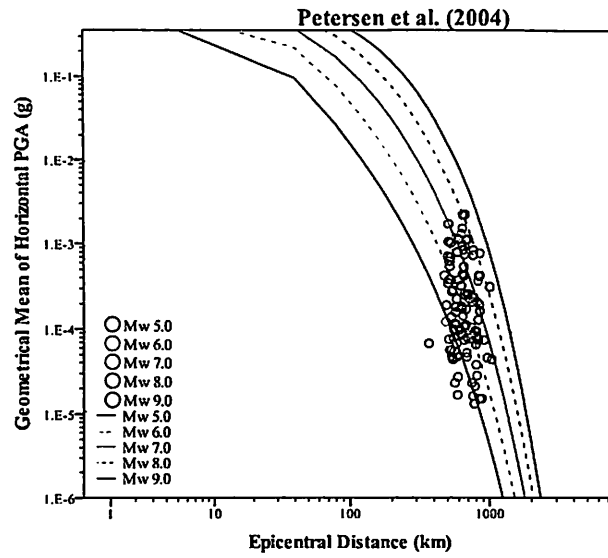


Figure 4.4 Continued

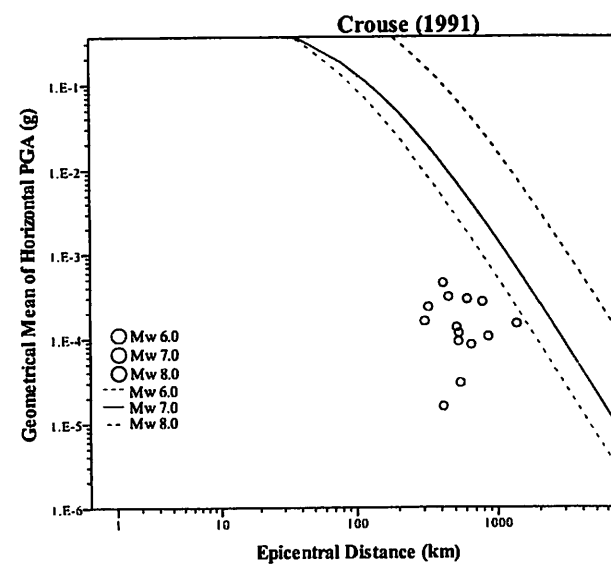
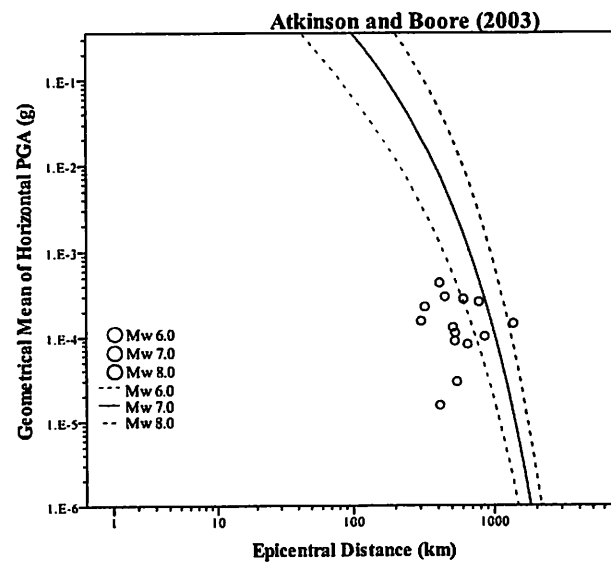
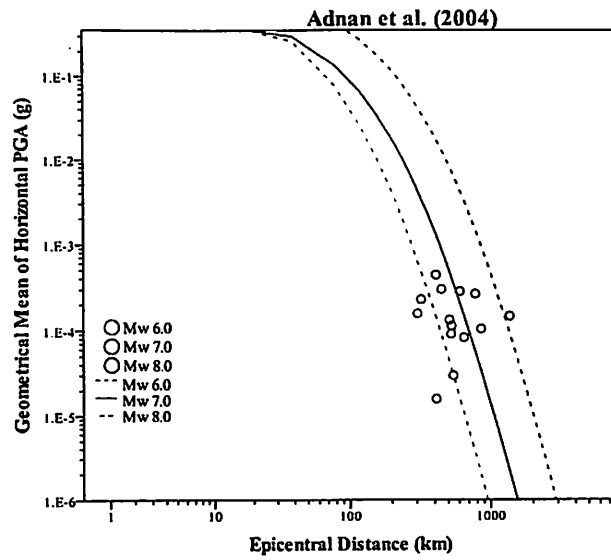


Figure 4.5 Attenuation curves and recorded PGA by seismic stations located on Class C sites for intraslab subduction earthquakes

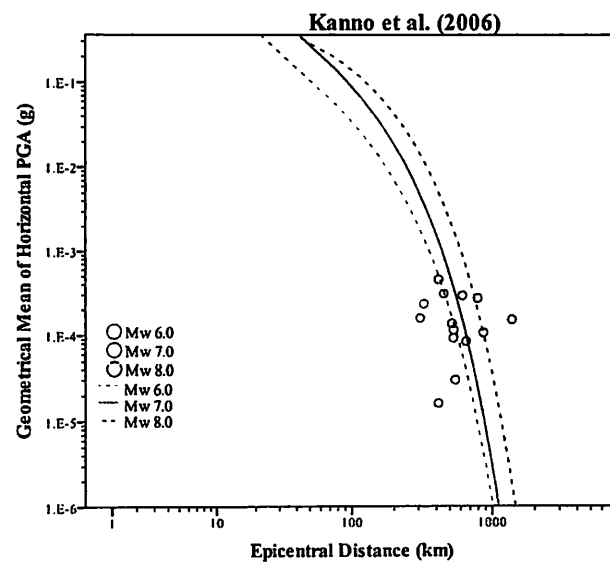
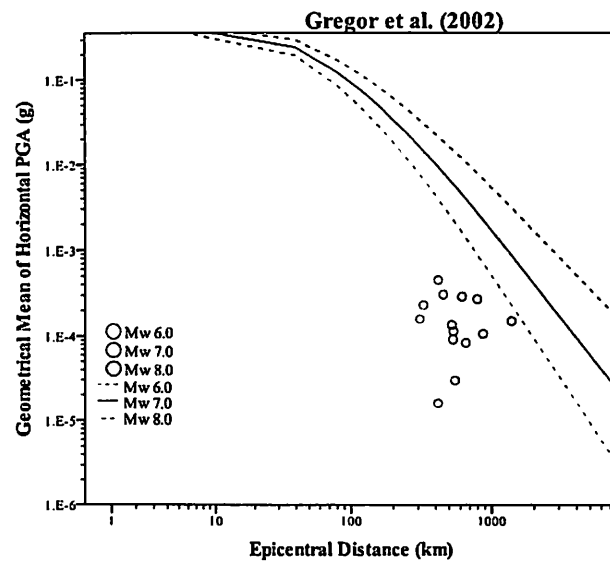
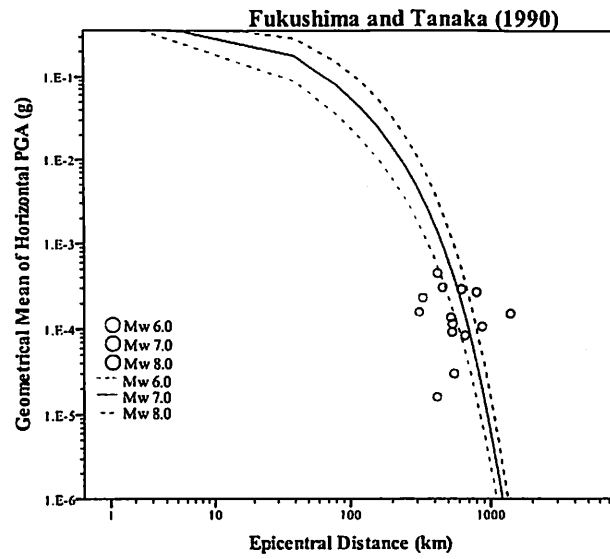


Figure 4.5 Continued

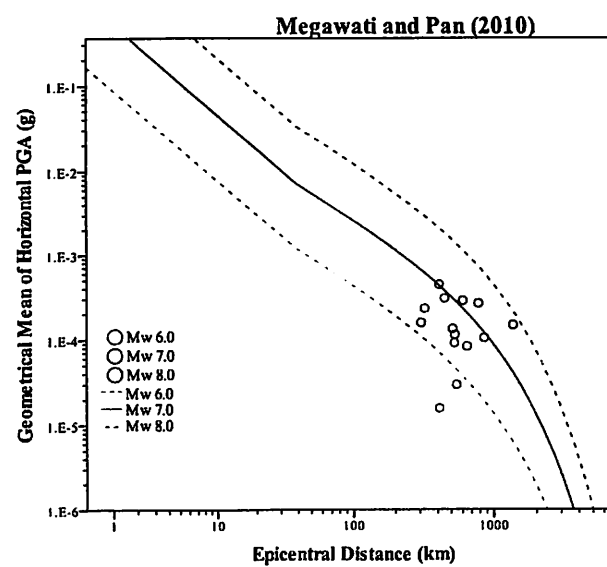
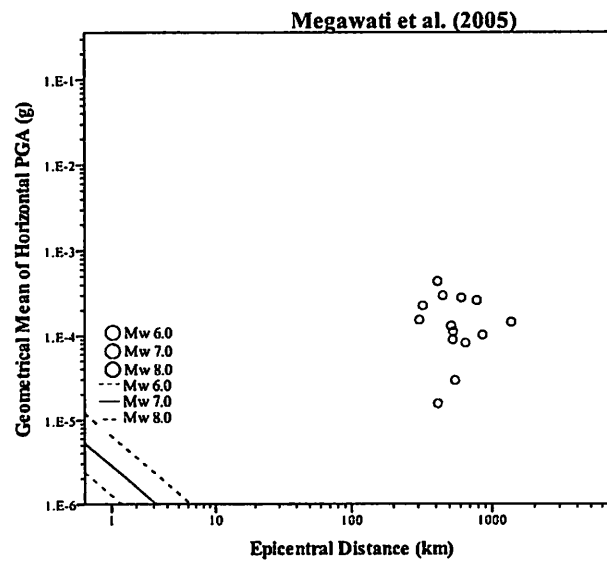
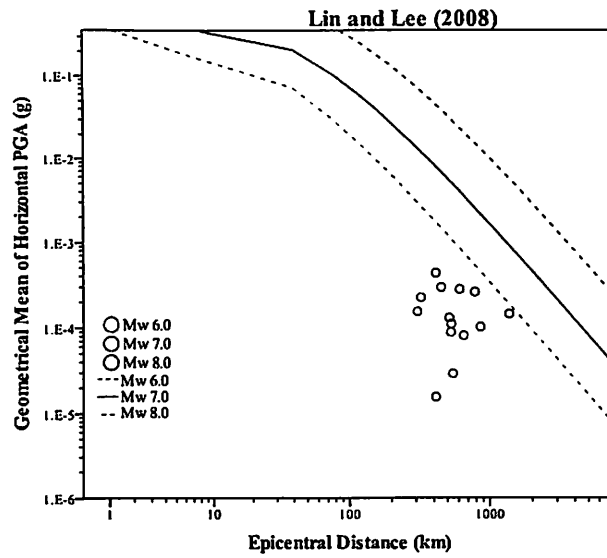


Figure 4.5 Continued

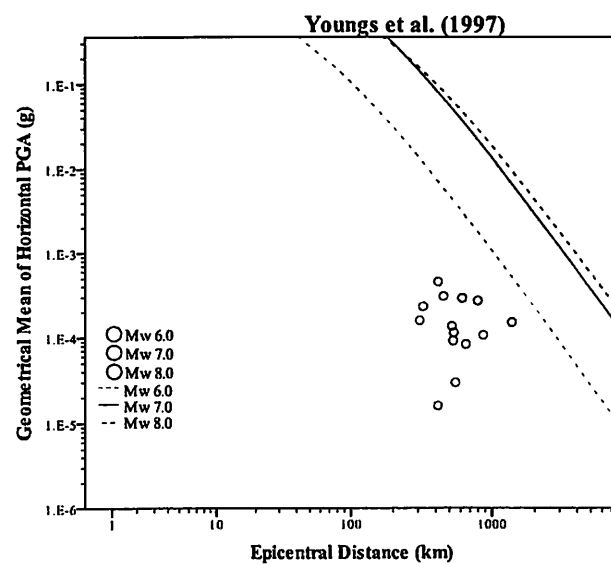
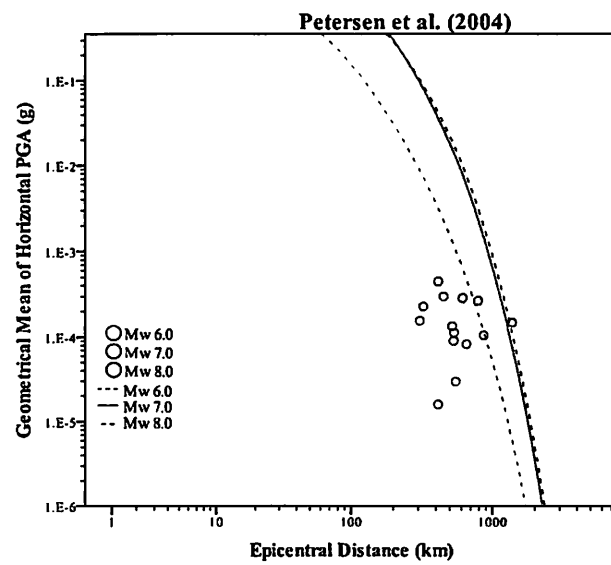
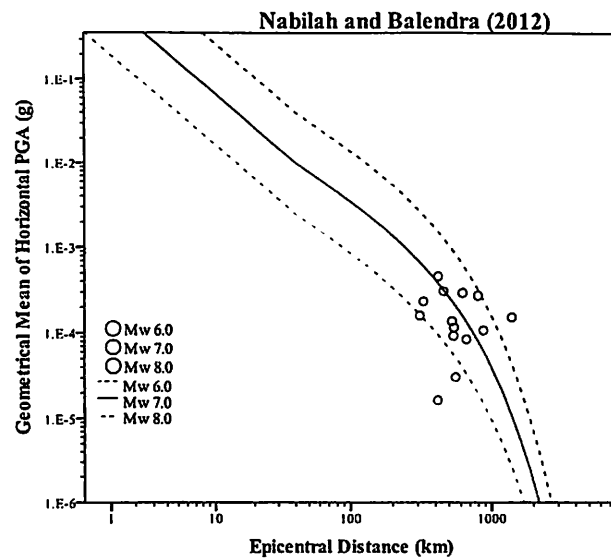


Figure 4.5 Continued

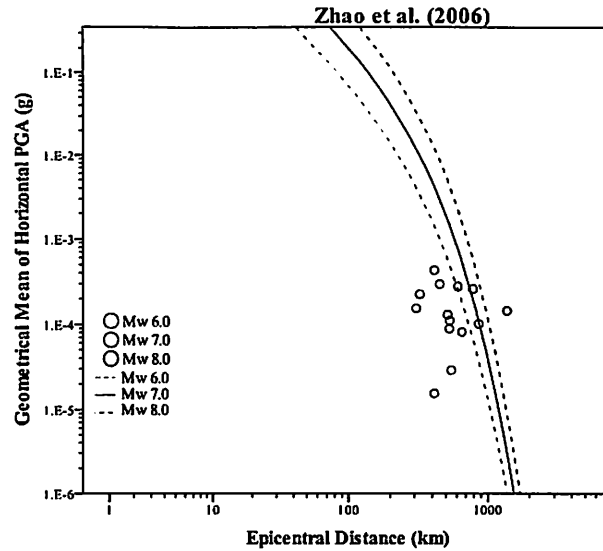


Figure 4.5 Continued

Models that were developed mostly considering shallower foci depth exhibits only characteristics for interface events and might not be able to cater for intraslab events. From the graphs plotted for intraslab events and Class C sites, such models are Gregor et al. (2002) and Megawati and Pan (2010). Both Gregor et al. (2002) and Megawati et al. (2005) models were derived to consider only interface earthquakes based on simulation of ground motion. This might be the reason for huge difference between predictions from these two models and the actual records. Crouse (1991), Youngs et al. (1997) and Lin and Lee (2008) curves are seen having lower attenuation rate at large distance and constantly laying above recorded data compare to other attenuation models. This caused those models to over-predict PGA for intraslab events. In contrast, Fukushima and Tanaka (1990), Atkinson and Boore (2003), Adnan et al. (2004), Petersen et al. (2004), Kanno et al. (2006) and Zhao et al. (2006) curves has steeper attenuation at larger distance. However, Atkinson and Boore (2003) and Petersen et al. (2004) are slightly deviated from the recorded data compare to Fukushima and Tanaka (1990), Adnan et al. (2004), Kanno et al. (2006) and Zhao et al. (2006). Megawati and Pan (2010) and Nabilah and Balendra (2012) have similar trends of curve and fit better for all 3 magnitudes of data.

The last set of graphs that depict the predictions of pre-selected subduction attenuation models is shown in Figure 4.6. These graphs portray prediction curves for intraslab events on Class D sites. As an overall view in this set of graphs, prediction curves for Class D sites are not much differ from curves for Class C sites. Nevertheless,

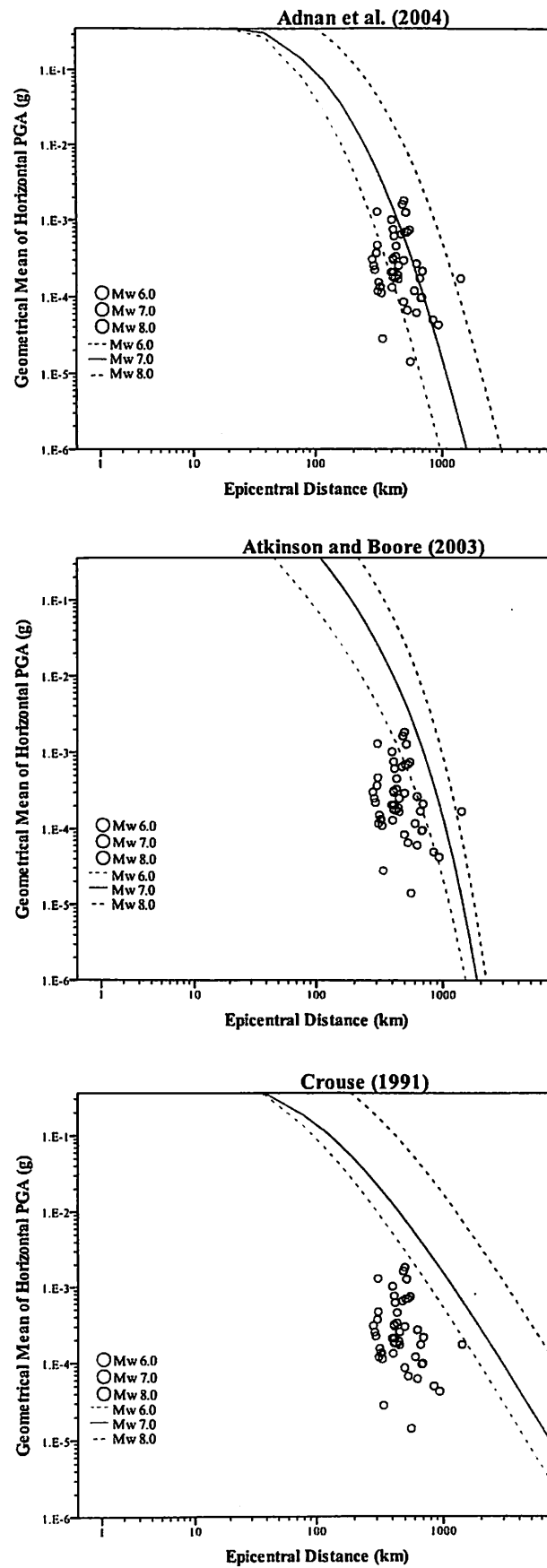


Figure 4.6 Attenuation curves and recorded PGA by seismic stations located on Class D sites for intraslab subduction earthquakes



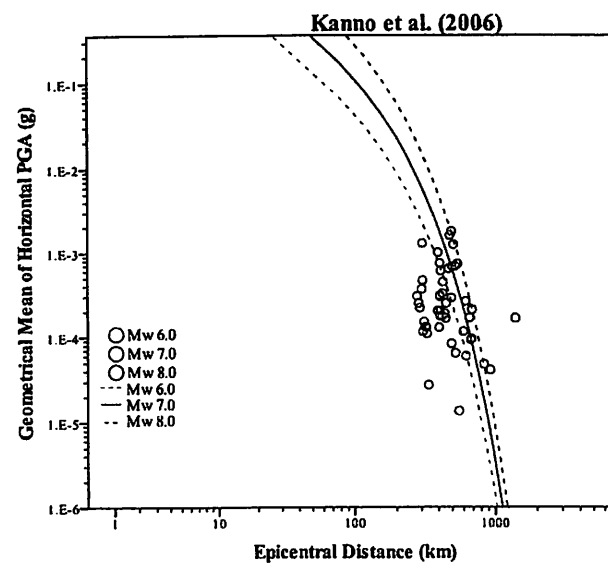
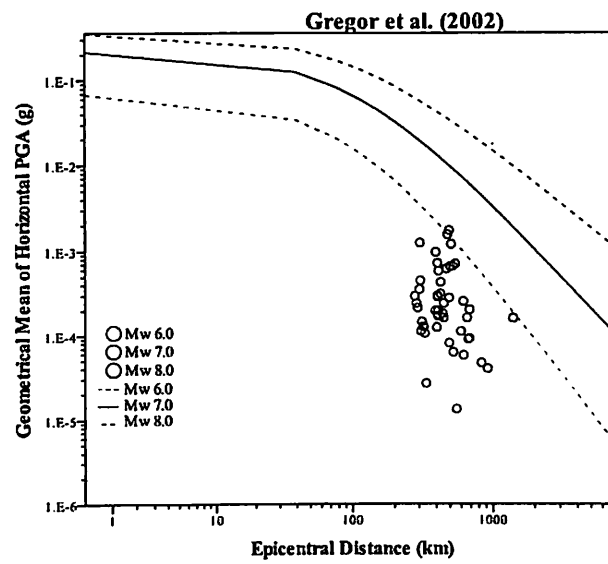
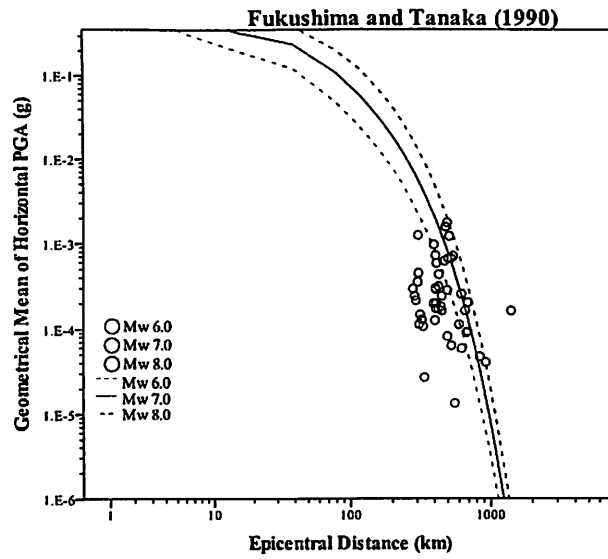


Figure 4.6 Continued

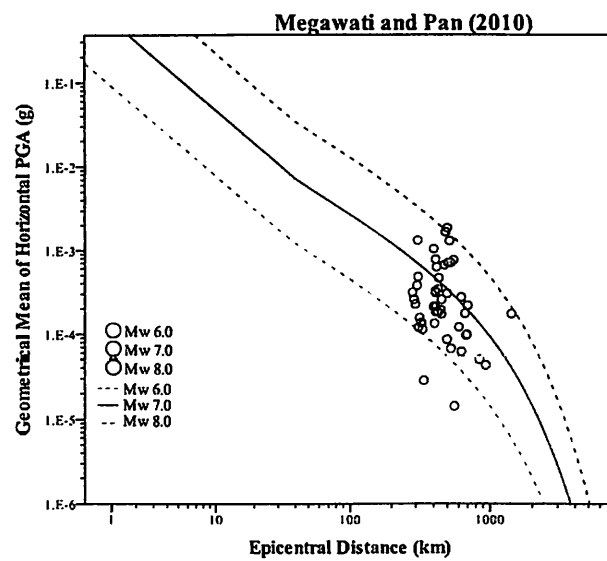
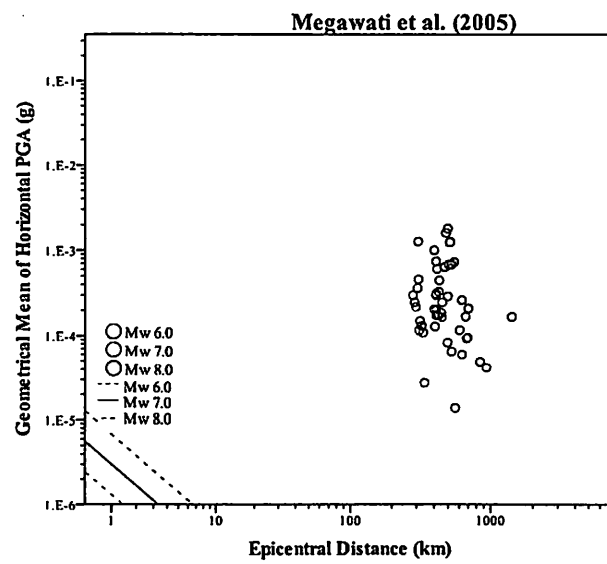
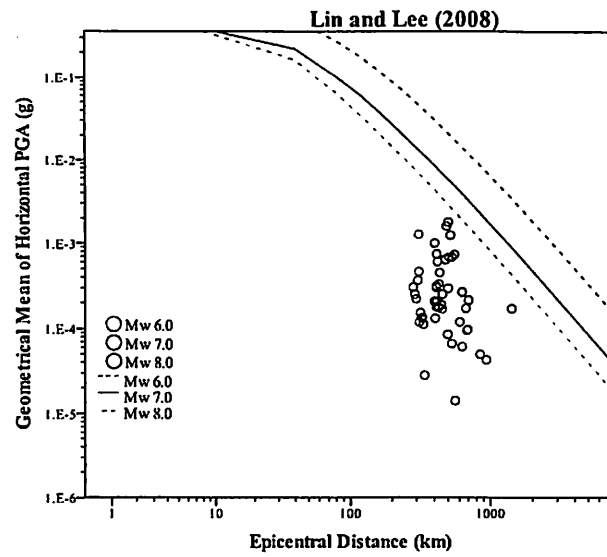


Figure 4.6 Continued

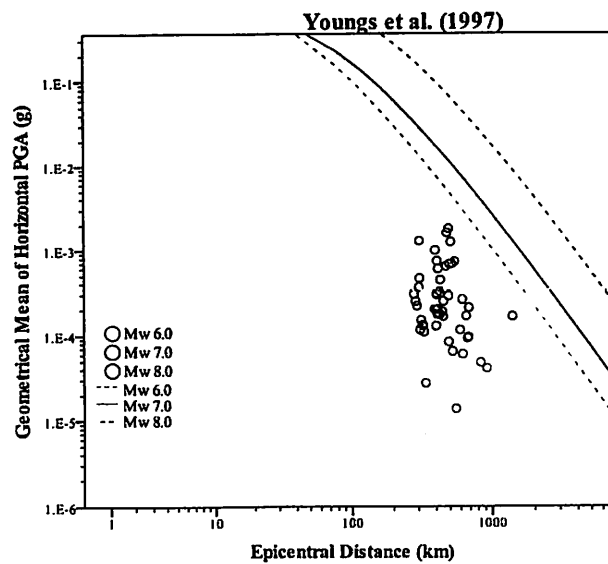
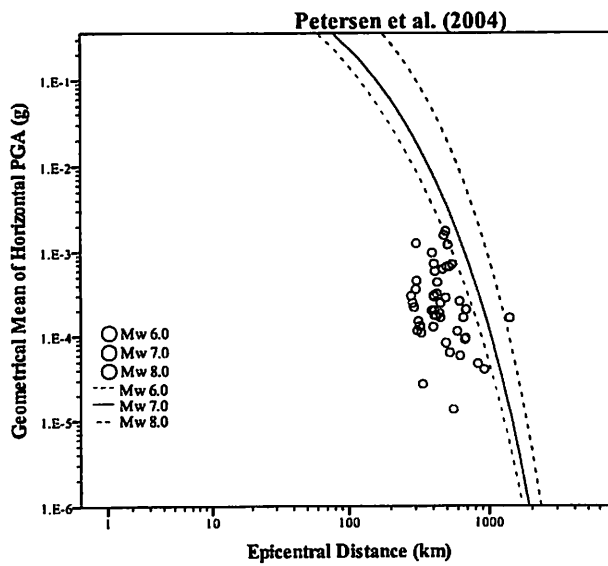
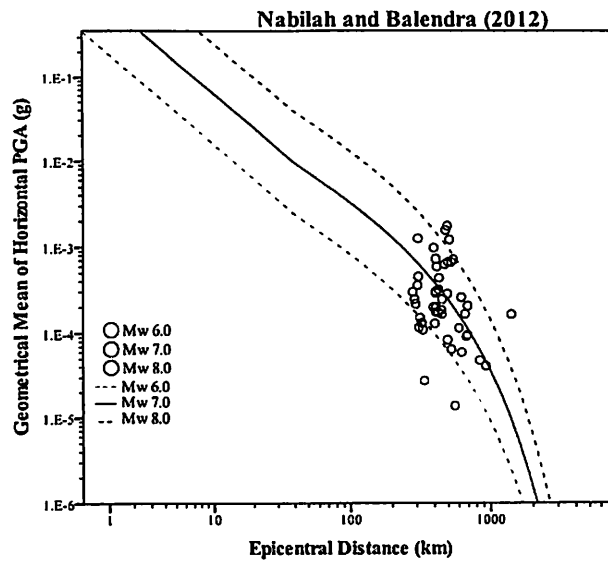


Figure 4.6 Continued

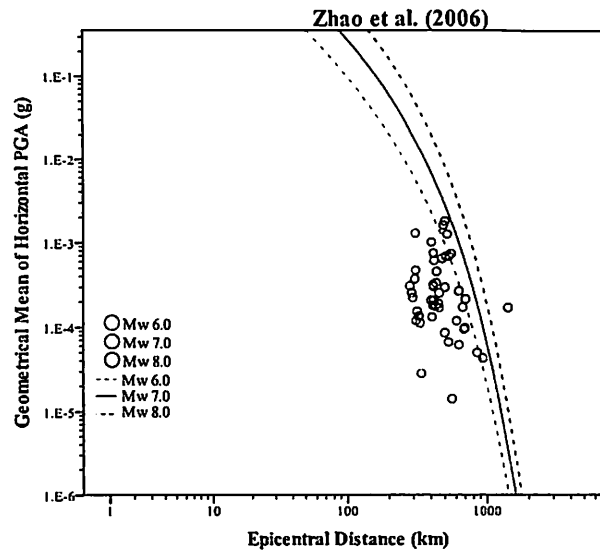


Figure 4.6 Continued

Fukushima and Tanaka (1990) and Zhao et al. (2006) did not give prediction as fit as for Class C site in predicting Class D site. These models tend to give higher prediction at  $M_W$  6.0 and  $M_W$  7.0. Megawati and Pan (2010) is also seen to be giving larger PGA for  $M_W$  8.0. However, Nabilah and Balendra (2012) model is still estimated closely to actual PGA despite neglecting provision of equation for different soil classes.

On the whole, it can be seen that models developed for Cascadian subduction zone or global, such as Crouse (1991), Youngs et al. (1997), Gregor et al. (2002) and Atkinson and Boore (2003) are tend to give higher prediction of PGA. This might be due to the global data used in deriving those models could not describe the characteristic of subduction earthquakes originated from Sumatra. The locally derived Lin and Lee (2008), which predicts higher PGA compare to observed data from Peninsular Malaysia is only suitable for Taiwan and Greece regions as stated by (Beauval et al., 2012a). In contrast, all attenuation curves derived specifically for Japan seems to have similar trends to the actual data from Peninsular Malaysia. Such models are Fukushima and Tanaka (1990), Kanno et al. (2006) and Zhao et al. (2006). This might be due to the abundance of Japanese data adopted in deriving those models are more specific and similar in geological and geographical features to Peninsular Malaysia. Petersen et al. (2004), Megawati et al. (2005), and Megawati and Pan (2010) models were derived for Singapore and Peninsular Malaysia. Among these three models, Megawati et al. (2005) produces curves that deviate far from actual data for intraslab events. The model is derived based

on simulation of shallow focal ground motion data and is not designed for intraslab events. Finally, the two models derived specifically for Peninsular Malaysia, namely Adnan et al. (2004) and Nabilah and Balendra (2012), seem to give reasonable correlation with the actual recorded data. However, the global data utilised in deriving Adnan et al. (2004) leads to higher prediction at large magnitude and lower prediction at small magnitude compare to actual data. Nabilah and Balendra (2012) were derived using ground motion in Peninsular Malaysia, therefore the model provides better fit for recorded PGA in Peninsular Malaysia.

#### 4.4.2 Comparison of pre-selected models for strike-slip earthquakes

There a total of 15 pre-selected ground motion attenuation models that were designed specifically for shallow crustal earthquakes. Records have been separated according to site classes to avoid soil amplification effect and ensure better representation of trend of ground motion characteristics. In this case, graphical presentations of these attenuation curves together with scatter plot of actual records are shown in Figure 4.7 and Figure 4.8 for Class C and Class D sites, respectively. The graph plots are arranged alphabetically and binned according to target regions of the model derivations, that are active tectonic region and stable continental region. Based on the scatter plot of actual ground motion record, for both Class C and Class D sites, there are large range of PGA recorded for a particular magnitude at similar distance. For example, PGAs recorded at Class C site is found range from 0.0002g to 0.003g for distance around 300 km to 400 km at  $M_W$  5.0. This makes the scatter of actual PGA to portray an almost vertical slope trend. Similar trends are also found in PGA recorded from Class D site. Thus, an attenuation model should have faster attenuation rate at larger distance in order to be claimed as appropriate in estimating ground motion originate from strike-slip earthquakes for Peninsular Malaysia.

Typically, there are two main types of curves showed by the graph plots. One type is one continuous linear line with two different slopes, particularly having steeper slope at long distance than short distance. The other type is one linear line at short distance merging with a curve with slope varies with distance. Different functional form adopted in different models shows different pattern or characteristics. Models that adopted the 4<sup>th</sup> and 5<sup>th</sup> functional forms shown in Table 2.5, show changes of slope at the same particular

distance for all magnitudes. Such models are Abrahamson and Silva (1997), Campbell (2003), Boore et al. (1997, 2005), Sadigh et al. (1997), Spudich et al. (1999) and Somerville et al. (2009). In these models, ground motion is assumed to be attenuated at slower rate once the waves travel beyond their defined near-source distance, regardless of the magnitude of the earthquake. Models that adopted the 3<sup>rd</sup> functional models are such as Frankel et al. (1996), Megawati et al. (2003), Atkinson and Boore (2006, 2011) and Pezeshk et al. (2011). These models illustrated a slight plateau after the cross point of short distance and long distance before a sudden steep drop of ground motion. On the other hand, the rest of the models, adopting other functional forms, showed dependencies of attenuation rate to magnitude of the earthquakes. Thus, the changes of slopes vary with distance at different magnitudes.

From the plotting of attenuation curves, Boore et al. (1997, 2005) and Spudich et al. (1999) has slow attenuation rate and deviate greatly from actual PGA. Abrahamson and Silva (1997) and Ambraseys et al. (2005) generate curves that diverge for different magnitude as the distance increase. This is because these two models are magnitude dependent model and were derived to give slower attenuation for higher magnitude. Campbell (2003) has constant attenuation rate for different magnitude, except for  $M_W$  9.0. Applicability of Campbell (2003) only lies within a magnitude constraint of  $M_W$  5.0 to  $M_W$  8.2. Nonetheless, the model trend could not fit the recorded data for magnitude that lies out of its applicability range. The rest of the models show steeper attenuation curve and converging for different magnitude as the distance increase. Even so, only Somerville et al. (2009) and Si and Midorikawa (2000) correspond quite well to the actual records for both site classes.

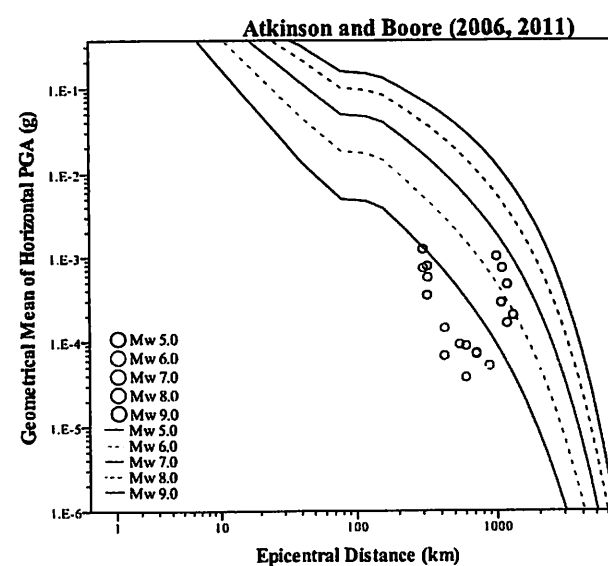
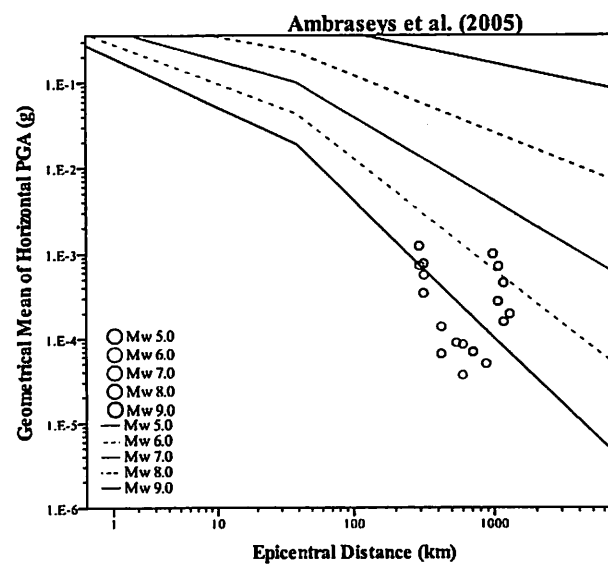
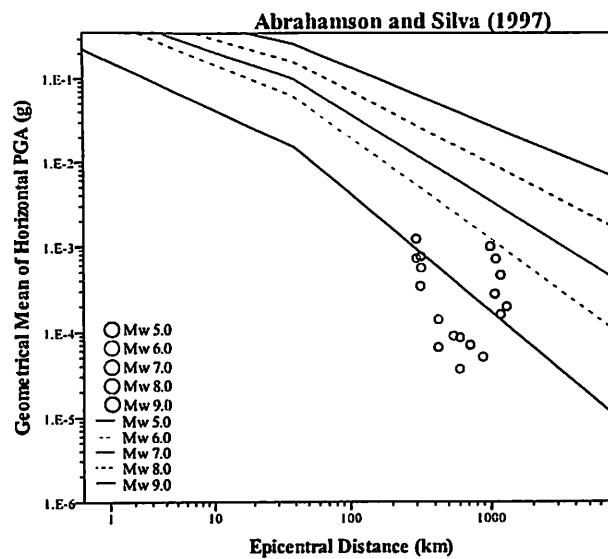


Figure 4.7 (a) Attenuation curves (active tectonic region) and recorded PGA by seismic stations located on Class C sites for strike-slip earthquakes

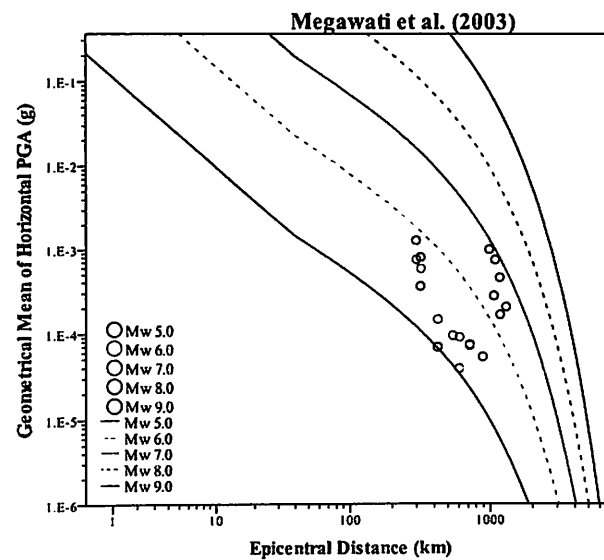
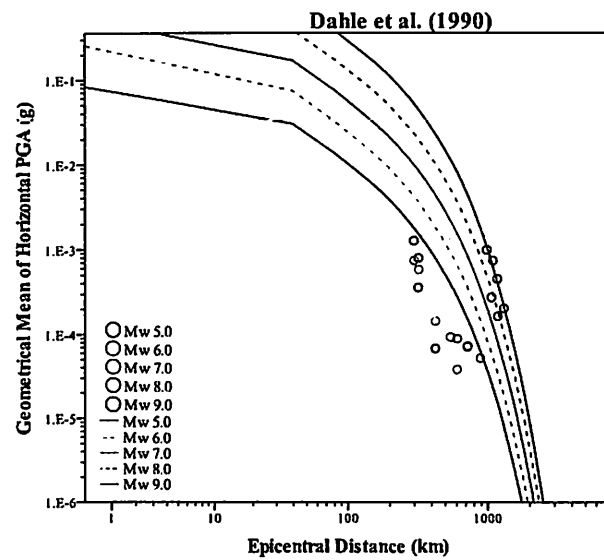
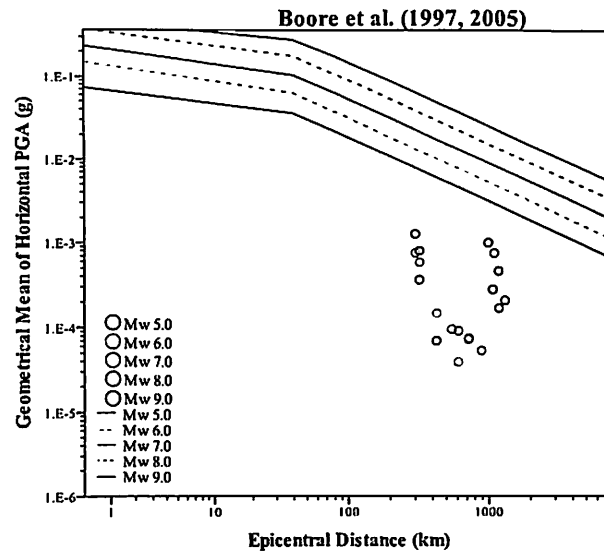


Figure 4.7 (a) Continued



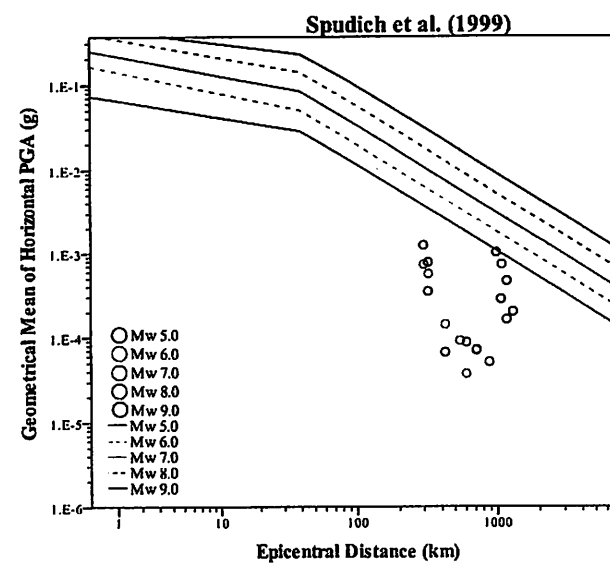
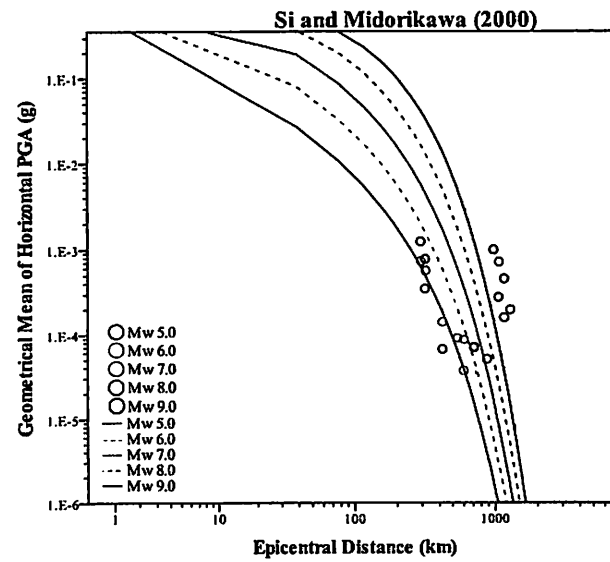
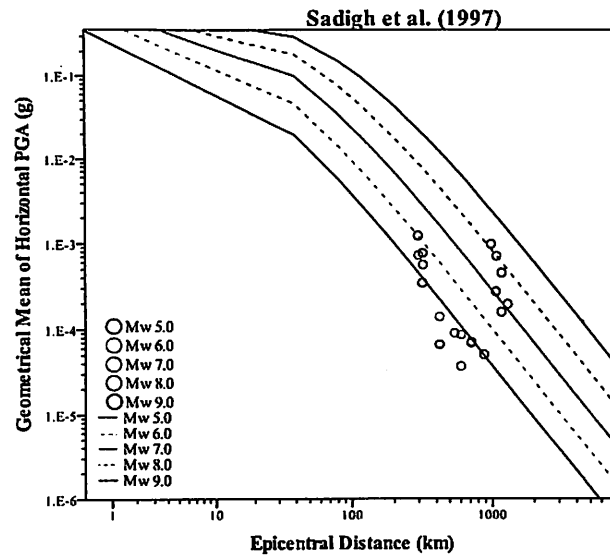


Figure 4.7 (a) Continued

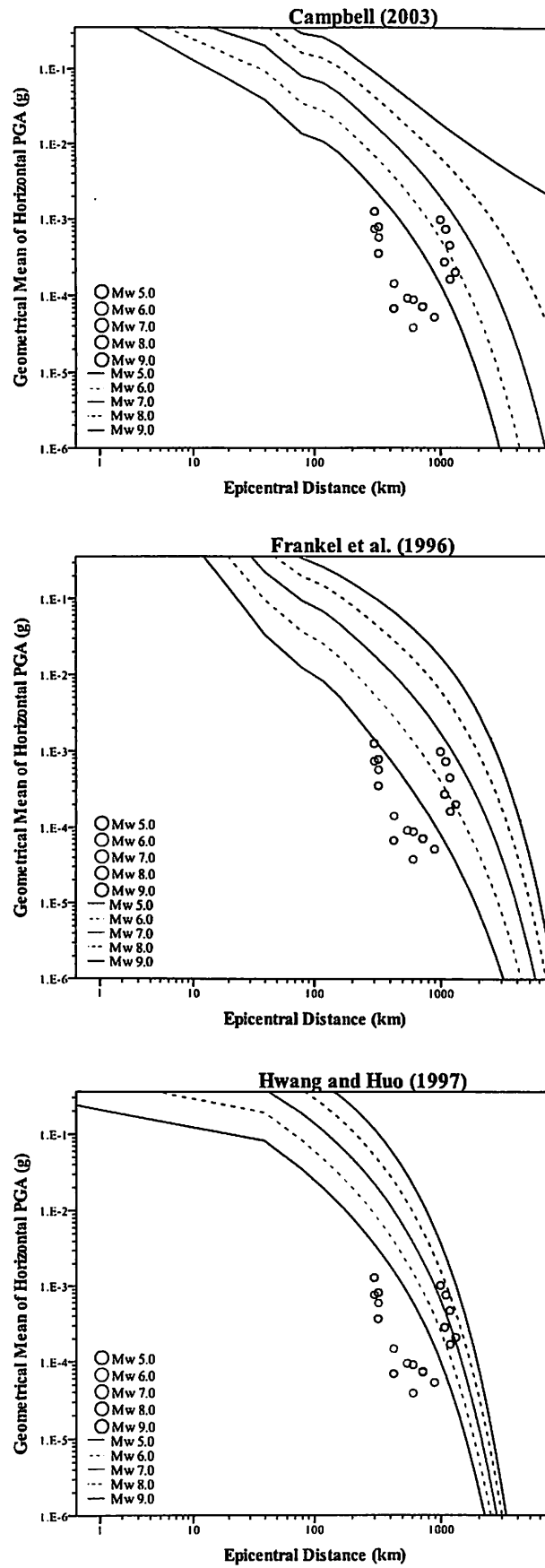


Figure 4.7 (b) Attenuation curves (stable continental region) and recorded PGA by seismic stations located on Class C sites for strike-slip earthquakes

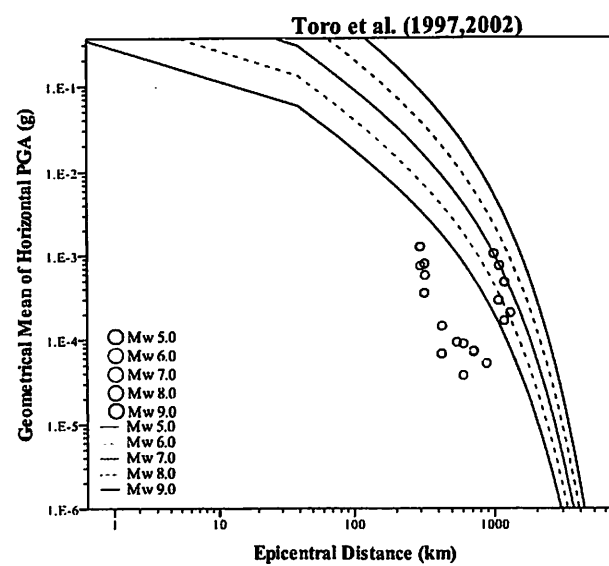
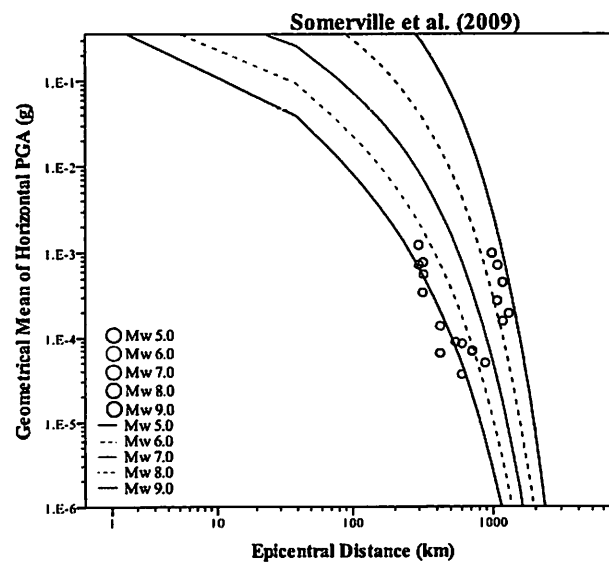
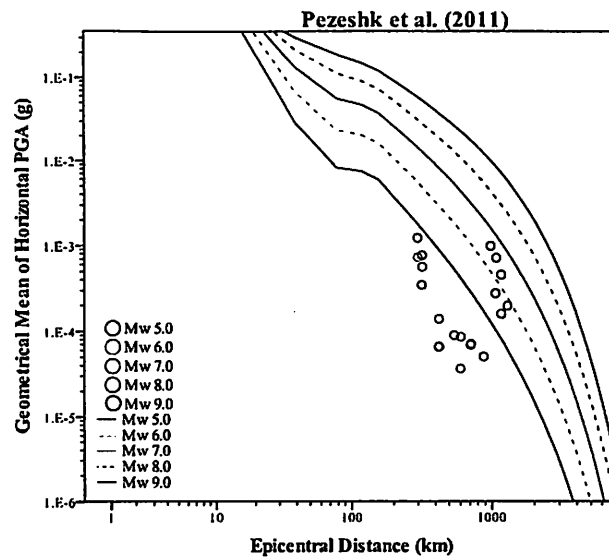


Figure 4.7(b) Continued

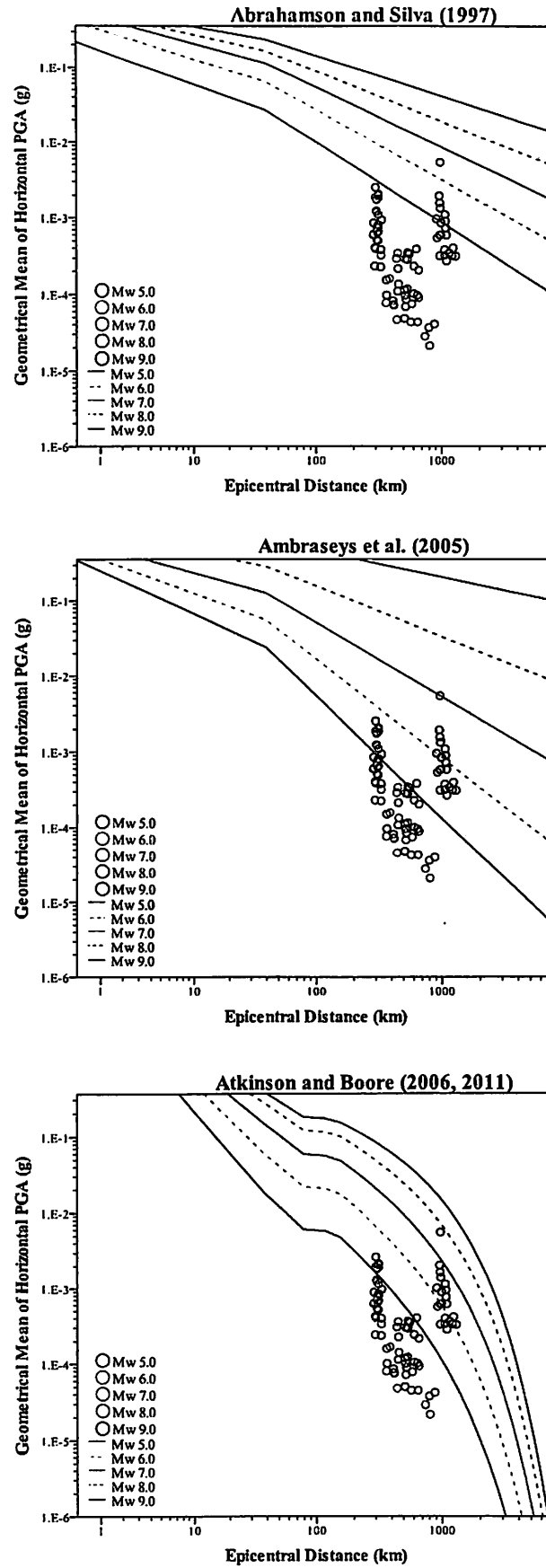


Figure 4.8 (a) Attenuation curves (active tectonic region) and recorded PGA by seismic stations located on Class D sites for strike-slip earthquakes

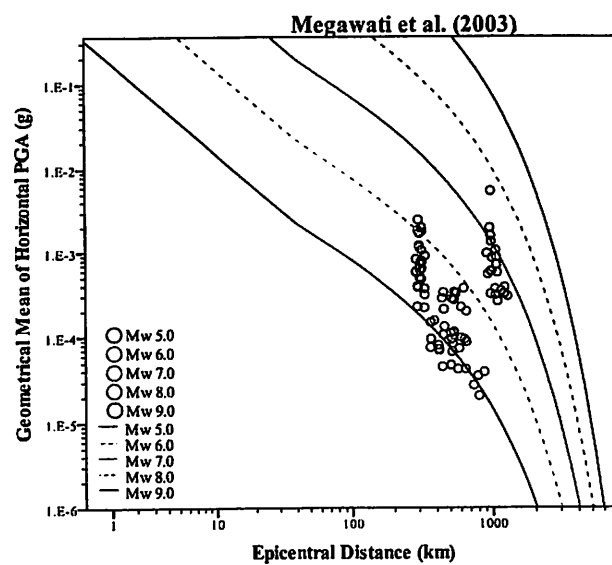
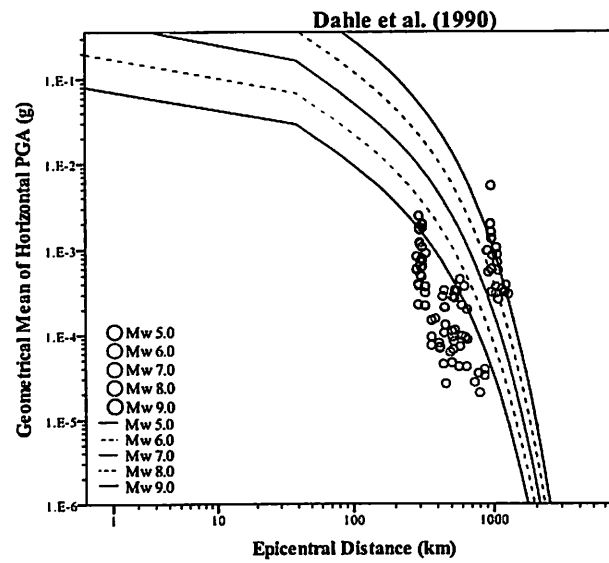
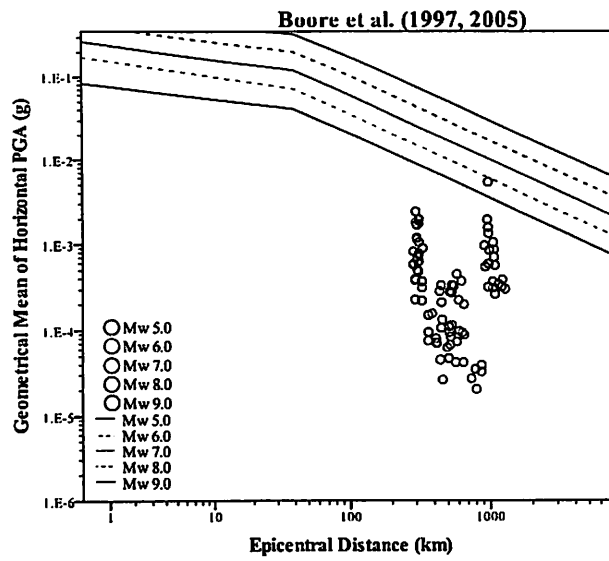


Figure 4.8 (a) Continued

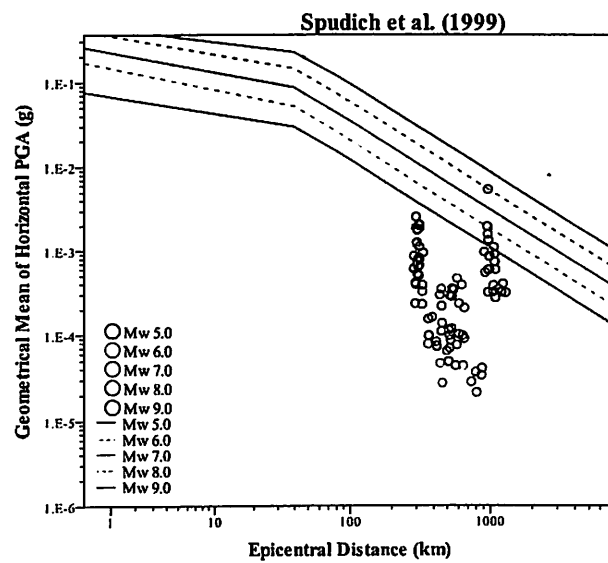
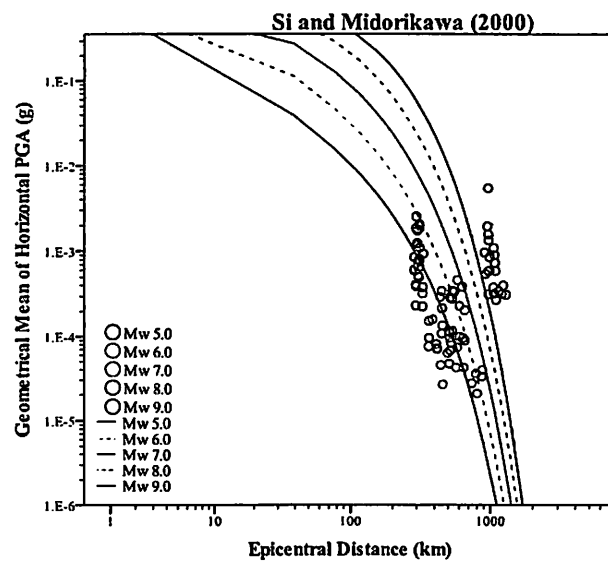
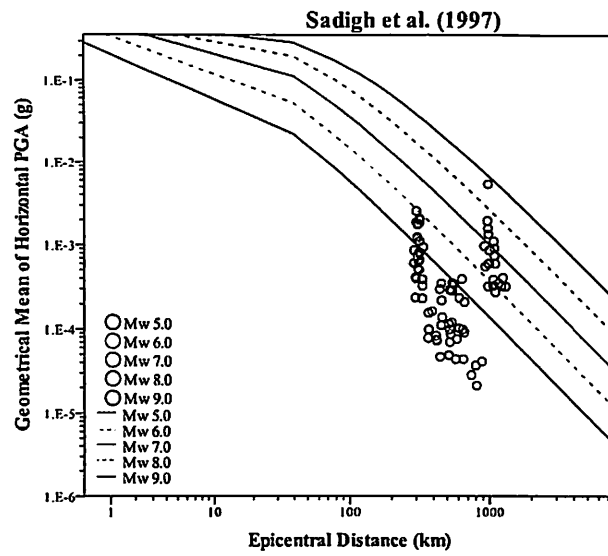


Figure 4.8 (a) Continued

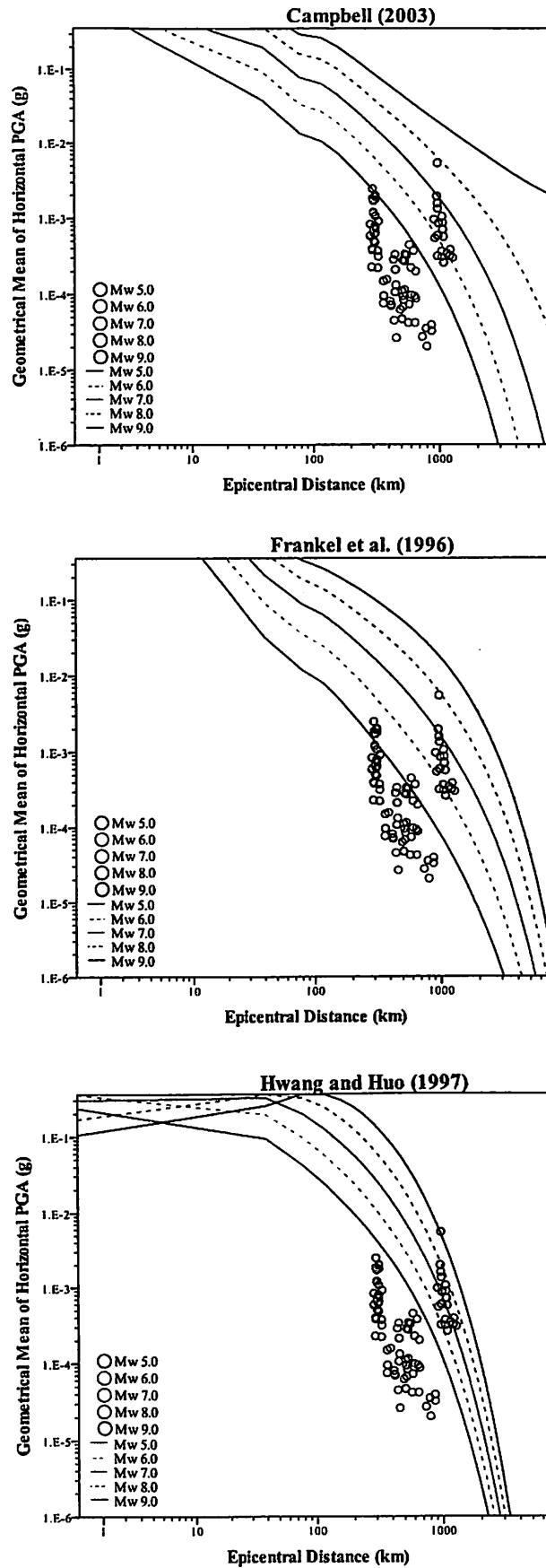


Figure 4.8 (b) Attenuation curves (stable continental region) and recorded PGA by seismic stations located on Class D sites for strike-slip earthquakes

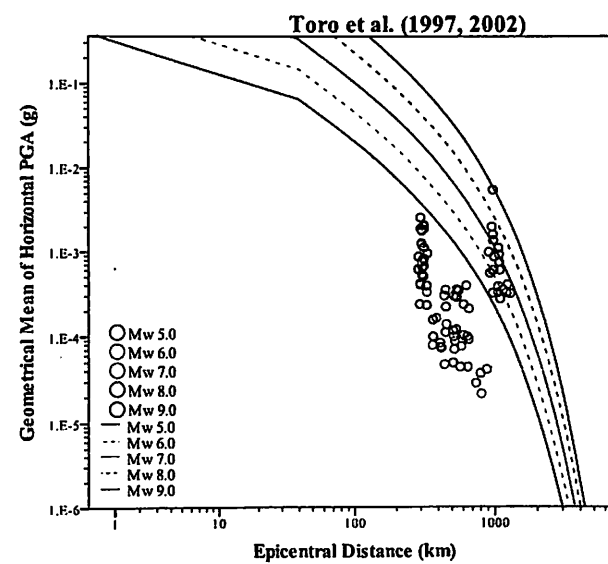
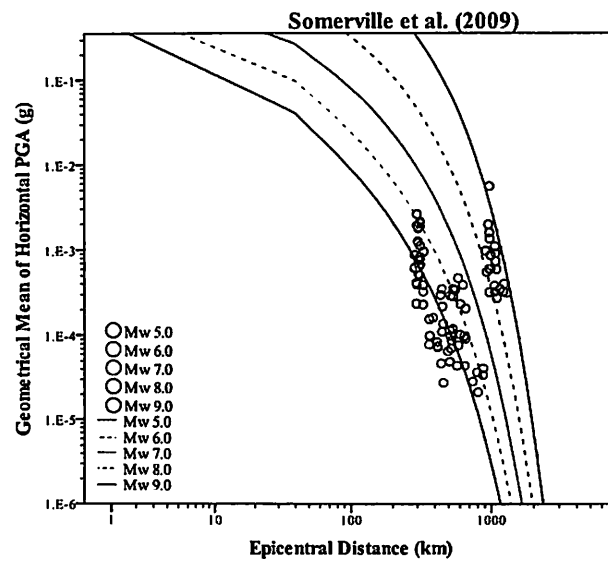
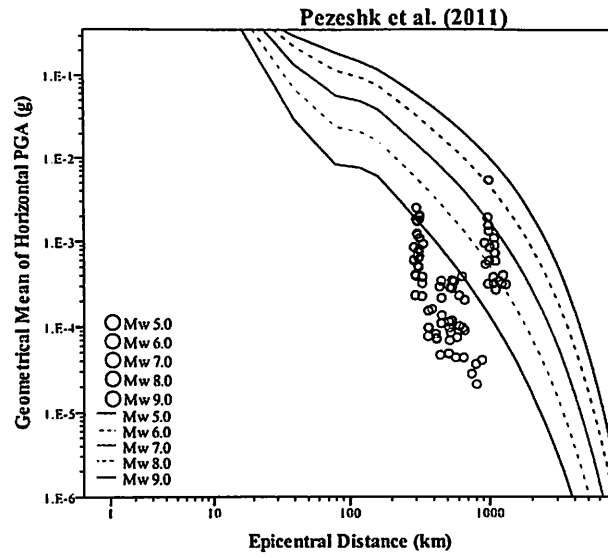


Figure 4.8 (b) Continued



#### 4.4.3 Quantification of adequacy of pre-selected models

Graphical presentation facilitates understanding. However, it could be hard to distinguish which model describes the best if there are some models that exhibited similar trend by using only visual interpretations. In this study, RMSE was calculated to quantify the goodness of fit for predicted and actual ground motion data. The smaller the RMSE value obtained the better the estimation to actual records. The RMSE has been normalized into the range of observed ground motion.  $RMSE_{Nor}$  values for each model are summarized in Table 4.5 and Table 4.6. These computed  $RMSE_{Nor}$  values were found agreeing well with plots of attenuation curves.

Table 4.5 Summary of computed normalised root mean squared error ( $RMSE_{Nor}$ ) for subduction earthquake ground motion attenuation models

Models	$RMSE_{Nor}$					
	Interface Class C	Interface Class D	Intraslab Class C	Intraslab Class D	Overall interface	Overall intraslab
Fukushima and Tanaka (1990)	0.045	0.045	0.045	0.045	0.045	0.045
Crouse (1991)	2.292	4.125	27.212	50.355	3.208	38.783
Youngs et al. (1997)	2.327	3.987	13.917	23.279	3.157	18.598
Gregor et al. (2002)	2.469	7.855	2.087	4.513	5.162	3.300
Atkinson and Boore (2003)	0.936	3.090	0.746	1.866	2.013	1.306
Adnan et al. (2004)	0.339	1.008	0.111	0.388	0.674	0.250
Petersen et al. (2004)	0.279	1.028	1.841	7.291	0.653	4.566
Megawati et al. (2005)	0.849	1.641	0.104	0.292	1.245	0.198
Kanno et al. (2006)	0.075	0.528	0.145	0.375	0.302	0.260
Zhao et al. (2006)	0.223	0.889	0.553	1.040	0.556	0.796
Lin and Lee (2008)	1.225	1.840	9.874	4.641	1.532	7.257
Megawati and Pan (2010)	0.249	0.429	0.080	0.157	0.339	0.119
Nabilah and Balendra (2012)	0.110	0.253	0.049	0.164	0.182	0.107

Table 4.6 Summary of computed normalised root mean squared error ( $RMSE_{Nor}$ ) for strike-slip earthquake ground motion attenuation models

Models	$RMSE_{Nor}$		
	Class C	Class D	Overall
Active tectonic region			
Si and Midorikawa (2000)	0.057	0.132	0.094
Megawati et al. (2003)	1.439	1.785	1.612
Ambraseys et al. (2005)	4.270	5.452	4.861
Abrahamson and Silva (1997)	4.124	5.839	4.981
Sadigh et al. (1997)	0.087	0.309	0.198
Spudich et al. (1999)	0.556	0.783	0.670
Dahle et al. (1990)	0.288	0.379	0.334
Atkinson and Boore (2006)	0.591	0.834	0.713
Boore et al. (1997)	2.072	2.673	2.372
Stable continental region			
Campbell (2003)	0.832	0.938	0.885
Hwang and Huo (1997)	0.321	0.532	0.426
Toro et al. (1997)	0.387	0.519	0.453
Pezeshk et al. (2011)	0.516	0.598	0.557
Frankel et al. (1996)	0.673	0.795	0.734
Somerville et al. (2009)	0.045	0.110	0.077

Among subduction earthquake ground motion attenuation models, Nabilah and Balendra (2012) model provides the lowest overall  $RMSE_{Nor}$  for both interface and intraslab events. Fukushima and Tanaka (1990) also predicts rather well for interface earthquakes while Megawati and Pan (2010) give second lower  $RMSE_{Nor}$  value for intraslab, after Nabilah and Balendra (2012). The lowest computed  $RMSE_{Nor}$  value for strike-slip earthquakes is provided by Somerville et al. (2009), following by Si and Midorikawa (2000) yielding the second lowest  $RMSE_{Nor}$  value and Sadigh et al. (1997) the third lowest  $RMSE_{Nor}$  value.

#### 4.5 Summary

Based from the results and validations conducted in this phase, it can be concluded that there are more than one model that can be considered as giving appropriate and consistent prediction of ground motion in relative to actual ground motion data.

For subduction events, Nabilah and Balendra (2012) model is good in predicting ground motion generated from both interface and intraslab events. However, Fukushima and Tanaka (1990) can also be a good alternative as the model estimates well for ground motion generated from interface events. Megawati and Pan (2010) curves also fit well to the PGA originated from intraslab events. Thus, the model can be another reliable option for estimating intraslab events.

Si and Midorikawa (2000) and Somerville et al. (2009) show similar consistency and closest fitting prediction curves to actual data for strike-slip events. The conducted  $RMSE_{Nor}$  has also proved the reliability of these two models to be used for distant strike-slip events for Peninsular Malaysia.

## CHAPTER 5

### CONCLUSION AND RECOMMENDATIONS

#### 5.1 Conclusions

A probable ground motion attenuation model is vital in seismic hazard analysis. Towards the end of this study, a comprehensive method in appraising the suitability of globally available ground motion attenuation models to be used in Peninsular Malaysia has been demonstrated. A set of pre-selected ground motion attenuation models has been reviewed and examined.

The site classification for seismic stations in Peninsular Malaysia is one of the most noteworthy findings to assist in accomplishing the first objective in this study. Based on the MASW test and computational analysis of shear wave velocity involved in the present study, the site classes of each seismic station are distinguished based on NEHRP site classifications standard. Seismic stations throughout Peninsular Malaysia are sitting on either Class C or Class D sites. With this finding, a set of 28 ground motion attenuation models has been examined and compared with the recorded ground motion in Peninsular Malaysia. In general, ground motion attenuation models that were developed for specific regions, especially Japan, are found to be producing trend that correspond well with the recorded field ground motion records. Global-based attenuation models, which were developed using worldwide events and ground motion data, tend to yield larger ground motion compare to recorded data in Peninsular Malaysia. Ground motion data in Peninsular Malaysia are predominantly attenuated due to the long propagation distance and thus, has different characteristic compare to the worldwide strong ground motion data utilised for development of global-based model. For non-subduction regions, models for stable continental regions have broader range of applicability. Therefore, they are more suitable in predicting the long distance and weak ground motion.

From the examination of ground motions model derived for subduction regions based on the dataset used in this analysis, Nabilah and Balendra (2012) model are found giving the smallest  $RMSE_{Nor}$  value. The model is considered suitable in predicting ground motion for distant subduction events for Peninsular Malaysia. Based from the computed  $RMSE_{Nor}$  value for strike-slip events, Somerville et al. (2009), which was derived based

on stochastic method, and Si and Midorikawa (2000), which was developed utilising historical ground motion records from Japan, gave the nearest PGA predictions to the actual records in Peninsular Malaysia. In final words, these three models are the most appropriate ground motion attenuation models for the application in Peninsular Malaysia, for respective tectonic mechanisms.

## REFERENCES

- Abrahamson, N. Empirical models of site response effects. *Proc. of the 11th World Conf. on Earthquake Engineering*. pp. 1-8.
- Abrahamson, N. A. & Shedlock, K. M. 1997. Overview of attenuation relations special issue. *Seismological Research Letters*, 68(1), pp. 9-23.
- Abrahamson, N. A. & Silva, W. J. 1997. Empirical response spectral attenuation relations for shallow crustal earthquakes. *Seismological Research Letters*, 68(1), pp. 94-127.
- Abrahamson, N. A. & Somerville, P. C. 1996. Effects of the hanging wall and footwall on ground motions recorded during the Northridge earthquake. *Bulletin of Seismological Society of America*, 86(1), pp. S93-S99.
- Adnan, A., Hendriyawan, Marto, A. & Irsyam, M., 2004. Selection and development of appropriate attenuation relationship for Peninsular Malaysia. In: *Malaysian Science and Technology Congress 2004 (MSTC 2004)*. Cititel Hotel, Midvalley Kuala Lumpur, 18-20 April 2005. pp. 9.
- Adnan, A., Hendriyawan, H. & Irsyam, M. 2002. The effect of the latest Sumatra earthquake to Malaysian Peninsular. *Jurnal Kejuruteraan Awam*, 14(2), pp. 12-252.
- Adnan, A., Marto, A. & Irsyam, M. 2011. Microzonation study for Kuala Lumpur and Putrajaya. *Malaysian Journal of Civil Engineering*, 23(1), pp. 63-85.
- Adnan, A., Tiong, P. L. Y. & Chow, Y. E. 2012. Usability of the Next Generation Attenuation equations for seismic hazard assessment in Malaysia. *International Journal of Engineering Research and Application (IJERA)*, 2(1), pp. 639-644.
- Adnan, A., Zaini Sooria, S., Sawada, S. & Goto, H. 2010. An investigation of the attenuation characteristics of distant ground motions in Peninsular Malaysia by comparing values of recorded with estimated PGA and PGV. *Malaysian Journal of Civil Engineering*, 2(1), pp. 38-52.
- Allen, T. The influence of attenuation in earthquake ground-motion and magnitude estimation: implications for Australian earthquake hazard. *Proceedings of the 2010 Australian Earthquake Engineering Society Conference*, Perth, Western Australia. pp. 1-13.
- Ambraseys, N., Douglas, J., Sarma, S. & Smit, P. 2005. Equations for the estimation of strong ground motions from shallow crustal earthquakes using data from Europe and the Middle East: horizontal peak ground acceleration and spectral acceleration. *Bulletin of Earthquake Engineering*, 3(1), pp. 1-53.
- Atkinson, G. M. & Boore, D. M. 1995. Ground-motion relations for eastern North America. *Bulletin of the Seismological Society of America*, 85(1), pp. 17-30.
- Atkinson, G. M. & Boore, D. M. 2003. Empirical ground-motion relations for subduction-zone earthquakes and their application to Cascadia and other regions. *Bulletin of the Seismological Society of America*, 93(4), pp. 1703-1729.

- Atkinson, G. M. & Boore, D. M. 2006. Earthquake ground-motion prediction equations for eastern North America. *Bulletin of the Seismological Society of America*, 96(6), pp. 2181-2205.
- Atkinson, G. M. & Boore, D. M. 2008. Erratum to empirical ground-motion relations for subduction zone earthquakes and their application to Cascadia and other regions. *Bulletin of the Seismological Society of America*, 98(5), pp. 2567-2569.
- Atkinson, G. M. & Boore, D. M. 2011. Modifications to existing ground-motion prediction equations in light of new data. *Bulletin of the Seismological Society of America*, 101(3), pp. 1121-1135.
- Azizan, N. Z. B. N. 2012. *Building performance with different bedrock response spectrum*. Master degree, Universiti Teknologi Malaysia.
- Balendra, T., Lam, N., Wilson, J. & Kong, K. 2002. Analysis of long-distance earthquake tremors and base shear demand for buildings in Singapore. *Engineering Structures*, 24(1), pp. 99-108.
- Beauval, C., Cotton, F., Abrahamson, N., Theodulidis, N., Delavaud, E., Rodriguez, L., Scherbaum, F. & Haendel, A. Regional differences in subduction ground motions. *World Conference on Earthquake Engineering Proceedings 2012*, Portugal. pp. 1-10.
- Beauval, C., Tasan, H., Laurendeau, A., Delavaud, E., Cotton, F., Guéguen, P. & Kuehn, N. 2012b. On the Testing of Ground-Motion Prediction Equations against Small-Magnitude Data. *Bulletin of the Seismological Society of America*, 102(5), pp. 1994-2007.
- Bolt, B. A. 1993. *Earthquake and geological discovery*, Scientific American Library, New York.
- Bommer, J. J., Hancock, J. & Alarcón, J. E. 2006. Correlations between duration and number of effective cycles of earthquake ground motion. *Soil Dynamics and Earthquake Engineering*, 26(1), pp. 1-13.
- Boore, D. M. 2005. Equations for estimating horizontal response spectra and peak acceleration from western North American earthquakes: a summary of recent work. *Seismological research letters*, 76(3), pp. 368-369.
- Boore, D. M. & Atkinson, G. M. 1987. Stochastic prediction of ground motion and spectral response parameters at hard-rock sites in eastern North America. *Bulletin of Seismological Society of America*, 77(1), pp. 440-467.
- Boore, D. M. & Joyner, W. B. 1997. Site amplifications for generic rock sites. *Bulletin of the Seismological Society of America*, 87(2), pp. 327-341.
- Boore, D. M., Joyner, W. B. & Fumal, T. E., 1993. *Estimation of response spectra and peak accelerations from western North American earthquakes: an interim report*. US Geological Survey Open-File Report 93-509.

- Boore, D. M., Joyner, W. B. & Fumal, T. E. 1997. Equations for estimating horizontal response spectra and peak acceleration from western North American earthquakes: A summary of recent work. *Seismological research letters*, 68(1), pp. 128-153.
- Bozorgnia, Y., Campbell, K. W. & Niazi, M. Observed spectral characteristics of vertical ground motion recorded during worldwide earthquakes from 1957 to 1995. *Proceedings of the 12th World Conference on Earthquake Engineering*.
- Bradley, B. A. 2011. Empirical correlation of PGA, spectral accelerations and spectrum intensities from active shallow crustal earthquakes. *Earthquake Engineering & Structural Dynamics*, 40(15), pp. 1707-1721.
- Brune, J. N. & Anooshehpour, A. 1999. Dynamic geometrical effects on strong ground motion in a normal fault model. *Journal of Geophysical Research: Solid Earth* (1978–2012), 104(B1), pp. 809-815.
- Building Seismic Safety Council (BSSC), 1998, 1997 Edition NEHRP Recommended Provisions for Seismic Regulations for New Buildings and Other Structures. (FEMA 302/303) Part 1: Provisions. Building Seismic Safety Council. United States Federal Emergency Management Agency. Washington D.C.
- Campbell, K. W. Ground motion model for the central United States based on near-source acceleration data. IN" *PROC. EARTHQUAKES & EARTHQUAKE ENG.: THE EASTERN U. S.*". pp. 213-232.
- Campbell, K. W., 1987. *Predicting strong ground motion in Utah*. In: " *Assesment of Regional Earthquake Hazards and Risk Along the Wasatch Front, Utah*"(P.L. Gori and W. W. Hays, Eds.). U.S. Geological Survey. Open-File Report 87.585. Reston, Virginia.
- Campbell, K. W. 2000. Predicting strong ground motion in Utah. In: " *Assesment of Regional Earthquake Hazards and Risk Along the Wasatch Front, Utah*"(P.L. Gori and W. W. Hays, Eds.). U.S. Geological Survey., *Professional Paper*, 1500(L), pp. L1-L31.
- Campbell, K. W. 2003. Prediction of strong ground motion using the hybrid empirical method and its use in the development of ground-motion (attenuation) relations in eastern North America. *Bulletin of the Seismological Society of America*, 93(3), pp. 1012-1033.
- Campbell, K. W. 2004. Prediction of strong ground motion using the hybrid empirical method and its use in the development of ground-motion (attenuation) relations in Eastern North America-Erratum. *Bulletin of Seismological Society of America*, 93(3), p. 1.
- Campbell, K. W., 2007. *Validation and update of hybrid empirical ground motion (attenuation) relations for the CEUS*. US Geological Survey Award 05HQGR0032.
- Campbell, K. W. & Bozorgnia, Y. New empirical models for predicting near-source horizontal, vertical, and V/H response spectra: Implications for design. In:



- "Proceedings., 6th International Conference on Siesmic Zonation", Nov. 12-15 2000, Palm Springs, CA, Earthquake Engineering Research Institute, Oakland, CA.
- Carlson, C. & Clay, D. 1999. The earth model—calculating field size and distances between points using GPS coordinates. *Site Specific Management Guidelines*, pp. 4.
- Chandler, A. & Lam, N. 2004. An attenuation model for distant earthquakes. *Earthquake Engineering & Structural Dynamics*, 33(2), pp. 183-210.
- Che Abas, M. R. Seismological activities in Malaysia. *Proceedings for the 5th ASEAN Science and Technology Week, Hanoi, Vietnam, 12-14 October 1998*. pp. 1-11.
- Chintanapakdee, C., Naguit, M. & Charoenyuth, M. Suitable attenuation model for Thailand. *Proceedings 14th World Conference on Earthquake Engineering*, 12-17 October 2008, Beijing, China. pp. 1-8.
- Cotton, F., Scherbaum, F., Bommer, J. J. & Bungum, H. 2006. Criteria for selecting and adjusting ground-motion models for specific target regions: Application to Central Europe and rock sites. *Journal of Seismology*, 10(2), pp. 137-156.
- Crouse, C. 1991. Ground-motion attenuation equations for earthquakes on the Cascadia subduction zone. *Earthquake spectra*, 7(2), pp. 201-236.
- Crouse, C., Vyas, Y. K. & Schell, B. A. 1988. Ground motions from subduction-zone earthquakes. *Bulletin of the Seismological Society of America*, 78(1), pp. 1-25.
- Dahle, A., Bungum, H. & Kvamme, L. B. 1990. Attenuation models inferred from intraplate earthquake recordings. *Earthquake Engineering & Structural Dynamics*, 19(8), pp. 1125-1141.
- Das, R., Wason, H. & Sharma, M. 2011. Global regression relations for conversion of surface wave and body wave magnitudes to moment magnitude. *Natural hazards*, 59(2), pp. 801-810.
- Dobry, R., Borcherdt, R., Crouse, C., Idriss, I., Joyner, W., Martin, G. R., Power, M., Rinne, E. & Seed, R. 2000. New site coefficients and site classification system used in recent building seismic code provisions. *Earthquake Spectra*, 16(1), pp. 41-67.
- Donohue, S. & Long, M. M. M. 2008. Assessment of an MASW technique incorporating discrete particle modelling. *Journal of Environmental & Engineering Geophysics*, 13(2), pp. 57-68.
- Douglas, J., 2011. *Ground-motion prediction equations 1964-2010*. Pacific Earthquake Engineering Research Center College of Engineering University of California, Berkeley: Bureau de Recherches Géologiques et Minières (BRGM).
- Douglas, J., Cotton, F., Di Alessandro, C., Boore, D. M., Abrahamson, N. & Akkar, S. Compilation and critical review of GMPEs for the GEM-PEER Global GMPEs Project. *Proceedings of the 15th World Conference on Earthquake Engineering 2012*, Lisbonne, Portugal

- Earthquake-Report.com. 2013. Earthquake Aceh, Sumatera, Indonesia becomes the second deadliest earthquake of 2013 (42 people killed and 6 remain missing) [Online]. [Accessed 31 December 2013], Available from World Wide Web: <http://earthquake-report.com/2013/07/02/very-strong-earthquake-northern-sumatra-indonesia-on-july-2-2013/>
- Electric Power Research Institute (EPRI), 2004. *CEUS ground motion project final report. 1009684*. Palo Alto, California.
- Electric Power Research Institute (EPRI), 1993. *Guidelines for site specific ground motions*. TR-102293. Palo Alto, California.
- Eurocode 8, 2004. EN 1998-1(2004) Eurocode 8: Design of Structures for Earthquake Resistance – Part 1: General rules, seismic actions and rules for buildings. *The European Union Per Regulation 305/2011, Directive 98/34/EC, Directive 2004/18/EC*.
- European-Mediterranean Seismological Centre (EMSC). 2011. Earthquake. [Online]. [Accessed 23 November 2012], Available from World Wide Web: <http://www.emsc-csem.org/Earthquake/earthquake.php?id=225446#providers>
- Fitch, T. J. 1972. Plate convergence, transcurrent faults, and internal deformation adjacent to Southeast Asia and the western Pacific. *Journal of Geophysical Research*, 77(23), pp. 4432-4460.
- Frankel, A. D., Mueller, C., Barnhard, T., Perkins, D., Leyendecker, E., Dickman, N., Hanson, S. & Hopper, M., 1996. *National seismic-hazard maps: documentation June 1996*.
- Fukushima, Y. & Tanaka, T. 1990. A new attenuation relation for peak horizontal acceleration of strong earthquake ground motion in Japan. *Bulletin of the Seismological Society of America*, 80(4), pp. 757-783.
- Gregor, N. J., Silva, W. J., Wong, I. G. & Youngs, R. R. 2002. Ground-motion attenuation relationships for Cascadia subduction zone megathrust earthquakes based on a stochastic finite-fault model. *Bulletin of the Seismological Society of America*, 92(5), pp. 1923-1932.
- Hanks, T. C. & Kanamori, H. 1979. A moment-magnitude scale. *Journal of Geophysical Research*, 84(1), pp. 2348-2350.
- Heaton, T. H., Tajima, F. & Mori, A. W. 1986. Estimating ground motion using recorded accelerograms. *Survey in Geophysics*, 8(1), pp. 25-83.
- Hendriyawan, H. 2010. Microzonation maps for Kuala Lumpur and Putrajaya. *Malaysian Journal of Civil Engineering*, 23(1), pp. 63-85.
- Husen, H., Majid, T., Nazri, F., Arshad, M. & Faisal, A. Development of design response spectra based on various attenuation relationships at specific location. *International Conference on Construction and Building Technology (ICCBT08)*.

- Hwang, H. & Huo, J.-R. 1997. Attenuation relations of ground motion for rock and soil sites in eastern United States. *Soil Dynamics and Earthquake Engineering*, 16(6), pp. 363-372.
- Hyndman, R. J. & Koehler, A. B. 2006. Another look at measures of forecast accuracy. *International Journal of Forecasting*, 22(4), pp. 679-688.
- Idriss, I. M. & Archuleta, R. J., 2005. *Evaluation of earthquake ground motions draft report for division of dam safety and inspections*. Office of Energy Projects and Federal Energy Regulatory Commission, Washington, D. C.
- International Code Council (ICC), 2000. International Building Code 2000. *International Conference of Building Officials*. Whittier, California, Alabama.
- Jeffrey, C. & Hee, M. 2008. Technical review of JKR's" Handbook on seismic design guidelines for concrete buildings in Malaysia".
- Jeffrey, C. C. L. & Mun, K. P., 2011. Gathering of Views and Opinions on Seismic Investigations in Peninsular Malaysia—Report on the IEM Workshop on Earthquake (part 1). *Bulletin of The Institution of Engineers Malaysia*. October 2011. pp. 44-47
- Joyner, W. B. & Boore, D. M. 1981. Peak horizontal acceleration and velocity from strong-motion records including records from the 1979 Imperial Valley, California, earthquake. *Bulletin of the Seismological Society of America*, 71(6), pp. 2011-2038.
- Kanno, T., Narita, A., Morikawa, N., Fujiwara, H. & Fukushima, Y. 2006. A new attenuation relation for strong ground motion in Japan based on recorded data. *Bulletin of the Seismological Society of America*, 96(3), pp. 879-897.
- Kramer, S. L. 1996. *Geotechnical Earthquake Engineering*, Prentice Hall, New Jersey.
- Lam, N., Wilson, J., Chandler, A. & Hutchinson, G. 2000. Response spectral relationships for rock sites derived from the component attenuation model. *Earthquake engineering & structural dynamics*, 29(10), pp. 1457-1489.
- Lau, T. L., Majid, T. A., Choong, K. K. & Zaini, S. S., 2005. Public Awareness On Earthquake And Tsunami Survey In Penang. *The Monthly Bulletin of The Institution of Engineers, Malaysia*. Vol.9. 4
- Lay, T., Kanamori, H., Ammon, C. J., Nettles, M., Ward, S. N., Aster, R. C., Beck, S. L., Bilek, S. L., Brudzinski, M. R. & Butler, R. 2005. The great Sumatra-Andaman earthquake of 26 december 2004. *Science*, 308(5725), pp. 1127-1133.
- Lay, T. & Wallace, T. C. 1995. *Modern global seismology*, Access Online via Elsevier,
- Lee, C.-T., Cheng, C.-T., Liao, C.-W. & Tsai, Y.-B. 2001. Site Classification of Taiwan Free-Field Strong-Motion Stations. *Bulletin of the Seismological Society of America*, 91(5), pp. 1283-1297.

- Lee, W. H., Jennings, P., Kisslinger, C. & Kanamori, H. 2002. *International Handbook of Earthquake & Engineering Seismology*, Academic Press,
- Lin, P.-S. & Lee, C.-T. 2008. Ground-motion attenuation relationships for subduction-zone earthquakes in northeastern Taiwan. *Bulletin of the Seismological Society of America*, 98(1), pp. 220-240.
- Madlazim & Santosa, B. J. 2010. Four Earthquakes of the Sumatran Fault Zone (Mw 6.0-6.4): Source Parameters and Identification of the Activated Fault Planes. *JSEE-Journal of Seismology and Earthquake Engineering*, 11(4), pp. 159-169.
- Malaysia Meteorological Department (MMD), 2008. Lokasi gempa bumi sekitar Bukit Tinggi [Earthquake locations around Bukit Tinggi] (unpublished)
- Malaysia Meteorological Department (MMD), 2012. MMD seismic stations code and location (unpublished)
- Mccaffrey, R., 2009. The tectonic framework of the Sumatran subduction zone. *Annual Review of Earth and Planetary Sciences*. 37. pp. 345-366
- Megawati, K., Pan, T.-C. & Koketsu, K. 2005. Response spectral attenuation relationships for Sumatran-subduction earthquakes and the seismic hazard implications to Singapore and Kuala Lumpur. *Soil Dynamics and Earthquake Engineering*, 25(1), pp. 11-25.
- Megawati, K. & Pan, T. C. 2010. Ground-motion attenuation relationship for the Sumatran megathrust earthquakes. *Earthquake Engineering & Structural Dynamics*, 39(8), pp. 827-845.
- Megawati, K., Pan, T. C. & Koketsu, K. 2003. Response spectral attenuation relationships for Singapore and the Malay Peninsula due to distant Sumatran-fault earthquakes. *Earthquake engineering & structural dynamics*, 32(14), pp. 2241-2265.
- Michael W., 2013. State seismologist Alaska Earthquake Center, University of Alaska Fairbanks : Faulting and earthquakes  
[Online]. [Accessed 17 December 2013], Available from World Wide Web: [http://www.aeic.alaska.edu/input/west/guides/amato\\_faulting/](http://www.aeic.alaska.edu/input/west/guides/amato_faulting/)
- Milne, W. G. & Davenport, A. G. 1969. Distribution of earthquake risk in Canada. *Bulletin of the Seismological Society of America*, 59(2), pp. 729-754.
- Nabilah, A. & Balendra, T. 2012. Seismic hazard analysis for Kuala Lumpur, Malaysia. *Journal of Earthquake Engineering*, 16(7), pp. 1076-1094.
- Naguit, M. E. 2007. *Estimation of probable earthquake ground motions in Bangkok*. Master thesis, Department of Civil Engineering, Faculty of Engineering, Chulalongkorn University.
- Natawidjaja, D. H. & Triyoso, W. 2007. The Sumatran Fault Zone—from Source to Hazard. *Journal of Earthquake and Tsunami*, 1(1), pp. 21-47.

- Numata, M. Earthquake resistant design for civil engineering structures: Earth-structures and foundations in Japan. *Proceedings of the Second World Conference on Earthquake Engineering Japan 1960*, Japan. pp. 1917-1946.
- Oglesby, D. D., Archuleta, R. J. & Nielsen, S. B. 1998. Earthquakes on dipping faults: the effects of broken symmetry. *Science*, 280(5366), pp. 1055-1059.
- Pacheco, J. F., Sykes, L. R. & Scholz, C. H. 1993. Nature of seismic coupling along simple plate boundaries of the subduction type. *Journal of Geophysical Research: Solid Earth*, 98(B8), pp. 14133-14159.
- Pappin, J. W., Yim, P. H. I. & Koo, C. H. R., 2011. An Approach for Seismic Design in Malaysia following the Principles of Eurocode 8. *Jurutera*. October 2011. pp. 22-28
- Petersen, M. D., Dewey, J., Hartzell, S., Mueller, C., Harmsen, S., Frankel, A. & Rukstales, K. 2004. Probabilistic seismic hazard analysis for Sumatra, Indonesia and across the Southern Malaysian Peninsula. *Tectonophysics*, 390(1), pp. 141-158.
- Pezeshk, S., Zandieh, A. & Tavakoli, B. 2011. Hybrid empirical ground-motion prediction equations for eastern North America using NGA models and updated seismological parameters. *Bulletin of the Seismological Society of America*, 101(4), pp. 1859-1870.
- Reid, H. F. 1913. Sudden Earth-movements in Sumatra in 1892. *Bulletin of the Seismological Society of America*, 3(2), pp. 72-79.
- Sadigh, K., Chang, C.-Y., Egan, J., Makdisi, F. & Youngs, R. 1997. Attenuation relationships for shallow crustal earthquakes based on California strong motion data. *Seismological Research Letters*, 68(1), pp. 180-189.
- Santosà, B. 2010. Four Earthquakes of the Sumatran Fault Zone (Mw 6.0-6.4): Source Parameters and Identification of the Activated Fault Planes. *JSEE-Journal of Seismology and Earthquake Engineering*, 11(4), pp. 159-169.
- Schnabel, P. B. & Seed, H. B. 1973. Accelerations in rock for earthquakes in the western United States. *Bulletin of the Seismological Society of America*, 63(2), pp. 501-516.
- Scordilis, E. M. 2006. Empirical Global Relations Converting  $M_S$  and  $m_b$  to Moment Magnitude. *Journal of Seismology*, 10(2), pp. 225-236.
- Shuib, M. K., 2009. The recent Bukit Tinggi earthquakes and their relationship to major geological structures. *Bulletin Geological Society of Malaysia*. 55. pp. 67-72
- Si, H. & Midorikawa, S. New attenuation relations for peak ground acceleration and velocity considering effects of fault type and site condition. *Proceedings of Twelfth World Conference on Earthquake Engineering*. pp. 1-8.
- Sieh, K. & Natawidjaja, D. 2000. Neotectonics of the Sumatran fault, Indonesia. *Journal of Geophysical Research: Solid Earth (1978–2012)*, 105(B12), pp. 28295-28326.

- Sieh, K., Ward, S. N., Natawidjaja, D. & Suwargadi, B. W. 1999. Crustal deformation at the Sumatran subduction zone revealed by coral rings. *Geophysical Research Letters*, 26(20), pp. 3141-3144.
- Sipkin, S. A. 2003. A correction to body-wave magnitude mb based on moment magnitude Mw. *Seismological Research Letters*, 74(6), pp. 739-742.
- Somerville, P. & Abrahamson, N., 2000. *Prediction of ground motions for thrust earthquakes*. Data Utilization Report No. CSMIP/00-01(OSM 00-03), California Strong Motion Instrumentation Program, Sacramento, CA.
- Somerville, P., Graves, R., Collins, N., Song, S. G., Ni, S. & Cummins, P. Source and ground motion models for Australian earthquakes. *Proc. 2009 Annual Conf. Australian Eqk. Eng. Soc.*
- Somerville, P. C. & Abrahamson, N. A. Ground motion prediction for thrust earthquakes. In: " *Proceedings SMIP95 Seminar on Seismological and Engineering Implications of Recent Strong-Motion Data*", May 16, 1995, San Francisco, California Strong Motion Instrumentation Program, Sacramento, CA. pp. 11-23.
- Spudich, P., Joyner, W., Lindh, A., Boore, D., Margaris, B. & Fletcher, J. 1999. SEA99: a revised ground motion prediction relation for use in extensional tectonic regimes. *Bulletin of the Seismological Society of America*, 89(5), pp. 1156-1170.
- Stein, S. & Wysession, M. 2009. *An introduction to seismology, earthquakes, and earth structure*, Wiley. com,
- Terrell, G. R. 1999. *Mathematical statistics: A unified introduction*, Springer.
- Toro, G. R. 2002. Modification of the Toro et al.(1997) attenuation equations for large magnitudes and short distances. *Risk Engineering*, Boulder, Colorado, pp. 1-10.
- Toro, G. R., Abrahamson, N. A. & Schneider, J. F. 1997. Model of strong ground motions from earthquakes in central and eastern North America: best estimates and uncertainties. *Seismological Research Letters*, 68(1), pp. 41-57.
- Trnkoczy, A., Bormann, P., Hanka, W., Holcomb, L. G., Nigbor, R. L., Shinohara, M., Shiobara, H. & Suyehiro, K. 2012. Site Selection, Preparation and Installation of Seismic Stations. Bormann, P. (Ed.), *New Manual of Seismological Observatory Practice 2 (NMSOP-2)*, Potsdam : Deutsches GeoForschungsZentrum GFZ.
- United States of Geological Survey (USGS). 2007. Significant earthquake: Summary of Magnitude 7.5-Java, Indonesia, 2007 August 08 17:04:58 UTC. [Online]. [Accessed 4 December 2013], Available from World Wide Web: <http://earthquake.usgs.gov/earthquakes/eqinthenews/2007/us2007fubd/#summary>
- United States of Geological Survey (USGS). 2012. Largest Earthquakes in the World since 1900. [Online]. [Accessed 17 December 2013], Available from World Wide Web: [http://earthquake.usgs.gov/earthquakes/world/10\\_largest\\_world.php](http://earthquake.usgs.gov/earthquakes/world/10_largest_world.php)

- United States of Geological Survey (USGS). 2013. An Updated Earthquake Catalogue for Stable Continental Regions: Intraplate Earthquake (495-2002) [Online]. [Accessed 11 December 2013], Available from World Wide Web: [http://earthquake.usgs.gov/data/scr\\_catalog.php](http://earthquake.usgs.gov/data/scr_catalog.php)
- United States of Geological Survey (USGS). 2012. Preliminary Determination of Earthquakes (PDE). [Online]. [Accessed 17 December 2013], Available from World Wide Web: <http://earthquake.usgs.gov/earthquakes/eqarchives/>
- United States of Geological Survey (USGS). 2013. Seismicity of Earth 1900-2012 [Online]. [Accessed 17 December 2013], Available from World Wide Web: [http://earthquake.usgs.gov/earthquakes/world/seismicity\\_maps/index.php](http://earthquake.usgs.gov/earthquakes/world/seismicity_maps/index.php)
- United States of Geological Survey (USGS). 2013. USGS Centroid Moment Solution [Online]. [Accessed 17 January 2014], Available from World Wide Web: [http://earthquake.usgs.gov/earthquakes/eqarchives/fm/neic\\_b000i4re\\_cmt.php](http://earthquake.usgs.gov/earthquakes/eqarchives/fm/neic_b000i4re_cmt.php)
- Villaverde, R. 2009. *Fundamental Concepts of Earthquake Engineering*, Taylor & Francis Group, United States of America.
- Weller, O., Lange, D., Tilmann, F., Natawidjaja, D., Rietbrock, A., Collings, R. & Gregory, L. 2012. The structure of the Sumatran Fault revealed by local seismicity. *Geophysical Research Letters*, 39(1), pp. 1-7.
- Xia, J., Miller, R. D., Park, C. B., Hunter, J. A. & Harris, J. B. 2000. Comparing shear-wave velocity profiles from MASW with borehole measurements in unconsolidated sediments, Fraser River Delta, BC, Canada. *Journal of Environmental & Engineering Geophysics*, 5(3), 1-13.
- Xia, J., Miller, R. D., Park, C. B., Hunter, J. A., Harris, J. B. & Ivanov, J. 2002. Comparing shear-wave velocity profiles inverted from multichannel surface wave with borehole measurements. *Soil dynamics and earthquake engineering*, 22(3), pp. 181-190.
- Xu, Y., Xia, J. & Miller, R. D. 2006. Quantitative estimation of minimum offset for multichannel surface-wave survey with actively exciting source. *Journal of Applied Geophysics*, 59(2), pp. 117-125.
- Yilmaz, O., Eser, M., Sandikkaya, A., Akkar, S., Bakir, S. & Yilmaz, T. 2008. Comparison of shear-wave velocity-depth profiles from downhole and surface seismic experiments.
- Youngs, R., Chiou, S.-J., Silva, W. & Humphrey, J. 1997. Strong ground motion attenuation relationships for subduction zone earthquakes. *Seismological Research Letters*, 68(1), pp. 58-73.
- Zhao, J. X., Dowrick, D. J. & Mcverry, G. H. 1997. Attenuation of peak ground acceleration in New Zealand earthquakes. *Bulletin of the New Zealand National Society for Earthquake Engineering*, 30(2), pp. 133-158.

Zhao, J. X., Zhang, J., Asano, A., Ohno, Y., Oouchi, T., Takahashi, T., Ogawa, H., Irikura, K., Thio, H. K. & Somerville, P. G. 2006. Attenuation relations of strong ground motion in Japan using site classification based on predominant period. *Bulletin of the Seismological Society of America*, 96(3), pp. 898-913.



## **APPENDICES**

# Appendix A Compilation of moment magnitude from various catalogues

No.	Date	Time	Coordinate		Magnitude				Source
			Lat.	Long.	$m_b$	$M_L$	$M_S$	$M_W$	
1	2013-07-02	07:37:02	4.611	96.6041	6.1	6.41	6.1	6.4	USGS
2	2012-07-25	00:27:45	2.657	96.126	5.99	-999	6.54	6.1	USGS
3	2012-06-23	04:34:53	2.9344	97.8058	6.62	6.21	7.13	6.1	USGS
4	2012-04-11 (a)	10:43:09	0.735	92.443	7.61	-	7.88	8.2	USGS
5	2012-04-11 (b)	08:38:38	2.36	93.0104	7.7	7.9	8.2	8.6	USGS
6	2012-03-05	06:55:28	4.187	97.093	5.2	5.48	6.52	5.5	USGS
7	2011-09-05	17:55:13	2.73	98	6.58	6.12	7.35	6.6	USGS
8	2011-06-18	11:58:05	1.784	99.315	4.92	5.37	5.77	5.2	MMD
9	2011-06-14 (a)	03:01:29	1.856	99.254	5.5	5.83	6.38	5.6	USGS
10	2011-06-14 (b)	00:08:33	1.813	99.29	5.23	5.69	6.01	5.3	USGS
11	2011-04-06	14:01:46	1.693	97.133	5.82	6.04	6.73	5.8	MMD
12	2010-12-01	00:50:23	2.758	98.95	5.45	5.09	6.5	5.9	MMD
13	2010-10-25	14:42:16	-3.838	99.604	6.14	4.78	7.29	7.7	USGS
14	2010-05-09	05:59:44	3.77	96.044	6.95	6.55	7.37	7.2	USGS
15	2010-04-06	22:15:06	2.412	97.145	7.24	-999	7.36	7.8	USGS
16	2009-12-23	01:11:52	-1.721	98.894	5.96	6.09	7.11	5.7	NEIC
17	2009-10-01	01:52:31	-2.49	101.685	6.2	6.49	6.88	6.6	USGS
18	2009-09-30	10:16:09	-0.873	99.746	7.46	6.86	7.6	7.6	USGS
19	2009-08-16	07:38:18	-1.699	98.597	6.5	-999	7.3	6.7	USGS
20	2008-05-19	14:26:00	1.7	99.1	6.1	-999	-999	6	NEIC
21	2008-02-25 (a)	18:06:00	-2.3	99.9	6.1	-999	-999	6.3	NEIC
22	2008-02-25 (b)	08:36:00	-2.6	99.7	6.5	-999	-999	7.2	USGS
23	2008-02-24	14:46:00	-2.5	99.6	6	-999	-999	6.2	NEIC
24	2008-02-20	08:08:00	2.7	95.8	6.5	-999	-999	7.4	USGS
25	2008-01-22	17:14:00	1.1	97.2	5.7	-999	-999	6.2	NEIC
26	2008-01-04	07:29:00	-3	100.5	6.1	-999	-999	6	NEIC
27	2007-09-20	08:31:00	-2.4	99.6	6.2	-999	-999	6.7	USGS
28	2007-09-13	03:35:00	-1.9	99.7	6.4	-999	-999	7	USGS
29	2007-09-12 (a)	23:49:00	-2.8	100.8	6.8	-999	-999	7.9	USGS
30	2007-09-12 (b)	11:10:00	-4.4	101.1	6.9	-999	-999	8.5	USGS
31	2007-08-08	17:04:00	-6.2	107.6	7	-999	-999	7.5	USGS
32	2007-07-21	12:53:00	5.1	97.8	5	-999	-999	5.2	DJA
33	2007-03-06 (a)	05:49:00	-0.6	100.4	5.8	-999	-999	6.1	MOS
34	2007-03-06 (b)	03:49:00	-0.5	100.4	5.6	-999	-999	6.4	USGS
35	2006-12-01	03:58:00	3.4	98.8	6.6	-999	-999	6.3	USGS
36	2006-05-16	15:28:00	0	97	6.7	-999	-999	6.8	USGS
37	2005-05-19	01:54:00	2	96.9	6.3	-999	-999	6.9	USGS
38	2005-05-14	05:05:00	0.8	98.2	6.7	-999	-999	6.8	USGS
39	2005-04-28	14:07:00	2.1	96.6	5.9	-999	-999	6.3	USGS
40	2005-04-10	10:29:00	-1.3	99.4	6.3	-999	-999	6.7	USGS
41	2005-04-03	03:10:00	2	97.5	5.8	-999	-999	6.3	USGS
42	2005-03-28	16:09:00	2	97.3	7.3	-999	-999	8.6	USGS
43	2004-12-26	00:58:53	3.2	95.9	7	7.3	-999	9.1	USGS
44	2004-07-25	14:35:19	-2.4	103.9	6.8	7	-999	7.3	USGS

Appendix B Computed epicentral distance between earthquake sources and seismic stations

Earthquake event					Distance (km)																		
No.	Date	Time (GMT)	Coordinate		PYSM_BO	SRSM	KNSM	BKSM	SASM	GTSM	JBSM	UYSM	DTSM	BRSM	FRM	KUM	IPM	KGM	KTM	JRM	KOM	PJSM	BTSM
			Lat.	Long.																			
1	2013-07-02	07:37:02	4.611	96.6041											577.9	454.8	490.6			657.0	863.3		
2	2012-07-25	00:27:45	2.657	96.126												580.3	584.1			718.7	864.2		
3	2012-06-23	4:34:53	2.9344	97.8058						444.1			448.9	451.1	425.9	409.2	401.3	621.2	648.0	529.7	683.7		448.6
4	2012-04-11 (a)	10:43:09	0.735	92.443			1047.3	1057.7		1078.7		1065.6	1078.2	1075.0	1058.1	1041.4	1044.3	1218.3	1291.6	1168.9	1274.6		1082.3
5	2012-04-11 (b)	8:38:38	2.36	93.0104	966.5	964.7	951.0	964.0		981.1		969.8	985.4	986.3	962.8	908.0	923.7	1147.1	1171.0	1065.7	1207.2		985.6
6	2012-03-05	6:55:28	4.187	97.093	529.0	512.0						520.1	540.0	548.7	514.3	412.9	438.6	732.2		598.8	796.1		
7	2011-09-05	17:55:13	2.73	98	410.2		395.3	407.8		426.0		414.0		430.0	406.9	408.2	393.5	596.6		513.7	658.6	411.1	
8	2011-06-18	11:58:05	1.784	99.315	291.8	311.1	294.8	299.7	284.1	326.2	330.4	310.7	317.8	309.2	303.0	415.0	363.0	445.9		421.5	504.3		
9	2011-06-14 (a)	3:01:29	1.856	99.254	294.7	312.4	296.2	301.7	286.0	327.7		312.4	320.2	312.4	304.7	410.1	359.9	452.3		422.9	511.1	297.6	
10	2011-06-14 (b)	0:08:33	1.813	99.29	293.0	311.6	295.3	300.5	284.9	326.8		311.4	318.8	310.5	303.7	413.0	361.7	448.5			507.1	296.0	
11	2011-04-06	14:01:46	1.693	97.133	524.0		517.6	526.8	511.0	549.3		535.5	547.0	542.8	527.9	557.4	537.6	688.9		641.7	747.2	526.2	
12	2010-12-01	0:50:23	2.758	98.95	304.5				287.2	321.7	329.7	309.3	323.8	324.3	302.1	337.6	306.2	492.5	544.6	411.4	555.1	305.6	
13	2010-10-25	14:42:16	-3.838	99.604	781.6	827.2			795.1	834.4		819.0	809.2	786.1	813.5	1015.0	943.4	767.4	1085.6	911.3	780.9		
14	2010-05-09	5:59:44	3.77	96.044	633.8	622.2		626.1	612.1	638.2	648.5		647.8	653.8	622.9	538.0	560.3	831.4	805.4	714.7	894.7		
15	2010-04-06	22:15:06	2.412	97.145	507.8			506.8	491.3			513.7			506.4	502.7	493.3	687.9	739.0	614.7	748.7		
16	2009-12-23	01:11:52	-1.721	98.894	599.4	639.2	624.1			649.5		633.2	628.5	608.5	626.6	799.0	735.7	642.4	910.3	736.8	674.3		
17	2009-10-01	1:52:31	-2.49	101.685	597.8			623.1		650.0				596.4	633.1	867.3	784.9	530.1	878.7	710.3	531.0		
18	2009-09-30	10:16:09	-0.873	99.746	471.3			492.0		522.5				479.2	500.2	688.5	619.4	509.7	781.9	607.6	543.3		
19	2009-08-16	7:38:18	-1.699	98.597	615.2	653.5	638.1	633.9	621.3	664.4			644.3	625.1	641.2	805.3	744.7		925.7	753.2	700.2		
20	2008-05-19	14:26:00	1.7	99.1													383.7		601.4				
21	2008-02-25 (a)	18:06:00	-2.3	99.9													770.7		916.2				
22	2008-02-25 (b)	8:36:00	-2.6	99.7													807.1		955.4		669.8		
23	2008-02-24	14:46:00	-2.5	99.6													798.4		949.8				
24	2008-02-20	08:08:00	2.7	95.8													616.6		864.6				
25	2008-01-22	17:14:00	1.1	97.2													573.5		808.1				

# Appendix B Continued

Earthquake event				Distance (km)																			
No.	Date	Time (GMT)	Coordinate		PYSM_B0	SRSM	KNSM	BKSM	SASM	GTSM	JBSM	UYSM	DTSM	BRSM	FRM	KUM	IPM	KGM	KTM	JRM	KOM	PJSM	BTSM
			Lat.	Long.																			
26	2008-01-04	07:29:00	-3	100.5													839.7		965.5				
27	2007-09-20	08:31:00	-2.4	99.6													787.6		939.8		661.8		
28	2007-09-13	03:35:00	-1.9	99.7													731.3		885.1				
29	2007-09-12 (a)	23:49:00	-2.8	100.8													816.0		934.7		610.4		
30	2007-09-12 (b)	11:10:00	-4.4	101.1													992.2		1097.9		749.4		
31	2007-08-08	17:04:00	-6.2	107.6													1395.8		1365.4				
32	2007-07-21	12:53:00	5.1	97.8													362.3		591.9		764.8		
33	2007-03-06 (a)	05:49:00	-0.6	100.4											445.6	651.6	576.9						
34	2007-03-06 (b)	03:49:00	-0.5	100.4											435.1	640.6	566.0		712.2				
35	2006-12-01	03:58:00	3.4	98.8											314.5	292.9	279.5	525.0	526.2				
36	2006-05-16	15:28:00	0	97												711.5	675.7	737.4	900.7				
37	2005-05-19	01:54:00	2	96.9											543.0	552.9	539.9		784.0				
38	2005-05-14	05:05:00	0.8	98.2											466.6	566.1	522.8	585.0	742.3				
39	2005-04-28	14:07:00	2.1	96.6											572.8	571.5	563.0	747.2	808.6				
40	2005-04-10	10:29:00	-1.3	99.4											559.3	741.4	674.7	569.4	841.8				
41	2005-04-03	03:10:00	2	97.5											478.7	504.6	484.6	647.1	725.9				
42	2005-03-28	16:09:00	2	97.3											500.0	520.3	502.8	669.3	745.1				
43	2004-12-26	00:58:53	3.2	95.9											636.4	575.6	589.3	835.0	836.8				
44	2004-07-25	14:35:19	-2.4	103.9											672.5	923.2	835.0	492.4	858.2				

# Appendix C Geometrical mean of two horizontal PGA for distant earthquakes

No.	Date	Time	Location	Focal Depth (km)	Mw	Stations	Epicentral Distance (km)	PGA(g) (mean horizontal)
1	2013-07-02	07:37:02	Northern Sumatra	10	6.1	KUM	454.84	0.000027
						IPM	490.55	0.000064
						FRM	577.92	0.000461
						KOM	863.26	0.000034
						JRM	656.96	0.000066
2	2012-07-25	00:27:45		22	6.4	KUM	580.28	0.000017
						IPM	584.07	0.000027
						KOM	864.15	0.000015
						JRM	718.71	0.000007
3	2012-06-23	04:34:53	Northern Sumatra	95	6.1	GTSM	444.10	0.000190
						DTSM	448.90	0.000308
						BRSM	451.10	0.000252
						FRM	425.90	0.000177
						KUM	409.20	0.000179
						IPM	401.30	0.000131
						KGM	621.20	0.000061
						KTM	648.00	0.000084
						JRM	529.70	0.000115
						KOM	683.70	0.000097
						BTSM	448.60	0.000169
4	11-4-2012 (a)	10:43:09	Off West Coast of Northern Sumatra	16.4	8.2	KNSM	1047.30	0.001085
						BKSM	1057.70	0.000895
						GTSM	1078.70	0.000270
						UYSM	1065.60	0.000725
						DTSM	1078.20	0.000735
						BRSM	1075.00	0.000586
						FRM	1058.10	0.000732
						KUM	1041.40	0.000377
						IPM	1044.30	0.000320
						KGM	1218.30	0.000397
						KTM	1291.60	0.000203
						JRM	1168.90	0.000164
						KOM	1274.60	0.000312
						BTSM	1082.30	0.000270
5	11-4-2012 (b)	08:38:38	Off West Coast of Northern Sumatra	22.9	8.6	PYSM 80	966.50	0.000322
						SRSM	964.70	0.005491
						KNSM	951.00	0.001983
						BKSM	964.00	0.001598
						GTSM	981.10	0.000602
						UYSM	969.80	0.001357
						DTSM	985.40	0.001001
						BRSM	986.30	0.000864
						FRM	962.80	0.000595
						KUM	908.00	0.000978
						IPM	923.70	0.000554
						KGM	1147.10	0.000350
						KTM	1171.00	0.000461
						JRM	1065.70	0.000280
						KOM	1207.20	0.000325
						BTSM	985.60	0.000870
6	2012-03-05	06:55:28	Northern Sumatra	10	5.5	PYSM 80	529.00	0.000118
						SRSM	512.00	0.000289
						UYSM	520.10	0.000086
						DTSM	540.00	0.000093
						BRSM	548.70	0.000336
						FRM	514.30	0.000069
						KUM	412.90	0.000074
						IPM	438.60	0.000046
						KGM	732.20	0.000028
						JRM	598.80	0.000038
						KOM	796.10	0.000021

Appendix C Continued.

No.	Date	Time	Location	Focal Depth (km)	Mw	Stations	Epicentral Distance (km)	PGA(g) (mean horizontal)
7	2011-09-05	17:55:13	Northern Sumatera	91	6.6	PYSM 80	410.15	0.000205
						KNSM	395.32	0.001002
						BKSM	407.75	0.000745
						GTSM	425.95	0.000328
						UYSM	414.03	0.000606
						BRSM	429.95	0.000448
						FRM	406.89	0.000312
						KUM	408.21	0.000300
						IPM	393.47	0.000205
						KGM	596.55	0.000117
						JRM	513.74	0.000135
						KOM	658.61	0.000170
						PJSM	411.10	0.000450
8	2011-06-18	11:58:05	Northern Sumatera	24.8	5.2	PYSM 80	291.81	0.000233
						SRSM	311.09	0.002060
						KNSM	294.78	0.001877
						BKSM	299.68	0.001230
						SASM	284.08	0.000599
						GTSM	326.15	0.000227
						JBSM	330.36	0.000931
						UYSM	310.71	0.000648
						DTSM	317.78	0.000356
						BRSM	309.20	0.000495
						FRM	303.00	0.000513
						KUM	415.00	0.000072
						IPM	362.98	0.000097
						KGM	445.90	0.000109
						JRM	421.48	0.000068
						KOM	504.28	0.000048
9	14-6-2011 (a)	03:01:29	Northern Sumatera	10	5.6	PYSM 80	294.69	0.000387
						SRSM	312.40	0.001828
						KNSM	296.15	0.001890
						BKSM	301.71	0.001165
						SASM	286.02	0.000615
						GTSM	327.66	0.000322
						UYSM	312.41	0.000776
						DTSM	320.20	0.000577
						BRSM	312.39	0.000659
						FRM	304.70	0.000636
						KUM	410.08	0.000082
						IPM	359.88	0.000077
						KGM	452.29	0.000136
						JRM	422.86	0.000144
						KOM	511.11	0.000097
						PJSM	297.60	0.000745
10	14-6-2011 (b)	00:08:33	Northern Sumatera	10	5.3	PYSM 80	292.97	0.000405
						SRSM	311.62	0.001984
						KNSM	295.33	0.002527
						BKSM	300.50	0.001743
						SASM	284.86	0.000851
						GTSM	326.76	0.000382
						UYSM	311.40	0.001092
						DTSM	318.76	0.000789
						BRSM	310.49	0.000807
						FRM	303.69	0.000746
						KUM	413.01	0.000074
						IPM	361.73	0.000153
						KGM	448.50	0.000216
						KOM	507.07	0.000113
						PJSM	296.00	0.001259

# Appendix C Continued.

No.	Date	Time	Location	Focal Depth (km)	Mw	Stations	Epicentral Distance (km)	PGA(g) (mean horizontal)
11	2011-04-06	14:01:46	Northern Sumatera	20	5.8	PYSM 80	524.02	0.000056
						KNSM	517.62	0.000374
						BKSM	526.84	0.000274
						SASM	511.04	0.000056
						GTSM	549.26	0.000054
						UYSM	535.50	0.000045
						DTSM	547.02	0.000073
						BRSM	542.84	0.000078
						FRM	527.94	0.000047
						KUM	557.37	0.000023
						IPM	537.61	0.000043
						KGM	688.88	0.001145
						JRM	641.74	0.000033
						KOM	747.17	0.000016
12	2010-12-01	00:50:23	Northern Sumatera	163.4	5.9	PYSM 80	526.20	0.000057
						PYSM 80	304.50	0.001289
						SASM	287.20	0.000252
						GTSM	321.70	0.000133
						JBSM	329.70	0.000111
						UYSM	309.30	0.000118
						DTSM	323.80	0.000233
						BRSM	324.30	0.000134
						FRM	302.10	0.000368
						KUM	337.60	0.000028
						IPM	306.20	0.000467
						KGM	492.50	0.000085
						KTM	544.60	0.000030
						JRM	411.40	0.000016
13	2010-10-25	14:42:16	Southwest of Sumatera	20.6	7.7	KOM	555.10	0.000014
						PYSM 80	305.60	0.000159
						PYSM 80	781.60	0.000080
						SRSM	827.20	0.000190
						SASM	795.10	0.000079
						GTSM	834.40	0.000160
						UYSM	819.00	0.000074
						DTSM	809.20	0.000079
						BRSM	786.10	0.000092
						FRM	813.50	0.000126
						KUM	1015.00	0.000043
						IPM	943.40	0.000045
						KGM	767.40	0.000093
						KTM	1085.60	0.000056
14	2010-05-09	05:59:44	Northern Sumatera	45	7.2	JRM	911.30	0.000056
						KOM	780.90	0.000065
						PYSM 80	633.80	0.000431
						SRSM	622.20	0.002215
						BKSM	626.10	0.002175
						SASM	612.10	0.001317
						GTSM	638.20	0.000408
						JBSM	648.50	0.002220
						DTSM	647.80	0.000817
						BRSM	653.80	0.000912
						FRM	622.90	0.000170
						KUM	538.00	0.000280
						IPM	560.30	0.000178
						KGM	831.40	0.000761
KTM	805.40	0.000147						
JRM	714.70	0.000141						
KOM	894.70	0.000073						

Appendix C Continued.

No.	Date	Time	Location	Focal Depth (km)	Mw	Stations	Epicentral Distance (km)	PGA(g) (mean horizontal)
15	2010-04-06	22:15:06	Northern Sumatera	31	7.8	PYSM 80	507.80	0.000532
						BKSM	506.80	0.000615
						SASM	491.30	0.000703
						UYSM	513.70	0.000684
						FRM	506.40	0.000676
						KUM	502.70	0.000373
						IPM	493.30	0.000341
						KGM	687.90	0.000251
						KTM	739.00	0.000386
						JRM	614.70	0.000345
KOM	748.70	0.000233						
16	2009-12-23	01:11:52	Southern Sumatera	22.6	5.7	PYSM 80	599.43	0.000097
						SRSM	639.22	0.000531
						KNSM	624.10	0.000938
						GTSM	649.51	0.000074
						UYSM	633.24	0.000141
						DTSM	628.48	0.000214
						BRSM	608.49	0.000319
						FRM	626.62	0.000086
						KUM	798.95	0.000028
						IPM	735.69	0.000023
						KGM	642.42	0.000737
						KTM	910.27	0.000084
						JRM	736.84	0.000038
						KOM	674.25	0.000052
17	2009-10-01	01:52:31	Southern Sumatera	15	6.6	PYSM 80	597.80	0.000100
						BKSM	623.11	0.000384
						GTSM	650.01	0.000205
						BRSM	596.36	0.000230
						FRM	633.07	0.000096
						KUM	867.33	0.000040
						IPM	784.86	0.000036
						KGM	530.06	0.000280
						KTM	878.72	0.000052
						JRM	710.29	0.000071
KOM	530.99	0.000345						
18	2009-09-30	10:16:09	Southern Sumatera	81	7.6	PYSM 80	471.34	0.000643
						BKSM	492.04	0.001798
						GTSM	522.54	0.000688
						BRSM	479.23	0.001610
						FRM	500.15	0.000684
						KUM	688.54	0.000212
						IPM	619.42	0.000265
						KGM	509.71	0.001252
						KTM	781.91	0.000270
						JRM	607.55	0.000290
KOM	543.27	0.000732						
19	2009-08-16	07:38:18	Southern Sumatera	20	6.7	PYSM 80	615.16	0.000182
						SRSM	653.50	0.000246
						KNSM	638.10	0.000897
						BKSM	633.90	0.000529
						SASM	621.31	0.001516
						GTSM	664.36	0.000168
						DTSM	644.29	0.000400
						BRSM	625.05	0.000430
						FRM	641.21	0.000252
						KUM	805.30	0.000075
						IPM	744.70	0.000085
						KTM	925.73	0.000091
						JRM	753.21	0.000130
						KOM	700.18	0.000222



# Appendix C Continued.

No.	Date	Time	Location	Focal Depth (km)	Mw	Stations	Epicentral Distance (km)	PGA(g) (mean horizontal)
20	2008-05-19	14:26:00	Northern Sumatera	14.8	6.0	IPM	383.72	0.000160
						KTM	601.36	0.000089
21	2008-02-25 (a)	18:06:00	Southern Sumatera	33.1	6.3	IPM	770.66	0.000021
						KTM	916.21	0.000028
22	2008-02-25 (b)	08:36:00	Southern Sumatera	35	7.2	IPM	807.10	0.000360
						KTM	955.38	0.000164
						KOM	669.76	0.000250
23	2008-02-24	14:46:00	Southern Sumatera	35	6.2	IPM	798.39	0.000206
						KTM	949.81	0.000023
24	2008-02-20	08:08:00	Simeulue, Northern	35	7.4	IPM	616.57	0.000313
						KTM	864.56	0.000165
25	2008-01-22	17:14:00	Nias Region, Northern	40.6	6.2	IPM	573.45	0.000046
						KTM	808.05	0.000037
26	2008-01-04	07:29:00	Southern Sumatera	40.6	6.0	IPM	839.74	0.000015
						KTM	965.46	0.000055
27	2007-09-20	08:31:00	Southern Sumatera	30	6.7	IPM	787.60	0.000037
						KTM	939.80	0.000066
						KOM	661.80	0.000109
28	2007-09-13	03:35:00	Southern Sumatera	20	7.0	IPM	731.30	0.000102
						KTM	885.10	0.000182
29	2007-09-12	23:49:00	Southern Sumatera	30	7.9	IPM	816.00	0.000419
						KTM	934.70	0.000457
						KOM	610.40	0.000932
30	2007-09-12	11:10:00	Southern Sumatera	34	8.5	IPM	992.20	0.000313
						KTM	1097.90	0.000510
						KOM	749.40	0.000742
31	2007-08-08	17:04:00	Java	289.2	7.5	IPM	1395.80	0.000169
						KTM	1365.40	0.000150
32	2007-07-21	12:53:00	Northern Sumatera	25.6	5.2	IPM	362.30	0.000067
						KTM	591.90	0.000033
						KOM	764.80	0.000013
33	2007-03-06 (a)	05:49:00	Southern Sumatera	30.1	6.1	FRM	445.60	0.000344
						KUM	651.60	0.000090
						IPM	576.90	0.000075
34	2007-03-06 (b)	03:49:00	Southern Sumatera	19	6.4	FRM	435.10	0.000293
						KUM	640.60	0.000043
						IPM	566.00	0.000043
						KTM	712.20	0.000073
35	2006-12-01	03:58:00	Northern Sumatera	206.1	6.3	FRM	314.49	0.000153
						KUM	292.91	0.000223
						IPM	279.48	0.000305
						KGM	524.99	0.000066
						KTM	526.16	0.000092
36	2006-05-16	15:28:00	Nias Region, Northern Sumatera	16.2	6.8	KUM	711.54	0.000076
						IPM	675.74	0.000078
						KGM	737.38	0.000204
						KTM	900.67	0.000072
37	2005-05-19	01:54:00	Northern Sumatera	30	6.9	FRM	542.95	0.000097
						KUM	552.88	0.000114
						IPM	539.94	0.000927
						KTM	784.02	0.000085
38	2005-05-14	05:05:00	Off West Coast of Northern Sumatera	34	6.8	FRM	466.64	0.000415
						KUM	566.05	0.000110
						IPM	522.82	0.000136
						KGM	584.98	0.000367
						KTM	742.28	0.000098
39	2005-04-28	14:07:00	Off West Coast of Northern Sumatera	29	6.3	FRM	572.75	0.000049
						KUM	571.49	0.000067
						IPM	563.03	0.001183
						KGM	747.24	0.000840
						KTM	808.63	0.000029

Appendix C Continued.

No.	Date	Time	Location	Focal Depth (km)	Mw	Stations	Epicentral Distance (km)	PGA(g) (mean horizontal)
40	2005-04-10	10:29:00	Kepulauan Mentawai Region	19	6.7	FRM	559.30	0.000155
						KUM	741.43	0.000075
						IPM	674.67	0.000046
						KGM	569.41	0.000220
						KTM	841.79	0.000070
41	2005-04-03	03:10:00	Off West Coast of Northern Sumatera	46.6	6.3	FRM	478.67	0.000120
						KUM	504.61	0.000075
						IPM	484.63	0.000189
						KGM	647.08	0.000105
						KTM	725.86	0.000103
42	2005-03-28	16:09:00	Off West Coast of Northern Sumatera	30	8.6	FRM	500.03	0.001759
						KUM	520.25	0.001033
						IPM	502.76	0.001073
						KGM	669.33	0.001130
						KTM	745.09	0.001130
43	2004-12-26	00:58:53	Off West Coast of Northern Sumatera	30	9.1	FRM	636.35	0.000856
						KUM	575.59	0.000810
						IPM	589.33	0.001151
						KGM	835.04	0.000422
						KTM	836.75	0.000708
44	2004-07-25	14:35:19	Southern Sumatera	576	7.3	FRM	672.48	0.000094
						KUM	923.24	0.000042
						IPM	835.00	0.000049
						KGM	492.40	0.000292
						KTM	858.16	0.000106

17	NURUL NADIA BINTI MOHD ZORKIPLI	Pembantu Penyelidik - SPM (N17)	21 Julai 2014	31 Oktober 2014	Pelantikan Baru
18	NURUL NADIA BINTI MOHD ZORKIPLI	Pembantu Penyelidik - SPM (N17)	1 November 2014	31 Januari 2015	Pelanjutan Perkhidmatan
19	NURUL SHAZWANI BINTI MOHD ZAIN	Pembantu Projek	1 Julai 2013	31 Ogos 2013	Pelantikan Baru
20	SHARIFAH AISHAH BINTI SYED SALIM	Penolong Pegawai Penyelidik - STPM (N27)	1 Mac 2013	31 Mei 2013	Pelantikan Baru
21	SHARIFAH AISHAH BINTI SYED SALIM	Penolong Pegawai Penyelidik - STPM (N27)	12 Mac 2015	31 Mei 2015	Pelantikan Baru
22	SHARIFAH AISHAH BINTI SYED SALIM	Penolong Pegawai Penyelidik - STPM (N27)	1 Jun 2013	31 Ogos 2013	Pelanjutan Perkhidmatan
23	SHARIFAH AISHAH BINTI SYED SALIM	Penolong Pegawai Penyelidik - STPM (N27)	1 September 2013	30 November 2013	Pelanjutan Perkhidmatan
24	SHARIFAH AISHAH BINTI SYED SALIM	Penolong Pegawai Penyelidik - STPM (N27)	1 Januari 2014	31 Mac 2014	Pelanjutan Perkhidmatan
25	SHARIFAH AISHAH BINTI SYED SALIM	Penolong Pegawai Penyelidik - STPM (N27)	1 April 2014	30 Jun 2014	Pelanjutan Perkhidmatan
26	SHARIFAH AISHAH BINTI SYED SALIM	Penolong Pegawai Penyelidik - STPM (N27)	1 Julai 2014	30 September 2014	Pelanjutan Perkhidmatan
27	SITI AMINAH BINTI HELL MEE	Pembantu Projek	1 Julai 2013	31 Ogos 2013	Pertukaran Akaun Projek
28	SITI LAILATUL MUNIRAH BT AHMAD TERMIZI	Pembantu Projek	1 Julai 2013	31 Ogos 2013	Pertukaran Akaun Projek
29	ZULFA AIZA BINTI ZULKIFLI	Pembantu Projek	1 Ogos 2013	31 Ogos 2013	Pertukaran Akaun Projek
30	'AQILAH BINTI GHAZALI	Pembantu Projek	1 Julai 2013	31 Ogos 2013	Pertukaran Akaun Projek

Purchase Requisition	Purchase Order	Suppliers	Maintenance	Financials	Coda Info	Reports	Admin
UserCode: SHALYDAH / USMKCTLIVE / PBAHAN		Program Code: Votebook9100		Current Program : Votebook (Header)			
Current Date : 02/08/2016 5:07:19 PM		Version: 15.124, Last Updated at 01/07/2016		DB: 13.00, 09/18/2010 VB: 13.01, 03/14/2011		Switch Language : English / Malay	
Wildcard : eg. Like 100%, Like 10%1, Like %1							
Element 1: 1001		Element 2: %		Element 4: PBAHAN			
Element 5: 814184		Year: 2016					

Detail	Excel	Budget Rule	Budget Control	Account Description	Budget Account Code	Roll over	Budget	Cash Received	Advanced	Commit	Actual	Available	Percentage
Detail	Excel	46	T	Projek Kumpulan Wang Uni Penyelidikan	1001.111.0.PBAHAN.814184	-24,406.24	0.00	0.00	0.00	0.00	28,172.10	-52,578.34	0.00%
		46	T	SubTotal		-24,406.24	0.00	0.00	0.00	0.00	28,172.10	-52,578.34	0.00%
Detail	Excel	47	T	Projek Kumpulan Wang Uni Penyelidikan	1001.221.0.PBAHAN.814184	15,091.50	0.00	0.00	0.00	0.00	775.30	14,316.20	0.00%
Detail	Excel	47	T	Projek Kumpulan Wang Uni Penyelidikan	1001.223.0.PBAHAN.814184	1,443.75	0.00	0.00	0.00	0.00	0.00	1,443.75	0.00%
Detail	Excel	47	T	Projek Kumpulan Wang Uni Penyelidikan	1001.224.0.PBAHAN.814184	-200.00	0.00	0.00	0.00	0.00	0.00	-200.00	0.00%
Detail	Excel	47	T	Projek Kumpulan Wang Uni Penyelidikan	1001.226.0.PBAHAN.814184	-5,599.50	0.00	0.00	0.00	627.00	5,476.40	-11,702.90	0.00%
Detail	Excel	47	T	Projek Kumpulan Wang Uni Penyelidikan	1001.227.0.PBAHAN.814184	28,251.60	0.00	0.00	0.00	0.00	669.00	27,582.60	0.00%
Detail	Excel	47	T	Projek Kumpulan Wang Uni Penyelidikan	1001.228.0.PBAHAN.814184	25,000.00	0.00	0.00	0.00	0.00	0.00	25,000.00	0.00%
Detail	Excel	47	T	Projek Kumpulan Wang Uni Penyelidikan	1001.229.0.PBAHAN.814184	2,003.20	0.00	0.00	0.00	0.00	4,802.83	-2,799.63	0.00%
		47	T	SubTotal		65,990.55	0.00	0.00	0.00	627.00	11,723.53	53,640.02	0.00%
Detail	Excel	50	T	Projek Kumpulan Wang Uni Penyelidikan	1001.552.0.PBAHAN.814184	-155.52	0.00	0.00	0.00	37.62	382.75	-575.89	0.00%
		50	T	SubTotal		-155.52	0.00	0.00	0.00	37.62	382.75	-575.89	0.00%
		9999		GrandTotal		41,428.79	0.00	0.00	0.00	664.62	40,278.38	485.79	0.00%